

UCSF

UC San Francisco Electronic Theses and Dissertations

Title

Discovery of Novel Inhibitors of Ornithine Decarboxylase in Trypanosoma brucei:
Development and Application of a Targeted High-Throughput Screening Program

Permalink

<https://escholarship.org/uc/item/8kk646b9>

Author

Smithson, David Carroll

Publication Date

2009

Peer reviewed|Thesis/dissertation

Discovery of Novel Inhibitors of Ornithine Decarboxylase in *Trypanosoma brucei*:
Development and Application of a Targeted High-Throughput Screening Program

by

David C. Smithson

DISSERTATION

Submitted in partial satisfaction of the requirements for the degree of

DOCTOR OF PHILOSOPHY

in

The Chemistry and Chemical Biology Program

in the

GRADUATE DIVISION

of the

Acknowledgements

A great many individuals have been a part of the completion of my degree. I would first like to thank my collaborators and advisors who have contributed invaluable advice and guidance over the years. Brian Shoichet and Jim McKerrow have served on my thesis committee and have provided valuable insights and guidance throughout the project. Kip Guy has been an excellent and understanding advisor throughout the many trials and tribulations which plagued this process. Jeremy Mallari has been a good friend and provided a great many useful discussions during my graduate career. The other members of the Guy lab including Alexander (Leggy) Arnold, Armand Guiguemde and Anang Shelat have also served as useful sounding boards and sources of inspiration during my years as a graduate student.

I would also like to thank my family, particularly my parents, Robert and Susan Smithson who have always supported my scientific interests and never shied away from my constant questioning. My father, who is never satisfied with the simple answers, is the reason that I am a scientist today. My grandparents, aunts, uncles and cousins on both sides have also contributed to my growth as an individual and have helped make me the man that I am today.

Finally, I would like to thank my loving wife Nicole Smithson, who has stood with me for the entirety of my graduate career, through the good times and the sleepless stress filled nights.

Discovery of Novel Inhibitors of Ornithine Decarboxylase in

Trypanosoma brucei:

Development and application of a Targeted High-Throughput Screening Program

David C. Smithson

Abstract

Human African Trypanosomiasis (HAT), caused by the eukaryotic parasite *Trypanosoma brucei*, is a serious health problem in much of central Africa. The only validated molecular target for treatment of HAT is ornithine decarboxylase (ODC), which catalyzes the first step in polyamine metabolism. Herein, we describe the optimization of high throughput screening protocols at St. Jude Children's Research Hospital as well as the development of a high-throughput compatible assay for ODC. We have used this assay to screen 316,114 unique molecules to identify potent and selective inhibitors of ODC. This effort identified four novel families of ODC inhibitors, including the first inhibitors selective for the parasitic enzyme. These compounds display unique binding modes, suggesting the presence of allosteric regulatory sites on the enzyme. Docking of a subset of these inhibitors, coupled with mutagenesis, also supports the existence of these allosteric sites.

Table of Contents

Abstract	iv
List of Tables	vii
List of Figures	viii
1 Introduction: An Overview of Human African Trypanosomiasis and it's Treatment	1
1.1 Origins of the Disease	2
1.2 Historical Efforts to Control Human African Trypanosomiasis	4
1.3 Current Disease Epidemiology	7
1.4 Current Vector Control Efforts	9
1.5 Current Chemotherapeutics	10
1.6 Parasite Biology	14
1.6.1 Life Cycle of <i>T. brucei</i>	15
1.6.2 Antigenic Variation and the Variant Surface Glycoprotein Coat	16
1.7 Modern Drug Discovery Methodology	18
1.7.1 Drug Target Validation	19
1.7.2 Assay Validation for High Throughput Screening	21
1.7.3 Library Selection	24
1.7.4 Automation Considerations	26
1.7.5 Data Analysis in High Throughput Screening – Picking Hits	28
1.8 Potential Targets for Chemotherapeutic Intervention	32
1.8.1 The Glycolytic Pathway	33
1.8.2 The Topoisomerases	34
1.8.3 Folate metabolism	35
1.8.4 Oxidative Stress Management	37
1.8.5 Proteases	38
1.8.6 Polyamine Biosynthesis	39
1.9 Project Goals	44
2 Combating Pin-Transfer Cross Contamination in High Throughput Screening	78
2.1 Introduction	79
2.2 Materials and Methods	82
2.3 Results	89
2.4 Discussion	102
3 Optimization of a Non-Radioactive High Throughput Assay for Decarboxylase Enzymes	106
3.1 Introduction	107
3.2 Materials and Methods	109
3.3 Results	116
3.4 Discussion	128

4	Discovery of Potent and Selective Inhibitors of <i>Trypanosoma brucei</i> Ornithine Decarboxylase	135
4.1	Introduction	136
4.2	Materials and Methods	137
4.3	Results	147
4.4	Discussion	161
5	Conclusions	174
	Appendix	181

List of Tables

4.1 – Inhibitors of TbODC	151
4.2 – Steady State Kinetic Analysis of TbODC Enzymes	159
4.3 – Whole Cell Cytotoxicity Results	161
S4.10 – Chapter 4 Compound Numbers to St. Jude Registry Key	189
S4.11 – Tables of All ODC HTS Screen Hits and Modes of Inhibition	207
S4.12 – Table of All ODC HTS Screen Hits Cytotoxicity Data	234
S4.13 – Table of All ODC HTS Screen Hits Purity and Concentration	243

List of Figures

1.1 – Chemotherapeutic Agents for Human African Trypanosomiasis	6
1.2 – Distribution of Human African Trypanosomiasis	9
1.3 – The <i>T. brucei</i> Lifecycle	16
1.4 – The Variant Surface Glycoprotein Coat	17
1.5 – The automated high-throughput screening deck at St. Jude Children’s Research Hospital	27
1.6 – The Polyamine Biosynthetic Pathway in Mammalian Systems and in <i>T. brucei</i>	42
2.1 – Detection of Carryover in Primary Screening Data	80
2.2 – Volumetric Data for Various Pin Sets	92
2.3 – Schematic of a Typical Cross Contamination Experiment	93
2.4 – Analysis of Carryover Patterns	95
2.5 – Comparison of Cleaning Methods	98
2.6 – Characteristics of the Carryover Test Set and Representative Structures	99
2.7 – Fluorescein Carryover Performance of Old and New Pins	101
3.1 – Linked Assay Mechanism	108
3.2 – Optimization of Primary Assay Conditions	117
3.3 – Optimization of PEPC-MDH Assay System	120
3.4 – Performance of Known Inhibitors	121
3.5 – ODC-PEPC-MDH Assay Scaling Assay Scatter Plot	123
3.6 – Comparing Curve Fitting Methods	125
3.7 – ROC Curve for Primary Assay	126
4.1 – Bisbiguanide Lineweaver-Burk Plots and Selectivity Curves	152
4.2 – Benzthiazole Lineweaver-Burk Plots	153
4.3 – Indole Lineweaver-Burk Plots	154
4.4 – Dithioamidine Lineweaver-Burk Plots and Selectivity Curves	156
4.5 – Proposed Dithioamidine Binding Site	158
S4.1 – Selectivity Curves for Compounds 1, 2, 6 and 8 (Ch. 4)	182
S4.2 – Reversibility Data for Representative Compounds	183
S4.3 – Reaction Linearity with Respect to [ODC]	183
S4.4 – K_m Determination for Enzymes Used in Chapter 4	183
S4.5 – D354E TbODC K_m Determination	184
S4.6 – Proposed Alternate Binding Sites for Dithioamidine Compounds	185
S4.7 – Proposed Alternate Binding Sites – Residue View	186
S4.8 – ROC Curves for Alternate Binding Site DOCKing Studies	187
S4.9 – Additional Benzthiazole Compounds Screened	188
Chapter 4 Compound UPLC-MS Data	190

Chapter 1

An Overview of Human African Trypanosomiasis, its Treatment and Modern Drug Discovery

1.1 Origins of the Disease

The earliest reports of African Trypanosomiasis, caused by subspecies of the eukaryotic parasite *Trypanosoma brucei*, are from ancient Egyptian papyri describing the cattle version of the disease (also known as nagana) dating back to the 2nd millennium BC.¹ In 1373, the death of the Emperor of Mali was attributed to a disease with similar characteristics to Human African Trypanosomiasis (HAT). Further reports of the disease do not appear until after European exploration of Africa began in the 1700's. In 1734 John Atkins, an English naval surgeon, published a report detailing the neurological effects of the disease in Negros.² Almost 75 years later in 1803 an English medical doctor named Thomas Winterbottom characterized the swollen lymph glands at the base of the neck that are indicative of early stage HAT. This swelling is now known as Winterbottom's sign.² The famous Scottish missionary David Livingstone was the first to suggest that the disease was spread by the tsetse fly after an encounter with nagana in the valleys of the Limpopo and Zambezi rivers in which all cattle he had brought with him died after being bitten.¹

By the mid 1800's, reports of trypanosomes in the blood of a wide range of animal species began to surface. Valentin, a professor of physiology at the University of Berne reported the presence of flagellates in the blood of brown trout in 1841 while Gluge, Mayer and Gruby (who created the *Trypanosoma* genus) published independent reports of trypanosomes in frog blood. Other reports quickly followed and were confirmed describing various trypanosome species in rats, camels, horses, mules, cattle and other wild animals.² In 1894, the Scottish army surgeon David Bruce discovered

Trypanosoma brucei brucei while studying nagana in the Umbombo district of Natal Province of South Africa.³ He further showed that the parasites were the causative agent of the disease by inoculating a healthy dog with the blood of an infected antelope.⁴ In addition, he clearly implicated the tsetse fly (*Glossina palpalis*) as the disease vector by dissecting the flies after they bit an infected animal and showing the presence of live parasites in the proboscis and stomach of the flies.⁴ However, due to the outbreak of war in the area he was unable to continue his experiments long enough to establish the presence of a developmental cycle within the fly and as a result hypothesized that transmission was simply mechanical.²

The first description of trypanosomes in humans was published in 1902 by Robert Michael Forde, a British Colonial surgeon who examined the blood of a Gambian steamboat captain and reported the presence of tiny worms. These were identified a few months later by Joseph Everett Dutton as trypanosomes and given the species name *Trypanosoma gambiense* (now known as *Trypanosoma brucei gambiense*).^{5, 6} Following this discovery, the field advanced rapidly for the next several decades. In 1903, Bruce reported that *T. brucei gambiense* was the causative agent of sleeping sickness in man, though Aldo Castellani, a young Italian doctor claimed to have made the observation first.⁷⁻¹⁰ This controversy has stretched on into modern times and is not likely to be cleanly resolved. In 1909, Friedrich Karl Kleine reported the full cyclical transmission cycle of *T. brucei* by tsetse flies, causing Bruce to revise his mechanical transmission theories and describe the full developmental cycle of the parasites within the insect.^{2, 11} Shortly after this, the second human pathogenic species *Trypanosoma rhodesiense* (now known as *Trypanosoma brucei rhodesiense*) was isolated from a patient in Northeast

Rhodesia (Zimbabwe) by John William Watson Stephens and Harold Benjamin Fantham.¹² This parasite strain was significantly more virulent in rats than *T. b. gambiense* and was found to be transmitted by *Glossina moristans*, a species of tsetse fly found in the East African savannah. In 1912 game animals were found to act as a reservoir for the parasite.¹³

1.2 Historical Efforts to Control Human African Trypanosomiasis

As European involvement in Africa increased during the 19th century so did their efforts to treat and control sleeping sickness. The first major recorded HAT epidemic occurred from 1896 to 1906 during which some 900,000 estimated deaths occurred in the Congo, Uganda and Kenya.^{1, 14} This devastation prompted colonial administrations to devote significant resources to the discovery of treatments for HAT as well as methods to control the tsetse fly vectors. The first reported chemotherapy for sleeping sickness was arsenic, which had been used by David Livingstone as a treatment for tsetse bite.¹⁵ This approach was confirmed in 1902 when Lavaren and Mesnil showed that sodium arsenite was able to reduce parasitemia in the blood of laboratory animals.² In 1904, the use of the experimental drug atoxyl (**Fig 1.1**) was reported by Harold Wofarstan Thomas and Anton Breinl to cure infections in infected animals. However, when Robert Koch used the compound in humans, it proved to be highly toxic, resulting in 22 cases of total blindness in a group of 1622 treated patients.¹ Koch consulted with Paul Ehrlich, who had already made progress in the field of anti-microbial agents by using methylene blue to treat malaria in 1891 – the first example of a synthetic compound being used as a drug.¹⁶

Ehrlich had already started work on Trypanosomiasis in 1904 and had shown that the trypan red dye was curative for *T. equinum*, a trypanosome species afflicting horses in the Americas. However, this agent was not effective versus *T. brucei*.¹ In 1916, Ehrlich's former assistant Wilhelm Roehl, with the assistance of Bayer pharmaceuticals developed suramin (**Fig 1.1**), a derivative of trypan red which is still in use today as a treatment for HAT. One year previously, in 1915, Michael Heidelberger developed an improved organo-arsenical drug which he named tryparsamide. (**Fig 1.1**) This was the first compound effective versus late stage HAT and was often used in combination with suramin.

During the second major sleeping sickness epidemic, which occurred from 1919 to the early 1940's, this combination was used to great effect by mobile treatment teams moving from one outbreak foci to the next. This approach led to a decrease in prevalence levels from 60% to 0.2%.¹ Besides chemotherapeutics, colonial powers attempted to control spread of the disease by both removing tsetse fly habitat and killing game animals serving as reservoirs for the parasite, which led to a significant decrease in the fly population.¹⁴ Pentamidine, a diamidine compound effective versus early stage HAT, was developed in 1937 by chemist Arthur James Ewins, though it was not used in the field until 1942.^{17, 18} (**Fig 1.1**) This drug remains in use as a front line therapy for HAT and resistance in the field is still low, despite extremely heavy use both as a single agent and in combination therapies.¹⁸

Following World War II, several other important advances were made. The first of these was the deployment of DDT to control tsetse fly populations in 1949.¹ At the same time, the arsenical melarsoprol (**Fig 1.1**) was developed by Ernst Friedheim. This is

still the only drug effective against late stage *T. b. rhodesiense*.¹ The combination of effective chemotherapeutics, tsetse fly control and active monitoring programs lead to a dramatic decrease in HAT, almost completely eliminating the disease by the 1960's.¹⁹ Disease levels remained low until the late 1970's, when decreased surveillance as a result of political instability in the region coupled with the world-wide ban of DDT lead to the third major HAT epidemic.¹⁹

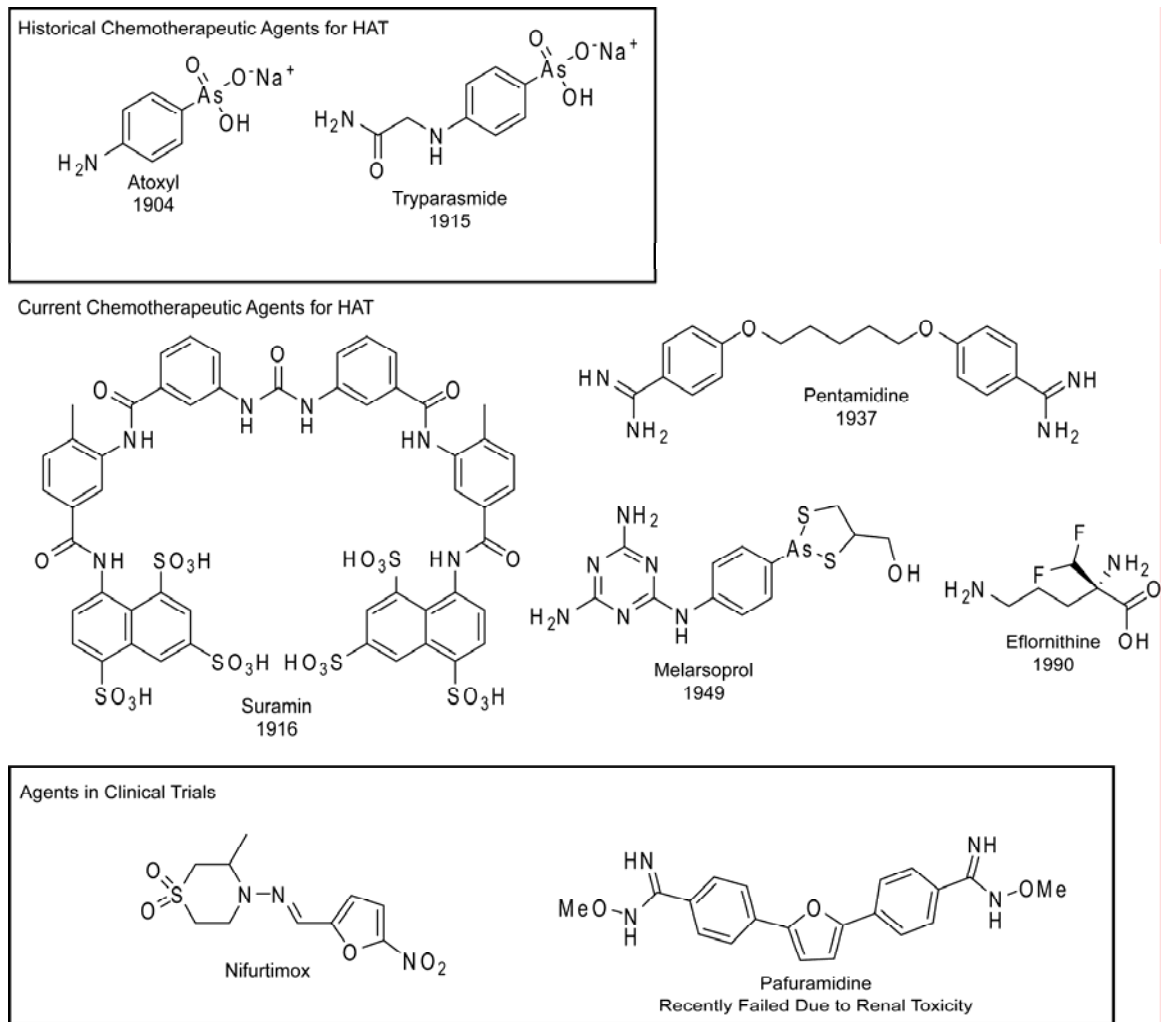


Figure 1.1 – Chemotherapeutic Agents for Human African Trypanosomiasis

This epidemic peaked in the mid 1990's and is now in decline (though levels are still not back to 1960's levels) thanks in large part to increased surveillance, tsetse fly trapping

programs and the introduction of the non-toxic drug eflornithine (**Fig 1.1**) in the early 1990's.^{1, 20, 21}

1.3 Current Disease Epidemiology

Of the three described subspecies of *Trypanosoma brucei*, *T. b. brucei*, *T. b. gambiense* and *T. b. rhodesiense*, only the last two cause disease in humans. The current combined infections of both *T. b. gambiense* and *T. b. rhodesiense* is estimated at approximately 50,000 to 70,000 active cases with 17,500 new cases per year.²² Since this disease predominately affects the productive age groups (15 to 45 years) it also has a major impact on the economies of endemic regions. In 2000, the WHO estimated that almost 2.05 million disability adjusted life years were lost due to sleeping sickness.²³ The disease is uniformly fatal if left untreated.

The difference between human infective and non-infective subspecies of *T. brucei* is largely due to their response to a lytic factor found in human plasma. As early as 1907 it had been noted that trypanosomes isolated from animals would lyse when exposed to human serum.²⁴ This has since been traced to the presence of the apolipoprotein L-I (apoL-I) in human serum which is thought to insert in the trypanosomal membranes creating pores and resulting in lysis.^{25, 26} *T. b. rhodesiense* expresses a membrane associated resistance protein (serum resistance associated protein, SRA) which grants resistance to this process. Interestingly, *T. b. gambiense* does not express this protein, and the genetic basis of its resistance to apoL-I is still unknown.²⁷ SRA has been isolated from a wide range of *T. b. rhodesiense* field samples and is used as a molecular marker to

distinguish the various subspecies.^{27, 28} It should be noted that it is possible for *T. b. brucei* to acquire resistance to apoL-I in laboratory settings through mechanisms other than SRA, suggesting that host switching may be possible in the field as well.²⁹

Although it does not infect humans *T. b. brucei* still has a major economic impact in Africa due to its effect on animal populations. It is able to infect a wide range of domestic livestock species and results in the wasting disease nagana which David Bruce originally began studying in the early 1900's.⁷ The presence of this disease severely limits the land area available for agricultural use in endemic areas.³⁰

T. b. rhodesiense, the causative agent of East African Trypanosomiasis, is often characterized as a host-range variant of *T. b. brucei* based on biochemical analysis of genomic DNA.¹⁴ However, classic taxonomical data disagrees with this assessment. East African Trypanosomiasis is a more acute form of sleeping sickness which typically results in death due to pancarditis or pulmonary edema several months after infection.³⁰ This disease progresses rapidly, often entering the CNS stage only weeks after infection. It is endemic to southeast Africa in relatively limited foci.²² (**Fig 1.2**) Although it accounts for only 10% of the reported cases the rapid progression leads to a higher mortality rate than the disease caused by *T. b. gambiense*.³¹

West African Trypanosomiasis, caused by *T. b. gambiense* is the more chronic version of the disease. These infections progress relatively slowly and take several months to progress to the CNS stage. This subspecies is more widespread and is endemic across western and central Africa, accounting for over 90% of HAT infections.²² (**Fig 1.2**)

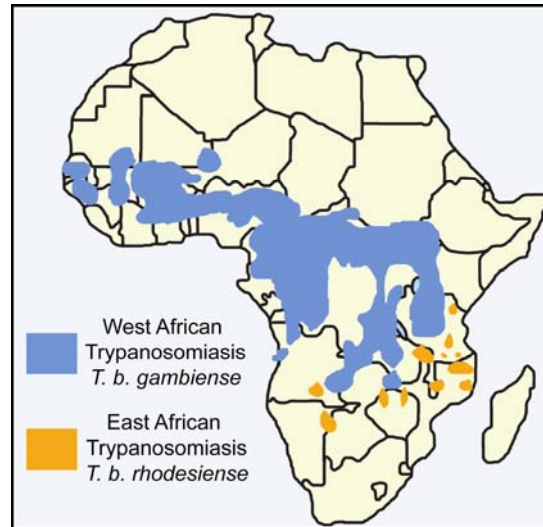


Figure 1.2 – Distribution of Human African Trypanosomiasis

1.4 Current Vector Control Efforts

Since the elimination of DDT spraying and ground clearing programs in the 1970's efforts to control the tsetse fly population efforts have largely centered on trapping of the flies. Traps were designed with shapes, colors and odors designed to attract the flies.³² Advances in insecticides which were toxic to the flies with minimal impact on mammals made it possible to use the traps to economically control the flies in limited areas.^{33, 34} Furthermore, it was shown that trap barriers could be created to protect tsetse free areas from infestation. Over 27,000 traps were deployed in Zimbabwe with a high degree of success.¹⁴ However, despite the success of traps in some regions widespread adoption has been limited, particularly in areas which are difficult to access. Pour-on insecticides which allowed farmers to treat livestock and prevent fly bites have also been used successfully.³⁵

In 2001 a major effort to eliminate the tsetse fly from Africa was launched by the Organization of African Unity.³⁶ This project combined traps, insecticide treated targets and aerial spraying approaches to reduce fly populations followed by release of sterile male flies to eliminate the target species. This technique relies on the creation of sterile male flies by brief exposure to high energy radiation and has been used to eliminate the fly population on the island of Zanzibar.³⁷ However, despite its success in a controlled island environment, many scientists are concerned that attempting this in a large open environment such as sub-Saharan Africa will fail.³⁸ This is due to both the cost of producing sterile flies as well the fact that there are at least 7 different species of fly which can serve as vectors for trypanosomiasis. In short, it seems unlikely that the vector responsible for spreading HAT will be eliminated soon.

1.5 Current Chemotherapeutics

There are currently four agents used therapeutically for the treatment of HAT, suramin, pentamidine, melarsoprol and eflornithine. (**Fig 1.1**) Of these, suramin and pentamidine are only used in pre-CNS infections, while melarsoprol and eflornithine are both effective in late-stage HAT.

Suramin is the recommended treatment for early stage *T. b. rhodesiense* infections. The drug is poorly bioavailable due to the fact that it has 6 negative charges at physiological pH. As a result, it must be administered intravenously and is unable to pass the blood-brain barrier. Once in the bloodstream it binds tightly to serum proteins and LDL components, resulting in a 44-54 day half-life.³⁹ The binding of suramin to LDL

also facilitates its uptake into the parasite.⁴⁰ The mechanism of action is not clear although several possibilities have been proposed including inhibition of glycolytic enzymes, lysosomal accumulation and inhibition of LDL uptake.⁴¹ Polyamine metabolism has also been suggested as a possible target since suramin is synergistic with eflornithine, a known inhibitor of polyamine biosynthesis.⁴² It is likely that the trypanocidal effects are due to a wide range of intracellular activities. This is supported by the fact that no clinical resistance to this drug has been reported, and efforts to raise resistant parasite strains in the laboratory have failed.⁴³ Immediate side effects of suramin include nausea, vomiting and collapse. Long term reactions include exfoliative dermatitis, kidney damage, agranulocytosis, hemolytic anemia, jaundice and severe diarrhea, all of which can be fatal.⁴³

Pentamidine is the drug of choice for early *T. b. gambiense* infections, though it is used as second line therapy for *T. b. rhodesiense* cases when suramin is contraindicated.⁴⁴ Like suramin, the drug is relatively poorly bioavailable, does not cross the blood-brain barrier and is typically administered intramuscularly. The drug is approximately 70-80% bound to plasma proteins with an average plasma half-life of 12 days. Elimination occurs via metabolic processes, only 11% is passed in the urine.⁴⁵ Pentamidine is accumulated in *T. brucei* species at concentrations in excess of 1 mM.⁴⁶ Several transporters have been implicated in this process, including the P2 aminopurine transporter, the high-affinity pentamidine transporter (HAPT1) and the low-affinity pentamidine transporter (LAPT1).^{47, 48, 49} Deletion of these transporters has been shown to result in resistance to the drug.⁵⁰ The mechanism of action is poorly characterized, though the compound has been shown to bind to DNA both in the nucleus and in the kinetoplast possibly interfering

with topoisomerase II activity.⁵¹ It has also been shown to inhibit S-adenosylmethionine decarboxylase, an enzyme in the polyamine biosynthetic pathway, though no changes in cellular polyamine levels are observed in pentamidine treated *T. b. brucei*, indicating that this is unlikely to be the mechanism for whole cell toxicity.⁵² Significant resistance in the field has not been reported despite heavy use as both a prophylactic and therapeutic agent for many years.⁴⁴ Side effects of pentamidine usage include nephrotoxicity, diabetes mellitus and hypotension.⁴³

Melarsoprol was the first drug developed effective versus late stage HAT. This drug contains a reactive arsenoxide group as well as a melaminophenyl group which is thought to be recognized by the P2 transporter system in *T. brucei*.⁵³ It is highly insoluble in water and is administered intravenously as a propylene glycol solution. The drug is highly toxic, resulting in a reactive encephalopathy in 5 to 10% of patients with a 50% fatality rate.⁴⁴ Other side effects include vomiting, peripheral neuropathy, abdominal colic, arthralgia and thrombophlebitis.⁴³ Despite this, the drug is the only therapeutic option for late stage *T. b. rhodesiense* infections with accumulations across the blood-brain barrier reaching 1-2% of peak plasma levels.⁵⁴ The compound acts as a pro-drug in which the active trivalent arsenic moiety is protected with 2, 3-dimercaptopropanol. Once injected it is rapidly converted into melarsen oxide and binds reversibly to serum proteins.⁵⁵ The metabolite is then rapidly eliminated from plasma with a half-life of 3.9 hours.⁵⁶ After transport into the trypanosomal cell, the drug, like the previous two, is likely to be acting through a wide range of mechanisms. Trivalent arsenic compounds are known to be promiscuous inhibitors and could conceivably be inhibiting a variety of cellular targets. The drug acts quickly, causing rapid lysis of trypanosomes following

exposure.⁵⁷ A small percentage of patients (5-10%) have relapsed following treatment for unknown reasons. In some regions this number increases to 30%, suggesting that resistance may eventually become limiting for this compound.^{58, 59}

The final and most recently developed drug in use versus HAT is eflornithine (diflouromethylornithine, DFMO), a selective inhibitor of ornithine decarboxylase (ODC). This compound is also effective in late stage disease, but only versus *T. b. gambiense* infections. It is the only HAT chemotherapeutic agent with a well defined mode of action, acting as an irreversible suicide inhibitor of ODC. Although it inhibits the human homologue with similar potency to the trypanosomal enzyme, eflornithine is relatively non-toxic due to a difference in turn-over rate between the mammalian and parasitic enzymes.⁶⁰ In addition to this difference, the mammalian polyamine pathway is substantially more robust than that of the trypanosome, meaning it is much less susceptible to chemotherapeutic perturbation.^{61, 62} As a result of both of these, eflornithine is relatively non-toxic with typical dosing at 400 mg/kg in four daily infusions over 2 hours for 7 or 14 days.⁴³ However, such dosing schedules makes the drug both expensive and difficult to use in the field. Eflornithine decreases polyamine levels in trypanosomes, resulting in a range of downstream effects including a general decrease in DNA, RNA and protein synthesis, preventing the synthesis of new surface glycoprotein and morphological and biochemical changes similar to those observed during transition to the non-dividing short stumpy form.⁴³ In cell culture, treatment with eflornithine results in cytostasis, while patients with intact immune systems the trypanosomes are rapidly cleared from the blood.⁴³

Two agents are currently undergoing (or have recently undergone) clinical trials for use versus *T. brucei* infections. The first of these is pafuramidine (DB289) a bioavailable analogue of pentamidine which is able to cross the blood-brain barrier.⁶³ (Fig 1.1) This compound has showed efficacy in murine models and has passed phase I trials in humans.^{63, 64} However, this compound has recently been removed from the clinic due to renal toxicity issues in the Phase II clinical trial. The second agent in clinical trials is nifurtimox, an agent used in the treatment of Chagas' disease. This compound is in phase II and III studies in combination with eflornithine, though early results indicate that toxicity will be problematic. Several of the trials were terminated prior to completion due to biochemical and hematological adverse events.⁶⁵ However, with different dosing schedules designed to minimize toxicity, it is possible that this compound will prove useful in the treatment of HAT.

1.6 Parasite Biology

Trypanosoma brucei belongs to a class of ancient eukaryotic flagellated single celled organisms known as the kinetoplastids and characterized by the presence of a single large mitochondria known as the kinetoplast. There are five major groups within the kinetoplastids, prokintoplastina, neobodonida, parabondonida, eubodonidia and trypanosomatida. Within the larger kinetoplastid group it appears that parasitism has evolved several times since each parasitic clade is closely related to a free-living organism.⁶⁶ As a whole kinetoplastids are most closely related to euglenoids with these two groups representing a unique branch separating them from two other related groups

of protozoa, the heterolobosid amoeboflagellates and small free-living bacterivorous flagellates known as jakobids.⁶⁷ The trypanosomatids are a large monophyletic group composed entirely of parasitic or symbiotic organisms infecting a wide range of animal hosts.⁶⁶ It has been hypothesized that *T. brucei* diverged from the American *T. cruzi* approximately 100 million years ago meaning that they have co-evolved with humans.⁶⁸ Most recent evidence supports the idea that the parasite originally infected biting insects and later adapted to life within the mammalian hosts giving rise to the two phase life cycle described below.⁶⁶ Seven species of tsetse fly (*Glossina spp*) are able to serve as vectors for *T. brucei*.⁶⁹

1.6.1 Life Cycle of *T. brucei*

T. brucei possesses a two stage lifecycle in which it passes from an infected fly into a mammalian host. (**Fig 1.2**) The process begins when a fly bites a host infected with *T. brucei*, taking up non-replicating short stumpy bloodstream form parasites pre-adapted to life in the insect. These parasites move to the fly midgut where they differentiate into the procyclic stage. The variant surface glycoprotein (VSG) coat which aids in evasion of the mammalian immune systems is replaced with a procyclin coat and the parasites undergo several morphological changes including loss of the flagella and repositioning of the kinetoplast. Eventually the procyclic parasites migrate to the salivary glands and differentiate into epimastigotes. At this point it is thought that the parasites undergo sexual reproduction prior to attaching to the gland walls.^{70, 71} The attached epimastigotes then undergo further replication prior to differentiating into metacyclic parasites. Metacyclic trypanosomes possess VSG coats and are pre-adapted for life in mammalian

systems. When the fly bites a suitable host, parasites in the salivary gland multiply at the site of the bite, resulting in a trypanosomal chancre. The parasites pass through the lymphatic system and into the bloodstream where they multiply as long slender bloodstream forms. During this time mitochondrial function is minimized and the parasite relies on glycolysis for energy production. Eventually these long slender parasites upregulate mitochondrial function and differentiate to the short stumpy form enabling another round of infection to take place.

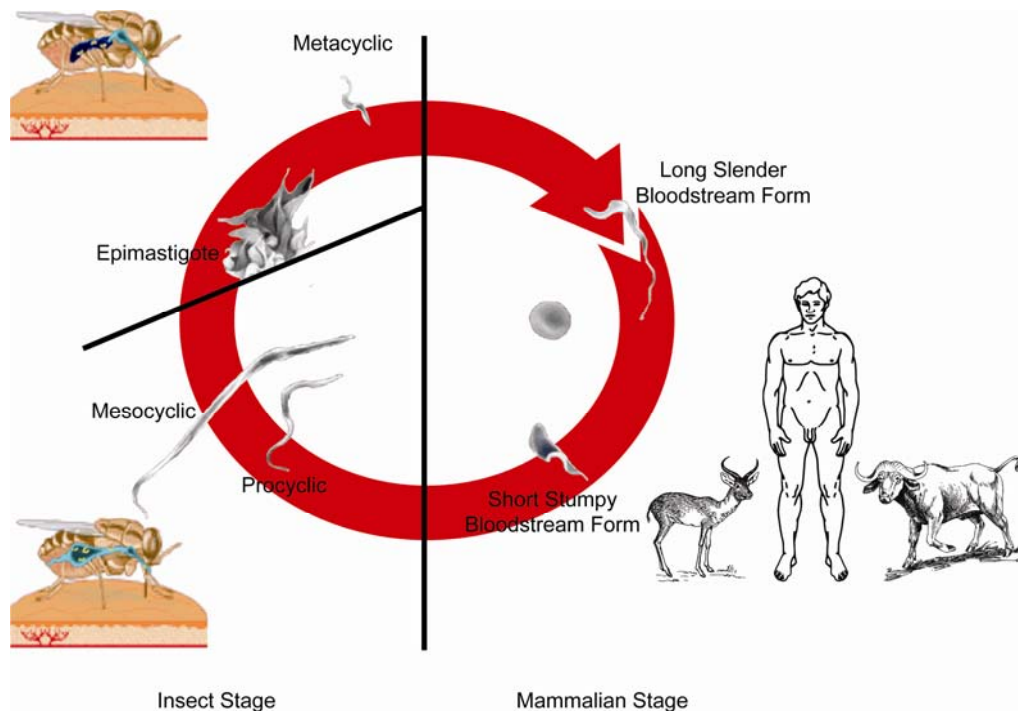


Fig 1.3 – The *T. brucei* Lifecycle

1.6.2 Antigenic Variation and the Variant Surface Glycoprotein Coat

As mentioned above, *T. brucei* is coated in a homogeneous protein coat while in the mammalian host. This coat is composed of a heterodimeric glycoprotein which covers

virtually the entire surface of the parasite with 10^7 copies per cell.⁷² Although each cell expresses only a single VSG, there are hundreds of active variants in the genome and over one thousand varied silent copies which can be activated.⁷³ The regulation of this process is highly complex and involves both recombination and transcriptional elements.⁷⁴ In a typical infection, several VSG variants will be expressed within the population, but one will dominate. The host immune system will respond to the dominant VSG, clearing the majority of the population, but leaving those cells expressing a different variant. This sub-population will then expand and multiply unopposed until the immune system recognizes and responds to the new VSG. This results in chronic infections following a characteristic sinusoidal pattern as the host responds to each epitope as it is presented. (Fig 1.4)

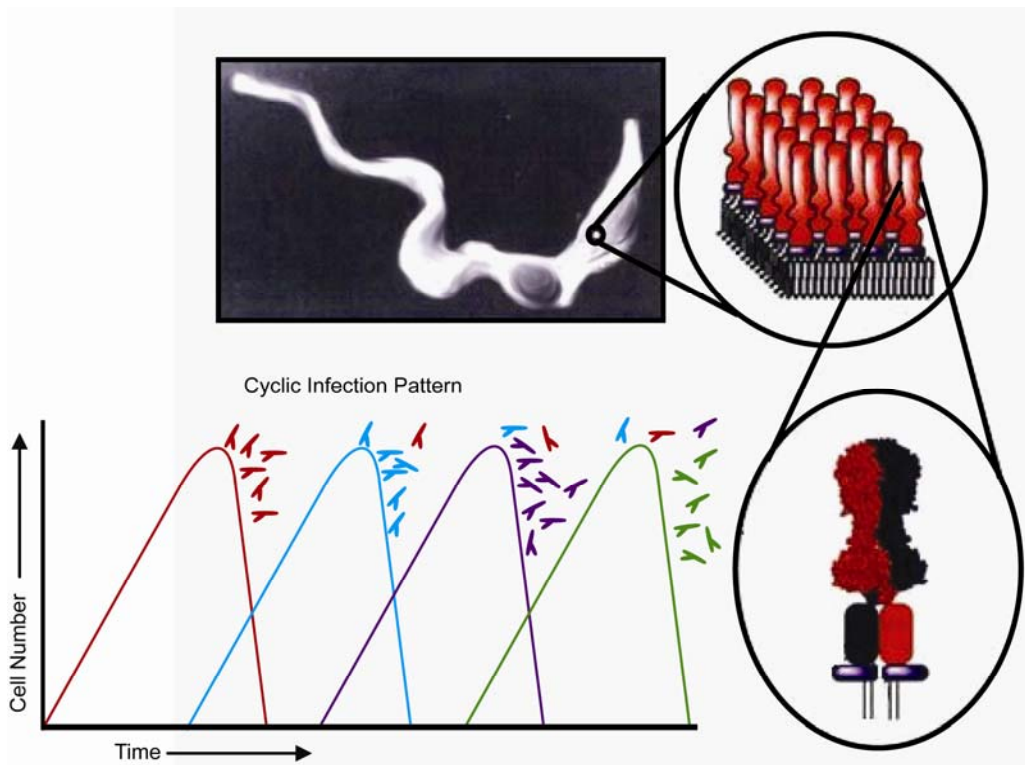


Fig 1.4 – The variant surface glycoprotein (VSG) coat and resultant chronic infection

The combination of the homogeneous coat coupled with rapid antigenic variation within infections means that vaccine development for *T. brucei* will be extremely difficult if not impossible. As a result it is likely that treatment of HAT will rely on traditional chemotherapeutic approaches for the foreseeable future. Drug discovery efforts have increased in recent years as increased knowledge of trypanosomal biology has yielded new potential targets.

1.7 Modern Drug Discovery Methodology

Before discussing modern drug discovery efforts in *T. brucei* specifically, it behooves us to examine the methodologies which are commonly employed today to discover novel therapeutic agents. The human practice of using specific agents for their therapeutic benefits can be traced back for as long as there have been written records, and possibly even before.^{75, 76} Discovery of biologically active substances was and continues to be a largely empirical process. The basic approach involves the collection of potential therapeutic material, testing of the material and observation of the results. In ancient times, testing was often performed directly on human patients and results were typically either the death of the patient or the elimination of the malady. This approach was limited both by the relative difficulty of obtaining test material and in obtaining test subjects, resulting in a slow and poorly replicable process. Progress in biological sciences eventually yielded animal disease models followed by cellular and biochemical models which were easier to test and alleviated the need for willing (or not-so willing) human volunteers. At this point the bottle-neck in drug discovery was often the sourcing of new

test material. Synthetic and analytical chemistry were still relatively nascent fields, and the production of test compounds was a slow and labor intensive process.⁷⁷

More recently, the advent of automation technology has allowed many of these processes to be streamlined, leading to the development of so-called high throughput technologies. These are typically based on performing both chemical and biological experiments in multi-welled microplates, resulting in the ability to synthesize and test thousands of compounds in days rather than months or years. These technologies have made testing of libraries of hundreds of thousands or even millions of compounds a relatively common occurrence in the modern pharmaceutical industry. With the ability to rapidly test a wide range of potential therapeutic agents in a large number of assay systems, the focus of many drug design efforts has shifted to target selection, assay validation and informatics technologies designed to aid in choosing the one or two agents which will prove successful from the milieu of possibilities.

1.7.1 Drug Target Validation

Biological target selection typically begins with efforts to identify homologues of proteins known to be important in other systems. This is generally accomplished by computational BLAST searches of the genome of interest. The optimal result of this process in the effort to select anti-parasitic targets is the discovery of pathways known to be vital in bacterial or plant cells, but which are not present in mammalian cells. Once putative sequences have been identified, efforts to clone and characterize the activity (particularly for enzymatic targets) are undertaken. Genetic knockouts or knockdowns via

RNAi are often performed at this point as well in order to establish the essentiality of the gene product. Non-selective inhibitors of specific target classes are also often used to help provide validation for specific approaches to chemotherapeutic development. Further validation can be accomplished by showing that a particular cellular phenotype can be rescued by addition of the enzymatic product (in the case of enzymatic target) or by over expression of the gene of interest (in the case of other targets). If a target passes these tests, it is often considered biologically validated and is turned over to medicinal chemists for inhibitor development.

The first step in chemically validating a target is often an assessment of its “drugability”, the ability of the target to bind and be inhibited by small, drug-like molecules. Many times this can be evaluated by examining the normal ligands which bind to the target. For example kinases bind adenosine-like molecules, which are relatively drug-like heterocyclic compounds easily modified by medicinal chemists. Other times, especially in cases where normal binding partners are large proteins or non-drug-like molecules, chemical validation requires testing large libraries of potential inhibitors. This can be accomplished using computational DOCKing methods (if sufficient known inhibitors exist to validate the computational model being used) or high-throughput screening approaches. Assuming that one of these proves successful, the molecular scaffolds identified as potential inhibitors can be optimized using medicinal chemistry approaches. During this process the activities of the small molecules being developed are tracked, typically both in biochemical and whole cell assays. Selectivity of the inhibitors for parasitic proteins versus their mammalian homologues is also typically addressed at this point. This is particularly important for highly conserved targets. Target

validation is further confirmed during this by establishing correlative relationships between biochemical activities and whole cell phenotypes. Other assays may be used to aid in this process including synergy studies with well characterized compounds, secondary assays in knock-out or over-expressing cell lines etc.. Assuming a target is well behaved with respect to all of these criteria, drug development of specifically targeted inhibitors can proceed.

1.7.2 Assay Validation for High Throughput Screening

Once a biological target has been selected, an appropriate high-throughput compatible assay must be designed and validated. The application of high-throughput technologies to the drug discovery process is often a costly process. A typical high-throughput screening (HTS) effort of a 350,000 member compound library can cost upwards of \$25,000 in reagents alone. Furthermore, the results of the initial testing can often focus the efforts of multiple groups for several years after the actual experiment. This is because a large number of potential compounds are typically identified in the primary screen which must then be validated using a range of much slower and more costly experiments. As a result of this, it is important for the initial assay used in the discovery process to be highly validated.

In most cases the target validation steps include the development of biochemical or cellular assays for the biological process of interest. However, these assays are generally performed in low-throughput formats (such as cuvettes or large cell culture dishes), or using methodologies which are not easily adapted to high-throughput

applications (such as gel-shift binding assays). Therefore, the initial step of assay validation is the transfer of these low-throughput assays to microplates or the design of novel, automation friendly techniques (for example, a fluorescence resonance transfer (FRET) based or fluorescence polarization (FP) assay in place of a gel-shift approach). Typically these techniques are based on homogeneous liquid phase experiments requiring a minimal number of additions or wash steps and having simple fluorescence, luminescence or absorbance based readouts which can be measured using standard microplate readers. Once this has been accomplished the plate based assay is used to replicate any characteristic low-throughput data which has been collected. (for example replicating K_m values for enzymes, K_i values for known inhibitors, K_d values for binding probes etc..)

If the plate-based assay is able to replicate the low-throughput results acceptably, further criteria are applied. The first of these is an assessment of the signal stability and magnitude. The typical statistical measurements of these used in HTS are Z-factor and Z-prime. The equations for both of these (see below) are highly similar. Both of these are

$$Z' = 1 - \frac{3(\sigma_{\text{pos}} + \sigma_{\text{neg}})}{(\mu_{\text{neg}} - \mu_{\text{pos}})}$$

Equation 1.1

$$Z = 1 - \frac{3(\sigma_{\text{pos}} + \sigma_{\text{variable}})}{(\mu_{\text{variable}} - \mu_{\text{pos}})}$$

Equation 1.2

σ_{pos} = standard deviation of positive controls
 σ_{neg} = standard deviation of negative controls
 σ_{variable} = standard deviation of all variable compounds
 μ_{pos} = mean of positive control signal
 μ_{neg} = mean of negative control signal
 μ_{variable} = mean of all variable compound signals

calculated on a per plate basis, and provide a quantitative measurement of the separation between the positive and negative control groups. Generally values of greater than 0.5 are considered acceptable in HTS applications, though any positive value reflects the ability to discriminate between positive and negative controls. If an HTS assay is shown to be acceptable in this respect, it is put through final validation steps in which the instrument set to be used during screening is used to run several control plates incorporating a range of signal levels (at minimum high, mid and low signal populations) across the full plate. This is then repeated over several days using several batches of reagents. The results of these experiments are evaluated for variation, either as a function of position on the plate (typically referred to as drift) or as a function of reagent batch. Typically signal variations of less than 15% are considered acceptable.

The final, and perhaps most important, step in validation of a high-throughput assay is typically referred to as the scaling screen. Most institutions have a smaller set of compounds used to assess the behavior of assays when exposed to a wide range of variable compounds. This is important since many assays are sensitive in ways which are difficult to predict a-priori. Generally the scaling screen will consist of anywhere from 5,000 to 30,000 compounds tested in the same manner as the eventual full-collection screen. Hits identified in this effort are then subjected to a panel of orthogonal secondary assays designed to determine if the compounds are indeed having the effect of interest. The results of these can be used to determine which compounds are the “true” hits and which are false positives. Using this data set, it is then possible to utilize other statistical tests, such as the receiver-operator characteristic (ROC plots) to ensure that the primary assay results are indeed predictive of the desired outcome. It should be noted that the

most important part of this is the use of orthogonal secondary assays. Simply verifying that compounds produce dose dependent effects in the primary assay system is insufficient for the determination of true hits versus false positives. A wide range of artifactual effects are capable of producing reproducible dose dependent effects in various systems, and it is important to evaluate the robustness of the assay with respect to these.⁷⁸⁻⁸¹ The hits identified in these early studies do not have to be potential drug leads. Rather, the emphasis should be placed on whether or not the generally desired effects are being observed. For example, is the enzyme being inhibited by the compound (the desired effect), or is the compound reducing the enzymatic substrate in a totally enzyme independent fashion? (a reproducible and misleading false positive result) Assuming the assay performs in a satisfactory manner in all of the above tests, high-throughput screening can proceed with the knowledge that if there are true positives in the test library, the primary assay is likely to detect them.

1.7.3 Library Selection

After the target has been chosen, and the assay validated, the sample library which will be tested must be selected. In the past, this has often meant simply testing everything available, an approach typically known as a full-deck screen. This can be appropriate in situations where little is known about potential inhibitors of a given process. In these cases, simply testing as many potential samples as possible will theoretically guarantee that if an active compound is in the library to begin with, it will be detected. However, as sample collections continue to grow it has become highly desirable

to minimize the number of compounds which must be tested in order to identify those of interest.

Several approaches have been applied to this problem. The first of these is pooled screening.⁸² This approach was a direct result of both the classical drug discovery practice of testing crude natural product extracts as well as the more recent advent of combinatorial chemistry, a process in which test chemicals are synthesized in large mixed batches and tested without further purification. This approach has largely been abandoned in the modern laboratory due to the difficulty in deconvoluting the source of the observed activities. Compounds in large mixtures often behave differently than they do as single agents and both false negatives and false positive signals plague pooled screening approaches as a result.^{82, 83} Due to this, most sample libraries are now tested as single agents.

The second methodology which is widely used to select screening libraries is commonly known as focused screening. This approach uses *a priori* knowledge about a target to bias the set of compounds tested. For example, if the target is a kinase, libraries composed of scaffolds known to be active versus kinases can be screened. Other approaches to generating focused libraries include virtual screening, in which compounds are DOCKed with the target using molecular modeling techniques. This requires significant *a priori* knowledge including a structure of the target as well as a set of compounds known to bind (preferably with known binding modes) with which to validate the computational model. However, if this data set is available, this approach can be quite effective and reduce the number of compounds to be tested from hundreds of thousands to a few hundred or even less.⁸⁴⁻⁸⁶

In the absence of significant amounts of *a priori* knowledge, the size of the library to be screened can also be decreased using a technique known as diversity analysis. The approach attempts to quantitatively describe a library using sets of molecular descriptors, group similar molecules together and then select representative compounds from each group.⁸⁷ Descriptors can include physiochemical properties, topological indices and molecular fingerprints derived from 2D connection tables or 3D conformations.⁸⁸ By only testing a small number of each molecular type, the size of any given library can be minimized, while the chemical space covered by said library can be maximized, theoretically improving the chances that an active scaffold type will be discovered in any given screening effort. It should be noted however, that it is common for small structural changes in a molecule (which may not be captured by typical molecular descriptors) can result in drastic shifts in observed activities.⁸⁹ Therefore, this approach may result in missing active compounds which would have been detected had a more thorough full-deck approach been used. However, this technique is often used to aid in guiding the efforts of chemists when expanding test libraries, either to ensure that new compounds are significantly different from those already in the collection, or conversely, that they match the characteristics of some desirable population (for example, orally bioavailable drugs).

1.7.4 Automation Considerations

Modern high throughput screening is generally carried out using some level of automation to perform the majority of the tasks. Some systems (including those at St.

Jude Children's Research Hospital, **Fig 1.5**) are fully automated, with no operator input required after reagents and supplies are loaded onto the system. These systems are typically one-of-a kind sets of instrumentation tailored to the needs of the particular screening group. As such, it often falls to the screener to perform many of the validation experiments necessary to ensure proper replicable behavior during the screening process.



Fig 1.5 The automated high-throughput screening deck at St. Jude Children's Research Hospital.

Almost all fully automated systems fulfill the same basic functions – bulk liquid additions of assay reagents, nano-scale liquid transfer of test compound, incubation of test mixtures and reading of assay output (typically light-based formats, either fluorescence, luminescence or absorbance). Generally, these functions are performed by separate instruments serviced by a robot capable of moving test microplates from one to the next. Each must be optimized using solutions with compositions as close as possible

to those which will be used in the actual screening run. For example, high-salt solutions can be problematic for bulk-liquid dispensing instrumentation over the course of a screening run, since evaporation can result in salt-buildup on the dispenser tips causing highly inaccurate performance. Other common problems are cross contamination caused by reusable tips or pins used for transfer of test compounds, assay temperature dependence, which can result in signal drift as the screening deck warms due to high levels of instrument activity and “traffic-jams” caused by improper optimization of plate transfer robots and algorithms. It is vital that several dry runs (test screening runs without liquid) as well as several wet-runs (test screening runs using simulated assay material) be performed prior to committing to the actual screening effort. These test runs should be as large as a typical single screening batch will be during the true HTS process. This will allow the operator to detect and correct any potential problems before the actual assay materials (which are often expensive or time consuming to replace) are loaded onto the system. Once the screening system has been shown to perform satisfactorily, the actual screen can proceed and data can be collected.

1.7.6 Data Analysis in High Throughput Screening – Picking Hits

After the actual screening process is finished, the new data set must be analyzed and potentially active compounds selected for further analysis. The first step in this process is to determine if the raw assay signal should be transformed or not. Most statistical methods for variance analysis assume that the populations to be examined exist in linear space. Therefore, if the assay readout is not linear in nature, it should be

transformed so that is. The best example of this is cell growth assays, which are logarithmic in nature. The raw assay signals from these types of experiments should be log-transformed prior to further analysis.

Once the data is in linear space, the behavior of the assay signal from the control groups can be evaluated. This is often done using normal statistical methods, such as calculating the mean and standard deviations for each population. “Hit” compounds are then selected using fairly simplistic criteria (for example, requiring that a the signal for a variable compound be three standard deviations away from the negative control population to be considered a hit) However, classical statistical methods are based on the assumption that the populations being considered follow normal or Gaussian distributions and are highly susceptible to the effects of outliers. In high throughput screening, populations are not necessarily well behaved Gaussian curves. Furthermore, outliers resulting from stochastic errors intrinsic to large scale automated processes are relatively common.

In order to combat the effects of these, robust statistical methods are often used in place of classical approaches.⁹⁰ These methods do not assume normal distributions and are resistant to outlier effects by virtue of the fact that the population extremes are removed from consideration prior to calculation of the mean or standard deviations. The robust mean is known as the 25% trimmed mean and is calculated by ordering the data points and calculating the average based on the central 50% of the data. The robust standard deviation is the scaled fourth spread and is calculated by ordering the data points, computing the difference between the third quartile and first quartile and dividing by a scaling factor (typically 1.349, a value selected so that this method matches the

classical result when applied to normally distributed populations). Finally, the robust method for determining statistically significant outliers from any population is the upper fourth plus 1.5 times the inter-quartile spread. It is calculated by multiplying 1.5 by the inter-quartile spread and adding this to third quartile to determine the upper outlier threshold, or subtracting this value from the first quartile to determine the lower outlier threshold. While this method is more resistant to outlier effects and can result in improved data quality, it also requires larger control populations (a minimum of 8 members for robust methods versus 3 for classical methods)

Once the behavior of the control groups has been modeled and the variable compounds which differ significantly from the negative control population have been identified (the minimum requirement to be designated a “hit” compound) further requirements to be a “hit” can be applied. These requirements are determined largely by the number of samples which can be reasonably subjected to the secondary assay panel and the number of preliminary hits resulting from the high-throughput screen. At this point, the experimental design of the screen becomes important. If, as in many cases, the variable samples were tested once at a single concentration, a simple “percent-activity” cut-off may be applied to reduce the number of compounds selected for follow-up experiments. To accomplish this, the raw assay signals are normalized to the positive and negative control populations, resulting in a percent-activity score which can then be used to rank-order hit compound from across the screen. The level at which the hit threshold is set is best determined by examining the results of the ROC analysis which should have been performed during the assay validation procedure. The ROC results can help focus attention on the section of the primary assay readout most likely to contain promising

hits. For example, it is often the case that the top 10% of the compounds (90-100% or greater activity) contains a large number of hits which are interfering with the assay in a non-specific manner. A properly designed ROC experiment will also allow a lower threshold to be determined below which the number of true positive compounds is likely to be small. Once these thresholds are determined, hit compounds can be subjected to orthogonal secondary assays designed to rapidly eliminate false positives.

It should be noted that an increasing number of high throughput screening efforts are no longer screening compounds in single concentration (a so-called single point assay). Rather, an approach known as quantitative high-throughput screening is gaining in popularity, largely as a result of further miniaturization of assay formats and specifically the advent of 1536-well screening.⁹¹ In this approach, compounds are tested in dilution series designed to detect concentration dependent effects. With these methods, outlier determination is no longer used for identification of hits. Rather, the normalized data for each compound dilution series is fit to a four parameter sigmoidal curve and the parameters from that fit are used to identify hits. Typically hits are those which have both lower and upper plateaus defined by at least two data points each as well as significant separation between those plateaus (generally at least 30% activity). Rank ordering hits from these types of screens is much easier than it the case of single point assays since actual IC_{50} values are determined for each test compound. However, this approach is still subject to all the requirements of a single point assay, and use of ROC analysis during assay validation is still vital for the selection of appropriate assays to be used in screening efforts.

1.8 Potential Targets for Chemotherapeutic Intervention

In the post genomics era, knowledge of trypanosomal biology has expanded rapidly. Tools such as RNAi have allowed rapid identification of critical cellular processes that offer potential points of chemotherapeutic intervention. However, despite the increase in biological knowledge, no new specifically targeted inhibitors have been approved for use in HAT therapeutics. This can be attributed in part to a breakdown in communication between the biologists responsible for initial target identification and characterization and the medicinal chemists responsible for developing inhibitors of the proposed targets. Lack of interest in *T. brucei* by the pharmaceutical industry and a paucity of funding are the other major issues.

There are currently over 18,000 protein coding genes known in *T. brucei*. Of these, 21% are specific to the parasite with no clear mammalian homologues. Only 5% of these genes have had their function characterized, with another 38% having putative functions inferred from sequence homology.⁹² It is clear that there are a large number of potential targets which must be validated. It should be noted that the idea of developing selective targeted inhibitors has been criticized, since many existing drugs actually target a wide range of cellular functions.⁹³ Despite this, targeted therapeutics remains the dominant paradigm in drug discovery. Only a relatively small number of pathways in *T. brucei* have been sufficiently characterized to justify medicinal chemistry efforts. These include the glycolytic pathway, various cysteine proteases, the topoisomerases, folate metabolism, oxidative stress management, and the polyamine metabolic pathway.

1.8.1 The Glycolytic Pathway

Bloodstream forms of *T. brucei* lack functional mitochondria. As a result, they are entirely dependent on glycolysis for energy production while in mammalian hosts.^{94, 95} Although the hosts also possess the glycolytic pathway, *T. brucei* has evolved a special organelle in which glycolysis takes place. This organelle, known as the glycosome, contains the first seven enzymes of the glycolytic pathway and separates them from the cytosol where they are normally found. The compartmentalization allows *T. brucei* to perform glycolysis at a much higher rate than would normally be expected.^{96, 97} Significant differences exist in the regulation and structure of this pathway between trypanosomes and their mammalian hosts.⁹⁸ This, coupled with the complete dependence of the parasite upon glycolysis for energy during mammalian infections has resulted in significant efforts to develop inhibitors of almost all stages of the pathway.⁹⁸

Particular attention has been paid to hexokinase,⁹⁹⁻¹⁰¹ phosphofructokinase¹⁰²⁻¹⁰⁴, fructose-1,6-bisphosphate aldolase¹⁰⁵, glyceraldehyde-3-phosphate dehydrogenase,^{103, 106-114} phosphoglycerate kinase^{101, 103, 115-117} and pyruvate kinase.^{102, 103} Structures are available for phosphofructokinase,¹¹⁸ glyceraldehyde-3-phosphate dehydrogenase,¹¹⁹⁻¹²¹ phosphoglycerate kinase,¹²² and pyruvate kinase,¹²³ raising the possibility of structure based drug design efforts for these enzymes. Despite the large amount of effort devoted to the development of selective inhibitors, compounds with acceptable potencies versus either the biochemical targets or whole cell parasites have been illusive thus far. Work is continuing in this area, and it remains to be seen if successful therapeutic agents targeting this pathway can be discovered.

1.8.2 The Topoisomerases

T. brucei possesses a single type IB topoisomerase as well as three distinct type II topoisomerases, two found in the nucleus and one active in the mitochondria.¹²⁴⁻¹²⁶ These enzymes are responsible for catalyzing DNA topological interconversions by making either single (Type IB) or double (Type II) stranded breaks in the DNA substrate, passing a new DNA segment through the break and then ligating the break. The trypanosomal type IB enzyme is composed of two subunits, a DNA binding domain and a catalytic domain.¹²⁷ RNAi experiments have shown that both are necessary for cellular growth.¹²⁴ Similar experiments examining the roles of the topoisomerase II enzymes showed that the mitochondrial enzyme (TbTOP2mt) as well as one of the nuclear enzymes (TbTOP2 α) are also necessary for growth.^{125, 126} Knockdown of the second nuclear enzyme (TbTOP2 β) did not result in any detectable phenotype in bloodstream *T. brucei*.

A wide range of topoisomerase inhibitors are available, primarily as a result of development as cancer chemotherapies and antibiotic agents. A suite of these inhibitors has been screened versus whole *T. brucei* with potencies ranging down to single digit nanomolar levels.¹²⁸ Camptothecin, a well characterized Topo I inhibitor, as well as analogues thereof, have shown promising activities in whole parasite assays, with potencies down to 70 nM.^{129, 130} Further chemical validation of these targets has been accomplished by showing that existing anti-trypanosomal drugs promote the accumulation of double-strand DNA breaks and that these breaks are linked with topo II enzymes. This is characteristic of topoisomerase poisons and suggests that inhibition of

these enzymes may explain at least part of the activities of several of the anti-trypanosomal drug classes.⁵¹

Although little work has been done to develop inhibitors specific for the trypanosomal enzymes, the relatively low homology (~50%) to the human homologues suggests that this may be possible.¹³¹ Several groups have synthesized analogue series of known topoisomerase inhibitors and assayed them versus whole cell trypanosomes, but no efforts have been made to screen the trypanosomal enzymes themselves.¹³²⁻¹³⁴ No structures are available for the parasitic enzymes, which complicates structure based drug design efforts. High throughput assays suitable for testing large numbers of compounds as topoisomerase inhibitors do exist.¹³⁵ However, the cloning and characterization of trypanosomal topoisomerases has not yet been reported, which complicates *in vitro* biochemical assessment of potential inhibitors. Despite this, the use of existing topoisomerase inhibitor scaffolds has so far proved extremely promising both *in vitro* and in preliminary animal infection models.¹³⁴

1.8.3 Folate Metabolism

The folate metabolic pathway has produced several clinical drug targets in many different systems, ranging from cancer to antibiotic agents.¹³⁶⁻¹³⁸ In particular, the thymidylate synthase (TS) and dihydrofolate reductase (DHFR) enzymes have proved to be useful targets. In *T. brucei*, these are linked together in a single bi-functional protein (DHFR-TS). This enzyme has been cloned and early biochemical analysis indicated that selective inhibition of this target versus its human homologue would not be

problematic.¹³⁹ Both single and dual knockouts of DHFR-TS established that it is necessary for cellular growth, and studies of knockout sensitivity to known DHFR inhibitors established that the compounds were in fact acting through DHFR-TS inhibition.¹⁴⁰ Computational models of the *T. brucei* enzyme based upon the crystal structure of the *Leishmania major* DHFR have highlighted residues likely to be important for the development of selective inhibitors.¹⁴¹

Efforts to develop inhibitors of the parasitic enzyme have focused primarily on dihydrofolate mimetics. The 2,4-diaminoquinoxaline scaffold has been used to produce compounds with potencies in the low nanomolar range versus whole cell parasites and displaying up to 50-fold selectivity for the parasitic enzyme.¹⁴² A second scaffold which has been used successfully to develop parasite selective inhibitors is 2,4-diaminopyrimidine. This scaffold resulted in compounds with low nanomolar potencies versus the enzyme, and low micromolar potencies versus whole cell parasites.^{143, 144} In addition, compounds based on this scaffold have shown some *in vivo* efficacy in rat models of *T. brucei* infection, though they are not curative.¹⁴³

A second folate metabolic enzyme which has attracted attention as a potential drug target is pteridine reductase. Knockdowns of the enzyme suggest that it is a vital enzyme, and efforts to develop inhibitors are underway. The protein has been expressed and both a crystal structure and an assay suitable for high-throughput screening are available making this target highly amenable to drug discovery efforts.^{145, 146} This data has been used to conduct fragment based DOCKing on the target, resulting in 7 nM inhibitors.¹⁴⁷ However, these compounds are less active versus whole cell parasites (10 μ M EC₅₀ values). It should be noted that drug discovery efforts versus this target are still

quite nascent, and it is possible that improved whole cell potencies will be possible to achieve.

1.8.4 Oxidative Stress Management

Management of intracellular oxidative potential is essential in all living cells. Most accomplish this task by utilizing the glutathione and glutathione reductase system.¹⁴⁸ However, the trypanosomatids utilize a modified version of this pathway in which two molecules of glutathione are reacted with the polyamine spermidine to produce a unique dimeric molecule known as trypanothione (N1,N8-bis-glutathionylspermidine).¹⁴⁹ This is then used as the reductant in a wide range of cellular processes.¹⁵⁰ Three key enzymes are used in the trypanothione pathway, γ -glutamylcysteine synthetase (γ -GCS), which catalyzes the first committed step in the biosynthesis of trypanothione, trypanothione synthase (TS), which is responsible for coupling the glutathione molecules to spermidine and trypanothione reductase (TR), which regenerates the reduced form of trypanothione after it has been oxidized.^{151, 152} A range of trypanothione dependant oxidases also rely upon this pathway in order to eliminate reactive oxygen species from the parasite.¹⁵⁰ Given the uniqueness of this pathway, it is hardly surprising that it has been heavily investigated as potential point of chemotherapeutic intervention.¹⁵³

γ -GCS has been validated both chemically and genetically in animal models of infections.^{154, 155} However, most recent work has focused on TS and TR. TR has been validated both biologically (*in vitro* and *in vivo*) and chemically (*in vitro* only).^{156, 157}

While many potent TR inhibitors have been synthesized which are highly active in whole cell assays, *in vivo* efficacy has proven difficult to achieve.¹⁵⁷⁻¹⁶⁸ Several groups have also reported the use of high-throughput screening methods to discover novel inhibitors of TR.¹⁶⁹⁻¹⁷¹ The structures of several trypanosomal TR enzymes are available for use in structure based drug design programs.¹⁷² *T. brucei* TS has been validated *in vitro* and *in vivo* biologically and *in vitro* chemically.¹⁷³⁻¹⁷⁵ Knockdown experiments have been performed on several of the trypanothione dependent peroxidases showing that they are vital for parasitic growth, though no inhibition by small molecules has yet been reported.¹⁷⁶⁻¹⁸⁰ Despite these successes, small molecule inhibition of the trypanothione pathway has not yet resulted in compounds with *in vivo* efficacy, casting some doubt on its potential as a potential point for chemotherapeutic intervention.

1.8.5 Proteases

While many of the proteases in *T. brucei* have been examined as potential drug targets, including the proteasome¹⁸¹⁻¹⁸⁵ and various metalloproteases^{186, 187}, the cysteine proteases have proved to be the most promising. It is well established that peptidyl and non-peptidyl cysteine protease inhibitors are effective versus whole cell parasites.¹⁸⁸⁻¹⁹² Furthermore, these inhibitors have proven efficacious in mouse models of infection, validating the general target class *in vivo*.¹⁹³ The presumed target of these inhibitors was rhodesain (also known as brucipain and trypanopain), a cathepsin-L like lysosomal protease which accounts for most of the proteolytic activity in the parasite.^{194, 195} However, the correlation between rhodesain inhibition and whole cell activity of most protease

inhibitors was poor, casting some doubt on the hypothesis that this was the relevant target.^{189, 190, 196, 197} Subsequent searches of the *T. brucei* genome lead to the discovery of TbCatB, a cathepsin B like protease expressed at low levels in the lysosome.

RNAi studies of TbCatB showed it to be necessary for parasite survival while knockdown of rhodesain did not lead to significant growth changes *in vitro* (though it did slow *in vivo* disease progression).^{198, 199} As a result of these studies, potent and selective inhibitors of TbCatB were synthesized as shown to be highly effective versus whole cell *T. brucei*.^{200, 201} In particular, the purine-nitrile based inhibitors of TbCatB show promise as potential chemotherapeutic agents. They are relatively non-toxic, orally bioavailable and cross the blood-brain barrier.(Mallari, personal communication) Furthermore, preliminary results suggest that they will be highly efficacious in mouse models of infection.(Mallari and Guy, personal communication) Further work to improve pharmacokinetic parameters of these compounds, as well as the development of other inhibitor scaffolds is certainly justified.

1.8.6 Polyamine Biosynthesis

The only clinically validated molecular target for treatment of *T. brucei* infections is ornithine decarboxylase (ODC), which catalyzes the first step in polyamine metabolism, the decarboxylation of ornithine to produce putrescine(**Fig 1.5**). The polyamines putrescine, spermidine and spermine are known to be necessary for cellular replication.^{202, 203} Increases in polyamine concentration have also been linked to carcinogenesis, and a variety of cancers have been shown to possess high levels of

intracellular polyamines. As such, inhibitors of the polyamine biosynthetic pathway have been extensively investigated as potential chemotherapeutic and chemopreventative compounds. (Reviewed in ²⁰⁴)

In mammalian systems, ODC, one of two rate-limiting enzymes in the polyamine biosynthetic pathway, is tightly controlled via transcriptional, translational, and post-translational mechanisms.²⁰⁴⁻²⁰⁶ (**Fig 1.5a**) It is active as a homodimer and is dependent upon binding to pyridoxal-5'-phosphate (PLP), a cofactor shared with many other enzymes.²⁰⁷ The ODC protein has one of the shortest known half-lives (~10-20 minutes), which is primarily regulated by antizyme (AZ), a polyamine inducible protein inhibitor which binds to ODC monomers. This prevents the formation of the active dimer and targets ODC for degradation.²⁰⁸ Antizyme, which is regulated by antizyme inhibitor(AZIN), also inhibits uptake of exogenous polyamines.²⁰⁹ In mammalian cells, the levels of the polyamines are further regulated by inter-conversion of individual pools as well as by a highly efficient transport system allowing import and export of polyamines and intermediates.²¹⁰ This highly redundant regulatory pathway means that mammalian cells are strongly resistant to changes in polyamine levels. Despite this tight regulation, it has been shown that even temporary inhibition of ODC can result in prolonged depletion of putrescine.²¹¹

The first ODC inhibitor developed with efficacy in cells was α -methylornithine (MO), a weak reversible inhibitor of ornithine decarboxylase (ODC).^{203, 212} Other more potent ornithine analogues have been synthesized, but were competitive with PLP.^{213, 214} Some of these inhibitors showed promise in animal models, but were later abandoned due to poor selectivity over other PLP dependent enzymes.²¹⁵ In the presence of reversible

inhibitors, ODC activity increases due to both stabilization of the enzyme and stimulation of mRNA translation.^{211, 216, 217} Despite this, reversible inhibitors have been shown to deplete putrescine levels effectively in cellular models, even in the presence of a 6 to 7 fold increase in ODC activity.²¹¹

The field rapidly shifted focus to irreversible inhibitors that did not increase ODC activity.²¹¹ This effort led to the discovery of α -difluoromethylornithine (DFMO), a highly selective compound that alkylates C360, a catalytic residue in the ODC active site.^{218, 219} DFMO is orally available but rapidly cleared ($t_{1/2}$ 1.5 (intravenous dosing) to 4 (oral dosing) hours).²²⁰ It is relatively non-toxic and can be dosed to extremely high levels (up to 3.75 g/M²) with only minor side effects.²²¹ Despite this, DFMO has largely been abandoned as a single agent chemotherapeutic due to low efficacy, which has been largely attributed to the robustness of the mammalian polyamine pool. Recently interest has risen in the use of DFMO as a chemopreventative in combination with other agents.²²²⁻²²⁴

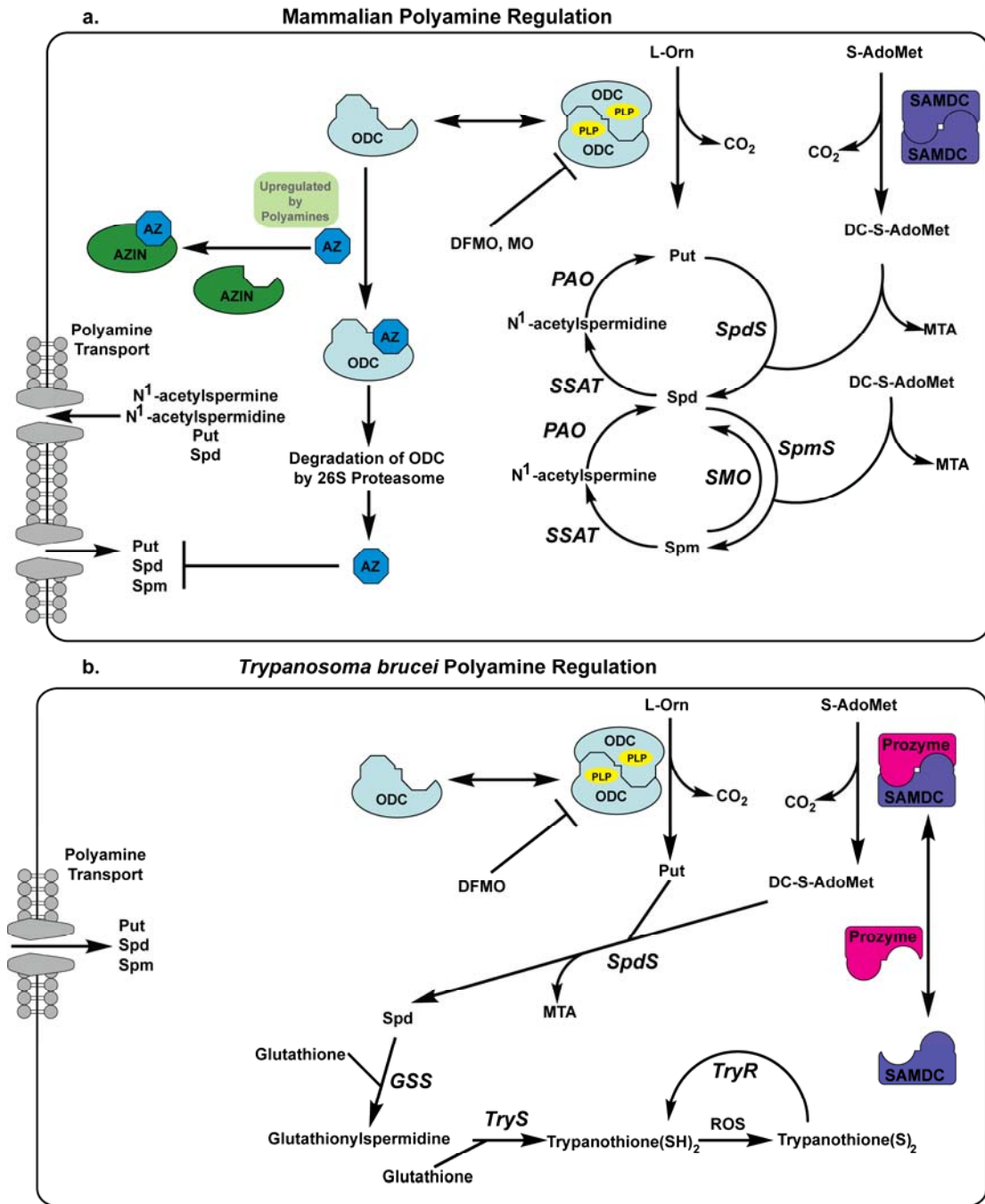


Fig 1.6 – The polyamine biosynthetic pathway in mammalian systems and in

T. brucei Extensive reviews of polyamine regulation in both systems can be found in:^{60, 210, 225, 226}

1.6a. *The mammalian polyamine regulatory pathway.* The mammalian polyamine regulatory pathway is highly regulated via transcriptional, translational and post-translational mechanisms. The rate limiting enzymes ODC and SAMDC have extremely short half-lives and are under strict control whereas the synthases SpdS and SpmS are constitutively expressed. The polyamine oxidases PAO and SMO along with the acetyl-transferase SSAT provide back conversion pathways between the three major polyamines. In addition, a highly efficient polyamine transport system aids in the maintenance of polyamine pools.

1.6b. The *Trypanosoma brucei* polyamine regulatory pathway. This pathway is much simpler than its mammalian counterpart. The rate limiting synthetic enzymes ODC and SAMDC have much longer half-lives. The main source of regulation in this pathway seems to be expression levels of prozyme, an inactive SAMDC homologue which binds to the SAMDC monomer, resulting in a 1200x active heterodimer. In addition, the end product of this pathway is trypanothione, a molecule implicated in management of oxidative stress. Though *T. brucei* is able to import exogenous polyamines, its transport system is not as efficient as the mammalian counterpart. *Universal abbreviations:* ornithine decarboxylase (ODC), pyridoxal-5'-phosphate (PLP), Sadenosylmethionine decarboxylase (SAMDC), S-adenosylmethionine (S-AdoMet), 5'-methylthioadenosine (MTA), decarboxylated S-adenosylmethionine (DC-S-AdoMet), putrescine (Put), spermidine (Spd), spermine (Spm), spermidine synthase (SpdS), spermidine/spermine N¹-acetyltransferase (SSAT), polyamine oxidase (PAO), spermine oxidase (SMO), antizyme (AZ), antizyme inhibitor (AZIN), α -methylornithine (MO), α -difluoromethylornithine (DFMO), glutathionyl spermidine synthase (GSS), TryS, trypanothione synthase, TryR, trypanothione reductase, ROS, reactive oxygen species.

In *T. brucei*, polyamine biosynthesis is much simpler. (**Fig 1.6b**) There are no inter-conversion pathways and transport of exogenous polyamines plays a lesser role.²²⁶ In addition *T. brucei* does not actively regulate ODC protein turnover.^{227, 228} Rather, the main source of polyamine regulation is the activation of S-adenosylmethionine decarboxylase (SAMDC) through binding to prozyme.²²⁹ Depletion of polyamines also reduces trypanothione, and has been shown to increase sensitivity to oxidative damage.²³⁰ DFMO has been used clinically to treat HAT by inhibition of polyamine biosynthesis. However, the poor pharmacokinetics of DFMO are a major limiting factor its use.²³¹ Furthermore, DFMO is only effective against one of two sub-species of *T. brucei* causing human disease.²³² As the parasite does not increase ODC levels in response to polyamine depletion, the development of potent reversible inhibitors may allow them to be used in a wider range of sub-species.²²⁶

To date, most discovery efforts directed towards ODC have been focused on analogues of ornithine (such as DFMO), putrescine, or PLP.²³³ None of these has proved as effective as DFMO for treatment of *T. brucei* infections. No large scale efforts to

discover novel inhibitors have been reported. The lack of prior high-throughput screening efforts directed at ODC is due in part to the difficulty in assaying its activity. Classical assay methods utilize capture of $^{14}\text{CO}_2$ from radiolabeled ornithine or derivatization of putrescine followed by HPLC analysis.^{234, 235} Neither of these techniques are tenable for a large scale inhibitor screening effort.

1.9 Project Goals

The main goal of this project was to expand the known inhibitor scaffolds able to act on *T. brucei* ODC. As the only clinically validated single molecular target for treatment of HAT, it is remarkable that the only known inhibitors remain simple product or substrate analogues, especially in light of the fact that this target was characterized over 30 years ago. In order to address this shortfall in the field, we set out to optimize a high-throughput assay and apply this assay to a library of 360,000 compounds. The hits from that assay were subjected to a rigorous set of secondary assays including assessment of mode of ODC inhibition, selectivity versus the human enzyme, analysis of potential binding sites and trypanocidal and general cytotoxicity for all compounds. This process has also involved the overall development of a high-throughput screening program at St. Jude Children's Research Hospital, where this project served as the first high-throughput effort for the new Chemical Biology and Therapeutics department. A side benefit of the high-throughput screening approach is the discovery of unexpected desirable compounds. During our high-throughput screening efforts, we also endeavored to pursue promising trypanocidal compounds, regardless of whether or not they inhibited ODC.

In order to accomplish all of this, the following aims were pursued, which will be discussed in the remaining chapters.

Aim 1. Optimize an ODC assay compatible with high throughput screening and optimize a high throughput assay system capable of performing said assay.

Aim 2. Apply this assay to a large chemical library in order to identify potential inhibitors of ODC.

Aim 3. Evaluate these compounds in terms of mode of inhibition, selectivity versus human ODC, potential binding sites, trypanocidal activity and general cytotoxicity.

References:

1. Steverding, D., The history of African trypanosomiasis. *Parasit Vectors* **2008**, 1, (1), 3.
2. Cox, F. E., History of sleeping sickness (African trypanosomiasis). *Infect Dis Clin North Am* **2004**, 18, (2), 231-45.
3. Joubert, J. J.; Schutte, C. H.; Irons, D. J.; Fripp, P. J., Ubombo and the site of David Bruce's discovery of *Trypanosoma brucei*. *Trans R Soc Trop Med Hyg* **1993**, 87, (4), 494-5.
4. Cook, G. C., Sir David Bruce's elucidation of the aetiology of nagana--exactly one hundred years ago. *Trans R Soc Trop Med Hyg* **1994**, 88, (3), 257-8.

5. Forde, R., Some Clinical notes on a European patient in whose blood a trypanosome was observed. *J. Trop. Med.* **1902**, 5, 261-263.
6. Dutton, J., Preliminary note upon a trypanosome occurring in the blood of man. *Thompson Yates lab Rep* **1902**, 4, (2), 455-468.
7. Bruce, D.; Nabarro, D.; Grieg, E., Further report of sleeping sickness in Uganda *Report of the Sleeping Sickness Commission* **1903**, 4, 3-87.
8. Anonymous, Reports of the Royal Society's Commission on Sleeping Sickness. *Br. Med. J.* **1903**, 2, (2233), 1008-1009.
9. Castellani, A., *Microbes, men and monarchs*. Gollanes: London, 1960.
10. Sodeman, W. A., Jr., A note on the early history of African trypanosomiasis. *Am J Trop Med Hyg* **1974**, 23, (4), 712-3.
11. Bruce, D., Classification of the African Trypanosomes Pathogenic to Man and Domestic Animals. *Trans R Soc Trop Med Hyg* **1914**, 8, (1), 1-22.
12. Stephens, J.; Fantham, H., On the peculiar morphology of a trypanosome from a case of sleeping sickness and the possibility of its being a new species (*T. rhodesiense*). *Proc R Soc Lond B* **1910**, 83, 28-33.
13. Kinghorn, A.; Yorke, W., On the transmission of human trypanosomes by *Glossina morsitans* and on the occurrence of human trypanosomes in game. *Ann Trop Med Parasitol* **1912**, 6, 1-23.
14. Hide, G., History of sleeping sickness in East Africa. *Clin Microbiol Rev* **1999**, 12, (1), 112-25.
15. Livingstone, D., Arsenic as a remedy for the tsetse bite. *Br. Med. J.* **1858**, 1, (70), 360-361.

16. Gensini, G. F.; Conti, A. A.; Lippi, D., The contributions of Paul Ehrlich to infectious disease. *J Infect* **2007**, 54, (3), 221-4.
17. Lourie, E.; Yorke, W., Studies in chemotherapy XXI. The trypanocidal action of certain aromatic diamidines. *Ann Trop Med Parasitol* **1939**, 33, 289-304.
18. Bray, P. G.; Barrett, M. P.; Ward, S. A.; de Koning, H. P., Pentamidine uptake and resistance in pathogenic protozoa: past, present and future. *Trends Parasitol* **2003**, 19, (5), 232-9.
19. WHO, Chapter 8 - African trypanosomiasis. In *WHO Report on Global Surveillance of Epidemic-prone Infectious Diseases*, World Health Organization: Geneva, 2000; pp 95-106.
20. Sjoerdsma, A.; Golden, J. A.; Schechter, P. J.; Barlow, J. L.; Santi, D. V., Successful treatment of lethal protozoal infections with the ornithine decarboxylase inhibitor, alpha-difluoromethylornithine. *Trans Assoc Am Physicians* **1984**, 97, 70-9.
21. Van Nieuwenhove, S.; Schechter, P. J.; Declercq, J.; Bone, G.; Burke, J.; Sjoerdsma, A., Treatment of gambiense sleeping sickness in the Sudan with oral DFMO (DL-alpha-difluoromethylornithine), an inhibitor of ornithine decarboxylase; first field trial. *Trans R Soc Trop Med Hyg* **1985**, 79, (5), 692-8.
22. WHO, Human African trypanosomiasis (sleeping sickness): epidemiological update. *Weekly epidemiological record* **2006**, 81, (8), 69-80.
23. WHO, *The world health report 2000: Health systems: Improving performance*. World Health Organization: Geneva, 2000.
24. Laveran, A.; Mesnil, F., *Trypanosomes and trypanosomiasis*. Balliere, Tindall and Cox: London, 1907.

25. Pays, E.; Vanhollebeke, B., Mutual self-defence: the trypanolytic factor story. *Microbes Infect* **2008**, 10, (9), 985-9.
26. Vanhamme, L.; Paturiaux-Hanocq, F.; Poelvoorde, P.; Nolan, D. P.; Lins, L.; Van Den Abbeele, J.; Pays, A.; Tebabi, P.; Van Xong, H.; Jacquet, A.; Moguelevsky, N.; Dieu, M.; Kane, J. P.; De Baetselier, P.; Brasseur, R.; Pays, E., Apolipoprotein L-I is the trypanosome lytic factor of human serum. *Nature* **2003**, 422, (6927), 83-7.
27. Picozzi, K.; Fevre, E. M.; Odiit, M.; Carrington, M.; Eisler, M. C.; Maudlin, I.; Welburn, S. C., Sleeping sickness in Uganda: a thin line between two fatal diseases. *Bmj* **2005**, 331, (7527), 1238-41.
28. De Greef, C.; Chimfwembe, E.; Kihang'a Wabacha, J.; Bajyana Songa, E.; Hamers, R., Only the serum-resistant bloodstream forms of *Trypanosoma brucei rhodesiense* express the serum resistance associated (SRA) protein. *Ann Soc Belg Med Trop* **1992**, 72 Suppl 1, 13-21.
29. Faulkner, S. D.; Oli, M. W.; Kieft, R.; Cotlin, L.; Widener, J.; Shiflett, A.; Cipriano, M. J.; Pacocha, S. E.; Birkeland, S. R.; Hajduk, S. L.; McArthur, A. G., In vitro generation of human high-density-lipoprotein-resistant *Trypanosoma brucei brucei*. *Eukaryot Cell* **2006**, 5, (8), 1276-86.
30. Maudlin, I., African trypanosomiasis. *Ann Trop Med Parasitol* **2006**, 100, (8), 679-701.
31. Barrett, M. P.; Burchmore, R. J.; Stich, A.; Lazzari, J. O.; Frasch, A. C.; Cazzulo, J. J.; Krishna, S., The trypanosomiasis. *Lancet* **2003**, 362, (9394), 1469-80.
32. Vale, G. A., Proceedings: Attractants for controlling and surveying tsetse populations. *Trans R Soc Trop Med Hyg* **1974**, 68, (1), 11.

33. Elliott, M.; Farnham, A. W.; Janes, N. F.; Needham, P. H.; Pulman, D. A.; Stevenson, J. H., A photostable pyrethroid. *Nature* **1973**, 246, (5429), 169-70.
34. Vale, G. A.; Hargrove, J. W.; Cockbill, G. G.; Phelps, R. J., Field trials of baits to control populations of *Glossinia morsitans moritans* Westwood and *G. pallidipes* Austen (Diptera: Glossinidae). *Bull. Entomol. Res.* **1986**, 76, 179-193.
35. Vale, G. A.; Mutika, G.; Lovemore, D. F., Insecticide-treated cattle for controlling tsetse flies (Diptera: Glossinidae): some questions answered, many posed. *Bull. Entomol. Res.* **1999**, 89, 569-578.
36. Kabayo, J. P., Aiming to eliminate tsetse from Africa. *Trends Parasitol* **2002**, 18, (11), 473-5.
37. Vreysen, M. J.; Saleh, K. M.; Ali, M. Y.; Abdulla, A. M.; Zhu, Z. R.; Juma, K. G.; Dyck, V. A.; Msangi, A. R.; Mkonyi, P. A.; Feldmann, H. U., *Glossina austeni* (Diptera: Glossinidae) eradicated on the island of Unguja, Zanzibar, using the sterile insect technique. *J Econ Entomol* **2000**, 93, (1), 123-35.
38. Bhalla, N., Pan African group takes lead against the tsetse fly. *Lancet* **2002**, 359, (9307), 686.
39. Collins, J. M.; Klecker, R. W., Jr.; Yarchoan, R.; Lane, H. C.; Fauci, A. S.; Redfield, R. R.; Broder, S.; Myers, C. E., Clinical pharmacokinetics of suramin in patients with HTLV-III/LAV infection. *J Clin Pharmacol* **1986**, 26, (1), 22-6.
40. Vansterkenburg, E. L.; Coppens, I.; Wilting, J.; Bos, O. J.; Fischer, M. J.; Janssen, L. H.; Opperdoes, F. R., The uptake of the trypanocidal drug suramin in combination with low-density lipoproteins by *Trypanosoma brucei* and its possible mode of action. *Acta Trop* **1993**, 54, (3-4), 237-50.

41. Nok, A. J., Arsenicals (melarsoprol), pentamidine and suramin in the treatment of human African trypanosomiasis. *Parasitol Res* **2003**, 90, (1), 71-9.
42. Clarkson, A. B., Jr.; Bienen, E. J.; Bacchi, C. J.; McCann, P. P.; Nathan, H. C.; Hutner, S. H.; Sjoerdsma, A., New drug combination for experimental late-stage African trypanosomiasis: DL-alpha-difluoromethylornithine (DFMO) with suramin. *Am J Trop Med Hyg* **1984**, 33, (6), 1073-7.
43. Fairlamb, A. H., Chemotherapy of human African trypanosomiasis: current and future prospects. *Trends Parasitol* **2003**, 19, (11), 488-94.
44. Pepin, J.; Milord, F., The treatment of human African trypanosomiasis. *Adv Parasitol* **1994**, 33, 1-47.
45. Doua, F.; Miezán, T. W.; Sanon Singaro, J. R.; Boa Yapo, F.; Baltz, T., The efficacy of pentamidine in the treatment of early-late stage *Trypanosoma brucei gambiense* trypanosomiasis. *Am J Trop Med Hyg* **1996**, 55, (6), 586-8.
46. Damper, D.; Patton, C. L., Pentamidine transport and sensitivity in brucei-group trypanosomes. *J Protozool* **1976**, 23, (2), 349-56.
47. Carter, N. S.; Berger, B. J.; Fairlamb, A. H., Uptake of diamidine drugs by the P2 nucleoside transporter in melarsen-sensitive and -resistant *Trypanosoma brucei brucei*. *J Biol Chem* **1995**, 270, (47), 28153-7.
48. de Koning, H. P.; Jarvis, S. M., Uptake of pentamidine in *Trypanosoma brucei brucei* is mediated by the P2 adenosine transporter and at least one novel, unrelated transporter. *Acta Trop* **2001**, 80, (3), 245-50.

49. De Koning, H. P., Uptake of pentamidine in *Trypanosoma brucei brucei* is mediated by three distinct transporters: implications for cross-resistance with arsenicals. *Mol Pharmacol* **2001**, 59, (3), 586-92.
50. Bridges, D. J.; Gould, M. K.; Nerima, B.; Maser, P.; Burchmore, R. J.; de Koning, H. P., Loss of the high-affinity pentamidine transporter is responsible for high levels of cross-resistance between arsenical and diamidine drugs in African trypanosomes. *Mol Pharmacol* **2007**, 71, (4), 1098-108.
51. Shapiro, T. A.; Englund, P. T., Selective cleavage of kinetoplast DNA minicircles promoted by antitrypanosomal drugs. *Proc Natl Acad Sci U S A* **1990**, 87, (3), 950-4.
52. Berger, B. J.; Carter, N. S.; Fairlamb, A. H., Polyamine and pentamidine metabolism in African trypanosomes. *Acta Trop* **1993**, 54, (3-4), 215-24.
53. Maser, P.; Sutterlin, C.; Kralli, A.; Kaminsky, R., A nucleoside transporter from *Trypanosoma brucei* involved in drug resistance. *Science* **1999**, 285, (5425), 242-4.
54. de Koning, H. P., Transporters in African trypanosomes: role in drug action and resistance. *Int J Parasitol* **2001**, 31, (5-6), 512-22.
55. Keiser, J.; Ericsson, O.; Burri, C., Investigations of the metabolites of the trypanocidal drug melarsoprol. *Clin Pharmacol Ther* **2000**, 67, (5), 478-88.
56. Burri, C.; Baltz, T.; Giroud, C.; Doua, F.; Welker, H. A.; Brun, R., Pharmacokinetic properties of the trypanocidal drug melarsoprol. *Chemotherapy* **1993**, 39, (4), 225-34.
57. Meshnick, S. R.; Blobstein, S. H.; Grady, R. W.; Cerami, A., An approach to the development of new drugs for African trypanosomiasis. *J Exp Med* **1978**, 148, (2), 569-79.

58. Brun, R.; Schumacher, R.; Schmid, C.; Kunz, C.; Burri, C., The phenomenon of treatment failures in Human African Trypanosomiasis. *Trop Med Int Health* **2001**, *6*, (11), 906-14.
59. Legros, D.; Evans, S.; Maiso, F.; Enyaru, J. C.; Mbulamberi, D., Risk factors for treatment failure after melarsoprol for *Trypanosoma brucei gambiense* trypanosomiasis in Uganda. *Trans R Soc Trop Med Hyg* **1999**, *93*, (4), 439-42.
60. Heby, O.; Roberts, S. C.; Ullman, B., Polyamine biosynthetic enzymes as drug targets in parasitic protozoa. *Biochem Soc Trans* **2003**, *31*, (2), 415-9.
61. Seiler, N., Thirty years of polyamine-related approaches to cancer therapy. Retrospect and prospect. Part 1. Selective enzyme inhibitors. *Curr Drug Targets* **2003**, *4*, (7), 537-64.
62. Bacchi, C. J.; Yarlett, N., Polyamine metabolism as chemotherapeutic target in protozoan parasites. *Mini Rev Med Chem* **2002**, *2*, (6), 553-63.
63. Wenzler, T.; Boykin, D. W.; Ismail, M. A.; Hall, J. E.; Tidwell, R. R.; Brun, R., New treatment option for second-stage African sleeping sickness: in vitro and in vivo efficacy of aza analogs of DB289. *Antimicrob Agents Chemother* **2009**, *53*, (10), 4185-92.
64. Nyunt, M. M.; Hendrix, C. W.; Bakshi, R. P.; Kumar, N.; Shapiro, T. A., Phase I/II evaluation of the prophylactic antimalarial activity of pafuramidine in healthy volunteers challenged with *Plasmodium falciparum* sporozoites. *Am J Trop Med Hyg* **2009**, *80*, (4), 528-35.
65. Priotto, G.; Fogg, C.; Balasegaram, M.; Erphas, O.; Louga, A.; Checchi, F.; Ghabri, S.; Piola, P., Three drug combinations for late-stage *Trypanosoma brucei*

gambiense sleeping sickness: a randomized clinical trial in Uganda. *PLoS Clin Trials* **2006**, 1, (8), e39.

66. Simpson, A. G.; Stevens, J. R.; Lukes, J., The evolution and diversity of kinetoplastid flagellates. *Trends Parasitol* **2006**, 22, (4), 168-74.

67. Baldauf, S. L.; Roger, A. J.; Wenk-Siefert, I.; Doolittle, W. F., A kingdom-level phylogeny of eukaryotes based on combined protein data. *Science* **2000**, 290, (5493), 972-7.

68. Stevens, J.; Noyes, H.; Gibson, W., The evolution of trypanosomes infecting humans and primates. *Mem Inst Oswaldo Cruz* **1998**, 93, (5), 669-76.

69. Fevre, E. M.; Picozzi, K.; Jannin, J.; Welburn, S. C.; Maudlin, I., Human African trypanosomiasis: Epidemiology and control. *Adv Parasitol* **2006**, 61, 167-221.

70. Gibson, W.; Peacock, L.; Ferris, V.; Williams, K.; Bailey, M., The use of yellow fluorescent hybrids to indicate mating in *Trypanosoma brucei*. *Parasit Vectors* **2008**, 1, (1), 4.

71. Tait, A.; Macleod, A.; Tweedie, A.; Masiga, D.; Turner, C. M., Genetic exchange in *Trypanosoma brucei*: evidence for mating prior to metacyclic stage development. *Mol Biochem Parasitol* **2007**, 151, (1), 133-6.

72. Turner, C. M.; Barry, J. D.; Maudlin, I.; Vickerman, K., An estimate of the size of the metacyclic variable antigen repertoire of *Trypanosoma brucei rhodesiense*. *Parasitology* **1988**, 97 (Pt 2), 269-76.

73. Pays, E.; Vanhamme, L.; Perez-Morga, D., Antigenic variation in *Trypanosoma brucei*: facts, challenges and mysteries. *Curr Opin Microbiol* **2004**, 7, (4), 369-74.

74. Stockdale, C.; Swiderski, M. R.; Barry, J. D.; McCulloch, R., Antigenic variation in *Trypanosoma brucei*: joining the DOTs. *PLoS Biol* **2008**, 6, (7), e185.
75. Sneader, W., *Drug Discovery A History*. John Wiley & Sons Ltd: West Sussex, England, 2005.
76. Kong, D. X.; Li, X. J.; Zhang, H. Y., Where is the hope for drug discovery? Let history tell the future. *Drug Discov Today* **2009**, 14, (3-4), 115-9.
77. Drews, J., Drug discovery: a historical perspective. *Science* **2000**, 287, (5460), 1960-4.
78. Feng, B. Y.; Shelat, A.; Doman, T. N.; Guy, R. K.; Shoichet, B. K., High-throughput assays for promiscuous inhibitors. *Nat Chem Biol* **2005**, 1, (3), 146-8.
79. McGovern, S. L.; Shoichet, B. K., Kinase inhibitors: not just for kinases anymore. *J Med Chem* **2003**, 46, (8), 1478-83.
80. Johnston, P. A.; Soares, K. M.; Shinde, S. N.; Foster, C. A.; Shun, T. Y.; Takyi, H. K.; Wipf, P.; Lazo, J. S., Development of a 384-well colorimetric assay to quantify hydrogen peroxide generated by the redox cycling of compounds in the presence of reducing agents. *Assay Drug Dev Technol* **2008**, 6, (4), 505-18.
81. Lor, L. A.; Schneck, J.; McNulty, D. E.; Diaz, E.; Brandt, M.; Thrall, S. H.; Schwartz, B., A simple assay for detection of small-molecule redox activity. *J Biomol Screen* **2007**, 12, (6), 881-90.
82. Kainkaryam, R. M.; Woolf, P. J., Pooling in high-throughput drug screening. *Curr Opin Drug Discov Devel* **2009**, 12, (3), 339-50.

83. Konings, D. A.; Wyatt, J. R.; Ecker, D. J.; Freier, S. M., Deconvolution of combinatorial libraries for Drug discovery: theoretical comparison of pooling strategies. *J Med Chem* **1996**, 39, (14), 2710-9.
84. Warren, G. L.; Andrews, C. W.; Capelli, A. M.; Clarke, B.; LaLonde, J.; Lambert, M. H.; Lindvall, M.; Nevins, N.; Semus, S. F.; Senger, S.; Tedesco, G.; Wall, I. D.; Woolven, J. M.; Peishoff, C. E.; Head, M. S., A critical assessment of docking programs and scoring functions. *J Med Chem* **2006**, 49, (20), 5912-31.
85. Sheridan, R. P.; McGaughey, G. B.; Cornell, W. D., Multiple protein structures and multiple ligands: effects on the apparent goodness of virtual screening results. *J Comput Aided Mol Des* **2008**, 22, (3-4), 257-65.
86. Pitera, J. W., Current developments in and importance of high-performance computing in drug discovery. *Curr Opin Drug Discov Devel* **2009**, 12, (3), 388-96.
87. Gillet, V. J., New directions in library design and analysis. *Curr Opin Chem Biol* **2008**, 12, (3), 372-8.
88. Gorse, A. D., Diversity in medicinal chemistry space. *Curr Top Med Chem* **2006**, 6, (1), 3-18.
89. Kubinyi, H., Similarity and dissimilarity: a medicinal chemist's view. *Perspect Drug Discov Des* **1998**, 9-11, 225-232.
90. Hoaglin, D. C., Mosteller, Frederick, Tukey, John W., *Understanding Robust and Exploratory Data Analysis*. John Wiley and Sons, Inc.: New York, 1983.
91. Inglese, J.; Auld, D. S.; Jadhav, A.; Johnson, R. L.; Simeonov, A.; Yasgar, A.; Zheng, W.; Austin, C. P., Quantitative high-throughput screening: a titration-based

approach that efficiently identifies biological activities in large chemical libraries. *Proc Natl Acad Sci U S A* **2006**, 103, (31), 11473-8.

92. Myler, P. J., Searching the Tritryp genomes for drug targets. *Adv Exp Med Biol* **2008**, 625, 133-40.

93. Luscher, A.; de Koning, H. P.; Maser, P., Chemotherapeutic strategies against *Trypanosoma brucei*: drug targets vs. drug targeting. *Curr Pharm Des* **2007**, 13, (6), 555-67.

94. Michels, P. A., Compartmentation of glycolysis in trypanosomes: a potential target for new trypanocidal drugs. *Biol Cell* **1988**, 64, (2), 157-64.

95. Bakker, B. M.; Westerhoff, H. V.; Opperdoes, F. R.; Michels, P. A., Metabolic control analysis of glycolysis in trypanosomes as an approach to improve selectivity and effectiveness of drugs. *Mol Biochem Parasitol* **2000**, 106, (1), 1-10.

96. Sommer, J. M.; Wang, C. C., Targeting proteins to the glycosomes of African trypanosomes. *Annu Rev Microbiol* **1994**, 48, 105-38.

97. Bakker, B. M.; Mensonides, F. I.; Teusink, B.; van Hoek, P.; Michels, P. A.; Westerhoff, H. V., Compartmentation protects trypanosomes from the dangerous design of glycolysis. *Proc Natl Acad Sci U S A* **2000**, 97, (5), 2087-92.

98. Michels, P. A.; Bringaud, F.; Herman, M.; Hannaert, V., Metabolic functions of glycosomes in trypanosomatids. *Biochim Biophys Acta* **2006**, 1763, (12), 1463-77.

99. Chambers, J. W.; Fowler, M. L.; Morris, M. T.; Morris, J. C., The anti-trypanosomal agent lonidamine inhibits *Trypanosoma brucei* hexokinase 1. *Mol Biochem Parasitol* **2008**, 158, (2), 202-7.

100. Hudock, M. P.; Sanz-Rodriguez, C. E.; Song, Y.; Chan, J. M.; Zhang, Y.; Odeh, S.; Kosztowski, T.; Leon-Rossell, A.; Concepcion, J. L.; Yardley, V.; Croft, S. L.; Urbina, J. A.; Oldfield, E., Inhibition of *Trypanosoma cruzi* hexokinase by bisphosphonates. *J Med Chem* **2006**, 49, (1), 215-23.
101. Trinquier, M.; Perie, J.; Callens, M.; Opperdoes, F.; Willson, M., Specific inhibitors for the glycolytic enzymes of *Trypanosoma brucei*. *Bioorg Med Chem* **1995**, 3, (11), 1423-7.
102. Nowicki, M. W.; Tulloch, L. B.; Worrall, L.; McNae, I. W.; Hannaert, V.; Michels, P. A.; Fothergill-Gilmore, L. A.; Walkinshaw, M. D.; Turner, N. J., Design, synthesis and trypanocidal activity of lead compounds based on inhibitors of parasite glycolysis. *Bioorg Med Chem* **2008**, 16, (9), 5050-61.
103. Nyasse, B.; Ngantchou, I.; Tchana, E. M.; Sonke, B.; Denier, C.; Fontaine, C., Inhibition of both *Trypanosoma brucei* bloodstream form and related glycolytic enzymes by a new kolavic acid derivative isolated from *Entada abyssinica*. *Pharmazie* **2004**, 59, (11), 873-5.
104. Claustre, S.; Denier, C.; Lakhdar-Ghazal, F.; Lougare, A.; Lopez, C.; Chevalier, N.; Michels, P. A.; Perie, J.; Willson, M., Exploring the active site of *Trypanosoma brucei* phosphofructokinase by inhibition studies: specific irreversible inhibition. *Biochemistry* **2002**, 41, (32), 10183-93.
105. Dax, C.; Duffieux, F.; Chabot, N.; Coincon, M.; Sygusch, J.; Michels, P. A.; Blonski, C., Selective irreversible inhibition of fructose 1,6-bisphosphate aldolase from *Trypanosoma brucei*. *J Med Chem* **2006**, 49, (5), 1499-502.

106. Gallo, M. B.; Marques, A. S.; Vieira, P. C.; da Silva, M. F.; Fernandes, J. B.; Silva, M.; Guido, R. V.; Oliva, G.; Thiemann, O. H.; Albuquerque, S.; Fairlamb, A. H., Enzymatic inhibitory activity and trypanocidal effects of extracts and compounds from *Siphoneugena densiflora* O. Berg and *Vitex polygama* Cham. *Z Naturforsch C* **2008**, 63, (5-6), 371-82.
107. Bressi, J. C.; Verlinde, C. L.; Aronov, A. M.; Shaw, M. L.; Shin, S. S.; Nguyen, L. N.; Suresh, S.; Buckner, F. S.; Van Voorhis, W. C.; Kuntz, I. D.; Hol, W. G.; Gelb, M. H., Adenosine analogues as selective inhibitors of glyceraldehyde-3-phosphate dehydrogenase of Trypanosomatidae via structure-based drug design. *J Med Chem* **2001**, 44, (13), 2080-93.
108. Ladame, S.; Bardet, M.; Perie, J.; Willson, M., Selective inhibition of *Trypanosoma brucei* GAPDH by 1,3-bisphospho-D-glyceric acid (1,3-diPG) analogues. *Bioorg Med Chem* **2001**, 9, (3), 773-83.
109. Aronov, A. M.; Suresh, S.; Buckner, F. S.; Van Voorhis, W. C.; Verlinde, C. L.; Opperdoes, F. R.; Hol, W. G.; Gelb, M. H., Structure-based design of submicromolar, biologically active inhibitors of trypanosomatid glyceraldehyde-3-phosphate dehydrogenase. *Proc Natl Acad Sci U S A* **1999**, 96, (8), 4273-8.
110. Aronov, A. M.; Verlinde, C. L.; Hol, W. G.; Gelb, M. H., Selective tight binding inhibitors of trypanosomal glyceraldehyde-3-phosphate dehydrogenase via structure-based drug design. *J Med Chem* **1998**, 41, (24), 4790-9.
111. Van Calenbergh, S.; Verlinde, C. L.; Soenens, J.; De Bruyn, A.; Callens, M.; Blaton, N. M.; Peeters, O. M.; Rozenski, J.; Hol, W. G.; Herdewijn, P., Synthesis and structure-activity relationships of analogs of 2'-deoxy-2'-(3-

methoxybenzamido)adenosine, a selective inhibitor of trypanosomal glycosomal glyceraldehyde-3-phosphate dehydrogenase. *J Med Chem* **1995**, 38, (19), 3838-49.

112. Verlinde, C. L.; Callens, M.; Van Calenbergh, S.; Van Aerschot, A.; Herdewijn, P.; Hannaert, V.; Michels, P. A.; Opperdoes, F. R.; Hol, W. G., Selective inhibition of trypanosomal glyceraldehyde-3-phosphate dehydrogenase by protein structure-based design: toward new drugs for the treatment of sleeping sickness. *J Med Chem* **1994**, 37, (21), 3605-13.

113. Willson, M.; Lauth, N.; Perie, J.; Callens, M.; Opperdoes, F. R., Inhibition of glyceraldehyde-3-phosphate dehydrogenase by phosphorylated epoxides and alpha-enones. *Biochemistry* **1994**, 33, (1), 214-20.

114. Duszenko, M.; Mecke, D., Inhibition of glyceraldehyde-3-phosphate dehydrogenase by pentalenolactone in *Trypanosoma brucei*. *Mol Biochem Parasitol* **1986**, 19, (3), 223-9.

115. Kotsikorou, E.; Sahota, G.; Oldfield, E., Bisphosphonate inhibition of phosphoglycerate kinase: quantitative structure-activity relationship and pharmacophore modeling investigation. *J Med Chem* **2006**, 49, (23), 6692-703.

116. Bressi, J. C.; Choe, J.; Hough, M. T.; Buckner, F. S.; Van Voorhis, W. C.; Verlinde, C. L.; Hol, W. G.; Gelb, M. H., Adenosine analogues as inhibitors of *Trypanosoma brucei* phosphoglycerate kinase: elucidation of a novel binding mode for a 2-amino-N(6)-substituted adenosine. *J Med Chem* **2000**, 43, (22), 4135-50.

117. Puech, J.; Callens, M.; Willson, M., Analysis of the kinetics of reversible enzyme inhibition by a general algebraic method. Application to multisite inhibition of the phosphoglycerate kinase from *Trypanosoma brucei*. *J Enzyme Inhib* **1998**, 14, (1), 27-47.

118. Martinez-Oyanedel, J.; McNae, I. W.; Nowicki, M. W.; Keillor, J. W.; Michels, P. A.; Fothergill-Gilmore, L. A.; Walkinshaw, M. D., The first crystal structure of phosphofructokinase from a eukaryote: *Trypanosoma brucei*. *J Mol Biol* **2007**, 366, (4), 1185-98.
119. Ladame, S.; Castilho, M. S.; Silva, C. H.; Denier, C.; Hannaert, V.; Perie, J.; Oliva, G.; Willson, M., Crystal structure of *Trypanosoma cruzi* glyceraldehyde-3-phosphate dehydrogenase complexed with an analogue of 1,3-bisphospho-d-glyceric acid. *Eur J Biochem* **2003**, 270, (22), 4574-86.
120. Vellieux, F. M.; Hajdu, J.; Hol, W. G., Refined 3.2 Å structure of glycosomal holo glyceraldehyde phosphate dehydrogenase from *Trypanosoma brucei brucei*. *Acta Crystallogr D Biol Crystallogr* **1995**, 51, (Pt 4), 575-89.
121. Vellieux, F. M.; Hajdu, J.; Verlinde, C. L.; Groendijk, H.; Read, R. J.; Greenhough, T. J.; Campbell, J. W.; Kalk, K. H.; Littlechild, J. A.; Watson, H. C.; et al., Structure of glycosomal glyceraldehyde-3-phosphate dehydrogenase from *Trypanosoma brucei* determined from Laue data. *Proc Natl Acad Sci U S A* **1993**, 90, (6), 2355-9.
122. Bernstein, B. E.; Hol, W. G., Crystal structures of substrates and products bound to the phosphoglycerate kinase active site reveal the catalytic mechanism. *Biochemistry* **1998**, 37, (13), 4429-36.
123. Rigden, D. J.; Phillips, S. E.; Michels, P. A.; Fothergill-Gilmore, L. A., The structure of pyruvate kinase from *Leishmania mexicana* reveals details of the allosteric transition and unusual effector specificity. *J Mol Biol* **1999**, 291, (3), 615-35.

124. Bakshi, R. P.; Shapiro, T. A., RNA interference of *Trypanosoma brucei* topoisomerase IB: both subunits are essential. *Mol Biochem Parasitol* **2004**, 136, (2), 249-55.
125. Kulikowicz, T.; Shapiro, T. A., Distinct genes encode type II Topoisomerases for the nucleus and mitochondrion in the protozoan parasite *Trypanosoma brucei*. *J Biol Chem* **2006**, 281, (6), 3048-56.
126. Wang, Z.; Englund, P. T., RNA interference of a trypanosome topoisomerase II causes progressive loss of mitochondrial DNA. *Embo J* **2001**, 20, (17), 4674-83.
127. Bodley, A. L.; Chakraborty, A. K.; Xie, S.; Burri, C.; Shapiro, T. A., An unusual type IB topoisomerase from African trypanosomes. *Proc Natl Acad Sci U S A* **2003**, 100, (13), 7539-44.
128. Deterding, A.; Dungey, F. A.; Thompson, K. A.; Steverding, D., Anti-trypanosomal activities of DNA topoisomerase inhibitors. *Acta Trop* **2005**, 93, (3), 311-6.
129. Bodley, A. L.; Shapiro, T. A., Molecular and cytotoxic effects of camptothecin, a topoisomerase I inhibitor, on trypanosomes and *Leishmania*. *Proc Natl Acad Sci U S A* **1995**, 92, (9), 3726-30.
130. Bodley, A. L.; Wani, M. C.; Wall, M. E.; Shapiro, T. A., Antitrypanosomal activity of camptothecin analogs. Structure-activity correlations. *Biochem Pharmacol* **1995**, 50, (7), 937-42.
131. Strauss, P. R.; Wang, J. C., The TOP2 gene of *Trypanosoma brucei*: a single-copy gene that shares extensive homology with other TOP2 genes encoding eukaryotic DNA topoisomerase II. *Mol Biochem Parasitol* **1990**, 38, (1), 141-50.

132. Gamage, S. A.; Figgitt, D. P.; Wojcik, S. J.; Ralph, R. K.; Ransijn, A.; Mauel, J.; Yardley, V.; Snowdon, D.; Croft, S. L.; Denny, W. A., Structure-activity relationships for the antileishmanial and antitrypanosomal activities of 1'-substituted 9-anilinoacridines. *J Med Chem* **1997**, 40, (16), 2634-42.
133. Jonckers, T. H.; van Miert, S.; Cimanga, K.; Bailly, C.; Colson, P.; De Pauw-Gillet, M. C.; van den Heuvel, H.; Claeys, M.; Lemiere, F.; Esmans, E. L.; Rozenski, J.; Quirijnen, L.; Maes, L.; Dommissie, R.; Lemiere, G. L.; Vlietinck, A.; Pieters, L., Synthesis, cytotoxicity, and antiplasmodial and antitrypanosomal activity of new neocryptolepine derivatives. *J Med Chem* **2002**, 45, (16), 3497-508.
134. Bakshi, R. P.; Sang, D.; Morrell, A.; Cushman, M.; Shapiro, T. A., Activity of indenoisoquinolines against African trypanosomes. *Antimicrob Agents Chemother* **2009**, 53, (1), 123-8.
135. Maxwell, A.; Burton, N. P.; O'Hagan, N., High-throughput assays for DNA gyrase and other topoisomerases. *Nucleic Acids Res* **2006**, 34, (15), e104.
136. Gangjee, A.; Jain, H. D.; Kurup, S., Recent advances in classical and non-classical antifolates as antitumor and antiopportunistic infection agents: part I. *Anticancer Agents Med Chem* **2007**, 7, (5), 524-42.
137. Gangjee, A.; Jain, H. D.; Kurup, S., Recent advances in classical and non-classical antifolates as antitumor and antiopportunistic infection agents: Part II. *Anticancer Agents Med Chem* **2008**, 8, (2), 205-31.
138. Then, R. L., Antimicrobial dihydrofolate reductase inhibitors--achievements and future options: review. *J Chemother* **2004**, 16, (1), 3-12.

139. Gamarro, F.; Yu, P. L.; Zhao, J.; Edman, U.; Greene, P. J.; Santi, D., Trypanosoma brucei dihydrofolate reductase-thymidylate synthase: gene isolation and expression and characterization of the enzyme. *Mol Biochem Parasitol* **1995**, 72, (1-2), 11-22.
140. Sienkiewicz, N.; Jaroslowski, S.; Wyllie, S.; Fairlamb, A. H., Chemical and genetic validation of dihydrofolate reductase-thymidylate synthase as a drug target in African trypanosomes. *Mol Microbiol* **2008**, 69, (2), 520-33.
141. Zuccotto, F.; Martin, A. C.; Laskowski, R. A.; Thornton, J. M.; Gilbert, I. H., Dihydrofolate reductase: a potential drug target in trypanosomes and leishmania. *J Comput Aided Mol Des* **1998**, 12, (3), 241-57.
142. Khabnadideh, S.; Pez, D.; Musso, A.; Brun, R.; Perez, L. M.; Gonzalez-Pacanowska, D.; Gilbert, I. H., Design, synthesis and evaluation of 2,4-diaminoquinazolines as inhibitors of trypanosomal and leishmanial dihydrofolate reductase. *Bioorg Med Chem* **2005**, 13, (7), 2637-49.
143. Chowdhury, S. F.; Villamor, V. B.; Guerrero, R. H.; Leal, I.; Brun, R.; Croft, S. L.; Goodman, J. M.; Maes, L.; Ruiz-Perez, L. M.; Pacanowska, D. G.; Gilbert, I. H., Design, synthesis, and evaluation of inhibitors of trypanosomal and leishmanial dihydrofolate reductase. *J Med Chem* **1999**, 42, (21), 4300-12.
144. Chowdhury, S. F.; Guerrero, R. H.; Brun, R.; Ruiz-Perez, L. M.; Pacanowska, D. G.; Gilbert, I. H., Synthesis and testing of 5-benzyl-2,4-diaminopyrimidines as potential inhibitors of leishmanial and trypanosomal dihydrofolate reductase. *J Enzyme Inhib Med Chem* **2002**, 17, (5), 293-302.

145. Dawson, A.; Gibellini, F.; Sienkiewicz, N.; Tulloch, L. B.; Fyfe, P. K.; McLuskey, K.; Fairlamb, A. H.; Hunter, W. N., Structure and reactivity of *Trypanosoma brucei* pteridine reductase: inhibition by the archetypal antifolate methotrexate. *Mol Microbiol* **2006**, 61, (6), 1457-68.
146. Shanks, E. J.; Ong, H. B.; Robinson, D. A.; Thompson, S.; Sienkiewicz, N.; Fairlamb, A. H.; Frearson, J. A., Development and validation of a cytochrome c-coupled assay for pteridine reductase 1 and dihydrofolate reductase. *Anal Biochem* **2009**.
147. Mpamhanga, C. P.; Spinks, D.; Tulloch, L. B.; Shanks, E. J.; Robinson, D. A.; Collie, I. T.; Fairlamb, A. H.; Wyatt, P. G.; Frearson, J. A.; Hunter, W. N.; Gilbert, I. H.; Brenk, R., One scaffold, three binding modes: novel and selective pteridine reductase 1 inhibitors derived from fragment hits discovered by virtual screening. *J Med Chem* **2009**, 52, (14), 4454-65.
148. Lopez-Mirabal, H. R.; Winther, J. R., Redox characteristics of the eukaryotic cytosol. *Biochim Biophys Acta* **2008**, 1783, (4), 629-40.
149. Fairlamb, A. H.; Blackburn, P.; Ulrich, P.; Chait, B. T.; Cerami, A., Trypanothione: a novel bis(glutathionyl)spermidine cofactor for glutathione reductase in trypanosomatids. *Science* **1985**, 227, (4693), 1485-7.
150. Castro, H.; Tomas, A. M., Peroxidases of trypanosomatids. *Antioxid Redox Signal* **2008**, 10, (9), 1593-606.
151. Fairlamb, A. H.; Cerami, A., Metabolism and functions of trypanothione in the Kinetoplastida. *Annu Rev Microbiol* **1992**, 46, 695-729.
152. Krauth-Siegel, L. R.; Comini, M. A.; Schlecker, T., The trypanothione system. *Subcell Biochem* **2007**, 44, 231-51.

153. Krauth-Siegel, R. L.; Coombs, G. H., Enzymes of parasite thiol metabolism as drug targets. *Parasitol Today* **1999**, 15, (10), 404-9.
154. Arrick, B. A.; Griffith, O. W.; Cerami, A., Inhibition of glutathione synthesis as a chemotherapeutic strategy for trypanosomiasis. *J Exp Med* **1981**, 153, (3), 720-5.
155. Huynh, T. T.; Huynh, V. T.; Harmon, M. A.; Phillips, M. A., Gene knockdown of gamma-glutamylcysteine synthetase by RNAi in the parasitic protozoa *Trypanosoma brucei* demonstrates that it is an essential enzyme. *J Biol Chem* **2003**, 278, (41), 39794-800.
156. Krieger, S.; Schwarz, W.; Ariyanayagam, M. R.; Fairlamb, A. H.; Krauth-Siegel, R. L.; Clayton, C., Trypanosomes lacking trypanothione reductase are avirulent and show increased sensitivity to oxidative stress. *Mol Microbiol* **2000**, 35, (3), 542-52.
157. Khan, M. O.; Austin, S. E.; Chan, C.; Yin, H.; Marks, D.; Vaghjiani, S. N.; Kendrick, H.; Yardley, V.; Croft, S. L.; Douglas, K. T., Use of an additional hydrophobic binding site, the Z site, in the rational drug design of a new class of stronger trypanothione reductase inhibitor, quaternary alkylammonium phenothiazines. *J Med Chem* **2000**, 43, (16), 3148-56.
158. O'Sullivan, M. C.; Zhou, Q.; Li, Z.; Durham, T. B.; Rattendi, D.; Lane, S.; Bacchi, C. J., Polyamine derivatives as inhibitors of trypanothione reductase and assessment of their trypanocidal activities. *Bioorg Med Chem* **1997**, 5, (12), 2145-55.
159. D'Silva, C.; Daunes, S., Structure-activity study on the in vitro antiprotozoal activity of glutathione derivatives. *J Med Chem* **2000**, 43, (10), 2072-8.
160. Lee, B.; Bauer, H.; Melchers, J.; Ruppert, T.; Rattray, L.; Yardley, V.; Davioud-Charvet, E.; Krauth-Siegel, R. L., Irreversible inactivation of trypanothione reductase by

unsaturated Mannich bases: a divinyl ketone as key intermediate. *J Med Chem* **2005**, 48, (23), 7400-10.

161. Parveen, S.; Khan, M. O.; Austin, S. E.; Croft, S. L.; Yardley, V.; Rock, P.; Douglas, K. T., Antitrypanosomal, antileishmanial, and antimalarial activities of quaternary arylalkylammonium 2-amino-4-chlorophenyl phenyl sulfides, a new class of trypanothione reductase inhibitor, and of N-acyl derivatives of 2-amino-4-chlorophenyl phenyl sulfide. *J Med Chem* **2005**, 48, (25), 8087-97.

162. Li, Z.; Fennie, M. W.; Ganem, B.; Hancock, M. T.; Kobaslija, M.; Rattendi, D.; Bacchi, C. J.; O'Sullivan, M. C., Polyamines with N-(3-phenylpropyl) substituents are effective competitive inhibitors of trypanothione reductase and trypanocidal agents. *Bioorg Med Chem Lett* **2001**, 11, (2), 251-4.

163. Salmon-Chemin, L.; Buisine, E.; Yardley, V.; Kohler, S.; Debreu, M. A.; Landry, V.; Sergheraert, C.; Croft, S. L.; Krauth-Siegel, R. L.; Davioud-Charvet, E., 2- and 3-substituted 1,4-naphthoquinone derivatives as subversive substrates of trypanothione reductase and lipoamide dehydrogenase from *Trypanosoma cruzi*: synthesis and correlation between redox cycling activities and in vitro cytotoxicity. *J Med Chem* **2001**, 44, (4), 548-65.

164. Chibale, K.; Visser, M.; Yardley, V.; Croft, S. L.; Fairlamb, A. H., Synthesis and evaluation of 9,9-dimethylxanthene tricyclics against trypanothione reductase, *Trypanosoma brucei*, *Trypanosoma cruzi* and *Leishmania donovani*. *Bioorg Med Chem Lett* **2000**, 10, (11), 1147-50.

165. Hamilton, C. J.; Saravanamuthu, A.; Poupat, C.; Fairlamb, A. H.; Eggleston, I. M., Time-dependent inhibitors of trypanothione reductase: analogues of the spermidine alkaloid lunarine and related natural products. *Bioorg Med Chem* **2006**, 14, (7), 2266-78.
166. Wenzel, I. N.; Wong, P. E.; Maes, L.; Muller, T. J.; Krauth-Siegel, R. L.; Barrett, M. P.; Davioud-Charvet, E., Unsaturated Mannich bases active against multidrug-resistant *Trypanosoma brucei brucei* strains. *ChemMedChem* **2009**, 4, (3), 339-51.
167. Stump, B.; Eberle, C.; Kaiser, M.; Brun, R.; Krauth-Siegel, R. L.; Diederich, F., Diaryl sulfide-based inhibitors of trypanothione reductase: inhibition potency, revised binding mode and antiprotozoal activities. *Org Biomol Chem* **2008**, 6, (21), 3935-47.
168. Patterson, S.; Jones, D. C.; Shanks, E. J.; Frearson, J. A.; Gilbert, I. H.; Wyatt, P. G.; Fairlamb, A. H., Synthesis and evaluation of 1-(1-(Benzo[b]thiophen-2-yl)cyclohexyl)piperidine (BTCP) analogues as inhibitors of trypanothione reductase. *ChemMedChem* **2009**, 4, (8), 1341-53.
169. Martyn, D. C.; Jones, D. C.; Fairlamb, A. H.; Clardy, J., High-throughput screening affords novel and selective trypanothione reductase inhibitors with anti-trypanosomal activity. *Bioorg Med Chem Lett* **2007**, 17, (5), 1280-3.
170. Richardson, J. L.; Nett, I. R.; Jones, D. C.; Abdille, M. H.; Gilbert, I. H.; Fairlamb, A. H., Improved tricyclic inhibitors of trypanothione reductase by screening and chemical synthesis. *ChemMedChem* **2009**, 4, (8), 1333-40.
171. Holloway, G. A.; Baell, J. B.; Fairlamb, A. H.; Novello, P. M.; Parisot, J. P.; Richardson, J.; Watson, K. G.; Street, I. P., Discovery of 2-iminobenzimidazoles as a new class of trypanothione reductase inhibitor by high-throughput screening. *Bioorg Med Chem Lett* **2007**, 17, (5), 1422-7.

172. Jones, D. C.; Ariza, A.; Chow, W. H.; Oza, S. L.; Fairlamb, A. H., Comparative structural, kinetic and inhibitor studies of *Trypanosoma brucei* trypanothione reductase with *T. cruzi*. *Mol Biochem Parasitol* **2009**.
173. Comini, M. A.; Guerrero, S. A.; Haile, S.; Menge, U.; Lunsdorf, H.; Flohe, L., Validation of *Trypanosoma brucei* trypanothione synthetase as drug target. *Free Radic Biol Med* **2004**, 36, (10), 1289-302.
174. Wyllie, S.; Oza, S. L.; Patterson, S.; Spinks, D.; Thompson, S.; Fairlamb, A. H., Dissecting the essentiality of the bifunctional trypanothione synthetase-amidase in *Trypanosoma brucei* using chemical and genetic methods. *Mol Microbiol* **2009**.
175. Torrie, L. S.; Wyllie, S.; Spinks, D.; Oza, S. L.; Thompson, S.; Harrison, J. R.; Gilbert, I. H.; Wyatt, P. G.; Fairlamb, A. H.; Frearson, J. A., Chemical validation of trypanothione synthetase: a potential drug target for human trypanosomiasis. *J Biol Chem* **2009**.
176. Tetaud, E.; Giroud, C.; Prescott, A. R.; Parkin, D. W.; Baltz, D.; Biteau, N.; Baltz, T.; Fairlamb, A. H., Molecular characterisation of mitochondrial and cytosolic trypanothione-dependent tryparedoxin peroxidases in *Trypanosoma brucei*. *Mol Biochem Parasitol* **2001**, 116, (2), 171-83.
177. Wilkinson, S. R.; Horn, D.; Prathalingam, S. R.; Kelly, J. M., RNA interference identifies two hydroperoxide metabolizing enzymes that are essential to the bloodstream form of the african trypanosome. *J Biol Chem* **2003**, 278, (34), 31640-6.
178. Wilkinson, S. R.; Kelly, J. M., The role of glutathione peroxidases in trypanosomatids. *Biol Chem* **2003**, 384, (4), 517-25.

179. Schlecker, T.; Schmidt, A.; Dirdjaja, N.; Voncken, F.; Clayton, C.; Krauth-Siegel, R. L., Substrate specificity, localization, and essential role of the glutathione peroxidase-type tryparedoxin peroxidases in *Trypanosoma brucei*. *J Biol Chem* **2005**, 280, (15), 14385-94.
180. Hillebrand, H.; Schmidt, A.; Krauth-Siegel, R. L., A second class of peroxidases linked to the trypanothione metabolism. *J Biol Chem* **2003**, 278, (9), 6809-15.
181. Nkemngu, N. J.; Rosenkranz, V.; Wink, M.; Steverding, D., Antitrypanosomal activities of proteasome inhibitors. *Antimicrob Agents Chemother* **2002**, 46, (6), 2038-40.
182. Mutomba, M. C.; To, W. Y.; Hyun, W. C.; Wang, C. C., Inhibition of proteasome activity blocks cell cycle progression at specific phase boundaries in African trypanosomes. *Mol Biochem Parasitol* **1997**, 90, (2), 491-504.
183. Steverding, D.; Wang, X., Trypanocidal activity of the proteasome inhibitor and anti-cancer drug bortezomib. *Parasit Vectors* **2009**, 2, (1), 29.
184. Kumar, P.; Wang, C. C., Depletion of anaphase-promoting complex or cyclosome (APC/C) subunit homolog APC1 or CDC27 of *Trypanosoma brucei* arrests the procyclic form in metaphase but the bloodstream form in anaphase. *J Biol Chem* **2005**, 280, (36), 31783-91.
185. Wang, C. C.; Bozdech, Z.; Liu, C. L.; Shipway, A.; Backes, B. J.; Harris, J. L.; Bogoy, M., Biochemical analysis of the 20 S proteasome of *Trypanosoma brucei*. *J Biol Chem* **2003**, 278, (18), 15800-8.
186. Bangs, J. D.; Ransom, D. A.; Nimick, M.; Christie, G.; Hooper, N. M., In vitro cytotoxic effects on *Trypanosoma brucei* and inhibition of *Leishmania major* GP63 by peptidomimetic metalloprotease inhibitors. *Mol Biochem Parasitol* **2001**, 114, (1), 111-7.

187. Grandgenett, P. M.; Otsu, K.; Wilson, H. R.; Wilson, M. E.; Donelson, J. E., A function for a specific zinc metalloprotease of African trypanosomes. *PLoS Pathog* **2007**, 3, (10), 1432-45.
188. Altmann, E.; Aichholz, R.; Betschart, C.; Buhl, T.; Green, J.; Irie, O.; Teno, N.; Lattmann, R.; Tintelnot-Blomley, M.; Missbach, M., 2-Cyano-pyrimidines: a new chemotype for inhibitors of the cysteine protease cathepsin K. *J Med Chem* **2007**, 50, (4), 591-4.
189. Fujii, N.; Mallari, J. P.; Hansell, E. J.; Mackey, Z.; Doyle, P.; Zhou, Y. M.; Gut, J.; Rosenthal, P. J.; McKerrow, J. H.; Guy, R. K., Discovery of potent thiosemicarbazone inhibitors of rhodesain and cruzain. *Bioorg Med Chem Lett* **2005**, 15, (1), 121-3.
190. Greenbaum, D. C.; Mackey, Z.; Hansell, E.; Doyle, P.; Gut, J.; Caffrey, C. R.; Lehrman, J.; Rosenthal, P. J.; McKerrow, J. H.; Chibale, K., Synthesis and structure-activity relationships of parasiticidal thiosemicarbazone cysteine protease inhibitors against *Plasmodium falciparum*, *Trypanosoma brucei*, and *Trypanosoma cruzi*. *J Med Chem* **2004**, 47, (12), 3212-9.
191. Ashall, F.; Harris, D.; Roberts, H.; Healy, N.; Shaw, E., Substrate specificity and inhibitor sensitivity of a trypanosomatid alkaline peptidase. *Biochim Biophys Acta* **1990**, 1035, (3), 293-9.
192. Troeberg, L.; Morty, R. E.; Pike, R. N.; Lonsdale-Eccles, J. D.; Palmer, J. T.; McKerrow, J. H.; Coetzer, T. H., Cysteine proteinase inhibitors kill cultured bloodstream forms of *Trypanosoma brucei brucei*. *Exp Parasitol* **1999**, 91, (4), 349-55.

193. Scory, S.; Caffrey, C. R.; Stierhof, Y. D.; Ruppel, A.; Steverding, D., Trypanosoma brucei: killing of bloodstream forms in vitro and in vivo by the cysteine proteinase inhibitor Z-phe-ala-CHN2. *Exp Parasitol* **1999**, 91, (4), 327-33.
194. Lonsdale-Eccles, J. D.; Grab, D. J., Lysosomal and non-lysosomal peptidyl hydrolases of the bloodstream forms of Trypanosoma brucei brucei. *Eur J Biochem* **1987**, 169, (3), 467-75.
195. Caffrey, C. R.; Hansell, E.; Lucas, K. D.; Brinen, L. S.; Alvarez Hernandez, A.; Cheng, J.; Gwaltney, S. L., 2nd; Roush, W. R.; Stierhof, Y. D.; Bogoyo, M.; Steverding, D.; McKerrow, J. H., Active site mapping, biochemical properties and subcellular localization of rhodesain, the major cysteine protease of Trypanosoma brucei rhodesiense. *Mol Biochem Parasitol* **2001**, 118, (1), 61-73.
196. Nkemgu, N. J.; Grande, R.; Hansell, E.; McKerrow, J. H.; Caffrey, C. R.; Steverding, D., Improved trypanocidal activities of cathepsin L inhibitors. *Int J Antimicrob Agents* **2003**, 22, (2), 155-9.
197. Caffrey, C. R.; Schanz, M.; Nkemngu, N. J.; Brush, M.; Hansell, E.; Cohen, F. E.; Flaherty, T. M.; McKerrow, J. H.; Steverding, D., Screening of acyl hydrazide proteinase inhibitors for antiparasitic activity against Trypanosoma brucei. *Int J Antimicrob Agents* **2002**, 19, (3), 227-31.
198. O'Brien, T. C.; Mackey, Z. B.; Fetter, R. D.; Choe, Y.; O'Donoghue, A. J.; Zhou, M.; Craik, C. S.; Caffrey, C. R.; McKerrow, J. H., A parasite cysteine protease is key to host protein degradation and iron acquisition. *J Biol Chem* **2008**, 283, (43), 28934-43.

199. Abdulla, M. H.; O'Brien, T.; Mackey, Z. B.; Sajid, M.; Grab, D. J.; McKerrow, J. H., RNA Interference of *Trypanosoma brucei* Cathepsin B and L Affects Disease Progression in a Mouse Model. *PLoS Negl Trop Dis* **2008**, *2*, (9), e298.
200. Mallari, J. P.; Shelat, A.; Kosinski, A.; Caffrey, C. R.; Connelly, M.; Zhu, F.; McKerrow, J. H.; Guy, R. K., Discovery of trypanocidal thiosemicarbazone inhibitors of rhodesain and TbcA. *Bioorg Med Chem Lett* **2008**, *18*, (9), 2883-5.
201. Mallari, J. P.; Shelat, A. A.; O'Brien, T.; Caffrey, C. R.; Kosinski, A.; Connelly, M.; Harbut, M.; Greenbaum, D.; McKerrow, J. H.; Guy, R. K., Development of potent purine-derived nitrile inhibitors of the trypanosomal protease TbcA. *J Med Chem* **2008**, *51*, (3), 545-52.
202. Russell, D.; Snyder, S. H., Amine synthesis in rapidly growing tissues: ornithine decarboxylase activity in regenerating rat liver, chick embryo, and various tumors. *Proc Natl Acad Sci U S A* **1968**, *60*, (4), 1420-7.
203. Abdel-Monem, M. M.; Newton, N. E.; Weeks, C. E., Inhibitors of polyamine biosynthesis. 1. Alpha-methyl-(plus or minus)-ornithine, an inhibitor of ornithine decarboxylase. *J Med Chem* **1974**, *17*, (4), 447-51.
204. Casero, R. A., Jr.; Marton, L. J., Targeting polyamine metabolism and function in cancer and other hyperproliferative diseases. *Nat Rev Drug Discov* **2007**, *6*, (5), 373-90.
205. Iwami, K.; Wang, J. Y.; Jain, R.; McCormack, S.; Johnson, L. R., Intestinal ornithine decarboxylase: half-life and regulation by putrescine. *Am J Physiol* **1990**, *258*, (2 Pt 1), G308-15.
206. Childs, A. C.; Mehta, D. J.; Gerner, E. W., Polyamine-dependent gene expression. *Cell Mol Life Sci* **2003**, *60*, (7), 1394-406.

207. Amadasi, A.; Bertoldi, M.; Contestabile, R.; Bettati, S.; Cellini, B.; di Salvo, M. L.; Borri-Voltattorni, C.; Bossa, F.; Mozzarelli, A., Pyridoxal 5'-phosphate enzymes as targets for therapeutic agents. *Curr Med Chem* **2007**, *14*, (12), 1291-324.
208. Coffino, P., Regulation of cellular polyamines by antizyme. *Nat Rev Mol Cell Biol* **2001**, *2*, (3), 188-94.
209. Mangold, U., Antizyme inhibitor: mysterious modulator of cell proliferation. *Cell Mol Life Sci* **2006**, *63*, (18), 2095-101.
210. Wallace, H. M.; Fraser, A. V.; Hughes, A., A perspective of polyamine metabolism. *Biochem J* **2003**, *376*, (Pt 1), 1-14.
211. Persson, L.; Oredsson, S. M.; Anehus, S.; Heby, O., Ornithine decarboxylase inhibitors increase the cellular content of the enzyme: implications for translational regulation. *Biochem Biophys Res Commun* **1985**, *131*, (1), 239-45.
212. Mamont, P. S.; Bohlen, P.; McCann, P. P.; Bey, P.; Schuber, F.; Tardif, C., Alpha-methyl ornithine, a potent competitive inhibitor of ornithine decarboxylase, blocks proliferation of rat hepatoma cells in culture. *Proc Natl Acad Sci U S A* **1976**, *73*, (5), 1626-30.
213. Abdel-Monem, M. M.; Newton, N. E.; Ho, B. C.; Weeks, C. E., Potential inhibitors of polyamine biosynthesis. 2. alpha-Alkyl- and benzyl-(+/-)-ornithine. *J Med Chem* **1975**, *18*, (6), 600-4.
214. Abdel-Monem, M. M.; Newton, N. E.; Weeks, C. E., Inhibitors of polyamine biosynthesis. 3. (+/-)-5-Amino-2-hydrazine-2-methylpentanoic acid, an inhibitor of ornithine decarboxylase. *J Med Chem* **1975**, *18*, (9), 945-8.

215. Kato, Y.; Inoue, H.; Gohda, E.; Tamada, F.; Takeda, Y., Effect of DL-alpha-hydrazino-delta-aminovaleric acid, an inhibitor of ornithine decarboxylase, on polyamine metabolism and growth of mouse sarcoma-180. *Gann* **1976**, 67, (4), 569-76.
216. Relyea, N.; Rando, R. R., Potent inhibition of ornithine decarboxylase by beta,gamma unsaturated substrate analogs. *Biochem Biophys Res Commun* **1975**, 67, (1), 392-8.
217. Harik, S. I.; Hollenberg, M. D.; Snyder, S. H., Ornithine decarboxylase turnover slowed by alpha-hydrazino-ornithine. *Mol Pharmacol* **1974**, 10, (1), 41-7.
218. Metcalf, B. W.; Bey, P.; Danzin, C.; Jung, M. J.; Casara, P.; Vever, J. P., Catalytic Irreversible Inhibition of Mammalian Ornithine Decarboxylase (E.D. 4.1.1.17) by Substrate and Product Analogues. *J. Am. Chem. Soc.* **1978**, 100, (8), 2551-2553.
219. Grishin, N. V.; Osterman, A. L.; Brooks, H. B.; Phillips, M. A.; Goldsmith, E. J., X-ray structure of ornithine decarboxylase from *Trypanosoma brucei*: the native structure and the structure in complex with alpha-difluoromethylornithine. *Biochemistry* **1999**, 38, (46), 15174-84.
220. Carbone, P. P.; Douglas, J. A.; Thomas, J.; Tutsch, K.; Pomplun, M.; Hamielec, M.; Pauk, D., Bioavailability study of oral liquid and tablet forms of alpha-difluoromethylornithine. *Clin Cancer Res* **2000**, 6, (10), 3850-4.
221. Griffin, C. A.; Slavik, M.; Chien, S. C.; Hermann, J.; Thompson, G.; Blanc, O.; Luk, G. D.; Baylin, S. B.; Abeloff, M. D., Phase I trial and pharmacokinetic study of intravenous and oral alpha-difluoromethylornithine. *Invest New Drugs* **1987**, 5, (2), 177-86.

222. Meyskens, F. L., Jr.; McLaren, C. E.; Pelot, D.; Fujikawa-Brooks, S.; Carpenter, P. M.; Hawk, E.; Kelloff, G.; Lawson, M. J.; Kidao, J.; McCracken, J.; Albers, C. G.; Ahnen, D. J.; Turgeon, D. K.; Goldschmid, S.; Lance, P.; Hagedorn, C. H.; Gillen, D. L.; Gerner, E. W., Difluoromethylornithine plus sulindac for the prevention of sporadic colorectal adenomas: a randomized placebo-controlled, double-blind trial. *Cancer Prev Res (Phila Pa)* **2008**, 1, (1), 32-8.
223. Simoneau, A. R.; Gerner, E. W.; Nagle, R.; Ziogas, A.; Fujikawa-Brooks, S.; Yerushalmi, H.; Ahlering, T. E.; Lieberman, R.; McLaren, C. E.; Anton-Culver, H.; Meyskens, F. L., Jr., The effect of difluoromethylornithine on decreasing prostate size and polyamines in men: results of a year-long phase IIb randomized placebo-controlled chemoprevention trial. *Cancer Epidemiol Biomarkers Prev* **2008**, 17, (2), 292-9.
224. Shantz, L. M.; Levin, V. A., Regulation of ornithine decarboxylase during oncogenic transformation: mechanisms and therapeutic potential. *Amino Acids* **2007**, 33, (2), 213-23.
225. Pegg, A. E., Regulation of ornithine decarboxylase. *J Biol Chem* **2006**, 281, (21), 14529-32.
226. Xiao, Y.; McCloskey, D. E.; Phillips, M. A., RNA interference-mediated silencing of ornithine decarboxylase and spermidine synthase genes in *Trypanosoma brucei* provides insight into regulation of polyamine biosynthesis. *Eukaryot Cell* **2009**, 8, (5), 747-55.
227. Ghoda, L.; Phillips, M. A.; Bass, K. E.; Wang, C. C.; Coffino, P., Trypanosome ornithine decarboxylase is stable because it lacks sequences found in the carboxyl

terminus of the mouse enzyme which target the latter for intracellular degradation. *J Biol Chem* **1990**, 265, (20), 11823-6.

228. Phillips, M. A.; Coffino, P.; Wang, C. C., Cloning and sequencing of the ornithine decarboxylase gene from *Trypanosoma brucei*. Implications for enzyme turnover and selective difluoromethylornithine inhibition. *J Biol Chem* **1987**, 262, (18), 8721-7.

229. Willert, E. K.; Fitzpatrick, R.; Phillips, M. A., Allosteric regulation of an essential trypanosome polyamine biosynthetic enzyme by a catalytically dead homolog. *Proc Natl Acad Sci U S A* **2007**, 104, (20), 8275-80.

230. Fairlamb, A. H.; Henderson, G. B.; Bacchi, C. J.; Cerami, A., In vivo effects of difluoromethylornithine on trypanothione and polyamine levels in bloodstream forms of *Trypanosoma brucei*. *Mol Biochem Parasitol* **1987**, 24, (2), 185-91.

231. Milord, F.; Pepin, J.; Loko, L.; Ethier, L.; Mpia, B., Efficacy and toxicity of eflornithine for treatment of *Trypanosoma brucei gambiense* sleeping sickness. *Lancet* **1992**, 340, (8820), 652-5.

232. Iten, M.; Matovu, E.; Brun, R.; Kaminsky, R., Innate lack of susceptibility of Ugandan *Trypanosoma brucei rhodesiense* to DL-alpha-difluoromethylornithine (DFMO). *Trop Med Parasitol* **1995**, 46, (3), 190-4.

233. Bey, P., Danzin, C, Jung, M, Inhibition of Basic Amino Acid Decarboxylases Involved in Polyamine Biosynthesis. In *Inhibition of Polyamine Metabolism - Biological Significance and Basis for New Therapies*, McCann, P. P., Pegg, A.E., Sjoerdsma, A., Ed. Academic Press: San Diego, 1987; pp 1-31.

234. Bitonti, A. J.; McCann, P. P.; Sjoerdsma, A., Restriction of bacterial growth by inhibition of polyamine biosynthesis by using monofluoromethylornithine,

difluoromethylarginine and dicyclohexylammonium sulphate. *Biochem J* **1982**, 208, (2), 435-41.

235. Thyssen, S. M.; Libertun, C., Quantitation of polyamines in hypothalamus and pituitary of female and male developing rats. *Neurosci Lett* **2002**, 323, (1), 65-9.

Chapter 2

Combating Pin-Transfer Cross Contamination in High Throughput Screening

Automated high throughput screening often involves many technical problems which must be resolved prior to and even during the assay process. The following chapter describes one such problem which was encountered and the procedures which were followed in order to minimize it.

Modified from: David C. Smithson, David Bouck, David Shook, Dario Campana, TaoSheng Chen, R. Kip Guy, and Anang A. Shelat *Journal of Biomolecular Screening*, **2009**, in preparation

2.1 Introduction

Modern drug discovery efforts typically involve parallel testing of hundreds of thousands of diverse small molecules. This generally involves the use of small assay volumes and high density formats such as 384 or 1536-well microplates. Testing in this manner necessitates the transfer of extremely small quantities of highly diverse compounds to assay plates reliably and quickly. Historically this has been accomplished by using air or liquid displacement pipetting techniques coupled with disposable tips to eliminate cross-contamination between wells, a phenomenon which can lead to increased false-positive rates. This approach has several drawbacks. The first is increased consumption of test compound. Since air and liquid based pipetting methods are generally limited to volumes above 1 μl , even in modern equipment, concentrated dimethyl sulfoxide (DMSO) stock solutions of test compounds are often diluted into aqueous daughter plates at intermediate concentrations before an aliquot is removed for addition to the assay plate. Once prepared and used for one screening effort, these dilution plates are not reusable. Generally compounds in high-throughput screening libraries are not available in large quantities. Therefore, the efficient use of these compounds is of utmost importance to any high-throughput screening group.¹ The second drawback to this method is the use of disposable tips. These are typically costly, especially if used for only one transfer, and require extensive wash protocols to eliminate cross-contamination if they are to be re-used.² The use of non-disposable fixed tips for

these methods reduces the cost, but leaves the cross-contamination and inefficient compound use problems in effect.

These limitations led to the development of improved liquid transfer technologies which are accurate into the low nano-liter range and allow the efficient transfer of concentrated DMSO solutions directly into assay plates. Currently, the most widely used methods to accomplish this are acoustic transfer (typified by the Labcyte Echo product line) and pin transfer methodologies (such as those developed by V&P Scientific).^{3,4} Acoustic transfer technologies rely on the use of focused acoustic energy to propel small droplets directly from the source plate to the assay plate. This method is accurate to volumes as low as pico-liters and provides a non-contact transfer, completely eliminating both cross contamination and lengthy wash protocols. However, these systems are currently high cost, limiting their use in smaller high-throughput facilities. Furthermore, their use also typically requires a re-working of compound handling procedures, limiting their adoption at larger organizations.

The second commonly used method for nano-scale transfers are pin-tools. These instruments are very simple, low cost and accurate into the single-digit nano-liter range.³ Transfer involves dipping pins (generally steel or coated steel) into the source solution and then into the destination plate. The volume transferred is proportional to the speed at which the pins are removed from the source solution. A faster withdrawal speed will leave a larger hanging droplet at the tip of the pin, while a slower speed will result in a smaller droplet and an overall lower transfer volume. Transfer volumes can also be controlled by changing the depth the pins are dipped into the source solution as well as the time they are left in contact with the destination plate. However, these dynamic

methods of controlling transfer volume typically only results in a two to three fold volumetric range. Greater changes in transfer volumes can be achieved using different pin types. Pins with calibrated slots in the tips which use capillary action to hold and dispense solutions can be used to transfer volumes up to five micro-liters. Since the pins are not disposable, wash protocols must be used to prevent compound carryover and prevent build-up of contaminants on the surface, which can then affect pin transfer performance.

There is very little literature available regarding the long-term use of pins and comparing the performance of different pin types in true high-throughput screening applications. Our group has been using pins for compound transfer since early 2006, while following the manufacturer's recommendations for pin cleaning and care. However, during a recent small-scale screen of our bioactive collection (typically used for the validation of new screens) we became aware of inconsistencies in our data. This triggered a full quality check on our liquid handling instrumentation and ultimately revealed a significant cross-contamination problem. After discovering the problem, we conducted a comprehensive study of the cross-contamination using several different pin types, several cleaning methods, including room-temperature plasma (TipCharger, IonFields, Inc) and a test set of 130 highly diverse compounds from our bioactive collection. Here we report both the detection of the cross-contamination problem as well as the results of our systematic efforts to eliminate it.

2.2 Materials and Methods

Compound Library Tested

The bioactive compound screening library at St. Jude Children's Research Hospital was assembled from commercially available collections including the Prestwick Chemical Library (Prestwick Chemical, Illkirch, France), the LOPAC Collection (Sigma-Aldrich, St. Louis, MO), the Spectrum Collection, the NINDS Collection, the Natural Product Collection and the Killer Plate Collection from Microsource (Microsource Discovery systems, Gaylordsville, CT). The total bioactive test set is approximately 5600 compounds, including many internal replicates. The total number of unique compounds in the collection is approximately 3200 molecules.

ES8 Cytotoxicity Assay

Ewing sarcoma cells with a stably integrated luciferase reporter gene, known as "ES8-luc" were kindly provided by D. Campana (St Jude Children's Research Hospital). Cells were checked for mycoplasma contamination and cultured using standard techniques in RPMI (Gibco) supplemented with 10% FBS (Hyclone) and penicillin-streptomycin (BioWhittaker).

For the cytotoxicity assay, 600 cells were seeded into each well of a white, tissue-culture treated, 384-well plate in 25 ul of growth medium. Cells were incubated overnight and test compounds were added (described below) on the following day. The cells were then incubated for an additional 72 hours prior to reading.

Cell proliferation was assayed by detecting the amount of luciferase generated luminescence from each well. Prior to reading, plates were allowed to cool to room temperature, after which 25 ul of HTS Steady-lite (Perkin Elmer) was added to each well. The plates were vortexed and incubated at room temperature 20 min prior to reading luminescence in an Envision plate reader (Perkin Elmer). Data were normalized to positive and negative controls, staurosporine (LC Labs) and DMSO, respectively, to determine percent activity. Screening run data were subsequently analyzed using custom Pipeline Pilot scripts (SciTegic).

Pins Used in Studies

Three pin sets were used in these studies. The first was labeled 10Hold. These pins were obtained in November, 2007 (FP1S10H, hydrophobic-coated 10 nl slotted steel pins, V&P Scientific, San Diego, CA) and had been used previously for one large-scale primary screen of approximately 350,000 compounds in 1000 source plates, as well as follow-up experiments resulting from this assay for a total of approximately 35,000 transfers. The pins have been cared for according to the manufacture's recommendations, with cleaning in V&P 110 solution before and after each screening run. They were stored dry in a closed drawer between uses.

The second pin set tested were 10 nl slotted un-coated stainless steel pins obtained in March of 2009. (FP1S10, V&P Scientific, San Diego, CA). These pins were used as received from the manufacture and had not been used in any studies prior to those reported in this paper. These pins are referred to as set 10Hstainless.

The third pin set tested were 10 nl slotted hydrophobic coated steel pins (FP1S10H, V&P Scientific, San Diego, CA). These pins were used as received from the manufacture. These pins are hereafter referred to as 10Hnew.

Pintool Wash Protocols

Wash liquids were contained in flat 50 ml polypropylene reservoirs. A dip is defined as entrance and exit from the liquid. All dips were performed to a depth of 0.5 cm below the surface of wash liquid. All wash protocols were performed on a BiomekFXP workstation (Beckman Coulter, Fullerton, CA). Speeds were programmed as percentages of maximal speed – 1% corresponded to approximately 1 mm/sec. All pins were subjected to complete cleaning before and after each use, as well as between carryover test-sets. Room temperature plasma was generated using a TipCharger instrument on loan from IonFields Inc.⁶

Complete Cleaning

1. 3 dips in VP110 (V&P Scientific, San Diego, CA), 15 mm/sec – 5 sec submerged pause on final dip
2. 1 blot on lint-free blotting paper (V&P Scientific, San Diego, CA), 15 mm/sec – 3 sec pause in contact with paper
3. Repeat steps 1 and 2 twice more (total of 3 dip/blots)
4. 3 dips in DI water, 15 mm/sec – 5 sec submerged pause on final dip
5. 1 blot on lint-free blotting paper (V&P Scientific, San Diego, CA), 15 mm/sec – 3 sec pause in contact with paper

6. Repeat steps 4 and 5 twice more (total of 3 dip/blots)
7. 3 dips isopropanol, 15 mm/sec – 5 sec submerged pause on final dip
8. 1 blot on lint-free blotting paper (V&P Scientific, San Diego, CA), 15 mm/sec – 3 sec pause in contact with paper

Total Cycle Time: 9.5 minutes

HTS Cleaning (HTS)

1. 3 dips in DMSO at 15 mm/sec – 5 sec submerged pause on final dip
2. 3 dips in isopropanol at 15 mm/sec – 5 sec submerged pause on final dip
3. 3 blots on lint-free blotting paper (V&P Scientific, San Diego, CA) at 15 mm/sec – 5 sec pause in contact with paper on final dip

Total Cycle Time: 37 seconds

V&P Cleaning (VP)

1. 3 dips in DMSO at 15 mm/sec – 5 sec submerged pause on final dip
2. 3 dips in DI water at 15 mm/sec – 5 sec submerged pause on final dip
3. 1 blot on lint-free blotting paper (V&P Scientific, San Diego, CA), 15 mm/sec – 3 sec pause in contact with paper
4. 3 dips in isopropanol at 15 mm/sec – 5 sec submerged pause on final dip
5. 1 blot on lint-free blotting paper (V&P Scientific, San Diego, CA), 15 mm/sec – 3 sec pause in contact with paper

Total Cycle Time: 70 seconds

TipCharger Cleaning (TC)

1. 3 dips in DI water at 15 mm/sec – 5 sec submerged pause on final dip
2. 1 dip in TipCharger (IonFields, Inc, Moorestown, NJ), 40 sec exposure to plasma

Total Cycle Time: 47 seconds

TipCharger-HTS Cleaning (TC-HTS)

1. 3 dips in DMSO at 15 mm/sec – 5 sec submerged pause on final dip
2. 3 dips in isopropanol at 15 mm/sec – 5 sec submerged pause on final dip
3. 1 dip in TipCharger (IonFields, Inc, Moorestown, NJ), 40 sec exposure to plasma

Total Cycle Time: 82 seconds

Pintool Volumetric Calibration

Volumetric calibration of the pintool was performed using fluorescein. A 10mM fluorescein (Fluka, Seelze, Germany) stock solution was prepared in DMSO. This stock solution was then used to make a 1 to 2 dilution series in 1X Dulbecco's Phosphate Buffered Saline (DPBS), pH 7.1, (Mediatech Inc, Herndon, VA) via hand pipetting in 150 μ l final volume. This was performed in octuplet. A 25 μ l aliquot of each dilution point was then transferred to a black-clear bottomed polystyrene microplate (#3702, Corning Life Sciences, Acton, MA) and the absorbance read using a 480 nM filter on an Envision Multilabel Reader (Perkin Elmer, Waltham, MA). The resulting data was fit using a linear regression model in Microsoft Excel, yielding a linear detection range from 0.2 to 25 μ M with an R^2 of 0.9997. Ten microliters of the 10 mM fluorescein stock was then added to a 384-well polypropylene plate (#3656, Corning Life Sciences, Acton,

MA) for use in pin transfer experiments. Calibration was performed on a BioMeckFXP (Beckman Coulter, Fullerton, CA) using pins and pin-racks from V&P Scientific (San Diego, CA). Typical calibration experiments transferred approximately 25 nl of 10 mM fluorescein stock solution into 25 μ l of DPBS in black, clear-bottomed polystyrene plates. Absorbance at 480 nm was read using the Envision plate reader. Data from the standard curve was then used to calculate actual volumes transferred by the pins. The exact calibration protocol is detailed below:

Alternatively, for low concentrations of fluorescein, calibration was performed utilizing fluorescence readout as opposed to absorbance. In this case the standard curve was linear from 0.78 μ M to 25 pM. Fluorescence readings were taken using an Envision Multilabel Reader (Perkin Elmer, Waltham, MA) equipped with a 480 nm excitation filter and a 535 nm emission filter. The calibration was performed as described above with the exception of the final plate reading method and the absolute concentrations of fluorescein used.

Carryover Detection

Carryover experiments were performed using a total of four assay plates and four drug plates. The first drug plate was filled with DMSO to control for any contamination that may be present on the pins prior to exposure to test compound. The second drug plate was filled with test compounds in 10 mM DMSO stocks. The third and fourth drug plates were again filled with DMSO. Carryover was defined as activity that was outliers from negative control populations on either the third or fourth assay plates as determined by robust statistical methods. The outlier cutoffs were calculated as the *upper fourth* plus

1.5 times the *fourth spread* (the upper fourth and fourth spread are similar to the third quartile and interquartile range, respectively), which corresponds to a *p*-value ~ 0.005 for normal distributions. However, such cutoff criteria are more robust to population deviations from normality.⁵ A typical carryover experiment is detailed below:

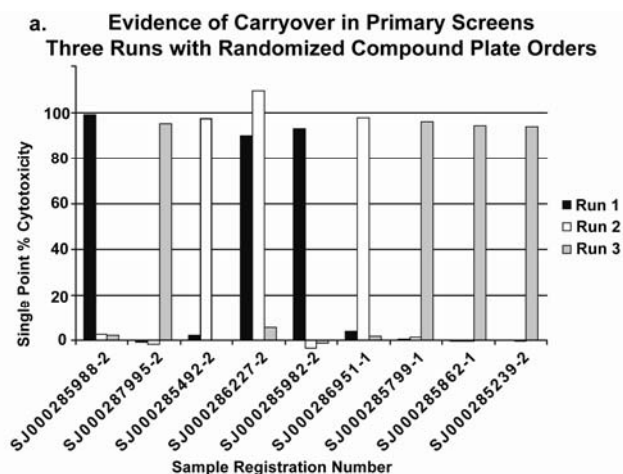
1. Complete cleaning of pins.
2. Standard cleaning of pins (methods used varied – see cleaning methods above)
3. Transfer of 25 nl DMSO from drug plate 1 to assay plate 1
4. Standard cleaning of pins
5. Transfer of 25 nl 10 mM variable test compound or fluorescein from drug plate 2 to assay plate 2
6. Standard cleaning of pins
7. Transfer of 25 nl DMSO from drug plate 3 to assay plate 3
8. Standard cleaning of pins
9. Transfer of 25 nl DMSO from drug plate 4 to assay plate 4
10. Complete cleaning of pins
11. Standard cleaning of pins
12. Transfer of 25 nl 10 mM staurosporine (positive control) to appropriate wells on all assay plates. (standard cleaning of pins between each assay plate)
13. Complete cleaning of pins

Each experiment was repeated in triplicate for a total of 12 assay plates for each carryover condition tested. Assay plates were drugged using a BiomekFXP workstation (Beckman Coulter, Fullerton, CA). Custom protocols were written for each pin-cleaning method tested.

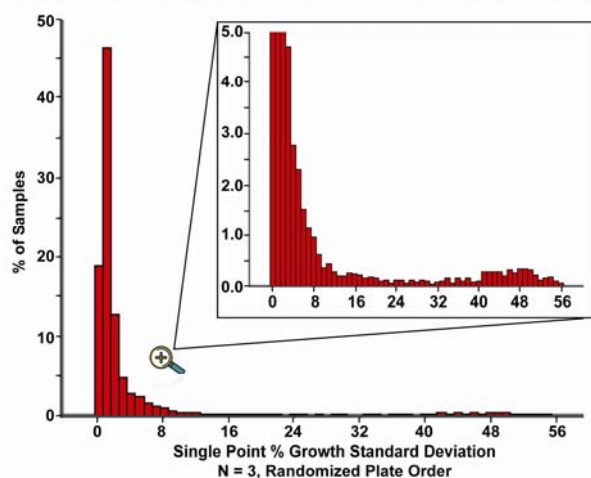
2.3 Results

Primary Screening Results and Initial Carryover Detection

The initial evidence for compound carryover was detected after using the ES8 cytotoxicity assay to screen the bioactive collection in triplicate. Each screen replicate consisted of 18 plates, for a total of 54 tested plates. Compound plate order was randomized between each replicate. The overall average Z' for all replicates was 0.89 indicating a well-behaved assay system. The EC_{50} of control compounds added in dose-response to each plate was also extremely replicable, with an average variance of 7.4%. However, it was noticed that a small sub-set of compounds were not behaving in a replicable manner. These compounds would appear as potent hits in one run, but not in the other two. (**Fig 1a**). The effect of these compounds can also be seen upon examination of the standard deviations of the replicate measurements. While most compounds have standard deviations less than 8%, a small bump can be seen at approximately 50%. (**Fig 1b**). Suspecting that this was the result of compound carryover, the Pearson correlation of well activity with the activity of the same well in neighboring plates was determined. (**Fig 1c**). This clearly indicated that the well activity in plate immediately prior to or immediately after the plate of interest was highly correlated.



b. Standard Deviations for All Wells Over Three Replicates



c. Correlation of Well Activity with Activities of the Same Well on Neighboring Plates

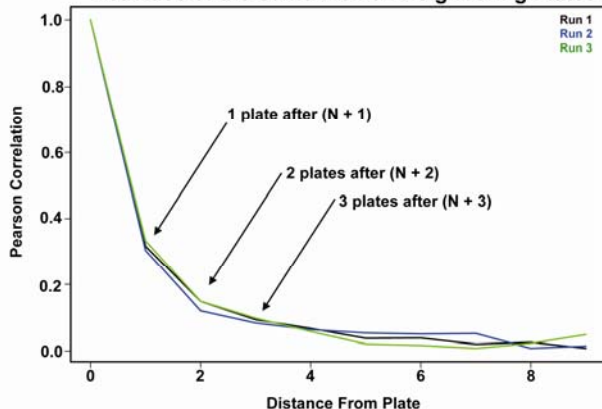


Fig 2.1

Fig 2.1 - Detection of carryover in primary screening data

1a. Data from replicate screening runs of the St. Jude Bioactive collection. Each run was performed using randomized compound plate order. Note the extreme differences between replicates in this set of compounds. **1b.** The standard deviation for all wells over the three replicates. Percent activity was defined as described in materials and methods. While most compounds have a standard deviation of less than 8 %, a small subset was observed to have standard deviations approaching 50%. **1c.** The Pearson correlation of well activity with the activity of the same well on neighboring plates. Note that plates either one plate prior to or one plate after the plate of interest are highly correlated, while the correlation decreases as a function of the distance from the plate of interest. The presence of this correlation is highly indicative of cross-contamination.

Selection of Probable Carryover Compounds

In order to study the carryover phenomena in greater detail, we applied a simple heuristic to the triplicate ES8 % growth inhibition values to select a test set composed of 52 compounds predicted to show carryover behavior and 78 “control” compounds predicted to behave normally. Since most compounds (>90%) showed little or no activity in the assay, the chance that an active compound in plate n would be preceded by another active compound in the corresponding well of plate $n+1$ in all three independent replicates of the assay (with randomized plate order) is small. Such an observation is more likely to result from active compound cross-contaminating inactive compound in the subsequent plate. A compound with growth inhibition >50% in all three replicates was defined as “active”. We defined potential carryover molecules as any “active” with median growth inhibition $Y\%$ in plate n that was followed by compounds showing $>1/2Y\%$ growth inhibition in all three $n+1$ plates. In contrast, any “active” in plate n followed by compounds with <10% activity in all three $n+1$ plates was defined as normal.

Pintool Quality Control

Immediately after the pintool cross contamination problem was detected, the pins used in the screening experiment (10Hold) were subjected to standard fluorescence intensity based volumetric calibration. As expected, these pins exhibited poor behavior, with a CV greater than 25% and a clear bio-modal distribution. (**Fig 2.2a**). Examination of the pins by light microscopy showed significant buildup of debris on the pin surface

and collecting in the slot. The pins were cleaned by repeated complete cleaning cycles and tested a second time with identical results.

Fig 2.2

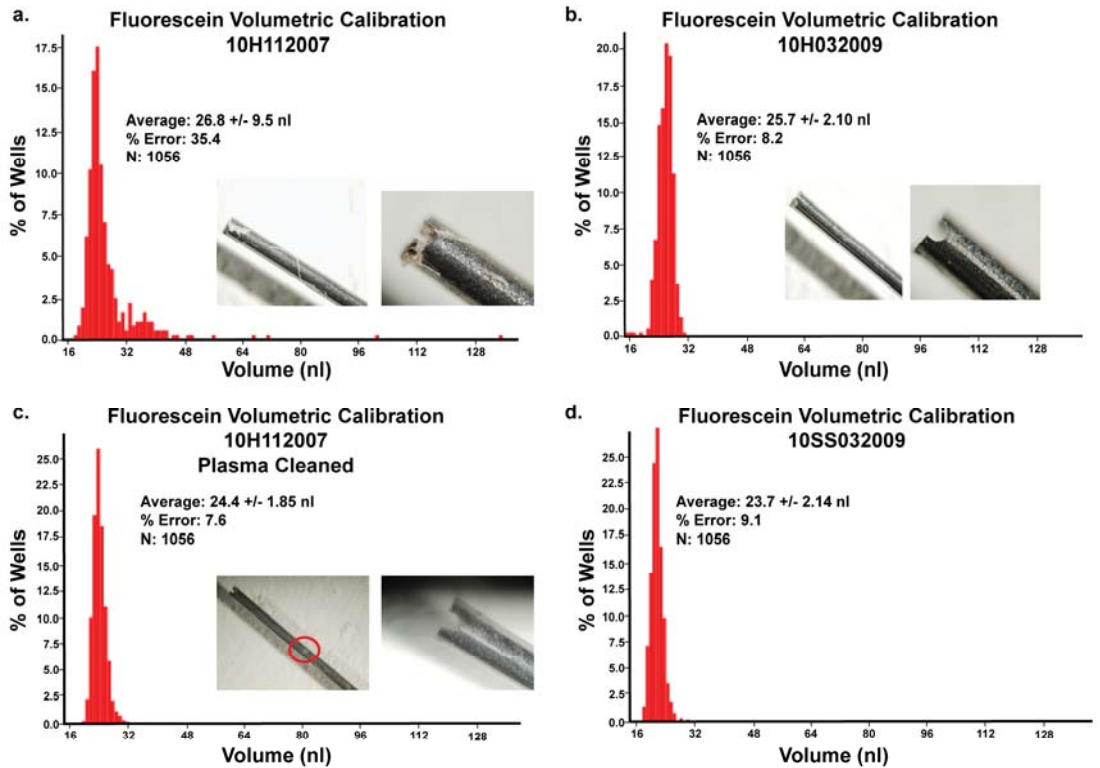


Figure 2.2 - Volumetric data for various pin sets. 2.2a. Volumetric performance of the old hydrophobic coated pins (10Hold). Note the bimodal character and poor overall percent error. Data was collected at 15 mm/sec withdrawal speed on the BiomekFX as described. Also note the extreme fouling seen the representative pin pictured here. **2.2b.** Volumetric performance of new hydrophobic coated pins (10Hnew). Note the lack of fouling and clean appearance of the representative pin seen here. Data was collected at 15 mm/sec withdrawal speed on the BiomekFX as described. **2.2c.** Volumetric performance of the plasma cleaned older hydrophobic coated pins (10Hold post-plasma). Note the lack of fouling visible on the representative pin and the presence of the cleaning line indicating the depth to which the pins were dipped in the plasma. Also note the like-new volumetric performance. These pins were cleaned using a single 40 second exposure to room temperature plasma prior to volumetric calibration. **2.2d.** Volumetric performance of non-coated stainless steel pins. This data was collected at 20 mm/sec withdrawal speed. The volumetric performance of these pins was comparable to that of the hydrophobic coated pins.

Comparison with new pins showed a significant deterioration of volumetric performance (Fig 2.2b). The pins were then subjected to 40 seconds of exposure to room temperature plasma generated using the TipCharger instrument resulting in a return to like-new volumetric performance (Fig 2.2c). Stainless steel pins were also shown to perform comparably with the hydrophobic coated pins in the volumetric transfer tests. (Fig 2.2d).

Testing of Probable Carryover Compounds

The test set of 130 compounds was subjected full dose response studies as well as our carryover detection experiment. (Fig 2.3) Of the 130 compounds selected, 107 displayed EC₅₀ values below 25 μM.

Figure 2.3

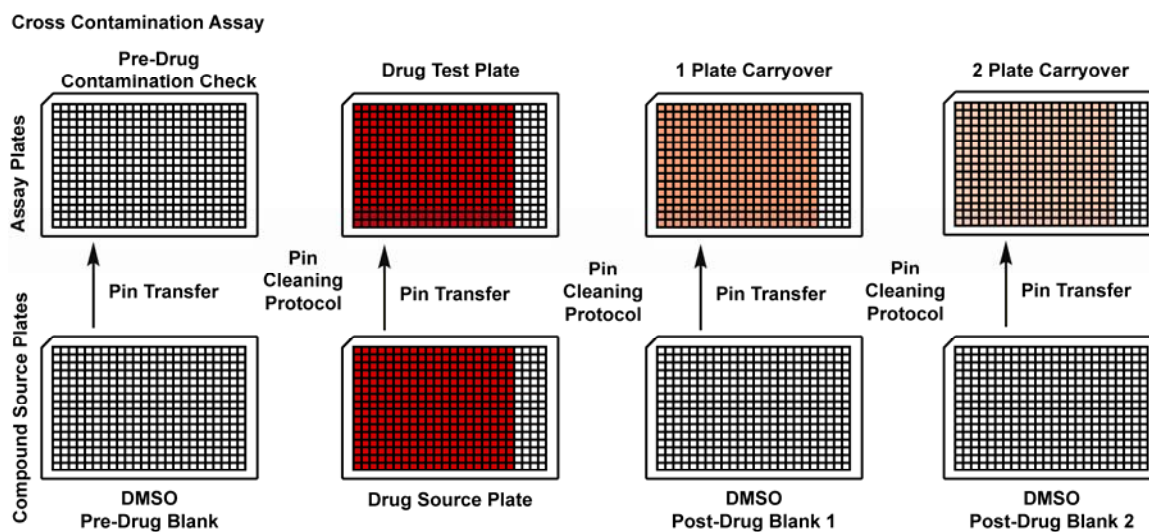


Figure 2.3 – Schematic of a typical cross contamination experiment. Before each replicate, pins were subjected to the complete cleaning protocol. Control compounds were added to test plates from a separate source plate.

Position was randomized during plating of the test compounds in the source plate in order to control for the effects of specific pin condition. The initial carryover experiment was performed using the HTS cleaning method along with the 10Hold pins prior to plasma

cleaning in order to establish a baseline for worst-case scenario behavior. Of the 52 predicted problematic compounds, 47 carried over one plate while 24 carried over two plates. From the 78 predicted non-carryover compounds, 6 carried over one plate and only one carried over two plates. This confirmed that the compounds we had predicted to be problematic were in fact causing cross-contamination artifacts.

To determine whether carryover was an effect of damage to specific pins, or characteristics of specific compounds, the 10Hold pre-plasma cleaning carryover compounds were mapped onto the volumetric data for each pin. (**Fig 2.4a**). Carryover compounds were observed to come preferentially from pins which were transferring abnormally large volumes. After plasma cleaning, the carryover and non-carryover pins were equally distributed. (**Fig 2.4b**). When compound potencies were compared to their carryover behavior, no strong correlations were observed. The pre-plasma 10Hold pins displayed higher % error on average when compared with their post-plasma cleaning performance. (**Fig 2.4c-d**) This analysis shows that detection of compound carryover is not simply a function of potency.

Figure 2.4

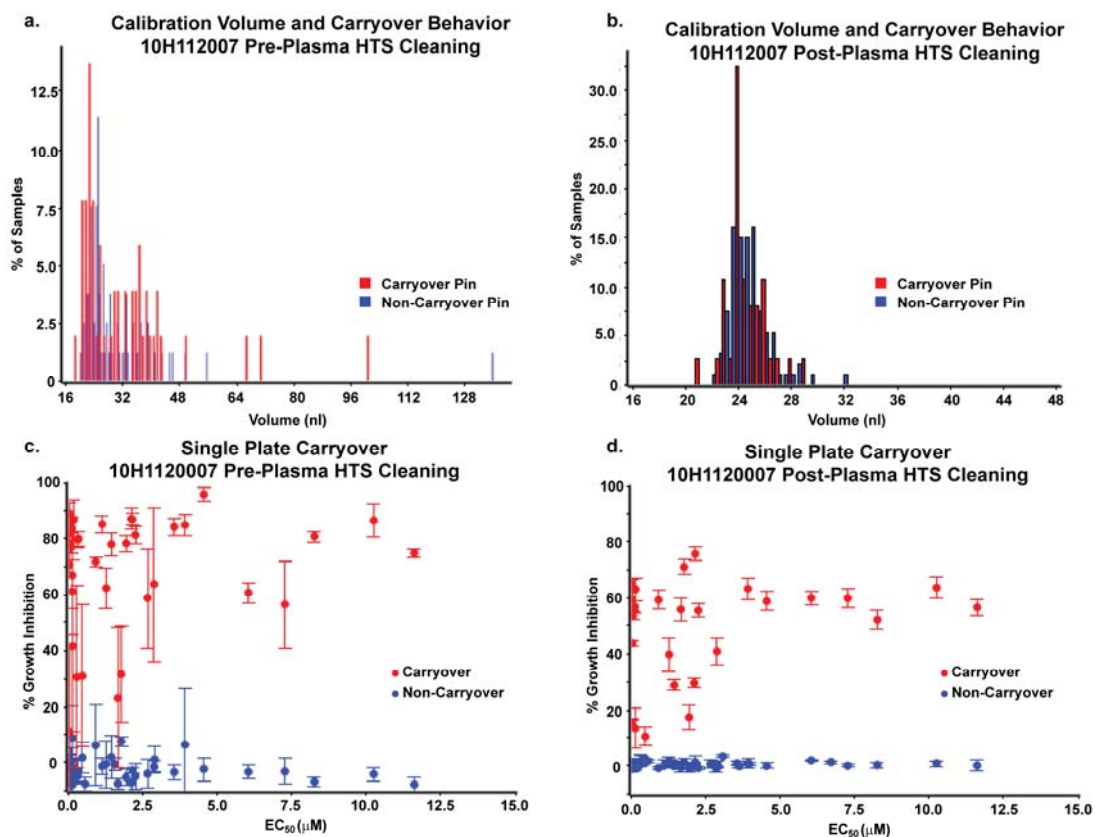


Figure 2.4 - Analysis of carryover patterns. 2.4a. Pin carryover performance mapped onto volumetric performance data for the pre-plasma cleaned old hydrophobic pins (10Hold). Note that carryover pins are preferentially located in the 2nd bump of the volumetric data. This is not unexpected, since pins which deliver larger volumes would logically be more susceptible to cross-contamination issues. **2.4b.** Pin carryover performance mapped onto volumetric performance data for post-plasma cleaned old hydrophobic pins (10Hold). Here carryover pins are equally distributed throughout the volumetric population, indicating that carryover is no longer a function of pin liquid volume delivery. **2.4c.** Single plate carryover data for the pre-plasma cleaned 10Hold pins as a function of compound EC₅₀. Note the high variability seen in this data set, as well as the fact that carryover is not a function of compound potency. **2.4d.** Single plate carryover data for the post-plasma cleaned 10Hold pins. Here the data is much less variable and while carryover is still present, the relative percent inhibition is slightly lower in all cases. This suggests that the high carryover signals were likely the result of fouling on the pin surface, a phenomena which could also lead to stochastic variability in the pin behavior. However, when the fouling is removed, the remaining carryover is likely to be the result of more permanent damage to the pin coating.

Testing of Pin Type and Cleaning Method Effects

The first pin type tested with diverse cleaning methods was the 10Hold pin set (**Fig 2.5a**). As noted previously, our standard HTS cleaning method resulted in 53 carryover compounds with these pins. The use of room temperature plasma cleaning (TC cleaning method) resulted in 34 of the predicted carryover and two of the predicted non-carryover compounds displayed detectable activities one plate away. Twenty-two of the predicted problematic and none of the predicted non-problematic compounds were also detectable two plates out. Combining this method with the standard HTS cleaning protocol (TC-HTS cleaning method) yielded 35 predicted carryover and one predicted non-carryover compounds with detectable activity one plate away. This number decreased to 15 predicted carryover compounds when data from two plates out was examined. Use of the more rigorous V&P cleaning protocol with post-plasma 10Hold pins showed 31 of the 52 predicted carryover compounds and two of the predicted non-carryover compounds with detectable activities one plate away. Only 17 of the predicted carryover and none of the predicted non-carryover compounds had detectable activities two plates out.

In a final effort to restore the 10Hold pins to “like-new” behavior, the pins were sonicated in undiluted V&P110 solution for 15 minutes, as recommended by V&P Scientific. Following this they were again tested for carryover using the V&P cleaning method. Under these conditions, 24 predicted carryover and one predicted non-carryover

compound were detectable one plate away. Twelve of the predicted carryover compounds also displayed detectable activity two plates out.

In contrast to the results with the 10Hold pins, use of the 10Hnew pins with the HTS cleaning method resulted in only 10 of the predicted carryover compounds with cross contamination one plate away, and none showing contamination two plates out (**Fig 2.5b**). None of the predicted non-carryover compounds showed detectable cross contamination. Using the TC cleaning method with these pins, only six predicted problematic compounds were detectable one plate away. None of the predicted non-carryover compounds displayed any detectable activities, and none of the test set was detectable two plates out. With the TC-HTS cleaning method, only six of the predicted problematic compounds were detectable one plate out. No compounds were detected two plates away. Using the V&P cleaning protocol, five compounds from the predicted carryover set displayed activities one plate out, with one compound from this set detectable two plates away. None of the predicted non-carryover compounds had detectable activities even one plate away. The uncoated stainless steel pins (10Hstainless) displayed similar performance to the 10Hnew pins (**Fig 2.5c**). Using the HTS cleaning method only six of the predicted carry over compounds were positive over one plate, and only one displayed detectable contamination two plates out. All other cleaning methods applied to these pins (TC, TC-HTS and V&P) resulted similar results.

Finally, the time dependence for effective cleaning using the TipCharger was determined utilizing the TC protocol outlined in materials and methods, but with the pins exposed to plasma for varying amounts of time. The pins used were the new hydrophobic coated pins (10Hnew). If the pins were not exposed to plasma at all, but were simply

dipped in water for cleaning, 117 of the 130 compounds, including all 52 predicted carry-over compounds displayed significant activity one plate out (**Fig 2.5d**). However, after only ten seconds of exposure to plasma, the number decreased to 15. The performance remained the same with 20 seconds of exposure, but after 40 seconds, the number of detectable cross-contamination compounds dropped to 6, the same level as all other cleaning methods tested.

Figure 2.5

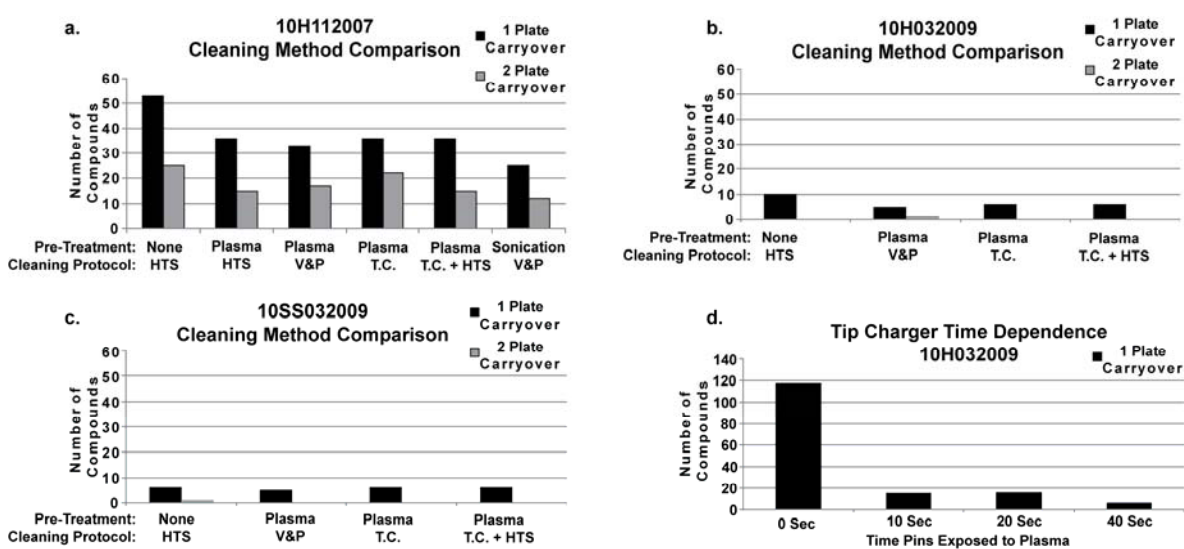


Figure 2.5 Comparison of cleaning methods. - **2.5a.** Performance of the old hydrophobic coated pins (10Hold) using various cleaning methods. While use of the TipCharger did decrease the number of carryover compounds, it did not eliminate the phenomenon. All cleaning methods performed in a fairly comparable manner for the test set. Further cleaning by sonication of the pins in undiluted VP110 for 15 minutes did decrease carryover somewhat, but was again unable to eliminate it, suggesting that the pins had become irreversibly damaged over time. **2.5b.** Performance of the new hydrophobic coated pins in the carryover experiments. Note that all methods performed similarly and that carryover is much reduced compared to the older hydrophobic pins. **2.5c.** Performance of the new non-coated stainless steel pins in the carryover experiments. Note that these pins perform comparably to the hydrophobic coated pins, and in some cases out-perform them. **2.5d.** Time dependence of the TipCharger instrument. Note that exposure to room temperature plasma for only 10 seconds is sufficient to reduce carryover behavior significantly, although a further decrease is seen after a 40 second exposure.

Figure 2.6

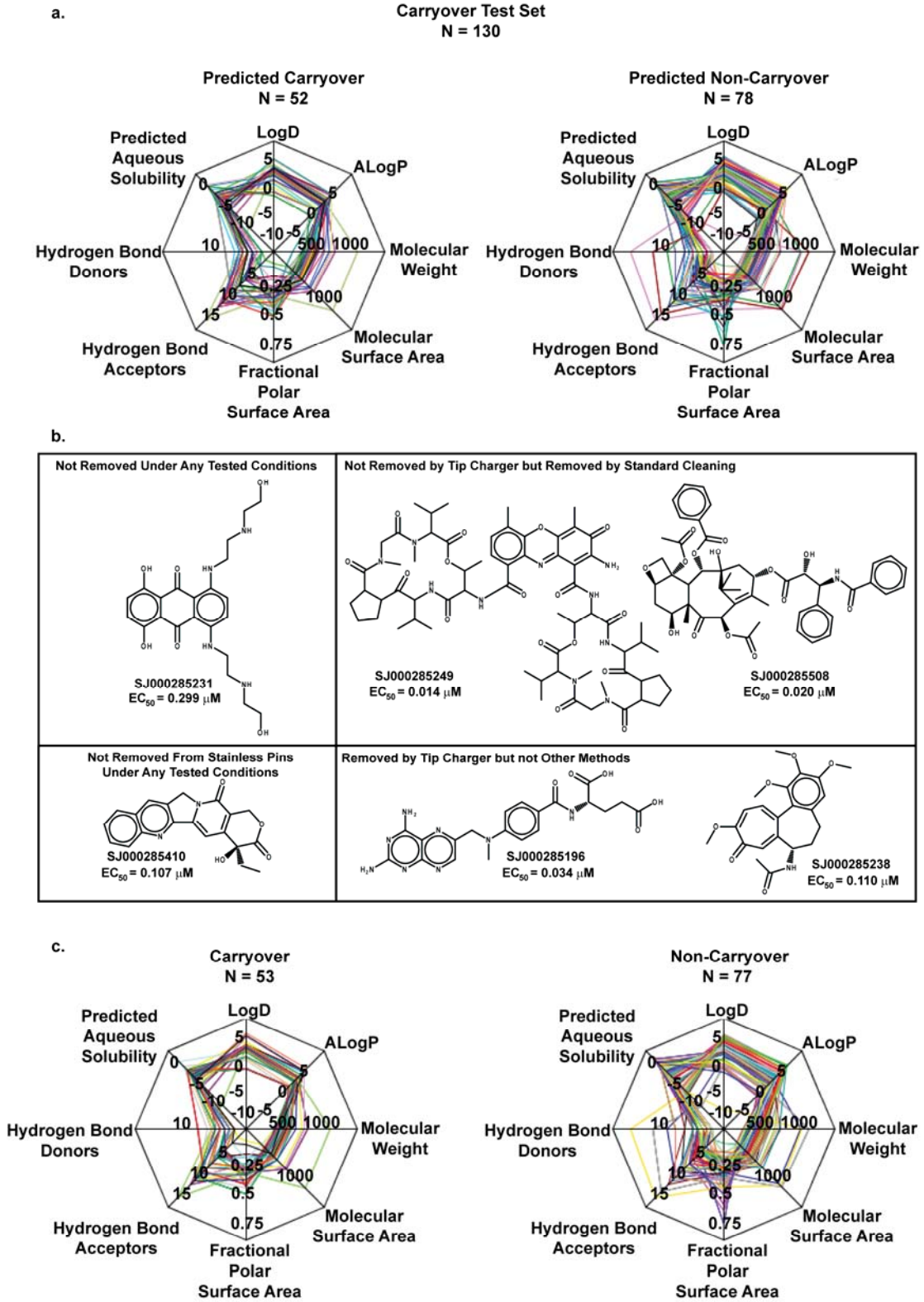


Figure 2.6 - Characteristics of the carryover test set and representative structures of problematic compounds. - **2.6a.** The full test set of predicted carryover and predicted non-carryover compounds. Note that both sets are highly diverse and are similar with respect to most chemical descriptors. **2.6b.** Representative structures of problematic compounds. SJ000285231 was particularly poorly behaved and was not removed under any conditions tested. **2.6c.** Characteristics of experimentally validated carryover and non-carryover compounds. These sets were classified using data from the pre-plasma 10Hold pins using the HTS cleaning method. Again, note the similarity between the two sets. This data suggests that carryover is a multi-faceted problem involving both the specific compound and the specific pin being used to transfer it.

Characterization of the compound test set using standard computed chemical descriptors along with the structures of particularly problematic compounds is shown in **Fig 2.6.**

Fluorescein Characterization of Carryover

After testing the pins using our variable compound test set, it was decided to attempt to detect carryover behavior using a non-biological assay, using fluorescein. The pins were calibrated in a manner identical to that used in the volumetric performance assays using the fluorescence readout, after which they were subjected to a typical carryover experiment. Carryover volume in plate immediately following the fluorescein stock plate was calculated based on the standard curve. The experiment was run in triplicate. An average carryover volume of 0.15 nl with a maximum of 1.68 nl was found using the post-plasma cleaning 10Hold pins. (**Fig 2.7a**) This corresponds to an in well concentration of 0.06 and 0.67 μM respectively. When the 10Hnew pins were tested, no repeatable carryover was detectable, and average concentrations were below the 0.025 pM detection limit of our assay. (**Fig 2.7b**). The replicates from both sets of pins were then compared to determine if carryover was pin specific or more stochastic in nature. In the case of the 10Hold pins, carryover was clearly related to specific pins (**Fig 2.7c**)

while in the case of the 10Hnew pins, carryover was much more stochastic in nature (**Fig 2.7d**).

Figure 2.7

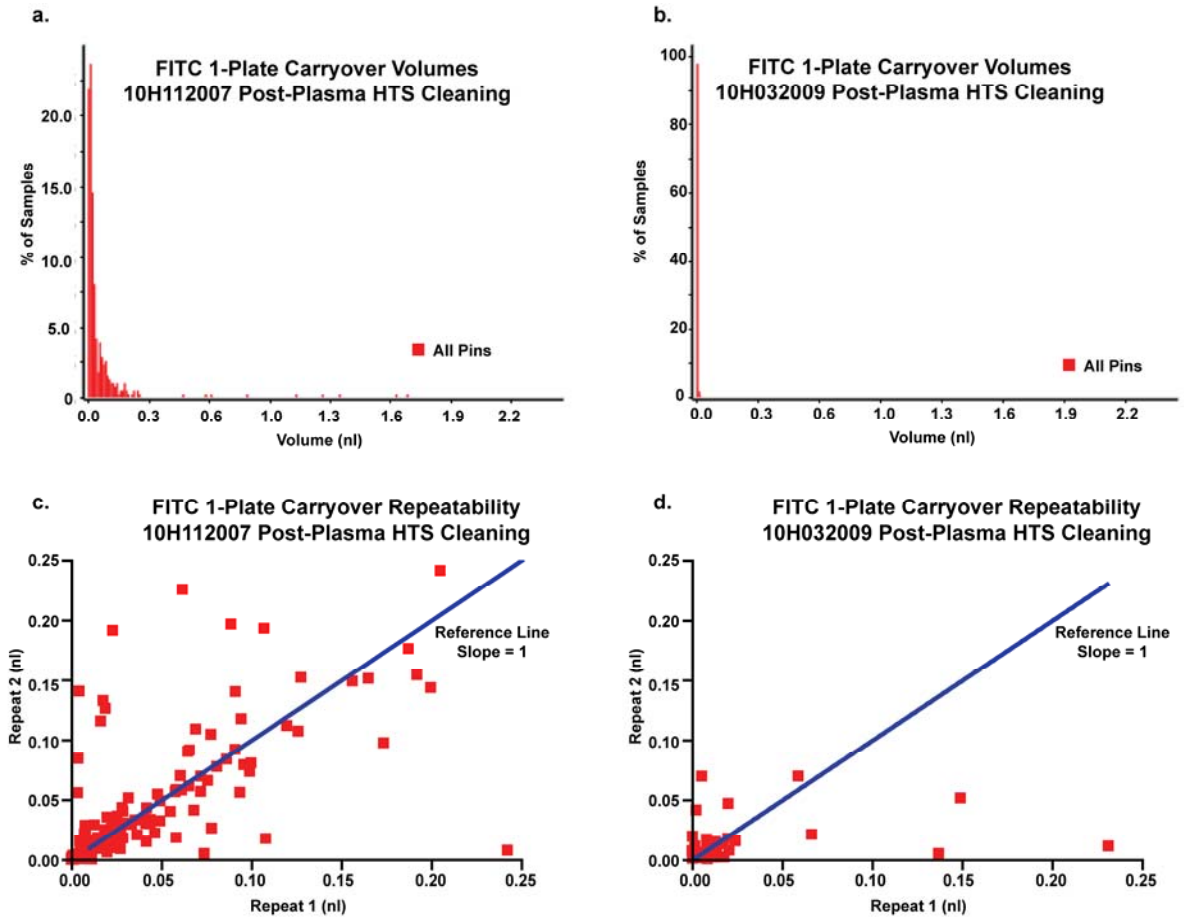


Figure 2.7 - Fluorescein carryover performance of 10Hold and 10Hnew pins. 2.7a.

Carryover volume as determined by FITC volumetric calibration for the post-plasma 10Hold pins. Average carryover volume was 0.1 nl with several pins carrying up to 2 nl FITC one plate out. **2.7b.** Carryover volume as determined by FITC volumetric calibration for the 10Hnew pins. Average carryover was below detectable limits. **2.7c.** Repeatability of carryover behavior for the 10Hold pins (post-plasma). Note that most pins were fairly replicable, with some exceptions, indicating that carryover is a function of pin condition. **2.7d.** Repeatability of the carryover behavior for the 10Hnew pins. Note that carryover behavior here is much more stochastic in nature, indicating that carryover is likely not a function of pin condition in this case.

2.4 Discussion

The results of this study indicate that compound carryover caused by pin-transfer instruments is a highly complex phenomenon. It is a function of both compound identity as well as pin type and pin condition. The greatest contribution to carryover is certainly pin condition. New pins out-perform old pins significantly under all conditions. Interestingly, volumetric performance did not correlate with carryover performance. This indicates that quality control measures that simply examine volumetric delivery variance will not be effective in detecting potential cross-contamination issues. However, the fluorescein carryover experiment was successful in detecting this variance, suggesting that experiments of this type would be more useful in tracking pin performance than simple volumetric calibration runs.

The comparison of pin cleaning protocols using a wide range of test compounds resulted in several interesting observations. The first is the absence of large differences between the various pin cleaning methods tested. However, of the methods tested, the best performing condition was the V&P cleaning protocol in conjunction with the new hydrophobic coated pins (10Hnew). Use of the stainless steel pins added only two compounds which were not problematic using the hydrophobic pins and decreased the absolute potencies of the observed carryover phenomena. This fact, coupled with the comparable volumetric performance seen between the un-coated and coated pins suggests that use of the 10-fold less expensive uncoated pins is a viable option in high-throughput screening. Furthermore, use of the stainless steel pins simplifies major cleaning efforts as damage to the coating of the pins is not a concern.

Another finding of this study was that the use of room-temperature plasma to clean small molecules is as effective as other methods. This plasma is generated by the TipCharger instrument by exposing normal atmosphere to high voltages, resulting in the production of a mixture of nitrogen and oxygen plasmas.⁶ The production of this plasma results in a large number of free electrons which interact with the surroundings, transferring large amounts of energy to both solvent and solute molecules on the surface of the pin. This results in the rapid breakdown of small molecules into theoretically inactive fragments. Interestingly, the TC-HTS cleaning method in association with the uncoated 10Hstainless pins was highly efficacious in removing all except three of the test compounds. Only the 10Hnew pins cleaned using the VP protocol resulting in comparable cross-contamination performance. A further advantage of using this method for pin cleaning was the remarkable removal of fouling from the 10Hold pins. A single 40-second exposure to the plasma was sufficient to restore the pins to like-new volumetric performance.

The use of this instrument in regular cleaning regimens would likely prevent the build-up of fouling on the pin surfaces, resulting in overall improved performance without the need to conduct other offline rigorous cleaning protocols. While the majority of our testing was performed using 40 seconds of exposure to the plasma, time dependency experiments showed that only a slight decrease in performance occurred with shorter exposures of 10 or 20 seconds. It should be noted that in its current form, it is necessary to dip pins in a secondary non-DMSO solvent before use of the TipCharger instrument, as large levels of DMSO can interfere with effective formation of plasma. However, by dipping in either water or isopropanol first, we were able to minimize this

phenomenon. While this cleaning method did result in much improved volumetric performance, the cross-contamination problems in the 10Hold pins was not removed, suggesting that further damage to the pins unrelated to fouling issues was likely contributing. Further cleaning of this pin set by sonication in undiluted VP 110 solution was also unable to recover the old pins to like new performance with respect to carryover.

Although we were not able to either completely eliminate carryover, or recover old-pins to like-new performance in this regard, we were able to develop a method that was highly successful in detecting the presence of carryover in real screening data. This relatively simple method, which correlates well activity on one plate with the activities of the same well on surrounding plates proved highly efficacious in predicting compounds which were indeed exhibiting cross contamination behavior. Utilization of this technique allows the detection of problematic pin performance without the need to perform more stringent tests such as those used in this study. Pin sets displaying this behavior can then be removed from service or subjected to more vigorous cleaning methods such as sonication in undiluted VP110.

In conclusion, we have rigorously tested a wide range of cleaning methods and pin types commonly used in high-throughput screening efforts using a large and diverse set of test compounds. We have found that while most cleaning methods perform relatively comparably when new pins are used, and that uncoated stainless steel pins perform as well as the more costly hydrophobic coated pins in typical high throughput screening settings. Furthermore, we have developed an algorithm capable of detecting deteriorating pin performance in normal screening data, without the need to perform rigorous cross-contamination experiments. This study represents the most thorough set of

experiments examining this phenomenon currently in the literature, and the data reported here will be valuable for all screening groups using pin transfer techniques.

References

1. Burr I, Winchester T, Keighley W, Sewing A: Compound management beyond efficiency: *J Biomol Screen* 2009; 14:485-91.
2. Astle T, Kowitz A: Accuracy and Tip Carryover Contamination in 96-Well Pipetting: *J. Biomol Screen* 1996; 1:211-216.
3. Cleveland P, Koutz PJ: Nanoliter dispensing for uHTS using pin tools: *Assay Drug Dev Technol* 2005; 3:213-25.
4. Ellson R, Mutz M, Browning B, Lee L, Miller M, Papen R: Transfer of Low Nanoliter Volumes between Microplates Using Focused Acoustics - Automation Considerations: *JALA* 2003; 8:29-34.
5. Hoaglin DC, Mosteller, Frederick, Tukey, John W.: *Understanding Robust and Exploratory Data Analysis*. New York: John Wiley and Sons, Inc., 1983.
6. Hensley P: TipCharger(R), A Breakthrough Wash Technology: *JALA* 2002; 7:64-65.

Chapter 3

Optimization of a Non-Radioactive High-Throughput Assay for Decarboxylase Enzymes

Before a large scale high throughput screening effort can take place, rigorous optimization of the primary assay as well as design and implementation of the secondary assay panel is necessary. The following details this process.

Modified from David C. Smithson, Anang A. Shelat , Jeffrey Baldwin, Margaret A. Phillips and R. Kiplin Guy, *Assay and Drug Development Technologies* **2009**, In Press

INTRODUCTION

Decarboxylase enzymes represent a significant target family for the development of therapeutic agents. Ornithine decarboxylase (ODC) and S-adenosylmethionine decarboxylase control the polyamine biosynthetic pathway, a therapeutic target in both oncology and parasitology.^{1, 2} Other medically relevant decarboxylases include histidine decarboxylase, a target in the inflammation pathway, DOPA decarboxylase, a Parkinson's disease target, and diaminopimelate decarboxylase, a potential antibiotic target.^{3,4,5} In spite of the importance of the enzyme class, few decarboxylases have been subjected to large scale drug discovery efforts, in part due to difficulty in quantifying their activities in a manner compatible with modern high-throughput approaches. Classical methods for assaying decarboxylase function often involve capture of ¹⁴CO₂ from radio-labeled substrates or derivatization of the enzyme products followed by HPLC analysis.^{6, 7} Neither of these techniques is suitable for high throughput screening (HTS) efforts, as they involve either formation of radioactive gas or lengthy, resource intensive detection procedures. Use of a commercial low-throughput method linking the production of CO₂ to the consumption of NADH using phosphoenolpyruvate carboxylase (PEPC) and malate dehydrogenase (MDH) to track decarboxylase activities has been reported.⁸ **(Fig 3.1)** Reaction progress was measured by the decrease in NADH absorbance at 340nm. We believed this assay was a good candidate for adaptation to HTS.

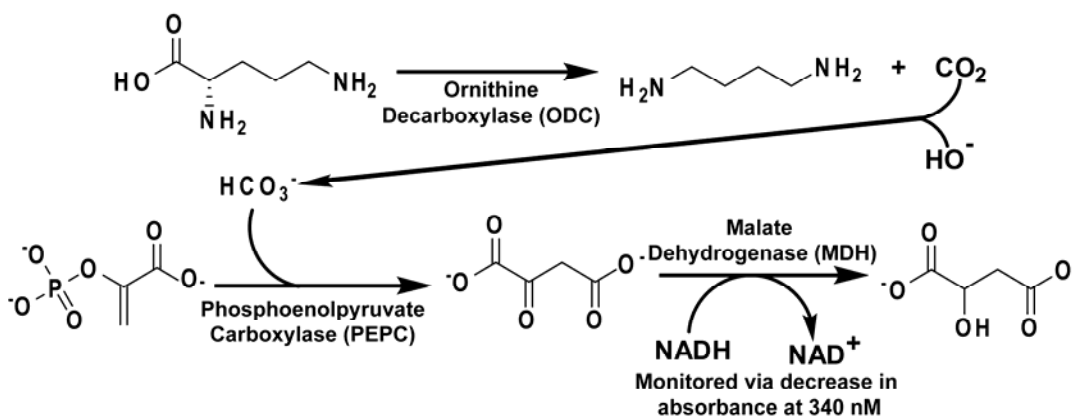


Figure 3.1 – Linked Assay Mechanism. ODC catalyzes the decarboxylation of ornithine, which releases CO_2 , which is captured by the basic buffer (pH 8.05) as bicarbonate. Phosphoenolpyruvate carboxylase (PEPC) uses this bicarbonate to generate oxaloacetate from phosphoenolpyruvate. The oxaloacetate is then reduced by malate dehydrogenase (MDH) to malate in a NADH dependant fashion. There is a 1:1 relationship between the amount of CO_2 produced by ODC and the amount of NADH oxidized by MDH, allowing kinetic parameters for ODC to be calculated from observing NADH levels as a function of time. The assay system has been optimized such that ODC is the rate limiting step.

The target chosen for optimization of this assay system was ODC from *Trypanosoma brucei*, the causative agent of Human African Trypanosomiasis. This disease is fatal if left untreated and is a major health problem in much of central Africa.⁹ The only clinically validated molecular target for treatment of *T. brucei* infections is ODC, which catalyzes the first step in polyamine metabolism, the decarboxylation of ornithine to produce putrescine. Putrescine and the other polyamines spermidine and spermine, are necessary for cellular reproduction, making their regulatory enzymes attractive drug targets in both parasitology and oncology. The biological roles of polyamines are numerous, and they have been implicated in the regulation of a wide range of important genes, including P53 and c-myc^{10, 11}

In mammalian cells, ODC is highly regulated and possesses a very short half-life of 10 to 20 minutes.¹² However, in protozoal parasites, particularly *T. brucei brucei* and

T. brucei gambiense, the enzyme is longer lived (~4 hours).¹³ This difference allows the use of irreversible and non-selective inhibitors of ODC such as difluoromethylornithine (DFMO) in clinical treatments for African Trypanosomiasis.¹⁴ Unfortunately, DFMO possesses poor pharmacokinetic properties, resulting in the need for multi-day high dosage intra-venous treatment regimens which limit its use in the third-world.¹⁵

To date, most drug discovery efforts directed towards ODC inhibitors have focused on analogues of ornithine (such as DFMO), putrescine, or pyridoxal-5'-phosphate (PLP), a cofactor necessary for ODC activity shared by many other enzymes.^{16,17} None of these have proved as effective as DFMO for treatment of *T. brucei* infections. No large scale efforts to discover inhibitors based on scaffolds other than substrate, product, or cofactor analogues have been reported. The lack of large scale drug discovery efforts has been due in part to the difficulty in assaying ODC activity in a high throughput manner.

Therefore, we have optimized a commercial enzyme linked bicarbonate detection system for use in high throughput screening of ODC. We report the results of this optimization and the performance of the assay on a proof-of-concept screen of approximately 3600 unique molecules.

MATERIALS AND METHODS

Materials

All chemicals assayed in this study were purchased from vendors without further purification. DI water was filtered with a MilliQ Synthesis Ultra-Pure water system

(Millipore, Billerica, MA) immediately before use. InfinityTM Carbon Dioxide Liquid Stable Reagent was purchased from Thermo Fisher Scientific. (Waltham, MA). L-Ornithine, pyridoxal 5'-phosphate (PLP) and dithiothreitol (DTT) were purchased from Sigma-Aldrich (St. Louis, MO). DFMO-HCl was purchased from Chem-Impex International (Wood Dale, IL). All plate based enzymatic assays were performed in 384-well black-sided, clear-bottomed polystyrene microplates (#3702) from Corning Life Sciences (Acton, MA). The bioactive compound screening library at St. Jude Children's Research Hospital was assembled from commercially available collections including the Prestwick Chemical Library (Prestwick Chemical, Illkirch, France); the LOPAC Collection (Sigma-Aldrich, St. Louis, MO); and the Spectrum Collection, the NINDS Collection, the Natural Product Collection, and the Killer Plate Collection from Microsource (Microsource Discovery systems, Gaylordsville, CT). The total bioactive test set contains approximately 7300 compounds, including many internal replicates. The total number of unique compounds in the collection is approximately 3600 molecules.

Purification of T. brucei ODC

ODC was expressed as an N-terminal 6xHis-tag fusion protein in *E. coli* BL21(DE3) cells as described.⁸ Protein was purified by Ni²⁺-NTA-agarose column followed by Superdex 200 gel-filtration column chromatography. Fractions containing the desired protein were identified by SDS-PAGE. Those containing pure ODC were combined and concentrated using an Amicon-Ultra centrifugal filter device (10Kda cutoff, UFC901024, Millipore, Billerica, MA) to concentrations of approximately 40 mg/mL. Yields of purified ODC were generally 7 to 13 mg/L of cultured cells.

Assay Automation and Nitrogen Atmosphere Generation

All screening data was generated on a High Resolution Engineering (Woburn, MA) integrated screening system using Liconic plate incubators (Woburn, MA) and a Stabuli T60 robotic arm (Stabuli, SC). This system is enclosed in a gas-tight Plexiglas enclosure allowing a nitrogen atmosphere to be generated by continual purging with approximately 30 psi nitrogen through twin 8 mm inner diameter tubes. Nitrogen was obtained by boil-off from liquid nitrogen using an inhouse dry-nitrogen system supplied by NexAir (Memphis, TN). Nitrogen consumption during screening was estimated to be approximately 200 liters per minute. Percent oxygen within the enclosure was monitored using an Air Aware oxygen detector (model 6810-0056, Industrial Scientific, Oakdale, PA) and maintained at less than 2.5% throughout all high throughput assays. Assay solutions were dispensed using Matrix Wellmates (Matrix Technologies, NH) equipped with 1µl rated tubes. Plates were centrifuged after all liquid additions using a Vspin plate centrifuge (Velocity11, Menlo Park, CA). Compound transfers were performed using a 384-well pin tool equipped with 10 nl slotted hydrophobic surface-coated pins (V&P Scientific, San Diego, CA). This allowed delivery of ~25nl of DMSO stock solution with CVs of less than 10%. All absorbance data was measured using an EnVision Multilabel Plate Reader equipped with a 340 nm narrow bandwidth filter (Perkin Elmer, 2100-5740). During automation, the screening system was operated offline and individual instruments were accessed using manual operation of the robot arm.

ODC-PEPC-MDH Linked Assay

This assay was performed under nitrogen atmosphere. Assay buffers were prepared under normal atmosphere while flushing with a stream of nitrogen and transferred to enclosed nitrogen atmosphere upon completion. Assay buffer (66 mM TRIS, 25 mM NaCl, 8 mM MgSO₄, 0.01% Triton-X, pH 8.05) was prepared daily. The assay reaction was prepared using two master mixes A and B, which were prepared immediately before use. Mix A contained ornithine (0 to 10 mM), PLP (0 to 937 μM) and 5.7 mM DTT in assay buffer. Mix A was prepared immediately before testing from frozen stocks prepared in water (0.5 M Orn, pH 7.5, 20 mM PLP and 1M DTT). Mix B contained InfinityTM Carbon Dioxide Liquid Stable Reagent (InfinityTM CO₂, Thermo-Fisher Scientific) and ODC (0 to 300 nM). Mix B was prepared immediately prior to testing from fresh InfinityTM Carbon Dioxide Liquid Stable Reagent and frozen ODC stocks. For testing, 15 μl Mix B was added to appropriate wells in a 384-well clear bottomed plate followed by compounds transferred by pin. 10 μl Mix A was then added to start the reaction.

Final optimized assay concentrations were 2.3 mM DTT, 600 μM ornithine, 60 μM PLP, 60% InfinityTM Carbon Dioxide Liquid Stable Reagent, 150 nM ODC, 10 μM test compound and 0.01% Triton-X, in a 25 μl final volume unless otherwise specified. Reaction progress was monitored by following absorbance at 340 nm using an Envision plate reader (Perkin Elmer) equipped with a narrow bandwidth 340 nm filter (Perkin Elmer, 2100-5740). Absorbance was monitored for 20 minutes, with time points taken every minute. Data from minutes 15 to 20 after addition of Mix A was fit to a linear model using statistical methods described below. The resulting slope of this fit was taken as the rate of the reaction and used as the endpoint for the assay.

Compounds for screening were placed in 384 well polypropylene plates (Corning Life Sciences, Acton, MA) at 10 mM concentration in DMSO with columns 1, 2, 13 and 14 empty. Positive controls (DFMO, 1 M, 10 μ l) were placed in a separate 384 well polypropylene plate in wells A2, B2, C2, D2, E14, F14, G14, H14, I2, J2, K2, L2, M14, N14, O14 and P14. Negative controls (DMSO, 10 μ l) were placed in the same plate as positive controls in wells A14, B14, C14, D14, E2, F2, G2, H2, I14, J14, K14, L14, M2, N2, O2 and P2. All microplate compound transfers were accomplished using a 384-well pin tool equipped with 10 nl hydrophobic surface coated pins (V&P Scientific, San Diego, CA). This allowed delivery of \sim 25nl of DMSO stock solution with CVs of less than 10%.

Cuvette assays were performed as described for above with the following minor modifications; the final assay volume in cuvettes was 500 μ l at 40% InfinityTM Carbon Dioxide Liquid Stable Reagent, 50 μ M PLP, 50 μ M DTT, 1% DMSO and varied ornithine concentrations from 10 mM to 100 μ M. As with microplate assays, assay buffer (66 mM TRIS, 25 mM NaCl, 8 mM MgSO₄, 0.01% Triton-X, pH 8.05) was prepared fresh daily.

PEPC-MDH Linked Assay - Microplate

For assay of the linking enzymes, assay buffer (66 mM TRIS, 25 mM NaCl, 8 mM MgSO₄, 0.01% Triton-X, pH 8.05) was prepared daily using water. The assay reaction was prepared in two master mixes. Mix A contained 1.25 mM sodium bicarbonate (Sigma Aldrich), 100 μ M PLP and 5.7 mM DTT in assay buffer. Mix B was 100% InfinityTM Carbon Dioxide Liquid Stable Reagent. For testing 15 μ l Mix B was

added to appropriate wells of a 384 well clear-bottom microplate followed by pin-transfer compound DMSO stocks. Compounds were allowed to equilibrate in the presence of enzymes for 20 minutes before substrate was added. The reaction was started by addition of 10 μ l Mix A and reaction progress was monitored by absorbance at 340 nm. Positive controls were wells with no sodium bicarbonate added, negative controls were DMSO.

Final assay concentrations were 2.3 mM DTT, 60 μ M PLP, 0.75 mM sodium bicarbonate, 60% InfinityTM Carbon Dioxide Liquid Stable Reagent, and 0.01% Triton-X. Reaction progress was monitored by decrease in absorbance at 340 nm using an Envision plate reader (Perkin Elmer) equipped with a narrow bandwidth 340 nm filter (Perkin Elmer, 2100-5740) for 10 minutes with time points taken every one minute. Data from minutes 1 to 5 was fit to a linear model using statistical methods as described below and normalized to the positive and negative controls.

Primary Screening Data Analysis and Reaction Rate Calculation

Primary screening data analysis was performed using custom protocols written in Pipeline Pilot (v. 6.1.1, Accelrys) and the R program (<http://www.r-project.org/>, v. 2.7.0).¹⁸ For rate determination, kinetic data were fit using 3 methods: a linear model using least squares (“linear”, calculated using the *lm* function in robustbase R package, v. 0.2-7), a linear model using only the difference between the first and last time points (“delta”), and a robust linear model using an iteratively re-weighted least squares algorithm (“robust”, calculated using the *lmrob* function in robustbase R package, v. 0.2-7).¹⁹ For hit identification, the final 5 minutes of data (6 data points in total including the 15 minute time point) were fit using the “linear” method. The fitted rates were the values

used in the calculations of all plate statistics. Only plates passing the minimum Z-prime and Z-factor thresholds of 0.4 and 0.4, respectively, were accepted. Initial screening hits were determined on a plate-by-plate basis by identifying compounds with activities that were simultaneously outliers from the negative control and variable compound populations. The outlier cutoffs were calculated as the *upper fourth* plus 1.5 times the *fourth spread* (the upper fourth and fourth spread are similar to the third quartile and interquartile range, respectively), a robust statistic which corresponds to a *p*-value ~ 0.005 for normal distributions.²⁰ For Z' calculations, 16 positive and 16 negative controls were used unless otherwise stated. Reaction rate was transformed from AU/min to mM NADH/min using an extinction coefficient of 6.349 AU mM⁻¹cm⁻¹ for NADH and an approximate path-length of 0.4 cm for assays performed at 25 μ l final volume in a 384 well plate.

Reaction rates for dose response data were calculated as described above. Rates were then normalized to DMSO and DFMO controls and sigmoidal curves with variable slopes were fit using Graphpad Prism 4.03. No constraints were used when fitting this data.

Receiver Operating Characteristic (ROC) Analysis

ROC analysis was performed using custom R scripts (<http://www.r-project.org/>, v. 2.9.0) and the R rocr package (v. 1.0.2). The ROC test set was composed of 63 compounds which uniformly sample from the distribution of observed primary screen activities (-7 – 103%). A compound was considered a true positive if it inhibited ODC in a dose dependent fashion, had no effect in the PEPC-MDH assay system, and showed a

2-fold increase in reaction rate when screened with 300 nM ODC. The ROC curve was formed by plotting the true positive rate vs. the false positive rate as a function of decreasing primary screen activity. Confidence intervals for the ROC area under the curve (AUC) were calculated from 200 bootstrap simulations.

RESULTS

Optimization of ODC-PEPC-MDH Linked Assay

The assay system was chosen in part because the linking system was available from Thermo Fisher Scientific, simplifying quality control and large-scale reagent sourcing. This system was designed for clinical detection of bicarbonate in bodily fluids, and is extremely sensitive to low levels of dissolved CO₂, which is in equilibrium with bicarbonate in aqueous solutions. Unfortunately, this sensitivity is a disadvantage in HTS applications. The background signal produced by atmospheric CO₂ reduces the assay linear time and causes reagents placed on the screening deck to rapidly degrade. However, if reagents are stored, dispensed, incubated and read under a nitrogen atmosphere, this liability is largely mitigated. When the assay is performed under nitrogen, the signal to noise ratio increases from 2.5 to 8.1 and there is a significant increase in reagent stability. (See Fig (3.2a)) For this reason, all optimization and screening experiments were performed under an inert nitrogen atmosphere as described.

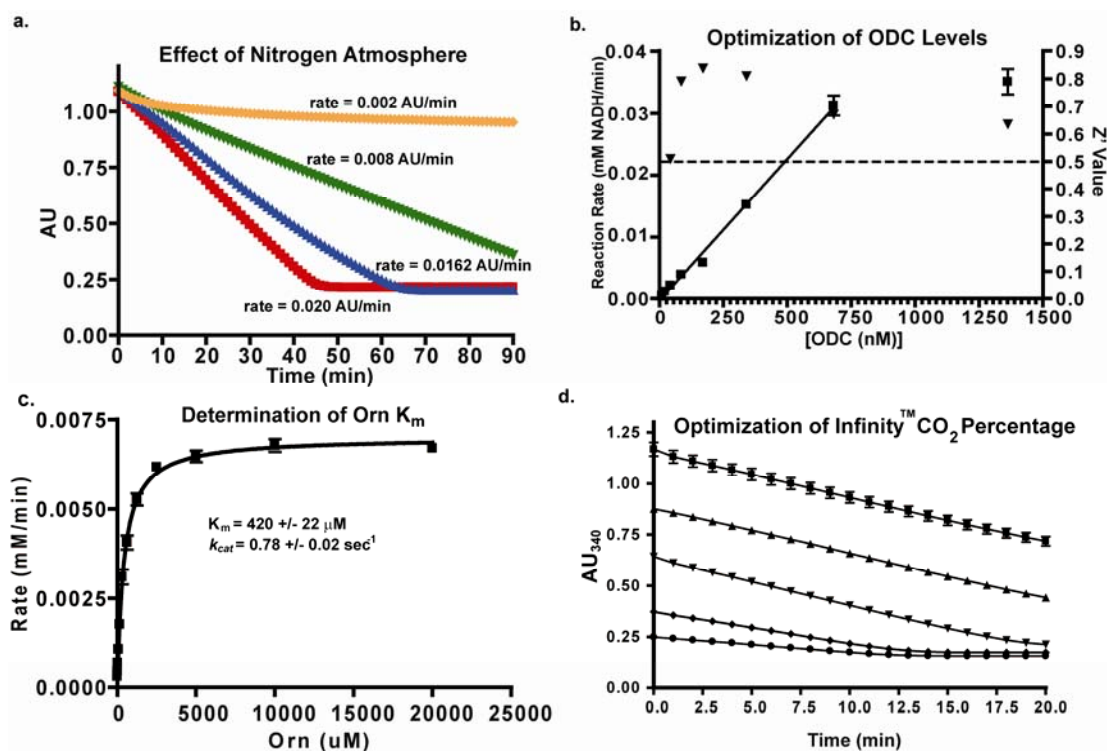


FIG. 3.2. Optimization of assay conditions. **3.2a:** Increase in background signal under normal atmosphere. The signal seen here in green is solely from atmospheric CO₂. (♦ = Nitrogen atmosphere, no ornithine, ▼ = standard atmosphere, no ornithine, ▲ = Nitrogen atmosphere, 625 μM ornithine, ■ = standard atmosphere, 625 μM ornithine) Quadruplicate data was collected in a 384 well microplate as described in the presence of the indicated concentrations of ornithine. All other reagent concentrations were identical to the optimized conditions described in materials and methods. The nitrogen atmosphere was maintained as described with O₂ levels under 2.5%. **3.2b:** Optimization of enzyme levels. ▼ = Z' values, ■ = reaction rates. Dashed line indicates standard Z' cutoff value of 0.5. Data was collected in a 384 well microplate using optimized assay conditions with varied final ODC concentrations. Z' Values were calculated using 8 positive (1mM DFMO) and 8 negative (DMSO) controls. The signal window at 150nM ODC is approximately 5 fold. **3.2c:** Determination of ODC K_m at 150 nM ODC and 60 μM PLP. Data was collected in a 384 well plate as described and fit to the Michaelis-Menten equation. **3.2d:** Optimization of InfinityTM CO₂ percentage. (■ = 60% InfinityTM CO₂, ▲ = 45% InfinityTM CO₂, ▼ = 30% InfinityTM CO₂, ♦ = 15 % InfinityTM CO₂, ● = 7.5% InfinityTM CO₂) Data was collected in 384 well plates as described at optimized assay conditions with varied InfinityTM CO₂. Data points were taken every 15 seconds in quadruplicate. The plot of AU₃₄₀ vs. time at 60% InfinityTM CO₂ represents a typical data set under optimized assay conditions with a ΔAU₃₄₀ of approximately 0.4 AU.

The assay rate was linear with respect to ODC concentration from 20 nM to approximately 600 nM. A final concentration of 150 nM ODC was chosen for the

primary screen, based upon signal to noise ratio and Z' score (>4 and >0.5 respectively, **Fig (3.2b)**). The final PLP concentration chosen was $60\ \mu\text{M}$, approximately 300-fold over the literature reported K_m .²¹ to minimize the probability of finding compounds that interfered directly with PLP, or competed for the PLP binding site. The assay buffer was not optimized, and was formulated to match the commercial linking buffer in order to maintain performance of the linking system. Several methods to remove dissolved CO_2 from the buffer were tested including vacuum degassing and nitrogen sparging. None offered significant reductions in background signal over using fresh MilliQ Synthesis grade water (data not shown). To ensure that the assay system was performing comparably to other literature methods, the K_m for ornithine was measured. The values obtained ($420 \pm 22\ \mu\text{M}$, **Fig (3.2c)**) were consistent with literature values (370 to $500\ \mu\text{M}$).^{22, 23} The relatively low ornithine concentration chosen for screening ($625\ \mu\text{M}$, $1.5 \times K_m$) was selected to maximize the probability of finding ornithine competitive inhibitors. The k_{cat} determined under screening conditions ($0.71\ \text{sec}^{-1}$ at $\sim 22^\circ\ \text{C}$) is approximately 10-fold lower than the reported literature values.²¹ This was determined to be a temperature effect, and it was possible to replicate literature values by performing the assay at $37^\circ\ \text{C}$. Due to limitations with our integrated plate reader, all high-throughput screening was performed at room temperature ($\sim 22^\circ\ \text{C}$).

Finally, the amount of linking enzyme mix (InfinityTM CO_2) was optimized (**Fig (3.2d)**). While the signal remained linear over the 20 minute assay window for both 60% and 45% InfinityTM CO_2 , 60% was chosen in order to maximize the linear time available during screening and reduce dependence on precise timing during the process. The percentage was not increased past 60% due to the fact that absorbance values were

already approaching 1.2 at this concentration. The assay system's tolerance for DMSO was also tested, and was shown to be up to 10% at optimized screening conditions (data not shown).

Optimization of Secondary PEPC-MDH Assay

In light of the fact that this assay is dependent upon the activity of the two linking enzymes as well as that of ODC, a secondary assay to test the effects of hits on the linking enzymes was designed. Titration of exogenous sodium bicarbonate into the reaction mixture showed a $K_{m,app}$ of 0.47 +/- 0.04 mM, which is consistent with reported literature values for the K_m of PEPC from *E. coli* (0.1 to 0.3 mM).^{24, 25} **(Fig (3.3a))** A bicarbonate concentration of 1.5 x $K_{m,app}$ (0.75 mM) was chosen for testing inhibitors. A final concentration of 60% Infinity CO₂ was used in order to mimic the primary assay screening conditions. At these reagent concentrations a linear time of 7 minutes was observed with a ΔAU of approximately 0.8. **(Fig (3.3b))** A signal window of 26 was observed and a Z' of 0.75 was calculated using no bicarbonate reagent as the positive control.

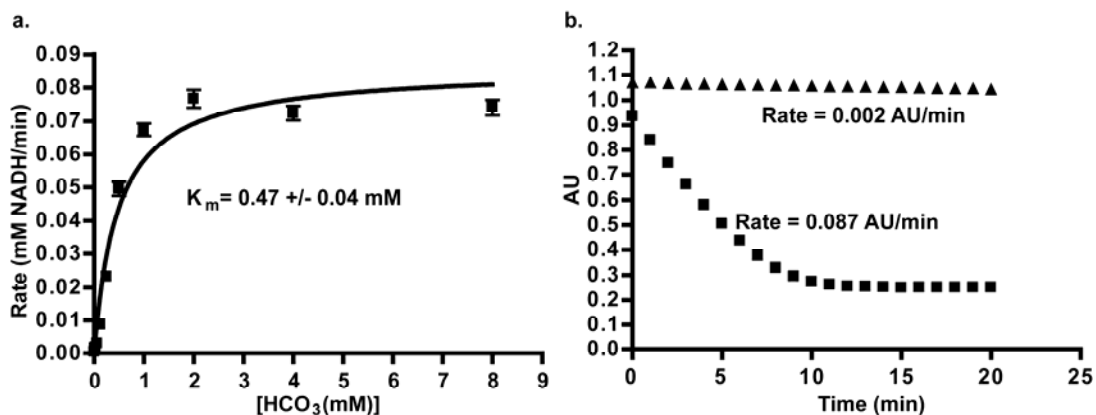


Fig 3.3. Optimization of PEPC-MDH assay system. Data was collected under nitrogen as described in materials and methods. All data was collected under nitrogen in 384 well microplates. **3.3a:** Determination of the K_m apparent with respect to bicarbonate. The value obtained is consistent with literature values.^{24,25} Data was fit to the Michaelis-Menton equation. **3.3b:** Determination of assay linear time. (■ = 0.75 mM HCO₃, ▲ = no HCO₃) Under optimized assay conditions, the bicarbonate signal was linear for approximately 7 minutes.

Testing of Known Inhibitors and Selection of Positive Controls

The only known ODC inhibitor available in large enough quantities for use as a high throughput screening control compound is DFMO. At optimized assay conditions in the ODC-PEPC-MDH linked system, DFMO exhibited an IC_{50} of 200 +/- 40 μ M, which is consistent with the literature K_{iapp} value of 160 μ M (**Fig (3.4a)**).²⁶ No effect on the IC_{50} value was seen when the amounts of linking enzyme present were changed. Additionally, it was possible to make 1 M stock solutions of DFMO in DMSO that were stable for several months at room temperature. Stock solutions at this concentration allowed efficient pin transfer of DFMO into the control wells in nano-liter volumes and permitted this compound to be used as positive control in screening at a final concentration of 1 mM. Inhibitors of the linking enzymes were ineffective under normal screening conditions (**Fig (3.4b)** and **(3.4c)**). Neither baicalein, a PEPC inhibitor, or isoquinoline, a

MDH inhibitor, had any effect at concentrations up to 1 mM under optimized assay conditions, well past their reported K_i values of 0.79 μM and 200 μM respectively.^{27, 28} However, if the percentage of InfinityTM CO₂ was reduced, inhibition by baicalein became apparent, with IC₅₀ values approaching literature values. Isoquinoline was not observed to have any inhibitory effects under any conditions tested; this is unsurprising given its poor potency.

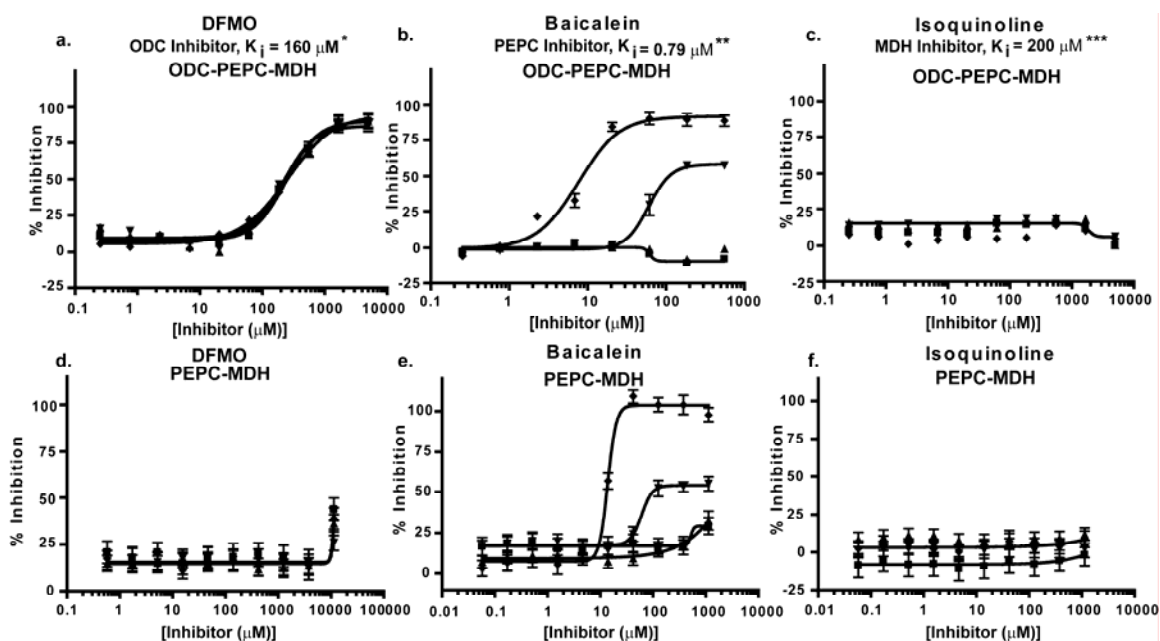


FIG. 3.4. Performance of known inhibitors in the ODC-PEPC-MDH and PEPC-MDH assays. (■ = 60% InfinityTM CO₂, ▲ = 45% InfinityTM CO₂, ▼ = 30% InfinityTM CO₂, ◆ = 15 % InfinityTM CO₂) Data was collected under optimized screening conditions as described unless otherwise noted. Compounds were allowed to equilibrate with enzymes for 20 minutes prior to addition of substrate. Percent inhibition is defined as $(1 - v_i/v_o) \times 100$. At InfinityTM CO₂ percentages lower than 45% reaction rates were calculated from the first 10 minutes of the reaction rather than the normal 20 minutes used at higher percentages due to limitations in assay linear time (see fig 1d). For PEPC-MDH assay results, rates were determined from the first 5 minutes. (see fig 2b). **3.4a:** Performance of DFMO, a known ODC inhibitor, in the ODC-PEPC-MDH assay with varying amounts of linking enzymes. Note that linking enzyme concentrations do not effect the performance of DFMO. **3.4b:** Performance of baicalein, a known inhibitor of PEPC at several different final linking mix concentrations in the ODC-PEPC-MDH assay. At normal screening conditions (60% InfinityTM CO₂) no inhibition is seen, even from this sub-micromolar inhibitor. However, upon dilution of the linking mix, inhibition becomes apparent. **3c:** Performance of isoquinoline, a known inhibitor of MDH in the

ODC-PEPC-MDH assay at several Infinity™ CO₂ percentages. No inhibition was seen in any condition tested. Reaction rates at Infinity™ CO₂ concentrations lower than 45% were calculated from the first 10 minutes of data due to limitations in assay linear time (see fig 1d). **3.4d**: Performance of DFMO in the PEPC-MDH assay system at varying levels of Infinity™ CO₂. **3.4e**: Performance of baicalein in the PEPC-MDH assay system at varying levels of Infinity™ CO₂. As with the ODC-PEPC-MDH system, a dependency on the amount of linking enzymes present greatly effects the amount of inhibition seen. **3.4f**: Performance of isoquinoline in the PEPC-MDH assay. No inhibition was observed under any conditions tested. *Literature value²⁶ **Literature value²⁷ ***Literature value²⁸

In the PEPC-MDH secondary assay system, DFMO did not have any effect below 10 mM concentrations. This inhibition is the result of a pH decrease in the assay solution due to the fact that the hydrochloride salt of DFMO was used to make inhibitor stock solutions. Baicalein, the PEPC inhibitor, was not observed to have any effect on the secondary assay at normal screening levels of Infinity™ CO₂. However, as in the case of the ODC-PEPC-MDH system, when linking enzyme levels were dropped, inhibition by baicalein was detected. Isoquinoline had no effect on the two enzyme system under any conditions tested.

Optimization of the High-Throughput Assay

Before performing any screening, the stability of the assay was tested using the fully automated system. Location-dependant effects were measured across a microplate prepared using the automated assay system. The only significant effect seen was a slight increase in high signal for the outside columns (**Fig 3.5a and 3.5b**). This did not affect Z' values significantly due to the fact that negative control wells were placed on both interior and edge columns (8 negative controls in columns 1 and 2, and 8 in columns 13

and 14). In order to maximize the amount of data gathered across a wide range of variable compounds, a twenty minute kinetic read with time points every minute was used during the initial screening efforts.

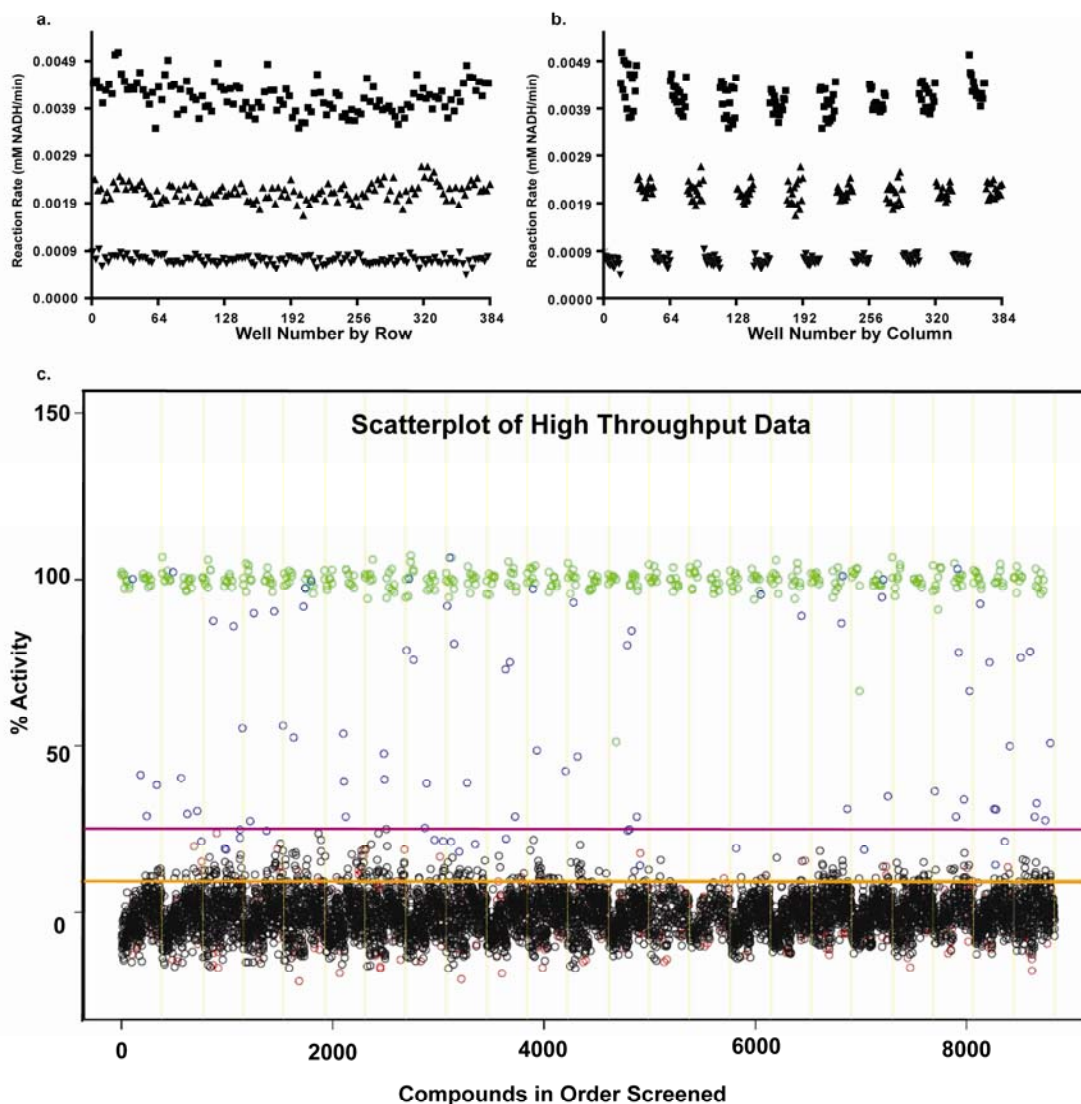


FIG. 3.5. ODC-PEPC-MDH linked plate geographic effects and high throughput data scatter plot. Assays were performed in 384 well plates as described and rates were calculated from the final 6 data points from a 20 minute observation. ■ = High Signal (DMSO), ▲ = Mid Signal (200 μ M DFMO), ▼ = Low Signal (1 mM DFMO) **3.5a:** Column effects resulting in a slight increase in signal on the outer columns. **3.5b:** Data from 3a arranged by row, showing that signal across rows is constant. The signal window for the assay is also apparent in these figures and is approximately 4.5. **3.5c:** Data from

the small scale high throughput assay of the bioactive compound collection at St. Jude Children's Research Hospital. Green circles = positive control (1 mM DFMO), Red circles = negative control (DMSO), Blue circles = hit compound, Black circles = inactive compound. Magenta line = 99th percentile cutoff, orange line = 95th percentile cutoff. Percent activity was calculated by normalizing kinetic reaction rates (20 minute data collection with the final 6 data points fit as described in materials and methods) to positive and negative controls. 8832 total data points were collected from ~3600 unique compounds. Absolute replicate number for each compound varied from 1 to 7, depending on vendor library composition and plating. The assay took 8.7 hours to complete using our automation system.

Primary Screen and Optimization of Kinetic Fitting Parameters

For the initial proof-of-concept screen, the bioactive collection at St. Jude Children's Research Hospital (8832 data points for ~3600 unique molecules in 23 384 well plates) was selected for testing. Absolute replicate number for each compound varied from 1 to 7 depending on vendor library composition and plating. The compounds were screened at 10 μ M against the ODC-PEPC-MDH system using a 20 minute kinetic read. Eight positive controls (1 mM DFMO) and eight negative controls (DMSO) were placed in columns 1, 2 and 13, 14 to help detect possible edge effects. The scatter plot for percent activity across the library is shown in **Figure 3.5c**. The screening run took 8.7 hours to complete using our automated system.

We tested three different methods for determining the assay rates (**Fig. 3.6**). Fitting using the later portion of the data (time points 10 to 20) improved Z' . The "delta" model performed similarly to the "linear" model on average, albeit with slightly higher variance. The "robust" model performed the best when all time points were included, but failed to converge without at least 15 time points. The "linear" method using time points

from 15 to 20 minutes was chosen to calculate endpoint values as a compromise between assay run time and Z' .

The overall data quality for the 3-enzyme assay was satisfactory, with an average Z' value of 0.68 across all plates. The robust outlier cutoff yielded 84 primary hits, of which 52 were unique. Internal duplication of compounds afforded an assessment of assay reproducibility. Active replicates were detected 86% of the time with an average activity CV of 16%, and 97% of the time with an average activity CV of only 3% when restricting replicates to those from the same vendor.

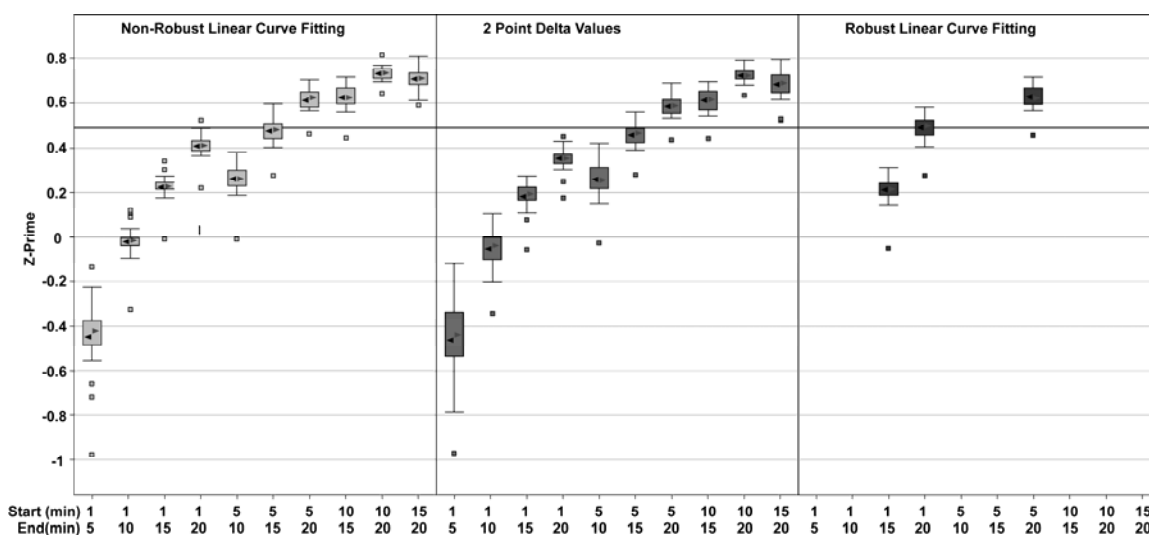


Fig 3.6. Effect of varying curve fitting methods on average Z' values for scaling screen. ► = Median, ◄ = Mean, solid line = standard Z' cutoff of 0.5. Data was collected as described in materials and methods under optimized assay conditions. Time points were taken every minute for 20 minutes. Note that the first five to ten minutes are poorly behaved and that eliminating them dramatically increases the average Z' for the run. This is primarily a result of a decrease in scatter rather than an increase in signal, since the average rates calculated were consistent for all methods tested.

Secondary Testing

To further characterize the hits, aliquots of each unique sample were cherry-picked and subjected to full dose response studies consisting of 10 points in a 1:3 dilution series (top = 100 μM). Thirty-three of the initial 52 unique hits displayed a full dose response while 15 displayed partial dose responses in the ODC-PEPC-MDH system—a 92% confirmation rate. None of the samples significantly affected the PEPC-MDH system at concentrations up to 100 μM at 60% InfinityTM CO₂ under optimized assay conditions. To further confirm that inhibition of ODC was the rate limiting step in the reaction cascade, the samples were re-screened at 300 nM ODC, and the rates at the IC₅₀ were compared to those determined at 150 nM ODC. All samples displayed the predicted two-fold increase at the higher enzyme concentration, confirming that inhibition of ODC was the rate limiting step. These compounds were designated as true positives for the ROC analysis.

ROC Analysis

Receiver-operator characteristic (ROC) analysis provides an assessment of the discriminatory power of an assay that is non-parametric (i.e., does not assume Gaussian distribution) and that is independent of both the number of true positives and the threshold for classifying hits. The ROC AUC is the probability that the assay will rank a randomly chosen true positive ahead of a randomly chosen true negative. A random assay—one which cannot discriminate true positives from true negatives—has an AUC = 0.5. The ROC AUC for the ODC assay is 0.90 (**Fig. 3.7**, 0.82-0.97 95% confidence

interval). Setting the cutoff at >30% in the primary screen would return >70% of all true positives, while yielding ~10% of all true negatives.

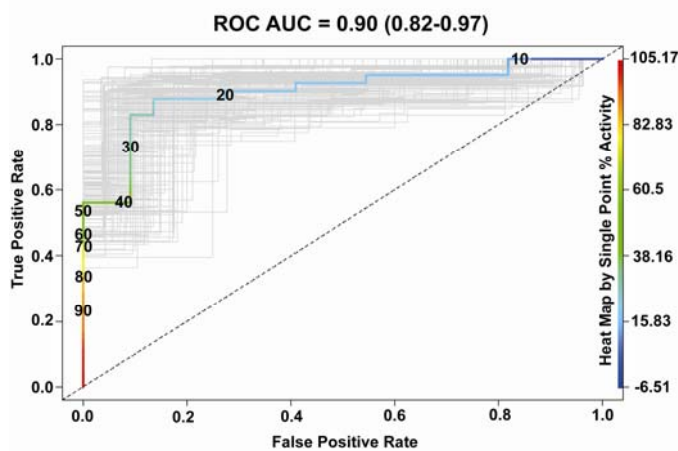


Fig 3.7. ROC curve for the ODC assay. The ROC AUC is 0.90 (0.82 – 0.97, 95% confidence interval). Bootstrap simulation curves are in light gray. The dotted-line is the curve for a random assay.

Hit Compounds

Due to the nature of the compound library, this proof-of-concept screen was not expected to yield many well behaved inhibitors with drug-like scaffolds. Indeed, a large number of quinone containing compounds were identified, along with several compound series containing Michael acceptors and other reactive groups. Though these compounds are not likely to be good lead candidates, they do inhibit the enzyme and were useful in the validation of the assay protocol. ODC has an active site cysteine residue and is known to require large amounts of reducing agent to be active in vitro. Therefore, it would be expected to be sensitive to potential alkylators as well as oxidizing compounds. ODC has historically been a difficult target to inhibit, and it is likely that screening a larger compound library will be necessary to find well-behaved inhibitors.

DISCUSSION

This study represents the first effort to develop an assay suitable for screening decarboxylases in a high throughput manner. Although it is a linked enzyme assay, the lack of susceptibility to known inhibitors of the linking enzymes suggests that relatively few false positive hits will be identified due to inhibition of the other enzymes in the mix. Baicalein, a known inhibitor of PEPC with a K_i of 0.79 μM , did not affect the assay appreciably until the linking enzyme mix had been diluted two-fold and even then, only inhibited the reaction by 50%. Isoquinoline, a known inhibitor of MDH with a literature K_i of 200 μM , did not inhibit the assay at any tested condition. Furthermore, none of the hits identified at 10 μM in the primary screen affected the dual enzyme linking system at concentrations up to 100 μM . Although the exact concentrations of the linking enzymes in the mixture are not disclosed by the manufacturer, these observations suggest that high concentrations of both PEPC and MDH are present, and that the assay is extremely resistant to inhibitors of the linking enzymes under optimized conditions (60% InfinityTM CO₂, 600 μM Orn, 60 μM PLP and 0.01% Triton-X).

However, the known ODC inhibitor, DFMO, exhibited an IC_{50} value of 206 +/- 40 μM after 20 minutes of pre-incubation, which is consistent with the literature $K_{i\text{app}}$ of 160 μM . ROC analysis, based on a definition of true positive which requires ODC specificity, quantitatively demonstrates the high discriminatory power of the assay. Moreover, the high degree of agreement found between replicate samples in the library further underscores the robustness of the assay system.

While the HTS assay requires a CO₂-free atmosphere in order to stabilize the reagents, other engineering controls may alleviate this need. For example, sealed reagent bottles equipped with nitrogen lines feeding bulk liquid dispensers would allow large amounts of the Infinity CO₂ reagent to be loaded into automated systems without degrading. It should be noted that performing the assay under normal atmosphere decreases linear time from approximately 60 minutes to 40 minutes, meaning that timing in the screening run must be monitored closely. The effect of moving to normal atmospheric conditions for screening is primarily an increase in background signal. This decreases the average Z' values observed from ~0.7 to ~0.5, a typical lower limit for high-throughput assay systems. Additionally, since this assay is based on absorbance values, it cannot be used in an endpoint fashion due to absorbance interference from the test compounds. To compensate for this, it is necessary to use a kinetic read. However, throughput was maximized by using a short kinetic read as it minimized movement of the plate, which is often rate limiting in high throughput screens on integrated systems. The throughput for this assay is approximately 10 plates per hour using our automated systems, when using a 5-minute kinetic read.

The relatively high primary hit rate of 1.4% reflects both the liberal primary hit cutoff in and the nature of the bioactive collection. It is likely that the hit rate would decline significantly for a more diverse compound library, particularly one curated to remove electrophiles and redox-active compounds. The identification of active scaffold series known to be redox active compounds and/or non-specific alkylators highlights the need for secondary assays that will address both of these liabilities in any true HTS-effort aimed at discovering novel inhibitors of ODC. However, since none of these compounds

were found to effect the linking enzymes, this sensitivity is due to the specific decarboxylase screened, not the assay method itself.

In conclusion, this study describes a quick and accurate method to screen ODC and other decarboxylases in high-throughput. The system is robust, generates hits with the desired biochemical effects, and is superior to existing assays that rely on either radiolabeled substrate or HPLC methods.

REFERENCES

1. Casero, R. A., Jr. and Marton, L. J.: Targeting polyamine metabolism and function in cancer and other hyperproliferative diseases. *Nature reviews* 2007;373-390.
2. Heby, O., Roberts, S. C. and Ullman, B.: Polyamine biosynthetic enzymes as drug targets in parasitic protozoa. *Biochem Soc Trans* 2003;415-419.
3. Moya-Garcia, A. A., Pino-Angeles, A., Gil-Redondo, R., Morreale, A. and Sanchez-Jimenez, F.: Structural features of mammalian histidine decarboxylase reveal the basis for specific inhibition. *British journal of pharmacology* 2009;4-13.
4. Bonifati, V. and Meco, G.: New, selective catechol-O-methyltransferase inhibitors as therapeutic agents in Parkinson's disease. *Pharmacology & therapeutics* 1999;1-36.
5. Ray, S. S., Bonanno, J. B., Rajashankar, K. R., Pinho, M. G., He, G., De Lencastre, H., Tomasz, A. and Burley, S. K.: Cocrystal structures of diaminopimelate decarboxylase: mechanism, evolution, and inhibition of an antibiotic resistance accessory factor. *Structure* 2002;1499-1508.

6. Bitonti, A. J., McCann, P. P. and Sjoerdsma, A.: Restriction of bacterial growth by inhibition of polyamine biosynthesis by using monofluoromethylornithine, difluoromethylarginine and dicyclohexylammonium sulphate. *The Biochemical journal* 1982;435-441.
7. Thyssen, S. M. and Libertun, C.: Quantitation of polyamines in hypothalamus and pituitary of female and male developing rats. *Neuroscience letters* 2002;65-69.
8. Osterman, A., Grishin, N. V., Kinch, L. N. and Phillips, M. A.: Formation of functional cross-species heterodimers of ornithine decarboxylase. *Biochemistry* 1994;13662-13667.
9. African trypanosomiasis (sleeping sickness).
<http://www.who.int/mediacentre/factsheets/fs259/en/> (Last accessed on [November 26, 2007]).
10. Ray, R. M., Zimmerman, B. J., McCormack, S. A., Patel, T. B. and Johnson, L. R.: Polyamine depletion arrests cell cycle and induces inhibitors p21(Waf1/Cip1), p27(Kip1), and p53 in IEC-6 cells. *The American journal of physiology* 1999;C684-691.
11. Celano, P., Baylin, S. B., Giardiello, F. M., Nelkin, B. D. and Casero, R. A., Jr.: Effect of polyamine depletion on c-myc expression in human colon carcinoma cells. *J Biol Chem* 1988;5491-5494.
12. Iwami, K., Wang, J. Y., Jain, R., McCormack, S. and Johnson, L. R.: Intestinal ornithine decarboxylase: half-life and regulation by putrescine. *The American journal of physiology* 1990;G308-315.

13. Phillips, M. A., Coffino, P. and Wang, C. C.: Cloning and sequencing of the ornithine decarboxylase gene from *Trypanosoma brucei*. Implications for enzyme turnover and selective difluoromethylornithine inhibition. *J Biol Chem* 1987;8721-8727.
14. Van Nieuwenhove, S., Schechter, P. J., Declercq, J., Bone, G., Burke, J. and Sjoerdsma, A.: Treatment of gambiense sleeping sickness in the Sudan with oral DFMO (DL-alpha-difluoromethylornithine), an inhibitor of ornithine decarboxylase; first field trial. *Transactions of the Royal Society of Tropical Medicine and Hygiene* 1985;692-698.
15. Abeloff, M. D., Slavik, M., Luk, G. D., Griffin, C. A., Hermann, J., Blanc, O., Sjoerdsma, A. and Baylin, S. B.: Phase I trial and pharmacokinetic studies of alpha-difluoromethylornithine--an inhibitor of polyamine biosynthesis. *J Clin Oncol* 1984;124-130.
16. Bey, P., Danzin, C, Jung, M: Inhibition of Basic Amino Acid Decarboxylases Involved in Polyamine Biosynthesis. In: *Inhibition of Polyamine Metabolism - Biological Significance and Basis for New Therapies*. P. P. McCann, Pegg, A.E., Sjoerdsma, A., (eds.), pp. 1-31. Academic Press, San Diego, 1987.
17. Amadasi, A., Bertoldi, M., Contestabile, R., Bettati, S., Cellini, B., di Salvo, M. L., Borri-Voltattorni, C., Bossa, F. and Mozzarelli, A.: Pyridoxal 5'-phosphate enzymes as targets for therapeutic agents. *Current medicinal chemistry* 2007;1291-1324.
18. Team, R. D. C.: *R: A language and environment for statistical computing*. R Foundation for Statistical Computing, Vienna, 2007.
19. Peter Rousseeuw, C. C., Valentin Todorov, Andreas Ruckstuhl, Matias Salibian-Barrera, Martin Maechler: *robustbase: Basic Robust Statistics R package 0.2-7*: 2006.

20. Hoaglin, D. C., Mosteller, Frederick, Tukey, John W.: Understanding Robust and Exploratory Data Analysis. John Wiley and Sons, Inc., New York, 1983.
21. Osterman, A. L., Brooks, H. B., Rizo, J. and Phillips, M. A.: Role of Arg-277 in the binding of pyridoxal 5'-phosphate to *Trypanosoma brucei* ornithine decarboxylase. *Biochemistry* 1997;4558-4567.
22. Myers, D. P., Jackson, L. K., Ipe, V. G., Murphy, G. E. and Phillips, M. A.: Long-range interactions in the dimer interface of ornithine decarboxylase are important for enzyme function. *Biochemistry* 2001;13230-13236.
23. Jackson, L. K., Baldwin, J., Akella, R., Goldsmith, E. J. and Phillips, M. A.: Multiple active site conformations revealed by distant site mutation in ornithine decarboxylase. *Biochemistry* 2004;12990-12999.
24. Terada, K. and Izui, K.: Site-directed mutagenesis of the conserved histidine residue of phosphoenolpyruvate carboxylase. His138 is essential for the second partial reaction. *European journal of biochemistry / FEBS* 1991;797-803.
25. Yano, M., Terada, K., Umiji, K. and Izui, K.: Catalytic role of an arginine residue in the highly conserved and unique sequence of phosphoenolpyruvate carboxylase. *Journal of biochemistry* 1995;1196-1200.
26. Bitonti, A. J., Bacchi, C. J., McCann, P. P. and Sjoerdsma, A.: Catalytic irreversible inhibition of *Trypanosoma brucei* ornithine decarboxylase by substrate and product analogs and their effects on murine trypanosomiasis. *Biochemical pharmacology* 1985;1773-1777.

27. Pairoba, C. F., Colombo, S. L. and Andreo, C. S.: Flavonoids as inhibitors of NADP-malic enzyme and PEP carboxylase from C4 plants. *Bioscience, biotechnology, and biochemistry* 1996;779-783.
28. Kapp, E. and Whiteley, C.: Protein ligand interactions: isoquinoline alkaloids as inhibitors for lactate and malate dehydrogenase. *Journal of enzyme inhibition* 1991;233-243.

Chapter 4

Discovery of Potent and Selective Inhibitors of *Trypanosoma brucei* Ornithine Decarboxylase

Modified from: David C. Smithson, Jeongmi Lee, Anang A. Shelat, Margaret A. Phillips and R. Kiplin Guy, *Journal of Biological Chemistry*, **2009**, submitted 11-2-2009

INTRODUCTION

The only clinically validated molecular target for treatment of HAT is ornithine decarboxylase (ODC), which catalyzes the decarboxylation of ornithine to produce putrescine, the first step in polyamine metabolism. The polyamines putrescine, spermidine, and spermine are known to be necessary for cellular replication.^{1,2} Increases in polyamine concentration have also been linked to carcinogenesis. Therefore, inhibitors of the polyamine biosynthetic pathway have been extensively investigated as potential chemotherapeutic and chemopreventative compounds. (Reviewed in ³)

To date, most discovery efforts directed towards ODC have been focused on analogues of ornithine (such as DFMO), putrescine, or PLP.⁴ None of these has proved as effective as DFMO for treatment of *T. brucei* infections. No large scale efforts to discover novel inhibitors have been reported. The lack of prior high-throughput screening efforts directed at ODC is due in part to the difficulty in assaying its activity. Classical assay methods utilize capture of ¹⁴CO₂ from radio-labeled ornithine or derivatization of putrescine followed by HPLC analysis.^{5, 6} Neither of these techniques is tenable for a large scale screening effort.

Therefore, we have optimized an enzyme linked assay suitable for high throughput screening of ODC. (See Chapter 3) Herein we report the use of this method to identify active compounds from a library of 316,114 unique compounds. This effort led to the discovery of four novel inhibitory chemotypes possessing previously

uncharacterized modes of inhibition. A subset of the inhibitors appeared to bind to a novel site that was characterized by molecular docking and mutagenesis techniques.

Materials and Methods

Materials

All chemicals were used as purchased from their vendors. DI water was filtered with a MilliQ Synthesis Ultra-Pure water system (Millipore, Billerica, MA) immediately before use. InfinityTM Carbon Dioxide Liquid Stable Reagent was purchased from Thermo Fisher Scientific (Waltham, MA). L-Ornithine, pyridoxal 5'-phosphate (PLP), and dithiothreitol (DTT) were purchased from Sigma-Aldrich (St. Louis, MO). DFMO was purchased from Chem-Impex International (Wood Dale, IL). All plate-based enzymatic assays were performed in 384-well black-sided, clear-bottomed polystyrene microtiter plates (#3702) from Corning Life Sciences (Acton, MA).

Screening Library

The compound library at St. Jude Children's Research Hospital was assembled from commercially available collections including the Prestwick Chemical Library (Prestwick Chemical, Illkirch, France); the LOPAC Collection (Sigma-Aldrich, St. Louis, MO); the Spectrum Collection, NINDS Collection, Natural Product Collection, and Killer Plate Collection (Microsource Discovery Systems, Gaylordsville, CT); Chemical Diversity (San Diego, CA); ChemBridge (San Diego, CA); Life Chemicals (Blulington, ON); and Tripos (St. Louis, MO). The library was constructed by filtering available

compounds using a combination of physiochemical metrics chosen to improve bioavailability and functional group metrics chosen to reduce the likelihood of non-specific or artifactual hits.^{7, 8} The filtered compound list was used to generate maximally diverse clusters by reducing the compounds to core fragments using the method of Bemis and Murcko.⁹ The clusters were prioritized based on the diversity of the existing library. Five to 20 compounds are required per cluster. Clusters of more than 20 available compounds were preferred, with a maximum of 20 compounds being purchased from within each cluster.

Purification of *T. brucei* ODC (TbODC) and human ODC (hODC)

TbODC and hODC were expressed as N-terminal 6xHis-tag fusion proteins in *E. coli* BL21(DE3) cells as described.¹⁰ Protein was purified by Ni²⁺-NTA-agarose column followed by Superdex 200 gel-filtration column chromatography. Fractions containing the desired protein were identified by SDS-PAGE. Those containing ODC were combined and concentrated using an Amicon-Ultra centrifugal filter device (10 KDa cutoff, Millipore, UFC901024) to concentrations of approximately 40 mg/ml. Yields of purified TbODC were generally 7 to 13 mg/liter of cultured cells. Protein concentration was determined by Bradford assay. Yields of purified hODC were approximately 2 to 5 mg/liter of cultured cells.

Site-directed mutagenesis of TbODC

The S369A and S402A TbODC) mutants were produced using the pODC29 plasmid that encodes the wild-type *TbODC* with the QuickChangeTM mutagenesis kit

(Stratagene, La Jolla, CA using the following forward primers: 5'-GTCGTAGGAACTTCTGCCTTTAATGGATTCCAG-3' and 5'-CCTTTAATGGATTCCAGGCTCCGACTATTTACTATG-3' for S396A and S402A, respectively (desired mutations in bold). The TbODC D364E mutant was generated using the standard Kunkel technique in the Bluescript vector (Stratagene, La Jolla, CA) using the M13 helper phage (Stratagene, La Jolla, CA) and the Kunkel strain BO265.¹¹ The primer used for this mutant was 5'ATGTGATGGGCTCGAGCAGATAG.

Assay Automation and Nitrogen Atmosphere Generation

All screening data was generated on a High Resolution Engineering (Woburn, MA) integrated screening system using Liconic plate incubators (Woburn, MA) and a Stabuli T60 robotic arm (Stabuli, SC). This system is enclosed in a virtually gas tight Plexiglass enclosure allowing a nitrogen atmosphere to be generated by continual purging with approximately 30 psi nitrogen through twin 8 mm inner diameter tubes. Nitrogen was obtained via an in-house dry-nitrogen system supplied by NexAir (Memphis, TN). Percent oxygen was monitored using an Air Aware oxygen detector (model 6810-0056, Industrial Scientific, Oakdale, PA) and maintained at less than 2.5% throughout all high throughput assays. Assay solutions were dispensed using Matrix Wellmates (Matrix Technologies, NH) equipped with 1µl rated tubes. Plates were centrifuged after all bulk liquid additions using a Vspin plate centrifuge (Velocity11, Menlo Park, CA). Compound transfers were performed using a 384-well pin tool equipped with 10 nl slotted hydrophobic surface coated pins (V&P Scientific, San Diego, CA). This allowed delivery of ~25 nl of DMSO stock solution with CVs of less than 10%. All absorbance data was

measured using an EnVision Multilabel Plate Reader equipped with a 340 nm narrow bandwidth filter (Perkin Elmer, 2100-5740).

ODC-PEPC-MDH Linked Assay

This assay was performed under nitrogen atmosphere. Assay buffers were prepared under normal atmosphere while flushing with a stream of nitrogen and transferred to the screening enclosure. Assay buffer (66 mM TRIS, 25 mM NaCl, 8 mM MgSO₄, 0.01% Triton-X, pH 8.05) was prepared daily in water. The assay reaction was prepared using two master mixes A and B, which were prepared immediately before use. Mix A contained ODC (375 to 750 nM), PLP (150 μM) and DTT (5.7 mM) in assay buffer. Mix B contained InfinityTM Carbon Dioxide Liquid Stable Reagent (InfinityTM CO₂) and L-ornithine (0 to 10 mM). For testing 10 μl Mix A was added to appropriate wells in a 384-well clear-bottomed plate followed by compounds transferred by pin. Plates and compounds were allowed to equilibrate in the presence of ODC for 20 minutes. Following this 15 μl Mix B was added to start the reaction. Plates were then incubated at room temperature for 15 minutes to allow the signal to stabilize before being moved to the plate reader. Final primary screening assay conditions were 2.3 mM DTT, 60 μM PLP, 625 μM L-Orn, 150 nM TbODC, 10 μM test compound and 60% InfinityTM CO₂ (v/v) in assay buffer with a final volume of 25 μl.

Reaction progress was monitored by decrease in absorbance at 340 nm using an Envision plate reader (Perkin Elmer) equipped with a narrow bandwidth 340 nm filter (Perkin Elmer, 2100-5740). Absorbance was monitored for 6 minutes, with time points taken every minute. These data were fit to a linear model using statistical methods

described below. The resulting slope of this fit was taken as the rate of the reaction and used as the endpoint for the assay.

Compounds for screening were placed in 384-well polypropylene plates (Corning Life Sciences, Acton, MA) at 10 mM concentrations in DMSO. Sixteen Positive controls (DFMO, 1 M in DMSO) and 16 negative controls (DMSO) were placed in a single separate 384-well polypropylene plate and pin-transferred to test plates after the addition of variable compounds.

Cuvette assays for low-throughput re-testing were performed as described above with the following minor modifications; the final assay volume in cuvettes was 500 μ l at 40% InfinityTM Carbon Dioxide Liquid Stable Reagent, 50 μ M PLP, 50 μ M DTT, 1% DMSO and varied ornithine concentrations from 10 mM to 100 μ M. As with microplate assays, assay buffer (66 mM TRIS, 25 mM NaCl, 8 mM MgSO₄, 0.01% Triton-X, pH 8.05) was prepared fresh daily. Cuvette assays were performed under normal atmosphere at 37 °C.

Primary Screening Data Analysis and Reaction Rate Calculation

Primary screening data analysis was performed using custom protocols (RISE 3.0) written in Pipeline Pilot (v. 7.0, Accelrys) and the R program (<http://www.r-project.org/>, v. 2.5.0).¹² Kinetic data from the full 6 minute observation (6 points in total) were fit to a linear model using a using a robust, iteratively re-weighted least squares algorithm (“lmrob” function in robustbase R package, v. 0.2-7) that reduces the influence of outliers compared to classical least squares.¹³ The slope values from kinetic data fits were taken as endpoints that were then used for the calculations of all other plate

statistics. Only plates passing the minimum Z-prime and Z-factor thresholds of 0.4 and 0.4, respectively, were accepted. Initial screening hits were determined on a plate-by-plate basis by identifying compounds with activities that were simultaneously outliers from the negative control and variable compound populations. The outlier cutoffs were calculated as the *upper fourth* plus 1.5 times the *fourth spread* (the upper fourth and fourth spread are similar to the third quartile and interquartile range, respectively), which corresponds to a *p*-value ~ 0.005 for normal distributions. However, such cutoff criteria are more robust to population deviations from normality.¹⁴ For calculations of Z-scores, 16 positive and 16 negative controls were used unless otherwise stated. Z-scores were calculated as described.¹⁵ Reaction rate was changed from AU/min to mM NADH/min using an extinction coefficient of $6.349 \text{ AU mM}^{-1}\text{cm}^{-1}$ for NADH and an approximate path-length of 0.4 cm for assays performed at 25 μl final volume in a 384-well plate. Dose response data were fit using a non-linear regression to a four parameter sigmoidal curve model, resulting in fit values for maximum and minimum responses, hill-slope and EC_{50} .

PEPC-MDH Linked Assay

For assay of the linking enzymes, assay buffer (66 mM TRIS, 25 mM NaCl, 8 mM MgSO_4 , 0.01% Triton-X, pH 8.05) was prepared daily using water. The assay reaction was prepared in two master mixes. Mix A contained 1.25 mM sodium bicarbonate (Sigma Aldrich), 100 μM PLP, and 5.7 mM DTT in assay buffer. Mix B was 100% InfinityTM Carbon Dioxide Liquid Stable Reagent. For testing 15 μl Mix B was added to appropriate wells of a 384-well clear-bottom microplate followed by pin-

transfer of compound DMSO stocks. Compounds were allowed to equilibrate in the presence of enzymes for 20 minutes before substrate was added. The reaction was started by addition of 10 μ l Mix A and reaction progress was monitored by decrease in absorbance at 340 nm.

Final assay concentrations were 2.3 mM DTT, 60 μ M PLP, 0.75 mM sodium bicarbonate, 60% InfinityTM Carbon Dioxide Liquid Stable Reagent, and 0.01% Triton-X. Reaction progress was monitored by decrease in absorbance at 340 nm using an Envision plate reader (Perkin Elmer) equipped with a narrow bandwidth 340 nm filter (Perkin Elmer, 2100-5740) for 10 minutes with time points taken every minute. Data from minutes two to seven was fit to a linear model using statistical methods as described below.

Radiolabeled Ornithine ODC Assay

¹⁴CO₂ released from L-[1-¹⁴C]ornithine by the decarboxylation activity of TbODC was directly measured as previously described^{16, 17} at pH 7.5 at 37 °C in the absence or presence of inhibitors. IC₅₀ values were determined in an 8-point dose response curve performed in singlicate. Data was fit to a simple IC₅₀ model as described.¹⁸

Reductive Assay

Reductive activity of all hits was determined using a high-throughput assay based on the detection of molecules capable of reducing resazurin (Cat Num R7017, Sigma-Aldrich, St. Louis, MO) to resorufin as described.¹⁹ Briefly: 25 μ l of assay solution (5 μ M resazurin, 50 mM HEPES, 50 mM NaCl, pH 7.5, 50 μ M DTT, prepared immediately

prior to usage) was added to a black 384-well polystyrene plate (Cat. Num. 3573, Corning, Lowell, MA) using a Matrix WellMate (Thermo Fisher, Hudson, NH). Test compounds were added by pin-transfer using 10 nL hydrophobic coated pins (FP1CS10H, V&P Scientific, San Diego, CA) to a final concentration of 10 μ M. Test plates were incubated in the dark at room temperature for 60 minutes and fluorescence intensity was read on an Envision (PerkinElmer, Waltham, MA) with Ex = 560 nm and Em = 590 nm. Each compound was read in quadruplicate and the signals averaged to generate relative activity levels. Compounds which differed significantly from DMSO levels as determined by use of in-house statistical software (RISE 3.0) were scored as being potentially redox active.

Reversibility Assay

Reversibility assays were performed by dialysis. ODC (1500 nM) was incubated with inhibitors at 10 x IC₅₀ concentrations for 40 minutes in assay buffer. Samples were then dialyzed in assay buffer overnight using 3000 MW cutoff Slide-A-Lyzer MINI dialysis units (Pierce, IL) and assayed at 600 μ M Orn, 60 μ M PLP and 150 nM ODC. Percent activity recovered was defined as the difference between the ratio of the dialyzed rate to the uninhibited rate and the ratio of the inhibited (10 x IC₅₀) rate to the uninhibited rate. Compounds were labeled reversible if >90% activity was recovered.

***T. brucei* Cytotoxicity Assay**

Culture adapted *T. brucei brucei* were grown at 37° C, 5% CO₂ in HMI-9 medium (HyClone) supplemented with penicillin/streptomycin (Gibco, 50 units/mL), 10% heat-

inactivated FBS (Omega Scientific, lot #3137) and 10% Serum Plus (JHR Biosciences) to a density of 1×10^6 cells/mL, then diluted to 1×10^4 cells/mL prior to screening. 100 μ l of diluted culture was added to each well of a white flat-bottom sterile 96 well plate (Greiner) and 0.5 μ l of test compound in DMSO was added. Plates were incubated for 48 hours at 37° C, 5% CO₂ before the addition of 50 μ l Cell Titer Glo (Promega) to each well. Plates were shaken for 2 minutes on an orbital shaker at 500 RPM. Luminescence was read after 8 minutes on an Envision plate reader (Perkin Elmer). To test for putrescine reversibility trypanosomes were cultured in the presence of 500 μ M putrescine during IC₅₀ determination experiments.

General Cytotoxicity Assays

BJ, Raji, HEK 293 and HEP G2 cell lines were purchased from the American Type Culture Collections (ATCC, Manassas VA) and were cultured according to recommendations. Cell culture media were purchased from ATCC. Cells were routinely tested for mycoplasma contamination using the MycoAlert Mycoplasma Detection Kit (Cambrex). Exponentially growing cells were plated in Costar 96 well custom assay plates, which were black with clear bottoms (Corning), and incubated overnight at 37° C in a humidified, 10% CO₂ incubator. DMSO inhibitor stock solutions were added the following day to a final DMSO concentration of 0.5%. Cytotoxicity was determined following a 72 hour incubation using the Cell Titer Glo assay (Promega). Luminescence was read on an Envision plate reader (Perkin Elmer).

Kinetic Analysis and Dose Response Analysis

Mode of inhibition for ornithine was determined by monitoring the reaction rate in the presence of increasing substrate concentration (0 to 10 mM Orn, in 1:3 dilution series; in the presence of 60 μ M PLP) with varying concentrations of inhibitors (0, IC_{50} , 3 x IC_{50} and 4 x IC_{50}). For PLP mode of inhibition studies, ornithine concentration was held constant at 600 μ M while PLP was varied from 0 to 600 μ M. All kinetic data were gathered from experiments performed in 384-well format, as described above. This data was used in *Lineweaver-Burke* analysis followed by fitting the data to the appropriate Michaelis-Menton inhibition equation (Competitive, Mixed-Competition with varied α values, Non-Competitive or Un-Competitive) for determination of K_i .²⁰ In specific cases reported in this manuscript, mode of inhibition and K_i values were confirmed by analysis using the cuvette-based assay. K_m for ornithine was calculated by fitting data to the Michaelis-Menton equation with a variable K_m and V_{max} . Data was fit using Graphpad Prism 4.03 (Graphpad Software, La Jolla, CA).

Reaction rates for dose-response data were calculated as described below. Rates were then normalized to DMSO and DFMO (1 mM) controls and sigmoidal curves with variable slopes (4-parameter fit) were fit using Graphpad Prism 4.03 or custom protocols in Pipeline Pilot (v. 7.0, Accelrys)

Computational Chemistry and Molecular Modeling

Structural data used in modeling experiments was taken from the protein databank (1QU4 – apo TbODC, 1D7K – apo hODC)^{21, 22}. All molecular modeling was performed

using MOE (v. 2007.09, Chemical Computing Group, Inc.). Site Finder, a geometric method for finding potential binding pockets similar to LigSite²³, was used to identify potential binding sites. The analysis was run with 1.4 and 1.8 Å probe radii for hydrophobic and hydrophilic probes respectively. A minimum site size of 25 alpha spheres was used, and a minimum bounding sphere radius of 2.5 Å were used to eliminate smaller pockets unlikely to bind with drug-like molecules. Dummy atoms were placed at the center of the alpha spheres generated by Site Finder and used as superposition targets for docking calculations.

Docking studies were also performed using MOE (v. 2007.09). Docking was performed using rigid ligand and receptors, using the Alpha Triangle placement method with 80,000 maximum generations for each ligand conformation. Scoring was done using the London dG scoring function. This is a five parameter function taking into account rotational and translational entropy, ligand flexibility, hydrogen bonding, metal ligations and desolvation energies. The predefined ligand conformer library was generated using the systematic conformational search function in MOE with a 10 kcal/mol cutoff. Results were visualized in Pymol (v. 0.99, Delano Scientific LLC) and receiver-operator curve (ROC) scores were generated in Pipeline Pilot (v. 7.0, Accelrys).

RESULTS

Primary Screen Results

For the purposes of identifying novel inhibitors of TbODC, a collection of 316,114 unique molecules was tested at St. Jude Children's Research Hospital. The

compounds were screened at 10 μM against the TbODC-PEPC-MDH linked enzyme system. Plates with Z' values of less than 0.4 were rejected for the purposes of identifying hits. This somewhat liberal data quality cutoff was chosen in order to maximize the number of hits chosen for further examination, since preliminary examination of the data showed that the hit rate was quite low. After filtering for poor Z' , 625 plates, with an average Z' of 0.52 and an average Z-factor of 0.47, containing a total of 240,000 unique compounds remained. These plates were used for selecting hits. Hits were picked using robust methods corresponding roughly to using a p -value cutoff of 0.005, resulting in 883 primary hits (0.3% hit rate).¹⁴ No minimum activity was required for characterization as a “hit.” This technique is more completely described in materials and methods.

To further characterize the hits, samples of each unique compound were cherry-picked and subjected to full dose-response studies using a dilution series of 10 points in a 1:3 dilution steps (top = 100 μM). Of the initial 883 compounds picked, 189 displayed a saturating dose response in the ODC-PEPC-MDH system, while 310 displayed partial dose responses. Upon retesting, 384 of the initially identified hits were inactive, giving a validated hit rate of 43.4%. None of the compounds detectably affected the PEPC-MDH system at concentrations up to 100 μM concentrations. Comparison of inhibited reaction rates at both 150 and 300 nM ODC showed that all compounds were acting via inhibition of ODC and that ODC inhibition was the rate limiting step in the coupled assay system. The remaining validated hits were filtered to remove those containing potentially undesirable chemical moieties, such as highly reactive groups or metal containing compounds and checked for commercial availability, leaving 179 commercially available

validated hits. These validated hits were re-ordered from their suppliers. At the same time, expanded sets were designed, centered on promising compound series, and sourced from the same vendors. This produced a total of 260 compounds which were subjected to the secondary assay panel.

Secondary Testing

The identity and purity of all 260 re-ordered compounds were validated using UPLC-MS.²⁴ The average purity was 79%, and any compound less than 90% pure was rejected from further analysis. Seventy-five of the compounds failed purity or identity checks. Stock solutions were prepared at a putative concentration of 10 mM in DMSO and the concentrations confirmed using CLND.²⁵ The remaining compounds were re-tested in the primary assay to validate their activities. Of the 185 pure compounds tested, 76 showed activity in the primary assay. At this point the compounds were also screened versus hODC and at high (300 nM) concentrations of TbODC to determine selectivity and verify that ODC inhibition was the rate limiting step in the system. Inhibition of TbODC was determined to be rate limiting in all cases. The compounds were also screened for redox activity to eliminate non-specific radical based inhibitors.¹⁹ A representative compound from each scaffold series was also tested using the radio-labeled ornithine assay to confirm inhibition of TbODC in an orthogonal assay system. The representative compound was also tested for reversibility by dialysis. Of the 76 compounds active in the primary assay, only 7 were acceptably active in all assays. The results of these are summarized in Table 1. The active compounds represented four scaffold classes. Following confirmation of activity in this fashion the compounds were

screened at varying L-ornithine (Orn) concentrations (0.31, 1.3, 2.5, 5.0 and 10 mM) as well as varying PLP concentrations (0.5, 1.5, 1, 3, 5 and 10 μ M) in order to determine mode of inhibition and K_i values. These compounds, spanning 4 scaffold series, along with small structure-activity groups are discussed below.

Novel Inhibitors of ODC

The first well-behaved inhibitor discovered during the course of this effort, (compound **1**, Table 4.1, **Fig 4.1**) was a bisbiguanide compound. This compound was quite potent, with a K_i value of 2.7 μ M, and displayed competitive inhibition with respect to ornithine but non-competitive inhibition with respect to PLP. However, despite its resemblance to the dithioamidines, it was not a selective inhibitor of TbODC, inhibiting hODC with a similar potency. This, as well as the difference in the mode of inhibition with respect to PLP, suggests that it has a different binding mode than the dithioamidines. This compound was reversible and inactive in the redox assay. No close analogs were available for structure-activity relationship studies.

Table 4.1 – Inhibitors of TbODC

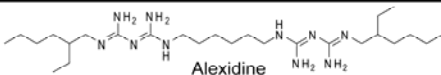
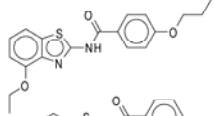
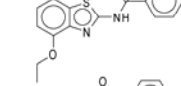
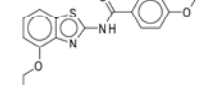
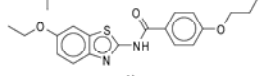
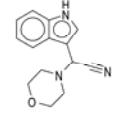
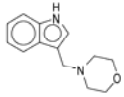
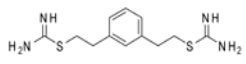
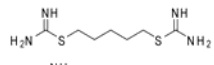
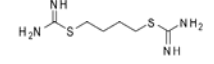
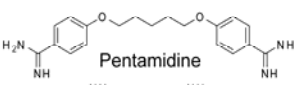
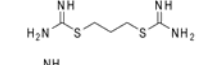
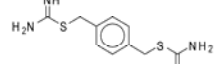
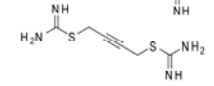
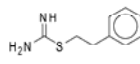
Number	Compound	WT TbODC K_i Linked Enzyme*	WT TbODC IC_{50} Linked Enzyme	WT TbODC IC_{50} C ¹⁵ Assay**	hODC IC_{50} Linked Enzyme	High:Low ODC Rate Ratio
1***	 Alexidine	2.7 (1.5 - 3.9)	24 ± 4.2	4.1	22 ± 2.8	1.9 ± 0.2
2***		14.0 (12.6 - 15.4)****	59.4 ± 6.5	180	24 ± 5.9	1.8 ± 0.2
3		>>100	>100	NT	>100	NA
4		>>100	>100	NT	>100	NA
5		>>100	>100	NT	>100	NA
6***		27.1 (24.3 - 30.0)****	20 ± 2	NT	62.8 ± 13	1.94 ± 0.20
7		>>100	>100	NT	>100	NA
8***		3.6 (2.1 - 5.7)	14 ± 4.2	12	>100	1.9 ± 0.2
9		10.2 (8.1 - 12.2)	15.3 ± 1.1	NT	>100	2.0 ± 0.3
10		28.8 (23.6 - 34.1)	30.3 ± 1.2	NT	>100	1.8 ± 0.3
11***	 Pentamidine	28.9 (22.3 - 37.0)	34.2 ± 1.7	NT	>100	1.8 ± 0.1
12		>100	~75‡	NT	>100	1.8 ± 0.2
13		>100	~75‡	NT	>100	1.9 ± 0.3
14		>>100	>100	NT	>100	NA
15		>>100	>100	NT	>100	NA

Table 4.1 – All values are μM unless otherwise noted. * K_i values were determined by global fitting of raw rate data to appropriate Michaelis-Menton equations and are expressed as fit value followed by 95% confidence limits. K_i values were determined using data from 3 separate triplicate experiments. ** IC_{50} determined at 37 °C at 400 μM L-Orn as described in materials and methods. Data was fit to simple IC_{50} model. ***Primary HTS hit compound. All other compounds were part of reordered analogue series. **** αK_i value from uncompetitive inhibition model. ‡Single point active at 100 μM All IC_{50} values were determined at isokinetic conditions (1.5 x K_m L-Orn, 60 μM PLP) as described in materials and methods. IC_{50} values are expressed as the mean of 3 measurements taken in triplicate \pm standard deviation. ODC concentrations were 150 nM

for all experiments. High and low ODC rates were determined at 150 and 300 nM ODC respectively in the presence of 625 μM L-Orn. NT: Not Tested, NA: Not Active.

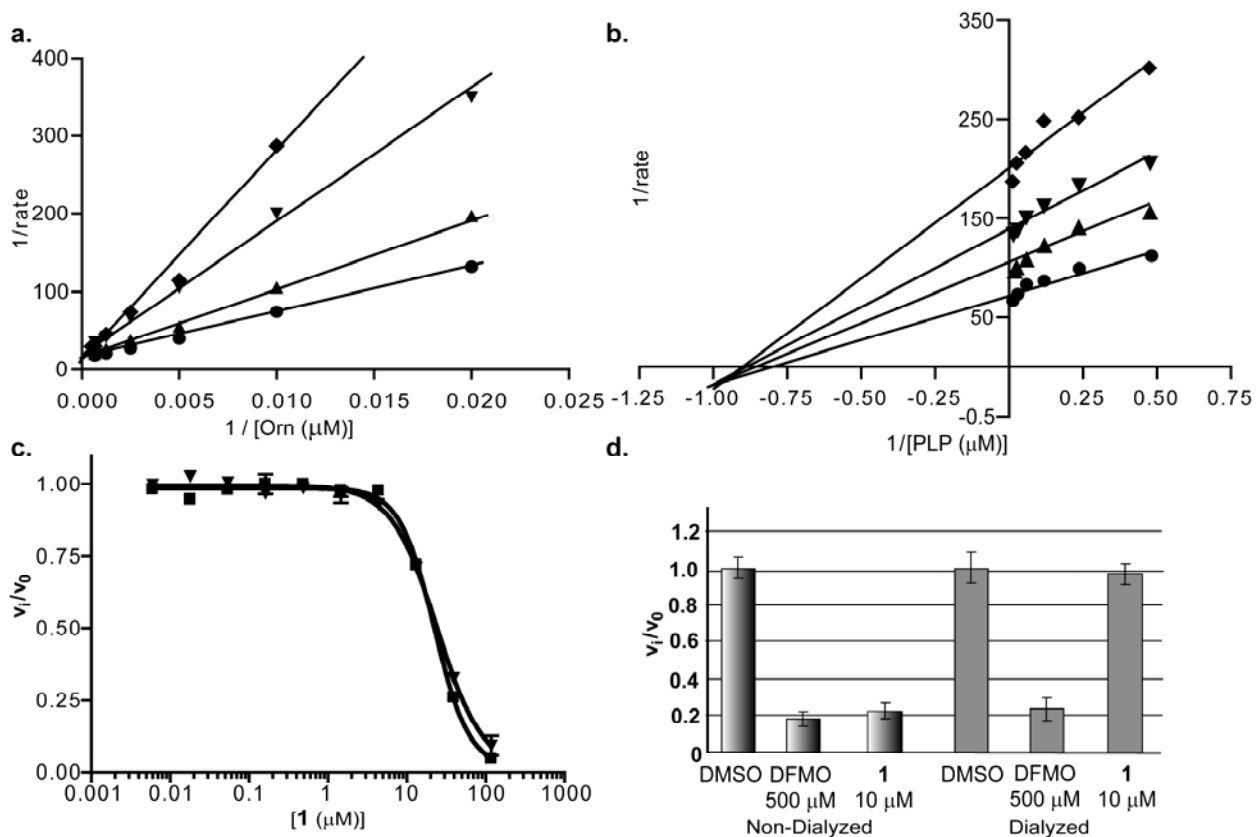


FIG. 4.1. Bisbiguanide inhibitor data. **4.1a** and **4.1b:** Lineweaver-Burk plots for Ornithine versus **1** and PLP versus **1**. (\blacklozenge = 10 μM , \blacktriangledown = 6 μM , \blacktriangle = 4 μM , \bullet = uninhibited) **4.1c:** Species selectivity analysis for **1**. Data for TbODC (\blacktriangledown) and hODC (\blacksquare) enzyme linked assays collected at 22°C in 384-well plates. Data was fitted to a 4 parameter sigmoidal dose response for determination of IC_{50} values. All data was collected under isokinetic conditions at $1.5 \times K_m$ for ornithine. **4.1d:** Reversibility of **1**. TbODC was incubated with inhibitor for 1 hour followed by overnight dialysis into assay buffer. Data was collected as described in materials and methods.

The second and third chemotypes were the benzthiazoles (compounds **2** to **5**, Table 1, **Fig 4.3**) and the indoles (compounds **5** and **6**, Table 1, **Fig 4.4**) which were moderately potent, with K_i values of 14.0 and 27.1 μM respectively. Both chemotypes were non-selective inhibitors, inhibiting both hODC and TbODC. Both chemotypes

displayed un-competitive inhibition with respect to PLP. The benzthiazoles were un-competitive with respect to ornithine, while the indoles were non-competitive. Both chemotypes were also reversible inhibitors of TbODC. Although there was only a single commercially available active member in each of these re-ordered series, the preliminary structure activity relationships from the screening collection suggest a specific binding interaction is responsible for the inhibition. This is particularly true for the benzthiazoles, which were heavily represented in the compound library.

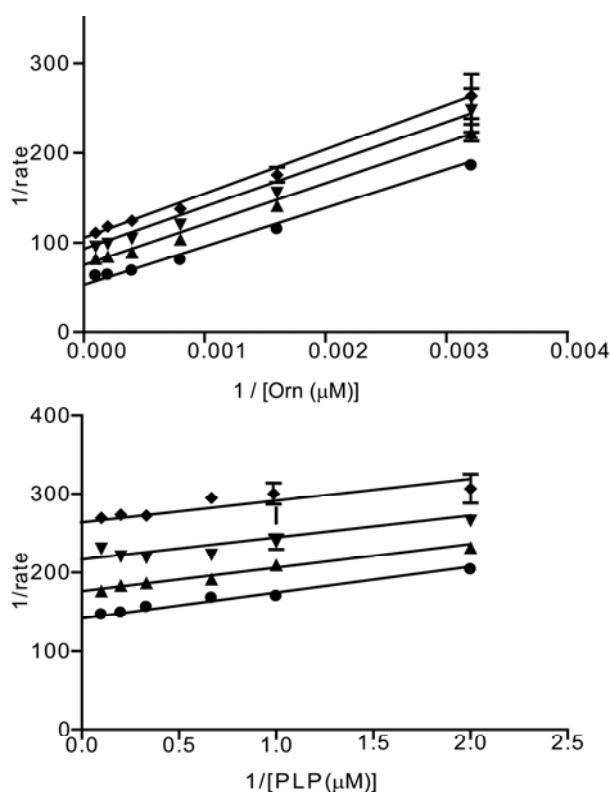


FIG. 4.2. Benzthiazole inhibitor data. Selectivity curves and reversibility data for these compounds can be found in supplementary data. Lineweaver-Burk plot for Ornithine versus **2** and PLP versus **2**. (♦ = 28 μM, ▼ = 9.5 μM, ▲ = 3.2 μM, ● = uninhibited)

After **2** was verified as a promising compound, all compounds containing the benzthiazole core were cherry-picked from our screening collection and subjected to full dose-response analysis. Though the small amounts of available compound prevented

determination of K_i values for these compounds, the IC_{50} values at 625 μM Orn, 60 μM PLP and 150 nM TbODC suggest that very little modification to the scaffold is acceptable. The structures and IC_{50} values for these compounds can be found in the supplementary data. In order to maintain activity, the 4-position ethoxy group must be present. Moving this group to the 6-position on the benzthiazole ring, or substitution with a methoxy group eliminates activity. Furthermore, the *p*-propoxy group on the phenyl amide moiety must also be preserved. This group can be substituted with a *p*-isopropoxyl moiety with a similar potency being maintained, but all other substitutions on this ring were inactive. In the case of the indole compounds, only one close analogue could be obtained for testing. This compound, SJ000360927, showed that the nitrile group was necessary for activity.

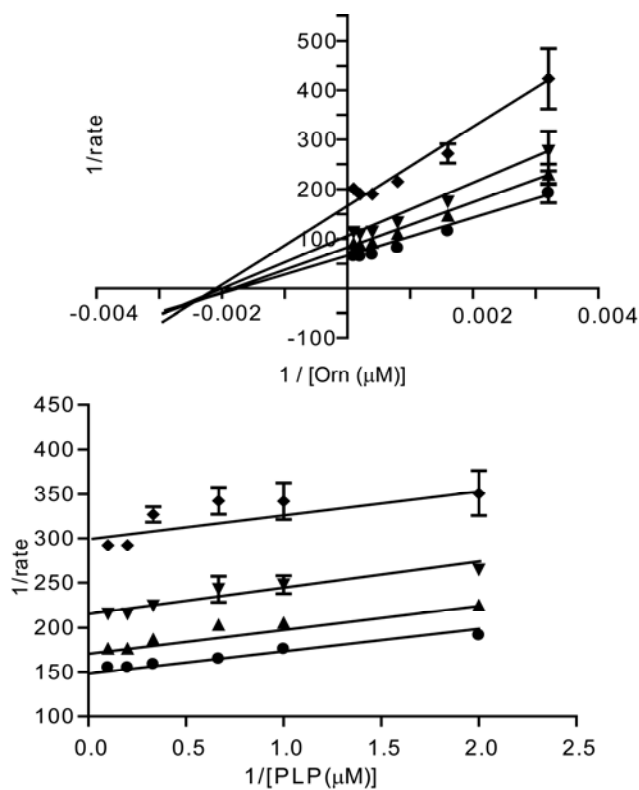


FIG. 4.3. Indole inhibitor data. Selectivity curves and reversibility data for these compounds can be found in supplementary data. Lineweaver-Burk plot for Ornithine versus **6** and PLP versus **6**. (◆ = 40 μM , ▼ = 13 μM , ▲ = 4.4 μM , ● = uninhibited)

The final novel chemotype discovered was the dithioamidines (compounds **8** to **15**, Table 1, Fig 4.5). These compounds were both selective and potent inhibitors of TbODC, with the most potent showing a K_i of 3.6 μM . Importantly, this compound has no detectable effect on hODC up to 100 μM . The compounds exhibit competitive inhibition with respect to ornithine and un-competitive inhibition with respect to PLP. They also displayed reversible inhibition. A reasonable preliminary structure-activity relationship exists in the series. To be active, these compounds must contain two thioamide moieties connected by a flexible linker of at least 4 atoms. Longer linkers were tolerated, with no upper limit on linker length being detected within the test set. These compounds were not active in the redox assay and are among the most potent reversible inhibitors of TbODC known. Interestingly, the anti-trypanosomal drug pentamidine (**11**) was also part of this inhibitor group, but does not appear to act by this mechanism in whole cells.

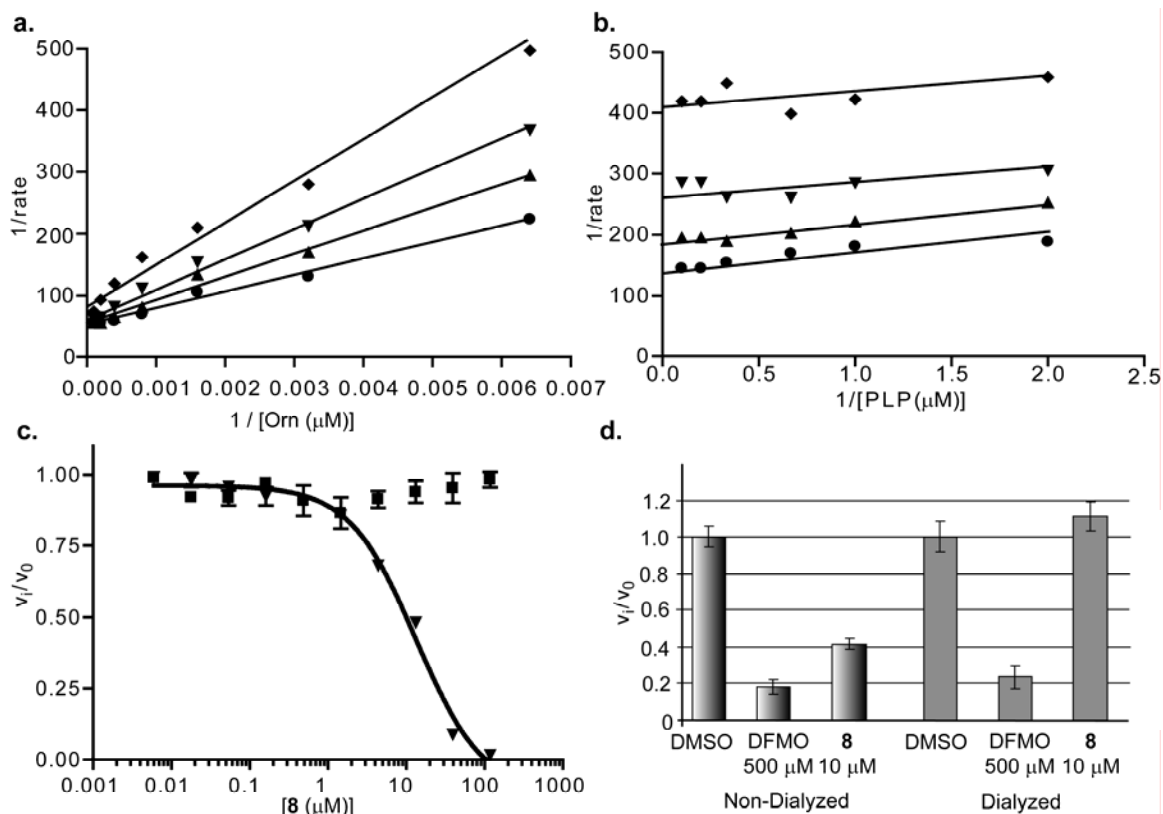


FIG. 4.4. Dithioamidine inhibitor data. **4.4a** and **b**: Lineweaver-Burk plots for Ornithine versus **8** and PLP versus **8**. ($\diamond = 40 \mu\text{M}$, $\nabla = 13 \mu\text{M}$, $\blacktriangle = 4.4 \mu\text{M}$, $\bullet =$ uninhibited). **4.4c**: Species selectivity analysis for **8**. Data for TbODC (∇) and hODC (\blacksquare) enzyme linked assays collected at 22°C in 384-well plates. Data was fitted to a 4 parameter sigmoidal dose response for determination of IC_{50} values. All data was collected under isokinetic conditions at $1.5 \times K_m$ for ornithine. **4.4d**: Reversibility of **8**. TbODC was incubated with inhibitor for 1 hour followed by overnight dialysis into assay buffer. Data was collected as described in materials and methods.

Identification of Potential Inhibitor Binding Sites on TbODC

Since the active sites of TbODC and hODC are highly homologous, it seemed unlikely that the TbODC selective dithioamidines were binding at the active site, despite the fact that they were competitive with ornithine.^{26, 27} Therefore, an effort was made to identify other potential binding sites on the surface of the TbODC homodimer. Site Finder was used to identify three major possible binding sites. The first of these (Site 1)

is a pocket just below the active site bounded by R337, H333, G201, and P245. The second (Site 2) is a groove at the dimer interface just above the active site bounded by K173, V168, P297, and F179. The final (Site 3) is a small, relatively deep pocket above and behind the active site bounded by D364, S396, and S402, with a possible entrance to the protein hydrophobic core defined by N92, D38, Q401, and E36. After computational identification, each site was utilized for DOCKing using a pre-generated conformer library containing all active dithioamidines as well as inactive analogues. Sites 1 and 2 were both predicted to be poor binding sites in comparison to the active site for all active compounds in the test set. However, Site 3 was predicted to be a better binding site for the dithioamidines than the active site. Furthermore, Site 3 yielded better discrimination between active and inactive dithioamidines than did any other site, with a receiver operator characteristic area under curve score (ROC AUC) of 0.99 versus scores of ~0.91 at the three other sites. The ROC AUC is the probability that the assay will rank a randomly chosen true positive ahead of a randomly chosen true negative. A score of >0.5 in this metric represents discriminatory ability. Binding at Site 3 would also explain the selectivity seen with this scaffold series. Residues at both possible entrances to the site are unconserved between TbODC and hODC. The apo structure of this site and the top docked pose of the dithioamide **9** at this site are pictured in **Fig 4.6a** and **4.6b** respectively. Enrichment plots (ROC Plots) of the docking results for the three alternate sites, as well as the active site can be found in supplementary materials.

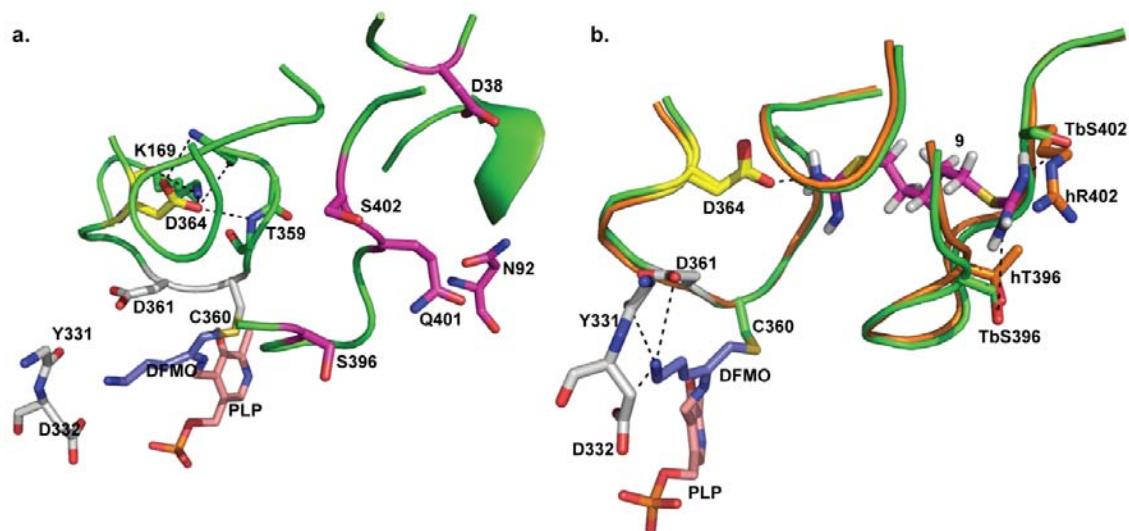


Fig 4.5. Proposed dithioamidine binding site. 4.5a: TbODC bound to DFMO. DFMO is in purple, PLP is salmon, active site residues are white, and residues that form the proposed binding site are indicated as follows: D364 is colored yellow and forms the bottom of the binding site and magenta residues form the two possible entrances to the proposed dithioamidine binding site. **4.5b: 9** docked into the proposed binding site on TbODC and superimposed with the apo human ODC structure. TbODC residues are orange, hODC residues are light blue. D364 is yellow, active site residues are white, DFMO is purple, and PLP is salmon. Note that S402 from TbODC is not conserved in hODC, and that the opening to the proposed site is completely occluded in the human enzyme. This could help account for the remarkable selectivity seen with the dithioamidine series of inhibitors.

As the DOCKing studies suggested that Site 3 might represent the *bone fide* site for the dithioamidenes, this site was examined in greater detail. The majority of the high scoring dock poses involved favorable interactions of one thioamidine moiety with D364, a negatively charged residue at the bottom binding site. The second thioamidine moiety assumed placements allowing a wide variety of interactions with charged or polar groups in and around the binding pocket. Previous studies have shown that D364 is critical to enzyme function, and that substitution with alanine renders the enzyme inactive.²⁸ In order to test our binding hypothesis, a more conservative mutant (D364E) was used to evaluate the role of the residue in the binding of the dithioamidine compounds. While this

mutant did have dramatically increased K_m (60 mM vs. 0.37 mM) and decreased k_{cat} (0.02 sec⁻¹ vs. 7 sec⁻¹) some activity was still measurable. This mutant was then used to test **1** and **8**, two competitive inhibitors with similar K_i values emerging from our studies that possess theoretically different binding modes. The non-TbODC selective inhibitor **1** was able to inhibit 20 μ M D364E TbODC with an IC_{50} value of approximately 40 μ M while **8** had no detectable effect up to 100 μ M, indicating that D364 does play a role in the binding of the dithioamidine compounds. The results of these assays, along with steady state kinetic data for all enzymes used in the comparison are included in **Table 4.2**.

Table 4.2 – Steady state kinetic analysis of TbODC enzymes with inhibition data

ODC protein	K_m (L-Orn) (mM)	k_{cat} (s ⁻¹)	k_{cat}/K_m (L-Orn)	Compound 1 IC_{50} (μ M)	Compound 8 IC_{50} (μ M)
Wild Type TbODC	0.37 \pm 0.03	7.0 \pm 0.2	19	5.1	6.2
D364E TbODC	66 \pm 16	0.025 \pm 0.003	0.00038	~40*	>>100
S396A TbODC	0.27 \pm 0.03	10 \pm 0.4	37.0	6.9	13

Table 4.2 – Steady state kinetic analysis of TbODC with inhibition data. All data were collected at 37 °C using the linked enzyme assay as described in materials and methods. All IC_{50} values were determined at isokinetic conditions (400 μ M L-Orn for WT-TbODC and S396A-TbODC, 60mM L-Orn for D364E TbODC, 150 μ M L-Orn for WT-hODC, 60 μ M PLP was used for all experiments). IC_{50} values were determined with the cuvette-based enzyme linked assay using the same protocol as for the ¹⁴CO₂ assay. ODC concentrations were 150 nM for all experiments except for D364E, in which 20 μ M ODC was used to compensate for the low k_{cat} of the mutant. *Single point active at 50 μ M (~60% inhibition).

Two other mutants, S402A and S396A, at one possible entrance to the binding site were also tested. The S402A mutant expressed as an insoluble aggregate, and S396A had no detectable effect on binding of **1** or **8**. However, in light of the fact that many

energetically close docked poses of **8** placed the second thioamidine moiety at the entrance defined by D38, this is not unexpected.

To further evaluate the effect of the D364E mutation on the geometry of Site 3, the residue was virtually modified using the apo structure 1QU4 as a template. After performing a rotamer search and minimizing all residues within 8 Å of the mutation using the AMBER99 forcefield, no large scale structural changes were seen. However, E364 is able to move closer to the backbone amine of T359 and assume a more optimal hydrogen bonding position (2.10 vs. 2.44 Å). Furthermore, E364 is able to move within hydrogen bonding distance of K169, a residue located in a loop whose flexibility is thought to be important for proper functioning of the catalytic cycle.²⁹ This movement also orients the carboxylate of the residue away from the thioamidine groups of the inhibitors, making the binding interaction less favorable.

Whole Cell Efficacy

Although all compounds able to inhibit TbODC were active in whole cell growth inhibition assays (with the exception of **6**), none showed statistically significant shifts in EC₅₀ values when tested in the presence of 500 µM putrescine, an amount sufficient to completely rescue growth inhibition caused by DFMO. Compound **1** displayed significant growth inhibition in all cell lines tested with 5 to 10 fold selectivity for *T. brucei*. Interestingly, the only benzthiazole active versus *T. brucei* or any of the mammalian cell lines was **2**. However, since **2** showed no shift in EC₅₀ when tested in the presence of putrescine, it is unlikely that this

Table 4.3 – Whole Cell Cytotoxicity Results

Compound	<i>T. brucei</i> EC ₅₀ (μ M) 0 μ M Put	<i>T. brucei</i> EC ₅₀ (μ M) 500 μ M Put	Raji EC ₅₀ (μ M)	HEPG2 EC ₅₀ (μ M)	HEK293 EC ₅₀ (μ M)	BJ EC ₅₀ (μ M)
1	0.67 (0.21)	0.63 (0.35)	3.2 (0.3)	6.3 (1.2)	8.6 (0.9)	11 (2.1)
2	4.6 (1.5)	6.5 (3.1)	15 (2)	>50	13 (7)	>50
3	>50	>50	>50	>50	>50	>50
4	>50	>50	>50	>50	>50	>50
5	>50	>50	>50	>50	>50	>50
6	>50	>50	>50	>50	>50	>50
7	>50	>50	>50	>50	>50	>50
8	0.63 (0.12)	0.83 (0.22)	>50	>50	>50	>50
9	1.5 (0.5)	7.1 (4)	>50	>50	>50	>50
10	18 (8)	22 (6)	>50	>50	>50	>50
11	0.10 (0.015)	0.078 (0.005)	>50	>50	>50	>50
12	28 (9)	34 (11)	>50	>50	>50	>50
13	3.1 (0.3)	4.2 (0.4)	>50	>50	>50	>50
14	25 (15)	28 (12)	>50	>50	>50	>50
15	29 (10)	54 (22)	>50	>50	>50	>50
DFMO	242 (63)	>10,000	696 (273)	>10,000	320 (57)	>10,000

Table 4.3 Whole cell cytotoxicity results. EC₅₀ values were determined using a 10 point dose response curve with a top concentration of 50 μ M with the exception of DFMO, which was tested with a top concentration of 10 mM. Data was normalized to positive and negative controls and fit to a four parameter sigmoidal curve with the top plateau limited to values below 125% growth. Values are expressed as the mean of three separate experiments with standard deviations in parentheses. *T. brucei* EC₅₀ values were determined in the presence or absence of 500 μ M putrescine.

activity is the result of ODC inhibition. Compounds **6** and **7** were completely inactive in all cell lines tested. The dithioamidienes were all active versus *T. brucei* and completely inactive in the cytotoxicity test panel. However, as in the case of **2**, no shifts in EC₅₀ were observed in the presence of high concentrations of putrescine, indicating that the observed toxicity is not ODC dependent.

DISCUSSION

This study was the first large scale screening effort to discover new chemotypes for ODC inhibition. Screening a large chemical library has led to the discovery of several

potent and selective inhibitors, including the first known inhibitors that are selective for TbODC over the highly homologous hODC. We also report the first non-substrate, non-product-based inhibitors of ODC. The identification of pentamidine, a known weakly binding inhibitor of TbODC ($K_i > 30 \mu\text{M}$), as a hit compound in the primary screen shows that our assay was sensitive.³⁰ This suggests that most reversible ODC inhibitors present in our screening library with K_i values below $30 \mu\text{M}$ are likely to have been identified.

The four classes of inhibitors identified in this screening effort represent novel chemotypes for ODC inhibition. They also possess novel modes of inhibition. The benzthiazoles, typified by **2**, are the most potent ornithine un-competitive inhibitors known for ODC, and are also uncompetitive with respect to PLP. While the exact binding modes of these compounds are unknown, it is unlikely to be at the active site, since addition of substrate increases the potency of the inhibitor. It is known that binding of ornithine stabilizes the dimerization of ODC.³¹ This suggests that the benzthiazoles bind to the ODC homodimer. While other uncompetitive inhibitors of ODC have previously been characterized, their K_i values have been in the mM range³², significantly weaker than **2**, which possesses a K_i of 12.6 to $15.4 \mu\text{M}$. Identification of the binding site for this inhibitor would allow further optimization with the potential for an improvement in binding affinity. Since the compound is non-selective for TbODC over hODC, it is also likely that the binding site is conserved between the human and trypanosomal enzymes. Interestingly, **2** is the only benzthiazole active versus whole cell *T. brucei*, as well as the only one active in the human cell line panel. However, the potency versus *T. brucei* does

not shift in the presence of high levels of putrescine, indicating that ODC is unlikely to be the primary mode of action.

The indole **6** is non-competitive with respect to ornithine, and un-competitive with respect to PLP, suggesting a binding mode that differs from the benzthiazoles and is not at the active site. Since this compound is non-selective for TbODC versus hODC, the binding site must be conserved between the two enzymes. While the presence of an electrophilic nitrile that is required for activity suggests the possibility of a covalent mechanism of action, the fact that inhibition is completely reversible indicates any modification is reversible. As with **2**, the identification of this binding site would prove useful in the further development of novel ODC inhibitors for both TbODC and hODC. All of the indoles tested were inactive in whole cell assays.

Two classes of potent competitive inhibitors were also discovered during the screen. The first of these, exemplified by **1** (alexidine), is bisbiguanides. Reports of alexidine's antimicrobial activity date back to the 1950's³³ and it has anti-fungal activity and has been assayed as a potential chemotherapeutic compound.^{34, 35} Alexidine represents an interesting molecule for use in characterizing ODC more fully. Although it is a competitive inhibitor, alexidine is too large to fit completely within the active site, suggesting that the binding mode is more than a simple interaction with a single active site. Prior studies have suggested that ODC is susceptible to allosteric modulation by G418, another large, basic antimicrobial compound.³⁶ However, G418 binds very weakly (K_i of 3-8 mM), severely hampering mechanistic studies. Alexidine, with the much lower K_i of 3.8 μ M, represents a much better opportunity to investigate the modulation of ODC through allosteric binding sites. While this compound does display whole cell anti-

trypanosomal effects, it is not affected by the presence of putrescine, indicating that it is unlikely to be acting via the polyamine pathway in this context.

The final class of inhibitors discovered in this screening effort is the most interesting. The dithioamidine series, and **8** in particular, represent the first selective inhibitors for TbODC. **8** is a known inhibitor of nitric oxide synthase and is one of the most potent reversible inhibitors of ODC known, with a K_i of 3.6 μM . This compound is structurally significantly different from the simple putrescine and ornithine analogues previously reported as reversible inhibitors of ODC^{4,37} suggesting that either the active site of ODC tolerates larger compounds or that these compounds are not binding at the active site. Because **8** is not highly functionalized it may be possible for medicinal chemistry efforts to improve its potency. This proposition is supported by the work of Tidwell et al, who have previously reported similar diamidine scaffolds as anti-trypanosomal compounds with unknown mechanism and shown clear structure activity relationships within these compound series.^{38,39} These results are replicated here, with all of the dithioamidine compounds being active versus whole cell *T. brucei*, though no correlation with ODC activity was observed. Furthermore, the EC_{50} of the compounds versus the parasite do not shift in the presence of high levels of putrescine, indicating that ODC inhibition is not responsible for the observed activities. All of the compounds were inactive to 50 μM in mammalian cytotoxicity assays.

Other diamidine compounds such as berenil have been shown to be effective inhibitors of SAMDC, another enzyme in the polyamine biosynthetic pathway.³⁰ This raises the possibility that diamidine or dithioamidine compounds could be developed that

are able to inhibit both TbODC and SAMDC, effectively shutting off both rate limiting steps in the polyamine biosynthetic pathway.

The remarkable selectivity for TbODC versus hODC displayed by the dithioamidines is likely due to the binding of these compounds to a secondary site, located behind the active site and bounded by tbD364, tbS396 and tbS402, with a second possible entrance defined by tbN92, tbD38, tbQ401, and tbE36. Binding at this site may explain selectivity, since the residues at the entrance to the site are not conserved between the trypanosomal and the human enzymes. In hODC, tbS402 is replaced by hR402, and tbN92 is substituted by hK92. Examination of the crystal structure of the human enzyme (17DK) shows these changes place greater positive charge density at the binding site entrances, and in the case of the tbS402 entrance, completely occlude access to the binding pocket. Both molecular modeling experiments and mutagenesis data support the idea that the dithioamidines interact directly with tbD364, a residue known to be important for ODC catalytic activity. This residue is conserved across a wide range of eukaryotic ODC enzymes, indicating an important role for maintaining enzymatic functionality.²⁸

D364 is uniquely positioned at the center of interaction between two important loops. The first loop, in which D364 resides, contains both D361 and C360. D361 is an active site residue involved in the stabilization of the terminal amine of ornithine during substrate binding. The precise positioning of the substrate by D361, along with D332 and the backbone carbonyl of Y331 has been hypothesized to be necessary for the substrate binding. The residue thought to be responsible for protonating the anion generated by decarboxylation, C360, is also in the same loop as D364, and shifts in this residue would

likely be detrimental to enzymatic function.⁴⁰ The second loop, which interacts with D364, contains K169 (directly hydrogen bonded to D364) and L166, a residue which has been predicted to interact with the carboxylate of L-ornithine.²⁹ This loop is known to be flexible, and that flexibility is thought to be important in the ODC catalytic cycle. Perturbations in the positioning of D364 would affect the populations of conformers available to this loop. In short, D364 is at the center of what is likely to be a highly dynamic set of hydrogen bond interactions involving many residues known to be vital to enzymatic function. The importance of its positioning is supported by mutagenic data for this residue, where substitution with an alanine renders the enzyme inactive, and even the relatively conservative substitution with glutamic acid increases K_m by more than 175-fold, and decreases k_{cat} by 280-fold.

The relatively small number of inhibitors discovered in this screen and the similarity of these inhibitors to polyamines underscores the difficulty of developing inhibitors for this enzyme. The bulk of available evidence, including the results of this screen, suggests that ODC's small and charged active site is unable to bind conventional drug-like molecules. However, this study has shown that TbODC is susceptible to inhibition by compounds likely to be acting at allosteric sites. Furthermore, allosteric inhibition of this enzyme may allow it to escape the stabilization typically seen in the presence of other reversible inhibitors in mammalian systems.

In conclusion, we have used a high-throughput assay to screen over 300,000 molecules, to identify potent and selective inhibitors of TbODC. Three of the four scaffold series presented display activity versus whole cell *T. brucei*, though not via the polyamine pathway, suggesting that the compounds are able to enter the cells. These

inhibitors are likely to bind at novel, non-active site locations on the enzyme, and represent valuable tools for further development of more drug-like inhibitors of this clinically relevant drug target.

REFERENCES

1. Russell, D.; Snyder, S. H., Amine synthesis in rapidly growing tissues: ornithine decarboxylase activity in regenerating rat liver, chick embryo, and various tumors. *Proc Natl Acad Sci U S A* **1968**, 60, (4), 1420-7.
2. Abdel-Monem, M. M.; Newton, N. E.; Weeks, C. E., Inhibitors of polyamine biosynthesis. 1. Alpha-methyl-(plus or minus)-ornithine, an inhibitor of ornithine decarboxylase. *J Med Chem* **1974**, 17, (4), 447-51.
3. Casero, R. A., Jr.; Marton, L. J., Targeting polyamine metabolism and function in cancer and other hyperproliferative diseases. *Nat Rev Drug Discov* **2007**, 6, (5), 373-90.
4. Bey, P., Danzin, C, Jung, M, Inhibition of Basic Amino Acid Decarboxylases Involved in Polyamine Biosynthesis. In *Inhibition of Polyamine Metabolism - Biological Significance and Basis for New Therapies*, McCann, P. P., Pegg, A.E., Sjoerdsma, A., Ed. Academic Press: San Diego, 1987; pp 1-31.
5. Bitonti, A. J.; McCann, P. P.; Sjoerdsma, A., Restriction of bacterial growth by inhibition of polyamine biosynthesis by using monofluoromethylornithine, difluoromethylarginine and dicyclohexylammonium sulphate. *Biochem J* **1982**, 208, (2), 435-41.
6. Thyssen, S. M.; Libertun, C., Quantitation of polyamines in hypothalamus and pituitary of female and male developing rats. *Neurosci Lett* **2002**, 323, (1), 65-9.

7. Shelat, A. A.; Guy, R. K., The interdependence between screening methods and screening libraries. *Curr Opin Chem Biol* **2007**, 11, (3), 244-51.
8. Hann, M.; Hudson, B.; Lewell, X.; Lively, R.; Miller, L.; Ramsden, N., Strategic pooling of compounds for high-throughput screening. *J Chem Inf Comput Sci* **1999**, 39, (5), 897-902.
9. Bemis, G. W.; Murcko, M. A., The properties of known drugs. 1. Molecular frameworks. *J Med Chem* **1996**, 39, (15), 2887-93.
10. Osterman, A.; Grishin, N. V.; Kinch, L. N.; Phillips, M. A., Formation of functional cross-species heterodimers of ornithine decarboxylase. *Biochemistry* **1994**, 33, (46), 13662-7.
11. Kunkel, T. A., Rapid and efficient site-specific mutagenesis without phenotypic selection. *Proc Natl Acad Sci U S A* **1985**, 82, (2), 488-92.
12. Team, R. D. C., *R: A language and environment for statistical computing*. R Foundation for Statistical Computing: Vienna, 2007.
13. Peter Rousseeuw, C. C., Valentin Todorov, Andreas Ruckstuhl, Matias Salibian-Barrera, Martin Maechler *robustbase: Basic Robust Statistics* R package 0.2-7; 2006.
14. Hoaglin, D. C., Mosteller, Frederick, Tukey, John W., *Understanding Robust and Exploratory Data Analysis*. John Wiley and Sons, Inc.: New York, 1983.
15. Zhang, J. H.; Chung, T. D.; Oldenburg, K. R., A Simple Statistical Parameter for Use in Evaluation and Validation of High Throughput Screening Assays. *J Biomol Screen* **1999**, 4, (2), 67-73.
16. Pegg, A. E.; McGill, S., Decarboxylation of ornithine and lysine in rat tissues. *Biochim Biophys Acta* **1979**, 568, (2), 416-27.

17. Lee, J.; Michael, A. J.; Martynowski, D.; Goldsmith, E. J.; Phillips, M. A., Phylogenetic diversity and the structural basis of substrate specificity in the beta/alpha-barrel fold basic amino acid decarboxylases. *J Biol Chem* **2007**, 282, (37), 27115-25.
18. Baldwin, J.; Michnoff, C. H.; Malmquist, N. A.; White, J.; Roth, M. G.; Rathod, P. K.; Phillips, M. A., High-throughput screening for potent and selective inhibitors of Plasmodium falciparum dihydroorotate dehydrogenase. *J Biol Chem* **2005**, 280, (23), 21847-53.
19. Lor, L. A.; Schneck, J.; McNulty, D. E.; Diaz, E.; Brandt, M.; Thrall, S. H.; Schwartz, B., A simple assay for detection of small-molecule redox activity. *J Biomol Screen* **2007**, 12, (6), 881-90.
20. Segel, I. H., *Enzyme Kinetics, Behavior and Analysis of Rapid Equilibrium and Steady-State Enzyme Systems*. John Wiley & Sons: New York, 1975.
21. Grishin, N. V.; Osterman, A. L.; Brooks, H. B.; Phillips, M. A.; Goldsmith, E. J., X-ray structure of ornithine decarboxylase from Trypanosoma brucei: the native structure and the structure in complex with alpha-difluoromethylornithine. *Biochemistry* **1999**, 38, (46), 15174-84.
22. Almrud, J. J.; Oliveira, M. A.; Kern, A. D.; Grishin, N. V.; Phillips, M. A.; Hackert, M. L., Crystal structure of human ornithine decarboxylase at 2.1 Å resolution: structural insights to antizyme binding. *J Mol Biol* **2000**, 295, (1), 7-16.
23. Hendlich, M.; Rippman, F.; Barnickel, G., LIGSITE: automatic and efficient detection of potential small molecule-binding sites in proteins. *J. Mol. Graph.* **1997**, 15, (6), 359-363.

24. Lemoff, A.; Yan, B., Dual detection approach to a more accurate measure of relative purity in high-throughput characterization of compound collections. *J Comb Chem* **2008**, 10, (5), 746-51.
25. Yan, B.; Zhao, J.; Leopold, K.; Zhang, B.; Jiang, G., Structure-dependent response of a chemiluminescence nitrogen detector for organic compounds with adjacent nitrogen atoms connected by a single bond. *Anal Chem* **2007**, 79, (2), 718-26.
26. Phillips, M. A.; Coffino, P.; Wang, C. C., Cloning and sequencing of the ornithine decarboxylase gene from *Trypanosoma brucei*. Implications for enzyme turnover and selective difluoromethylornithine inhibition. *J Biol Chem* **1987**, 262, (18), 8721-7.
27. Steglich, C.; Schaeffer, S. W., The ornithine decarboxylase gene of *Trypanosoma brucei*: Evidence for horizontal gene transfer from a vertebrate source. *Infect Genet Evol* **2006**, 6, (3), 205-19.
28. Osterman, A. L.; Kinch, L. N.; Grishin, N. V.; Phillips, M. A., Acidic residues important for substrate binding and cofactor reactivity in eukaryotic ornithine decarboxylase identified by alanine scanning mutagenesis. *J Biol Chem* **1995**, 270, (20), 11797-802.
29. Jackson, L. K.; Baldwin, J.; Akella, R.; Goldsmith, E. J.; Phillips, M. A., Multiple active site conformations revealed by distant site mutation in ornithine decarboxylase. *Biochemistry* **2004**, 43, (41), 12990-9.
30. Bitonti, A. J.; Dumont, J. A.; McCann, P. P., Characterization of *Trypanosoma brucei brucei* S-adenosyl-L-methionine decarboxylase and its inhibition by Berenil, pentamidine and methylglyoxal bis(guanyldrazone). *Biochem J* **1986**, 237, (3), 685-9.

31. Solano, F.; Penafiel, R.; Solano, M. E.; Lozano, J. A., Equilibrium between active and inactive forms of rat liver ornithine decarboxylase mediated by L-ornithine and salts. *FEBS Lett* **1985**, 190, (2), 324-8.
32. Henley, C. M., 3rd; Mahran, L. G.; Schacht, J., Inhibition of renal ornithine decarboxylase by aminoglycoside antibiotics in vitro. *Biochem Pharmacol* **1988**, 37, (9), 1679-82.
33. Rose, F. L., Swain, G, Bisdiguandines having Antibacterial Activity. *J. Chem. Soc.* **1956**, 4422-4425.
34. Ganendren, R.; Widmer, F.; Singhal, V.; Wilson, C.; Sorrell, T.; Wright, L., In vitro antifungal activities of inhibitors of phospholipases from the fungal pathogen *Cryptococcus neoformans*. *Antimicrob Agents Chemother* **2004**, 48, (5), 1561-9.
35. Yip, K. W.; Ito, E.; Mao, X.; Au, P. Y.; Hedley, D. W.; Mocanu, J. D.; Bastianutto, C.; Schimmer, A.; Liu, F. F., Potential use of alexidine dihydrochloride as an apoptosis-promoting anticancer agent. *Mol Cancer Ther* **2006**, 5, (9), 2234-40.
36. Jackson, L. K.; Goldsmith, E. J.; Phillips, M. A., X-ray structure determination of *Trypanosoma brucei* ornithine decarboxylase bound to D-ornithine and to G418: insights into substrate binding and ODC conformational flexibility. *J Biol Chem* **2003**, 278, (24), 22037-43.
37. Garvey, E. P.; Oplinger, J. A.; Tanoury, G. J.; Sherman, P. A.; Fowler, M.; Marshall, S.; Harmon, M. F.; Paith, J. E.; Furfine, E. S., Potent and selective inhibition of human nitric oxide synthases. Inhibition by non-amino acid isothioureas. *J Biol Chem* **1994**, 269, (43), 26669-76.

38. Athri, P.; Wenzler, T.; Ruiz, P.; Brun, R.; Boykin, D. W.; Tidwell, R.; Wilson, W. D., 3D QSAR on a library of heterocyclic diamidine derivatives with antiparasitic activity. *Bioorg Med Chem* **2006**, 14, (9), 3144-52.
39. Mathis, A. M.; Holman, J. L.; Sturk, L. M.; Ismail, M. A.; Boykin, D. W.; Tidwell, R. R.; Hall, J. E., Accumulation and intracellular distribution of antitrypanosomal diamidine compounds DB75 and DB820 in African trypanosomes. *Antimicrob Agents Chemother* **2006**, 50, (6), 2185-91.
40. Jackson, L. K.; Brooks, H. B.; Osterman, A. L.; Goldsmith, E. J.; Phillips, M. A., Altering the reaction specificity of eukaryotic ornithine decarboxylase. *Biochemistry* **2000**, 39, (37), 11247-57.

Chapter 5
Conclusions

The work presented herein represents the first fruits of a new high-throughput screening facility along with the first large scale drug discovery effort targeted at trypanosomal ODC. The lessons learned during this process, and particularly during the ODC project will be invaluable to future high-throughput screening efforts at St. Jude Children's Research Hospital as well as to other investigators interested in polyamine biosynthesis in *Trypanosoma brucei*.

The set-up and optimization of a fully automated high-throughput screening facility is always a challenging endeavor. Many of the systems are one of a kind or small production run models and are relatively poorly tested before release. Additionally, many of the most experienced high-throughput screening groups are in industry, meaning that their knowledge is largely inaccessible to the academic researcher. As such, a wide range of preliminary experiments, from timing optimization to wash protocol development (chapter 2) were performed both before and during the process described in this thesis. The results of these experiments, when appropriate, have been published, allowing other screening organizations to learn from our efforts and streamline their own. This is becoming increasingly important as academic high-throughput screening groups become more and more common. However, while the general approaches used to solve these problems can be shared with others, specific solutions are often highly application specific, meaning that each screening group must conquer their own systems before a successful screening program can begin full-time operation.

TbODC was the first full deck screen attempted at St. Jude. As such, everything from relatively simple automation issues including robotic programming and instrument integration to more complex issues such as data handling, curve fitting, cherry-picking

procedures and automated liquid handling protocols for the production of dose response plates had to be developed and optimized during the screening process. Many of the protocols implemented during the TbODC assay are still in use at St. Jude and have proved invaluable for other screening efforts. In particular, our experiences with automating low volume liquid handling in a flexible, user-friendly manner has proved invaluable across a wide range of projects institution wide.

Optimization of an assay for use in a high-throughput screen is not a simple process. The assay in question must be highly robust, and a suitable panel of secondary assay systems must be in place which is capable of dealing with false positives from the primary screen. In this effort, an assay suitable for the screening of any carbon dioxide producing enzyme has been optimized and shown to be highly sensitive. The main drawback to this screening effort had nothing to do with the assay system itself, but rather with the sensitivity of ODC to various redox stressors. The majority of false positives resulted from incubating the enzyme in the presence of test compound without dithiothreitol (DTT). This resulted in the identification of compounds capable of irreversibly inhibiting the enzyme in its oxidized state rather than its active reduced state. If this assay system were to be used in the future for screening of ODC, the compounds should be incubated in the presence of ODC and DTT. However, this may not prove to be any better, since it is known that a wide range of small molecules are able to react with DTT to produce free radicals which can then inhibit enzymes non-specifically.^{1, 2} In short, it is most likely necessary to screen potential hit compounds under both conditions. Well behaved inhibitors should behave identically in both.

This phenomena may be worthy of additional investigation since a significant portion the DTT-sensitive false positive compounds were not identified as redox active in the proxy-assay for oxidative potential.² It should be noted that the false positive compounds contained ~10 to 15 compound series with varying levels of internal structure activity relationships and including compounds which were selective for TbODC versus hODC. However, since none of these compounds replicated in the ¹⁴CO₂ assay or in the whole cell putrescine rescue experiments, they must still be regarded as screening artifacts rather than ODC inhibitors. The compounds were not tested for their H₂O₂ production potential, and this remains a possible mechanism for the observed DTT-sensitivity. However, since sensitivity to the presence of a reducing agent was observed with both DTT and β-mercaptoethanol, which is known to be less susceptible to H₂O₂ production, it seems unlikely that the remaining false positives are due to this. It is well known that ODC requires large amounts of reducing agents (preferably DTT) to maintain activity *in vitro*.^{3, 4} This level of sensitivity to reductive potential likely results in ODC being abnormally sensitive to oxidative compounds in the absence of a protective amount of reducing agent.

The ODC inhibitors identified in this high-throughput screening effort represent potentially useful tools in the quest to create clinically useful ODC targeted drugs. In particular, the identification of potential allosteric sites and novel modes of inhibition may allow the development of more potent compounds suffering from fewer off-target effects. Towards that end, crystallographic studies of both the dithioamidine and the benzthiazole based compounds are ongoing in collaboration with Margaret Phillip's laboratory. It should be noted that these compounds have significant off-target effects in

addition to their ODC inhibiting properties. They are trypanocidal rather than trypanostatic and cannot be rescued by addition of putrescine (as would be expected if they were acting solely via ODC). Therefore, these compounds should not be regarded as potential drug leads themselves, but rather as tools to be used in the development of other less toxic inhibitors of ODC.

If further work is pursued on these scaffold series, the allosteric benzthiazole based inhibitors seems the most promising. The benzthiazole scaffold is present in FDA approved drugs and is known to have a wide range of biological activities.⁵⁻⁷ Furthermore, the preliminary structure activity relationships within the benzthiazole series suggest that some optimization may be possible. The fact that the compound is uncompetitive with L-ornithine is also beneficial, since inhibition of ODC is expected to result in accumulation of substrate. This means that it may be possible to for an inhibitor with lower overall binding affinities to be efficacious. However, since it is clear that the benzthiazole inhibitors presented herein are not acting in a putrescine dependent it is likely that significant effort will be required to eliminate off target effects. Therefore, any effort to optimize this scaffold should be regarded as a relatively high-risk project.

The relatively low number of ODC inhibitors found in this screening effort, along with the fact that none of the hits were active at whole cell levels via polyamine dependent pathways casts some doubt on the feasibility of developing more ODC inhibitors. The overall low hit rate of this screen demonstrates that ODC is not a particularly druggable target. Therefore, despite the successes detailed above, further work to develop novel inhibitors based on anything other than simple substrate or product analogues is likely to be unsuccessful.

However, this does not mean that the polyamine pathway itself is invalidated. Screening of other enzymes in this pathway, particularly SAMDC could be quite productive. In fact, the same assay system presented herein to screen ODC could be used to screen large libraries for SAMDC inhibitors. A second approach which would be useful in identifying polyamine pathway inhibitors would be to screen whole *T. brucei* and evaluate all hits for their ability to be rescued by addition of either putrescine or spermidine to the culture media. Preliminary efforts to identify compounds using both of these approaches are underway both in our laboratory and in the laboratories of our collaborators. Still other groups have pursued polyamine dependent enzymes further down the pathway. A recent publication by the Fairlamb and Frearson groups has used an approach similar to that presented here to chemically validate trypanothione synthetase as a drug target in *T. brucei*.⁸ In light of these results, coupled with those presented herein, it seems prudent to focus on other targets within the *T. brucei* polyamine pathway in the future.

References:

1. Johnston, P. A.; Soares, K. M.; Shinde, S. N.; Foster, C. A.; Shun, T. Y.; Takyi, H. K.; Wipf, P.; Lazo, J. S., Development of a 384-well colorimetric assay to quantify hydrogen peroxide generated by the redox cycling of compounds in the presence of reducing agents. *Assay Drug Dev Technol* **2008**, 6, (4), 505-18.
2. Lor, L. A.; Schneck, J.; McNulty, D. E.; Diaz, E.; Brandt, M.; Thrall, S. H.; Schwartz, B., A simple assay for detection of small-molecule redox activity. *J Biomol Screen* **2007**, 12, (6), 881-90.

3. Janne, J.; Williams-Ashman, H. G., On the purification of L-ornithine decarboxylase from rat prostate and effects of thiol compounds on the enzyme. *J Biol Chem* **1971**, 246, (6), 1725-32.
4. Coleman, C. S.; Stanley, B. A.; Pegg, A. E., Effect of mutations at active site residues on the activity of ornithine decarboxylase and its inhibition by active site-directed irreversible inhibitors. *J Biol Chem* **1993**, 268, (33), 24572-9.
5. Lacomblez, L.; Bensimon, G.; Leigh, P. N.; Guillet, P.; Meininger, V., Dose-ranging study of riluzole in amyotrophic lateral sclerosis. Amyotrophic Lateral Sclerosis/Riluzole Study Group II. *Lancet* **1996**, 347, (9013), 1425-31.
6. Hutchinson, I.; Bradshaw, T. D.; Matthews, C. S.; Stevens, M. F.; Westwell, A. D., Antitumour benzothiazoles. Part 20: 3'-cyano and 3'-alkynyl-substituted 2-(4'-aminophenyl)benzothiazoles as new potent and selective analogues. *Bioorg Med Chem Lett* **2003**, 13, (3), 471-4.
7. Scozzafava, A.; Briganti, F.; Ilies, M. A.; Supuran, C. T., Carbonic anhydrase inhibitors: synthesis of membrane-impermeant low molecular weight sulfonamides possessing in vivo selectivity for the membrane-bound versus cytosolic isozymes. *J Med Chem* **2000**, 43, (2), 292-300.
8. Torrie, L. S.; Wyllie, S.; Spinks, D.; Oza, S. L.; Thompson, S.; Harrison, J. R.; Gilbert, I. H.; Wyatt, P. G.; Fairlamb, A. H.; Frearson, J. A., Chemical validation of trypanothione synthetase: a potential drug target for human trypanosomiasis. *J Biol Chem* **2009**.

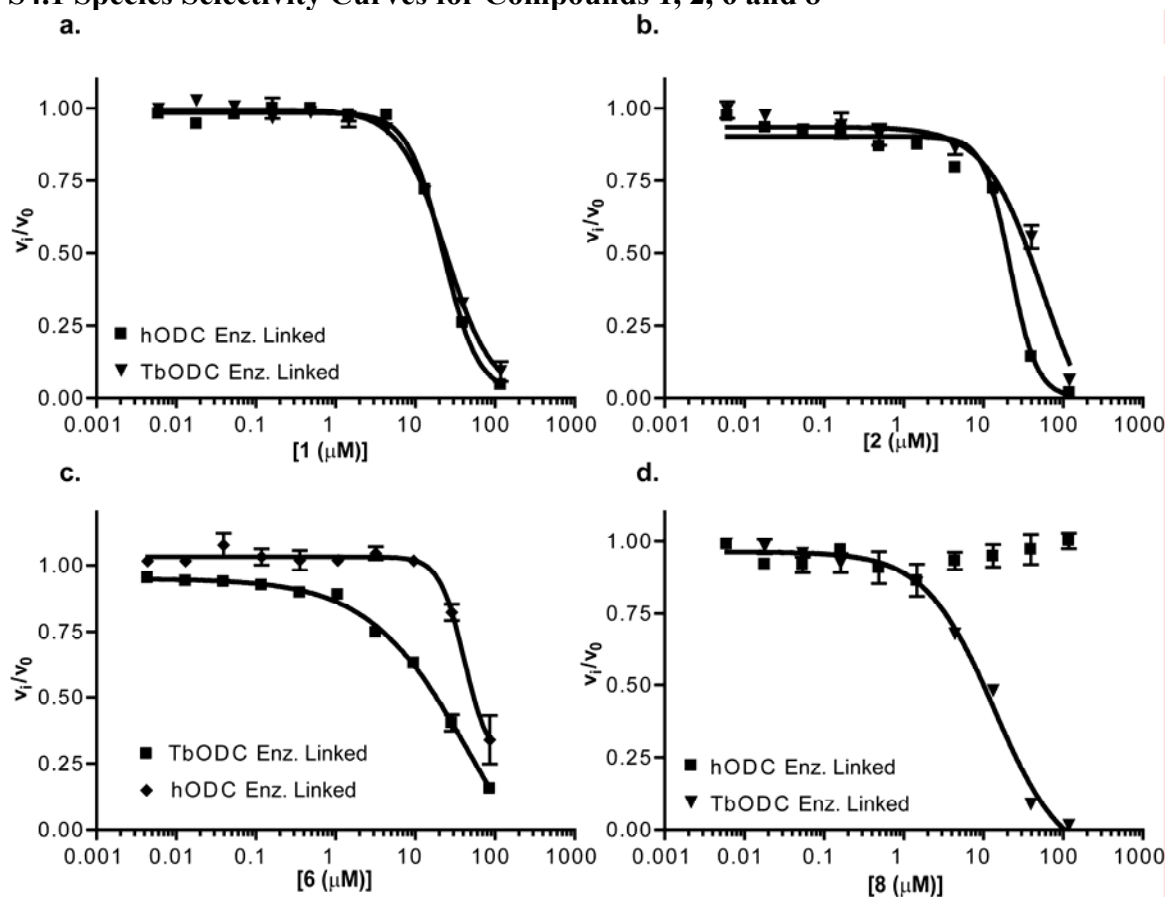
Appendix

Appendix

Chapter 4 Supplementary Data

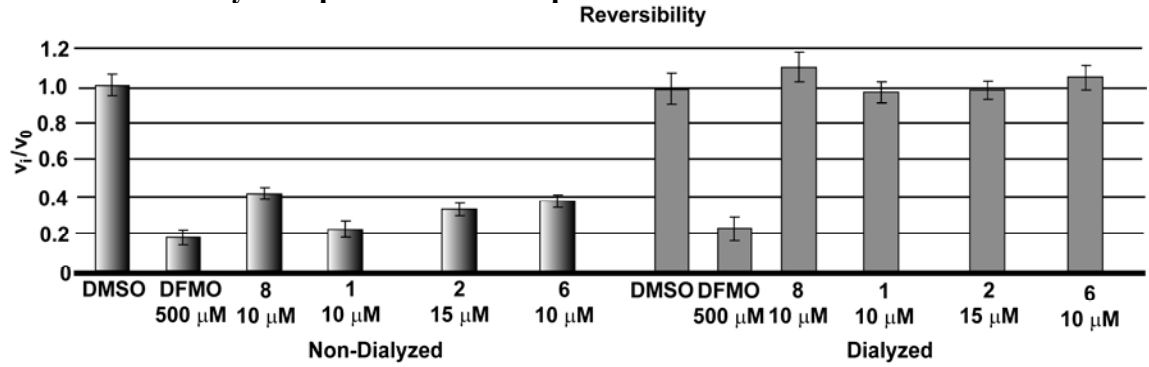
Supplementary Data for: Smithson et al. - Discovery of Potent and Selective Inhibitors of *Trypanosoma brucei* Ornithine Decarboxylase.

S4.1 Species Selectivity Curves for Compounds 1, 2, 6 and 8



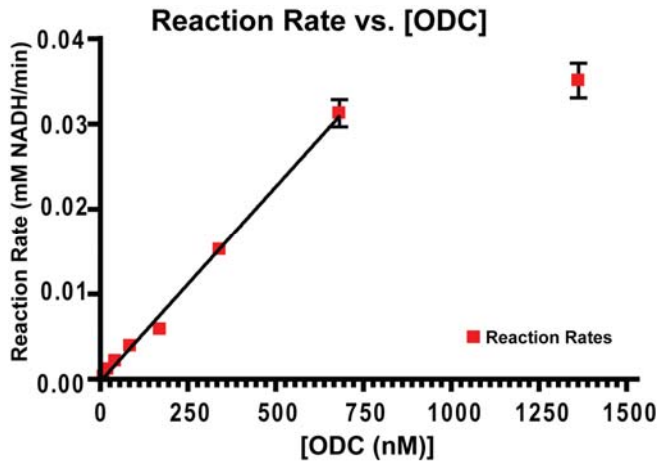
Data was gathered in 384 well plates as described in materials and methods. All curves were determined under isokinetic conditions at $[1.5 \times K_m]$ L-ornithine. (625 μM L-Orn for TbODC, 150 μM L-Orn for hODC) IC_{50} experiments were performed in independent triplicates.

S4.2 Reversibility of representative compounds



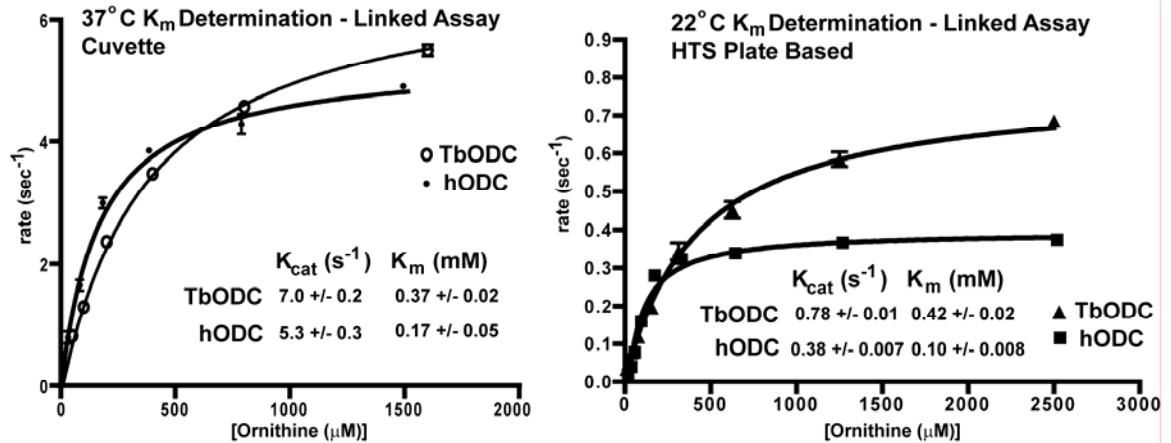
Reversibility was determined as described in materials and methods.

S4.3 Reaction Linearity with Respect to [ODC]



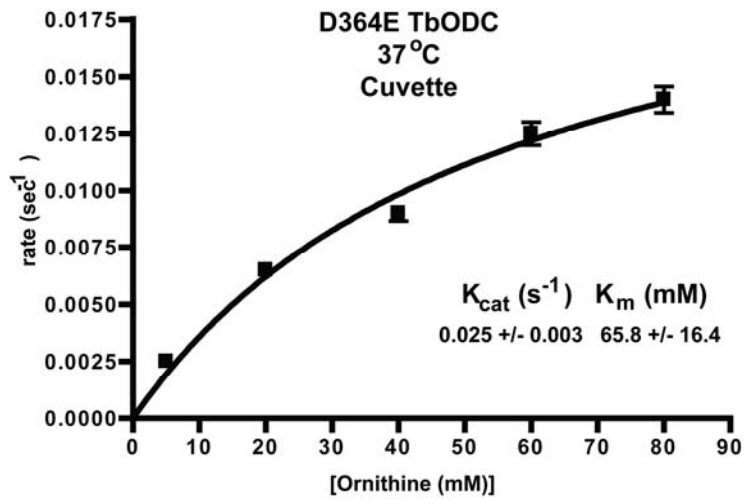
Linearity was determined at 625 μM Orn and 60 μM PLP in 384-well plates using HTS assay protocol under a nitrogen atmosphere.

S4.4 K_m Determination for Enzymes used in Study



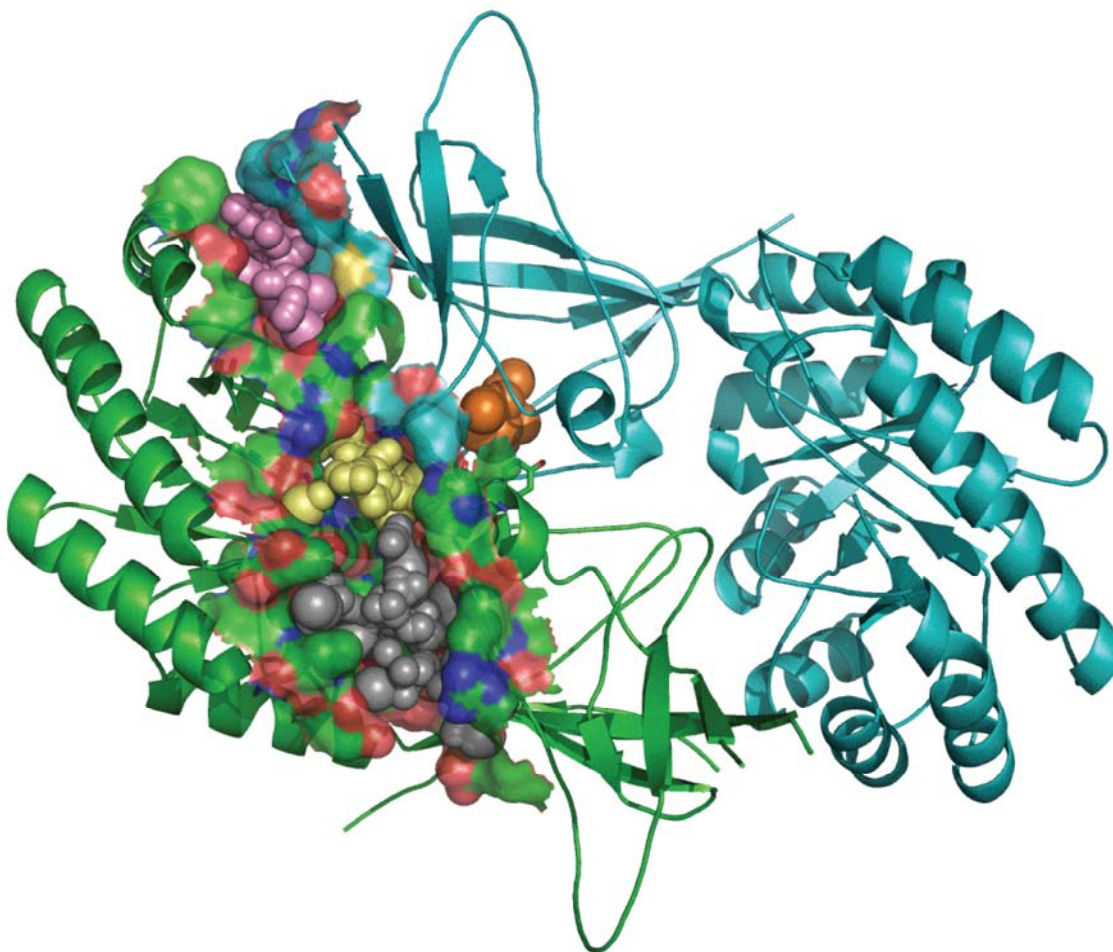
TbODC and hODC in plate based assay were 150nM, TbODC and hODC in cuvette assays were at 100nM.

S4.5 D364E TbODC K_m Determination



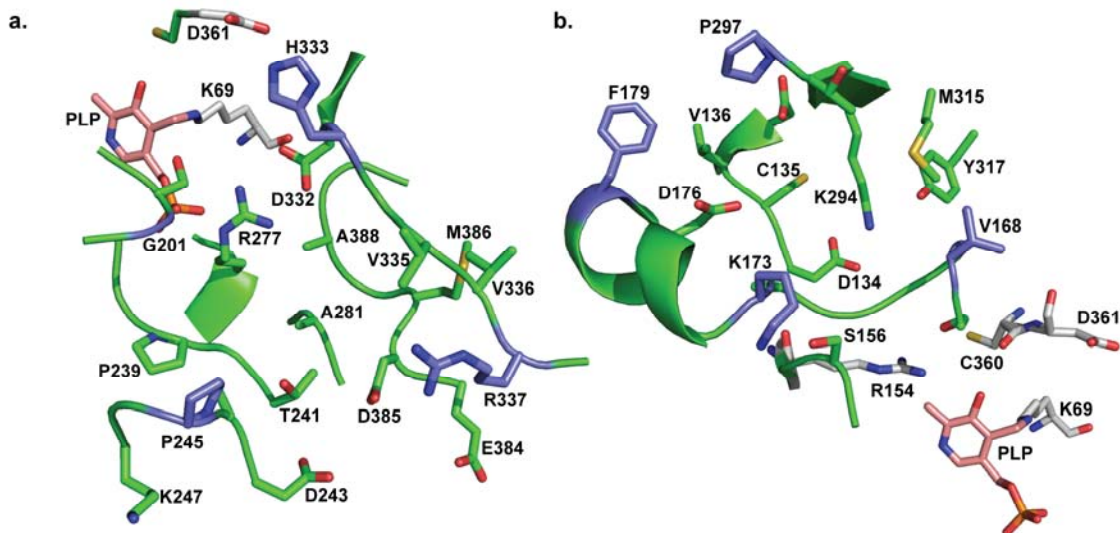
D364E TbODC was tested in cuvettes at 20 μM ODC due to low activity of the enzyme.

S4.6 Proposed Alternate Binding Sites for Dithioamidine Compounds



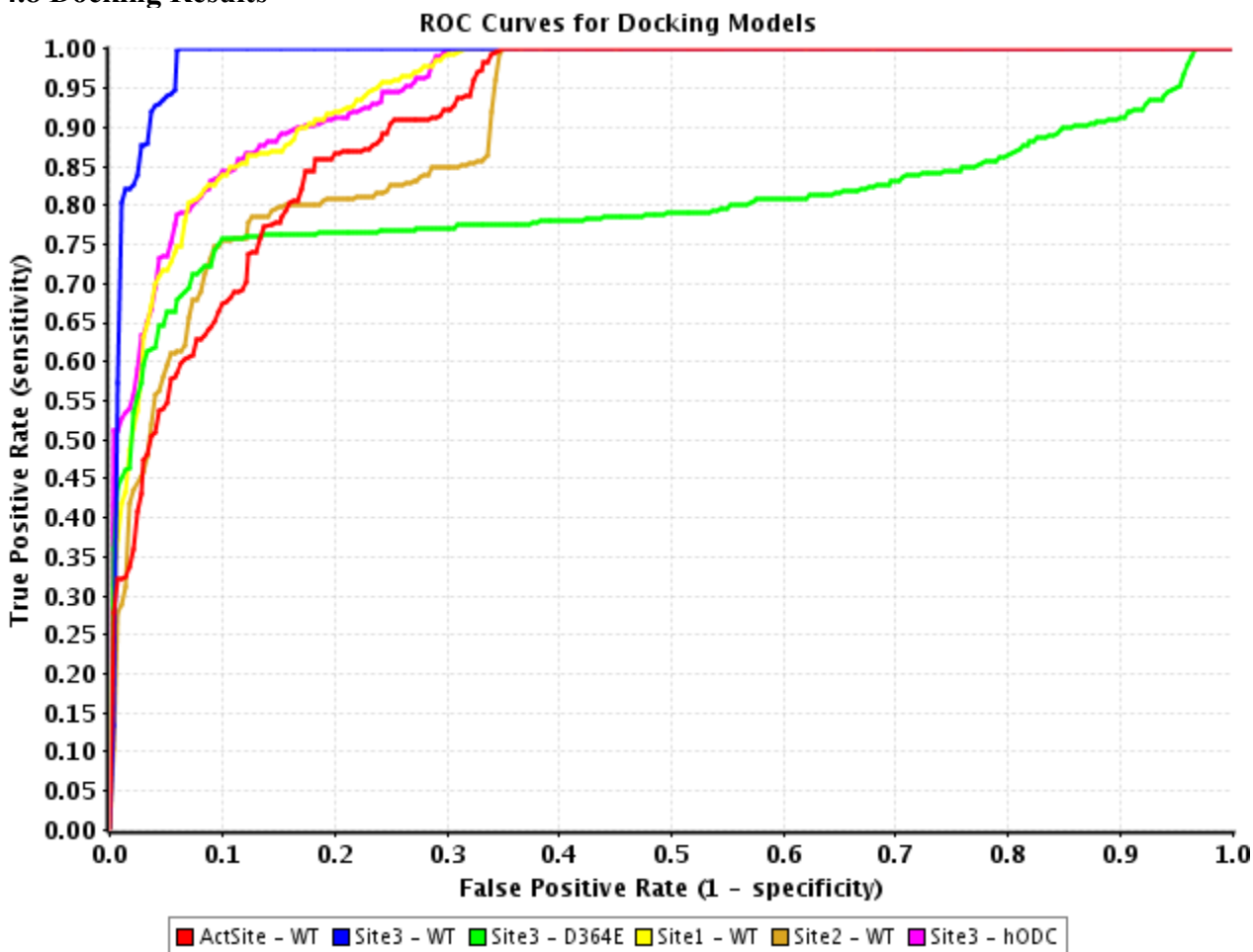
The above structure is based on the TbODC structure 1QU4. Green coloration represents chain C of the dimer and blue coloration represents chain D of the dimer. Yellow spheres represent the enzyme active site where ornithine and PLP bind. Gray spheres represent potential alternate binding site 1, pink spheres represent potential alternate binding site 2 and orange spheres represent potential alternate binding site 3.

S4.7 Proposed Alternate Binding Sites – Residue View



- a.** Site 1. Apo TbODC structure. PLP is salmon, active site residues are white and residues that form the boundaries of the entrance to the proposed binding site are purple.
- b.** Site 2. Apo TbODC structure. PLP is salmon, active site residues are white and residues that form the boundaries of the entrance to the proposed binding site are purple.

S4.8 Docking Results

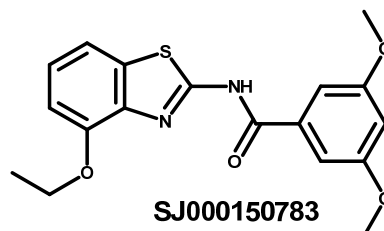
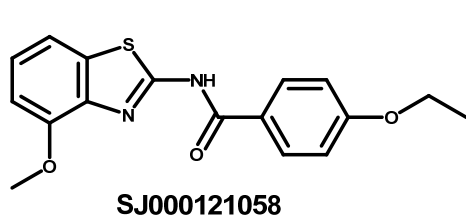
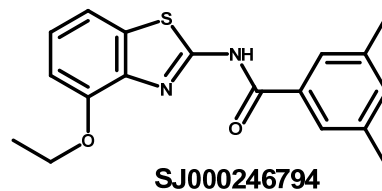
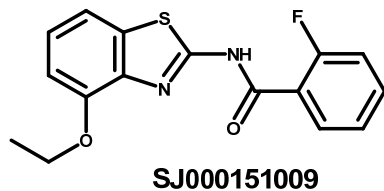
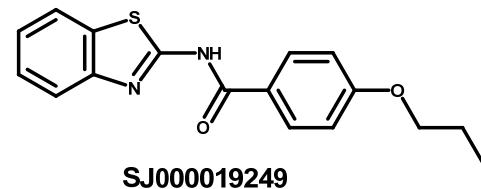
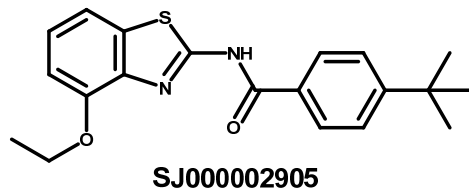
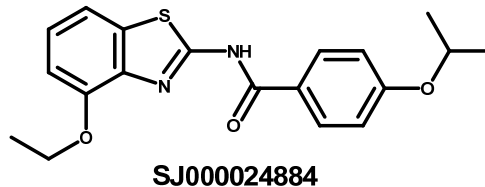
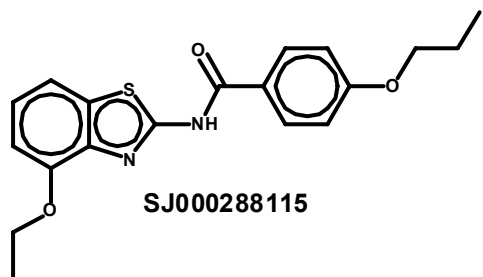


ROC Curves for Docking Models – Enrichment plots for each alternate binding site tested using molecular docking approaches. Note that Site 3 outperforms other models, while the remaining sites perform similarly. Site 3 in the D364E mutant model performs much worse than the same site in the wild-type TbODC enzyme. The top 100 poses of each compound were used for calculating enrichment, and true positives were defined as those compounds with K_i values less than 50 μM . AUC scores are as follows: ActSite – WT (Active Site, wild-type TbODC): 0.91, Site3-WT (Site 3, wild-type TbODC): 0.99, Site3-D364E (Site3, D364E TbODC model): 0.80, Site1-WT (Site 1, wild-type TbODC): 0.93, Site2-WT (Site 2, wild-type TbODC): 0.91, Site3-hODC (Site 3, wild-type hODC): 0.93.

S4.9 Additional Benzthiazoles Screened

Note that these compounds did not have K_i values determined, and while identities were confirmed by mass spec, purities were not able to be accurately assessed due to the limited amount of available compound. IC_{50} values were obtained at 625 μ M L-ornithine, 60 μ M PLP and 150 nM TbODC, fit as described in materials and methods, and are expressed as 95% confidence intervals.

Compound ID	IC_{50} (μ M)
SJ000288115	4.6 to 7.8
SJ000024884	3.7 to 10.1
SJ000002905	Inactive (>100 μ M)
SJ000019249	Inactive (>100 μ M)
SJ000151009	Inactive (>100 μ M)
SJ000246794	Inactive (>100 μ M)
SJ000121058	Inactive (>100 μ M)
SJ000150783	Inactive (>100 μ M)



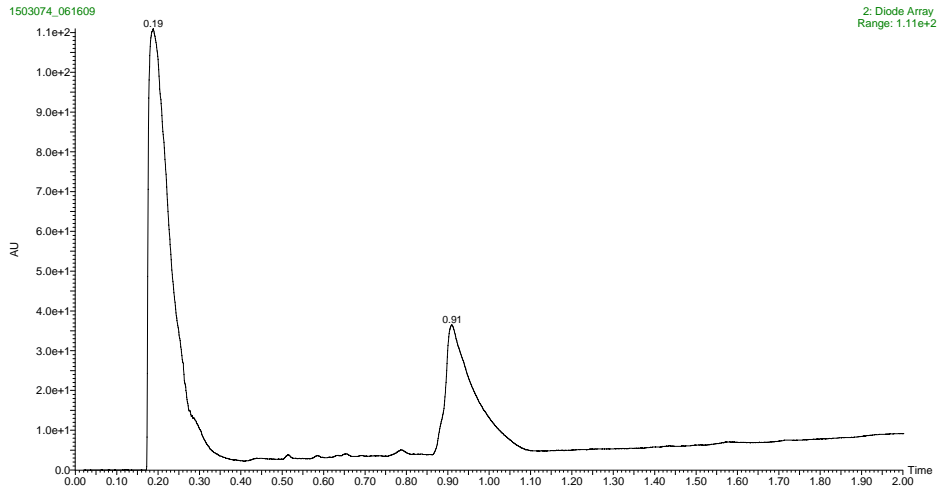
S4.10 Paper numbering to St. Jude Registry Number Key – please use the below designations when requesting additional information regarding compounds included in this report.

SJREGNO	Internal Manuscript Numbering
SJ000285319	1
SJ00026125	2
SJ000360936	3
SJ000122887	4
SJ000298934	5
SJ000126684	6
SJ000360927	7
SJ000288115	8
SJ000359132	9
SJ000359141	10
SJ000285200	11
SJ000359413	12
SJ000359140	13
SJ000359137	14
SJ000354134	15

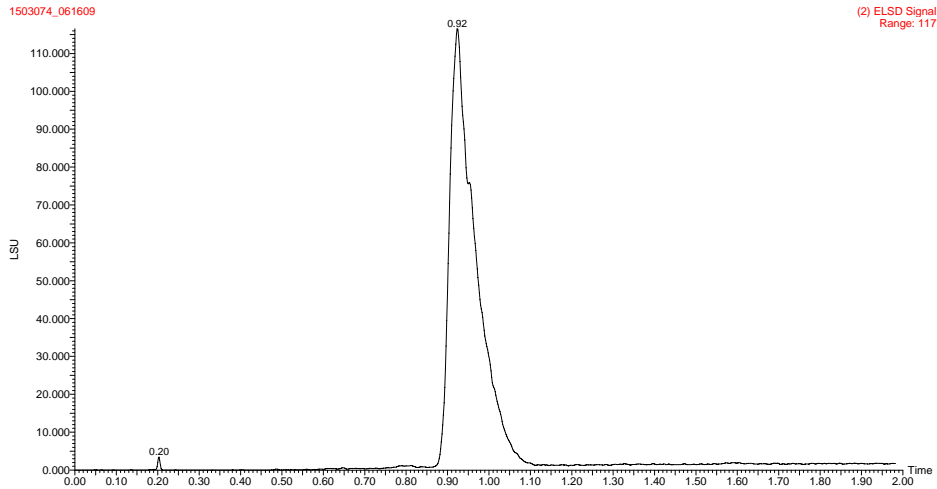
Compound UPLC-MS Data

(Peaks at 0.2 min are DMSO solvent peaks)

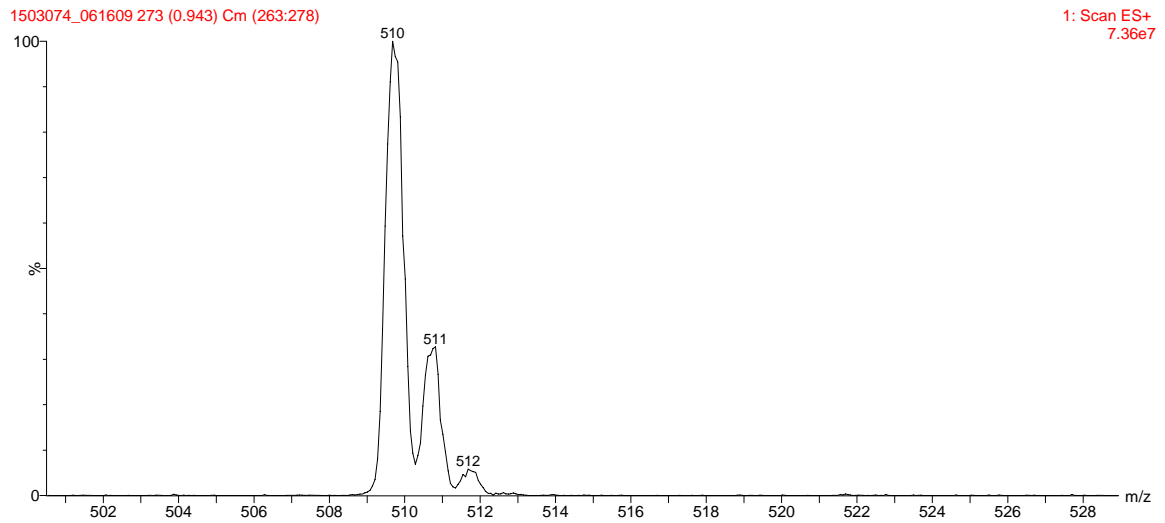
1 (SJ000285319) UV-TIC – Purity = >95% - Product Mass at 0.91 min



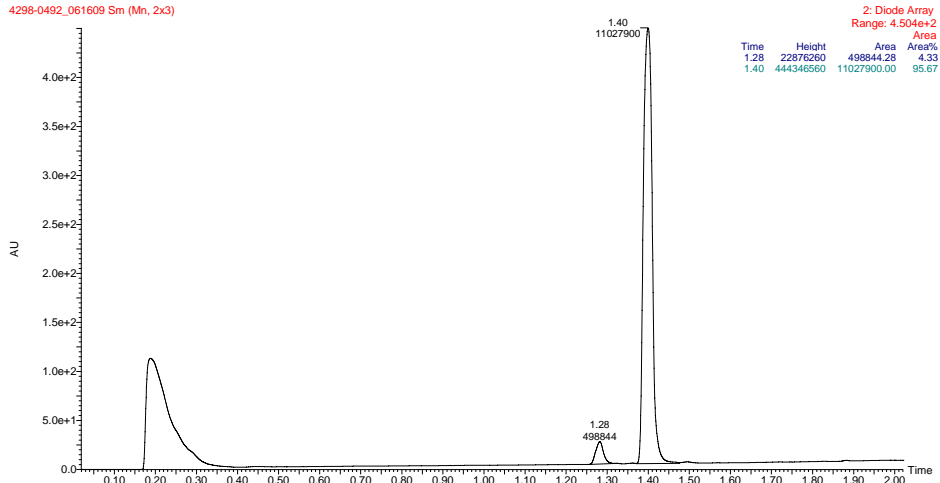
1 (SJ000285319) ELSD Signal – Purity = >95% - Product Mass at 0.92 min



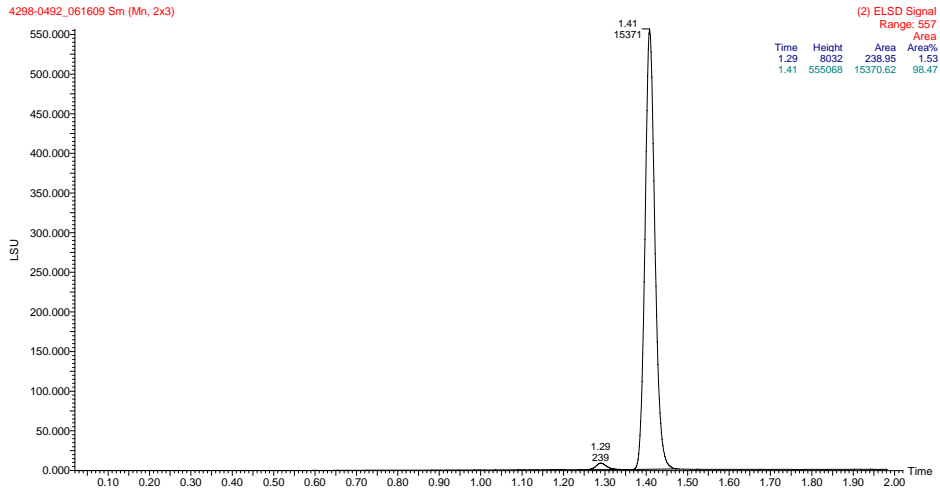
1 (SJ000285319) Parent Ion – Expected Mass+1: 509.8



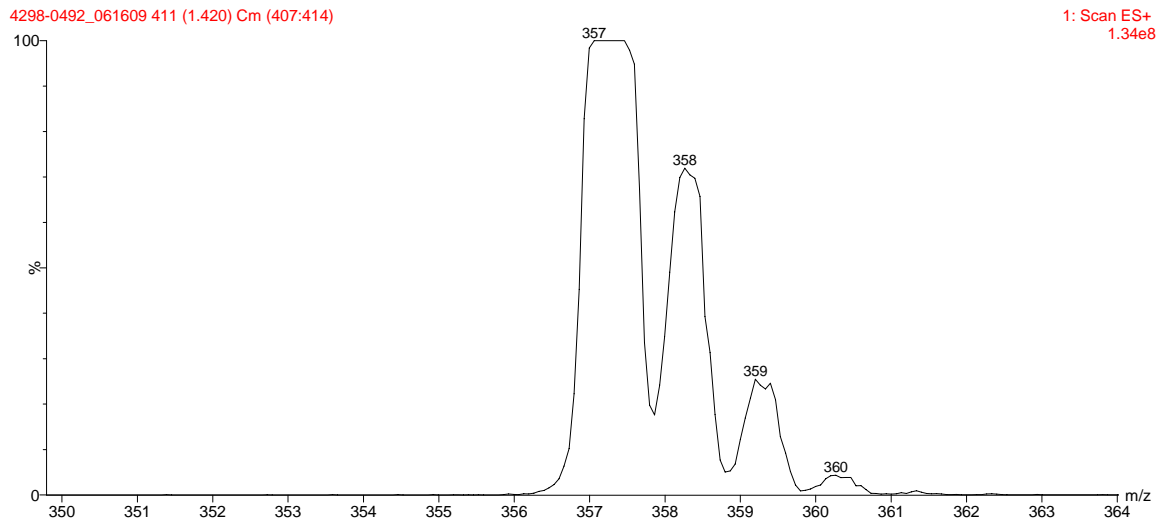
2 (SJ000026125) UV-TIC – Purity = 95% - product mass at 1.40 min



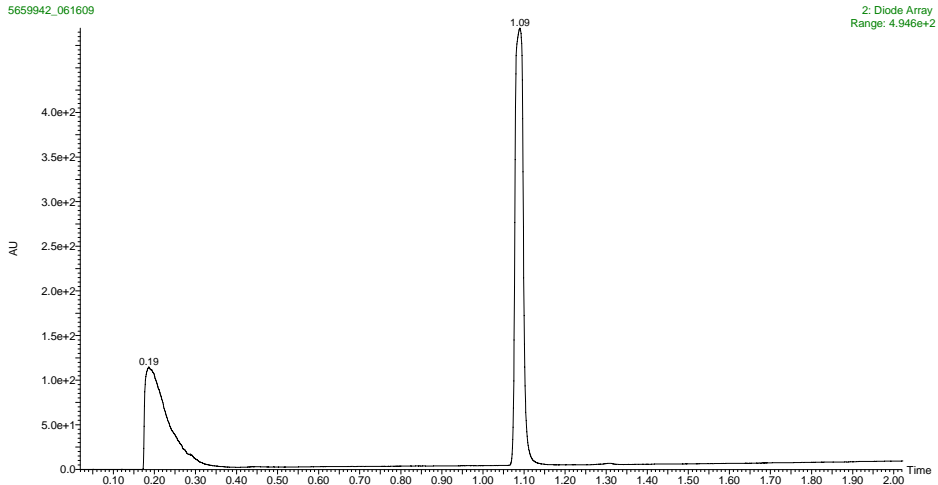
2 (SJ000026125) ELSD Signal – Purity = 98 % - product mass at 1.41 min



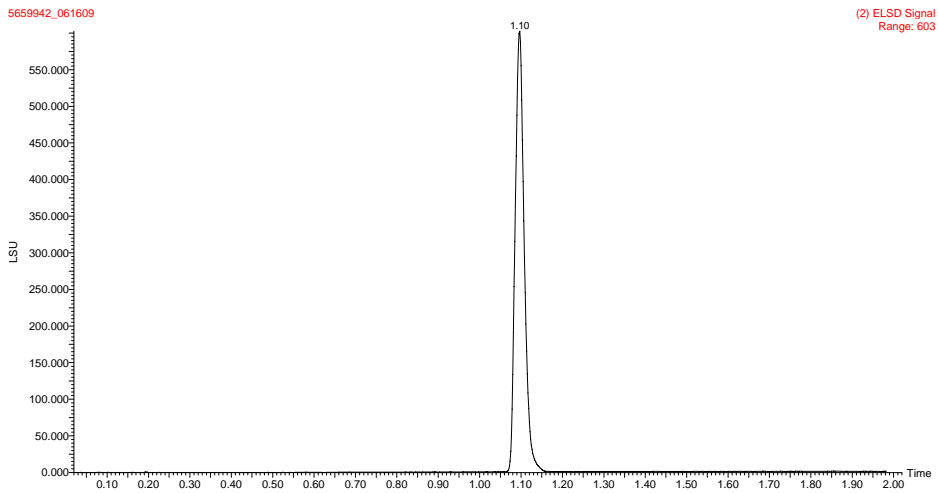
2 (SJ000026125) Parent Ion – Expected Mass +1: 357.7



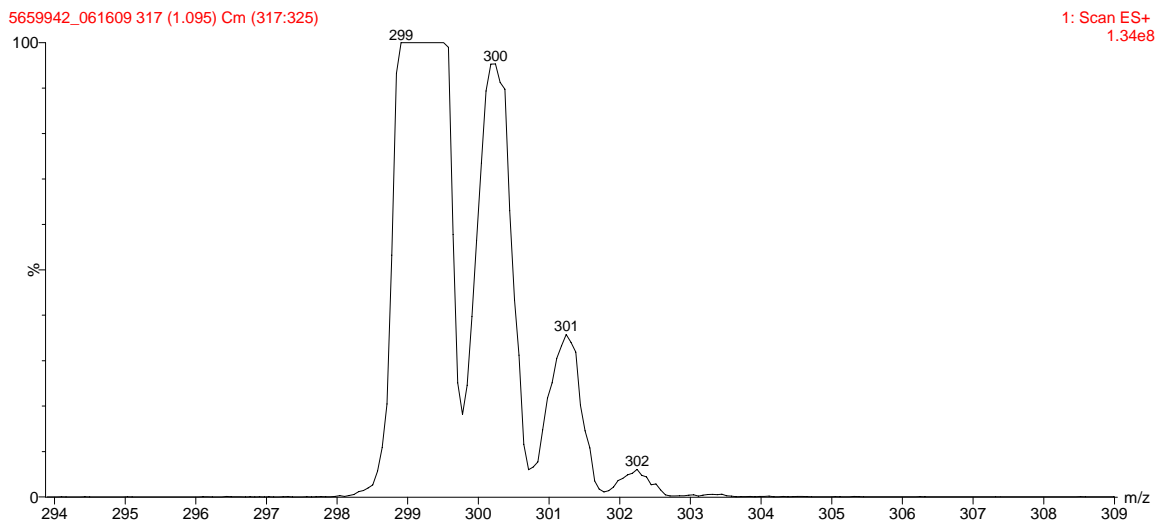
3 (SJ000360936) – UV-TIC – Purity = >95% - product mass at 1.09 min



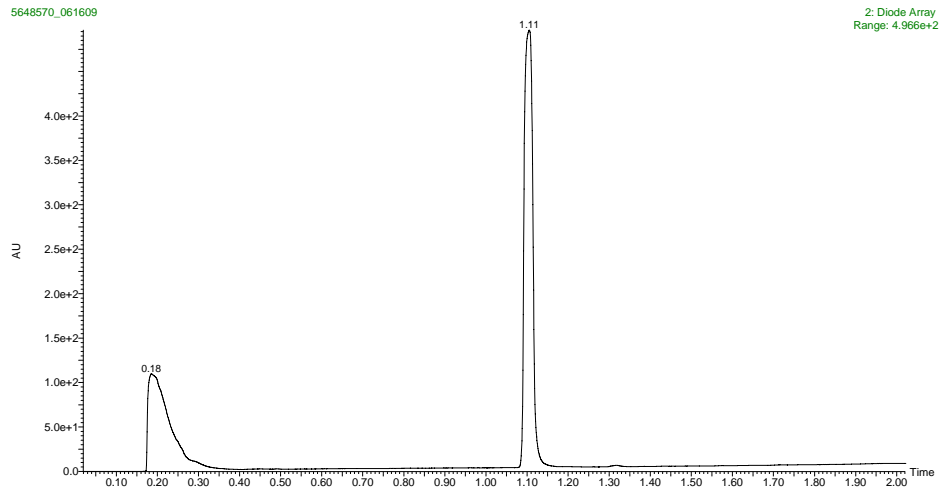
3 (SJ000360936) – ELSD Signal – Purity = >95% - product mass at 1.10 min



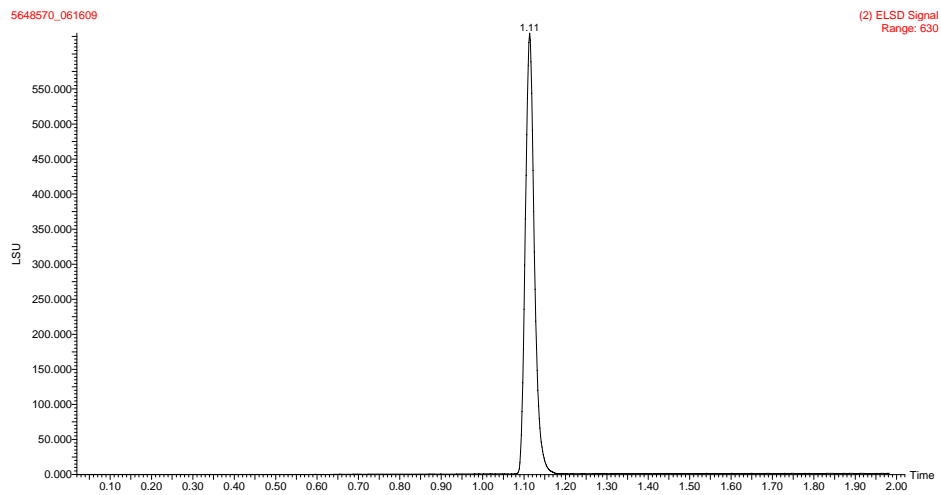
3 (SJ000360936) Parent Ion – Expected Mass +1: 299.1



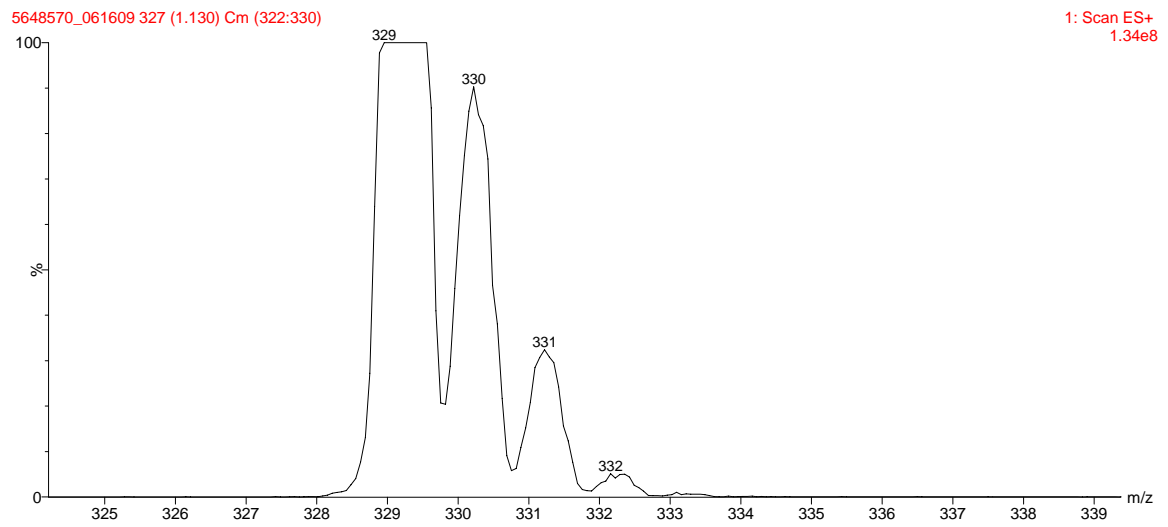
4 (SJ000122887) UV-TIC – Purity = >95% - product mass at 1.11 min



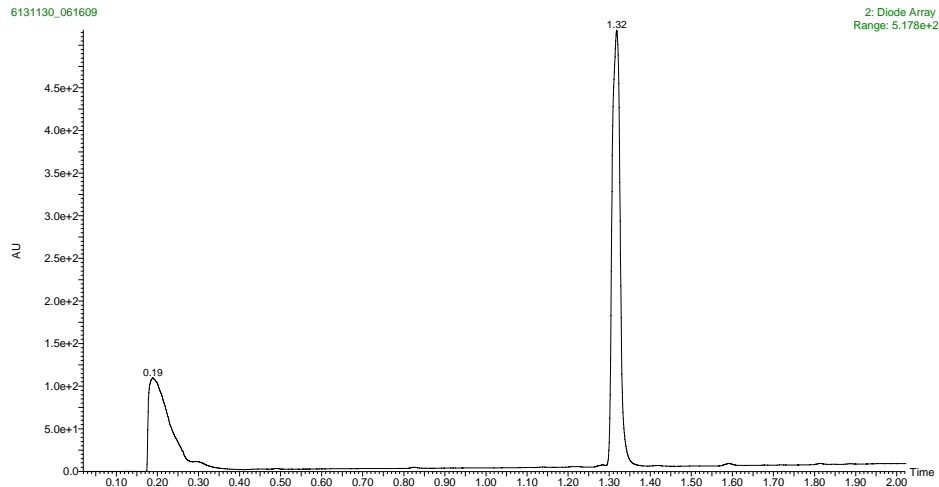
4 (SJ000122887) ELSD Signal – Purity = >95% - product mass at 1.11 min



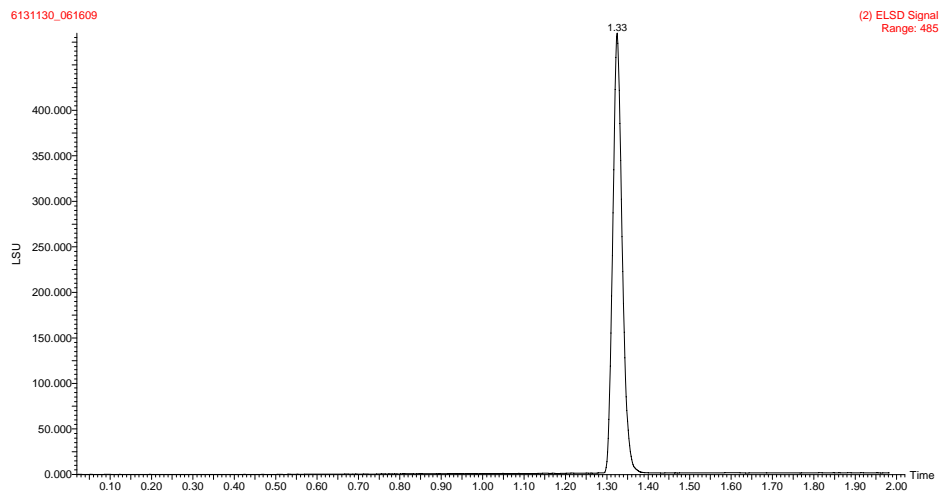
4 (SJ000122887) Parent Ion – Expected Mass +1: 329.1



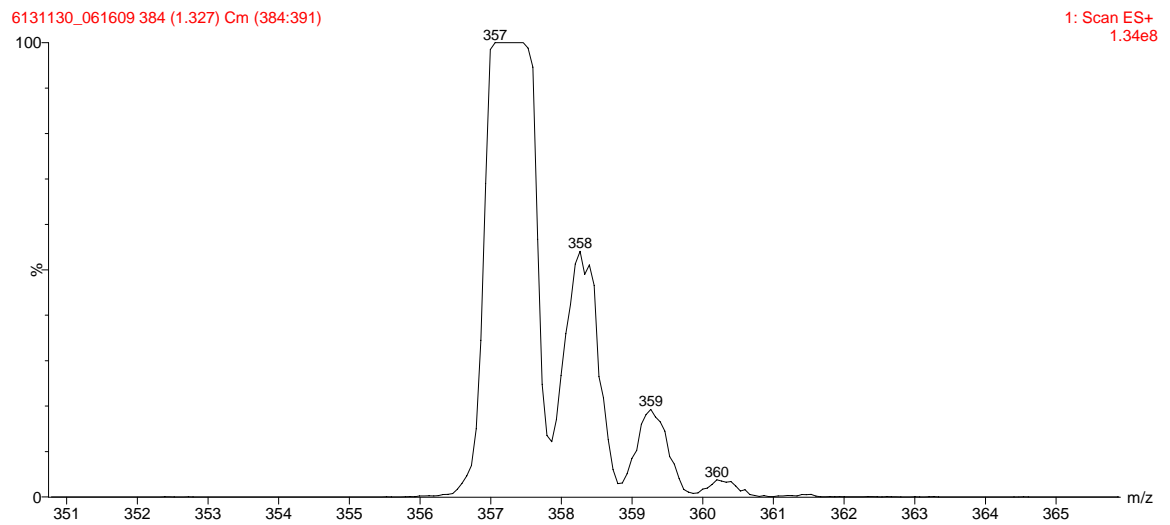
5 (SJ000298934) UV-TIC – Purity = 100 % - product mass at 1.32 min



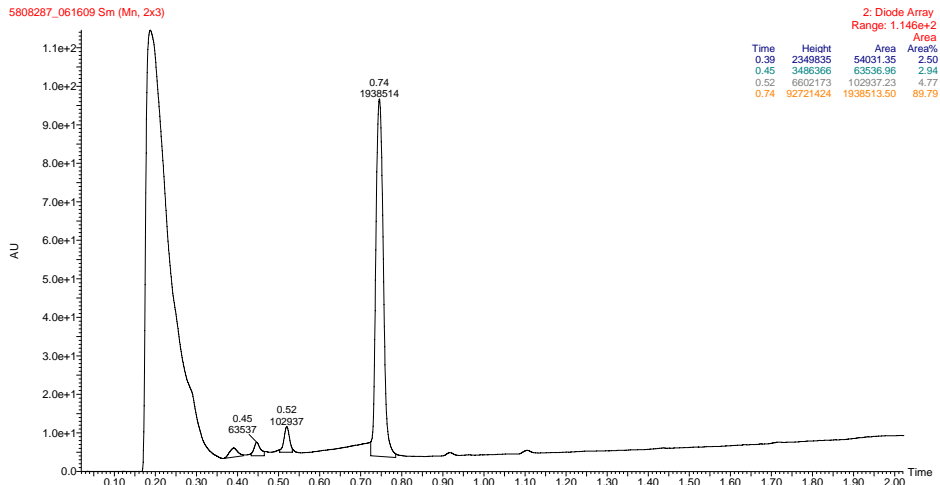
5 (SJ000298934) ELSD – Purity = 100 % - product mass at 1.33 min



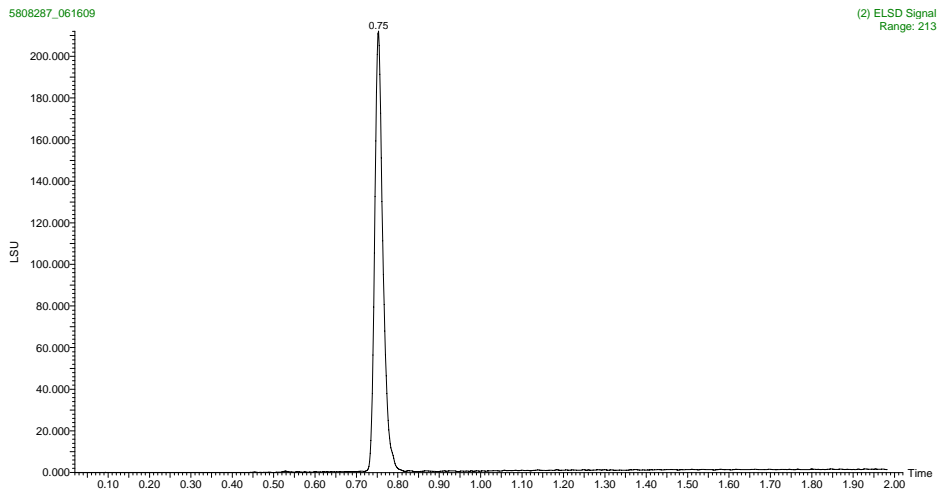
5 (SJ000298934) Parent Ion – Expected Mass +1: 357.1



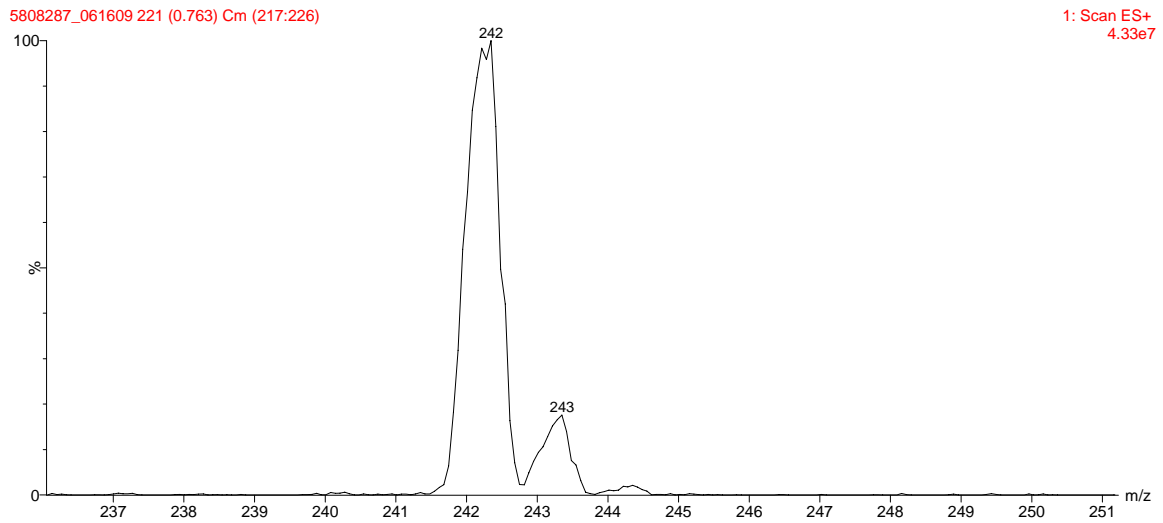
6 (SJ000126684) – UV-TIC – Purity = 90% - product mass at 0.74 min



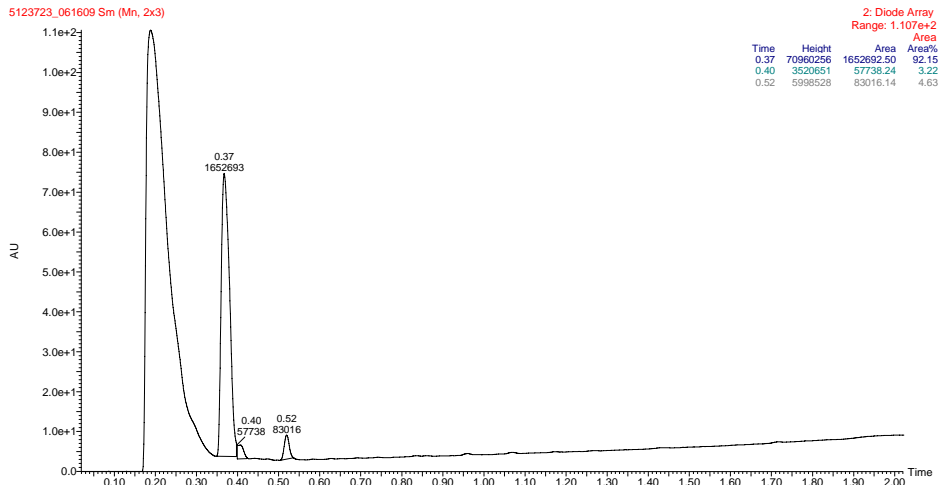
6 (SJ000126684) – ELSD Signal – Purity = >95% - product mass at 0.75 min



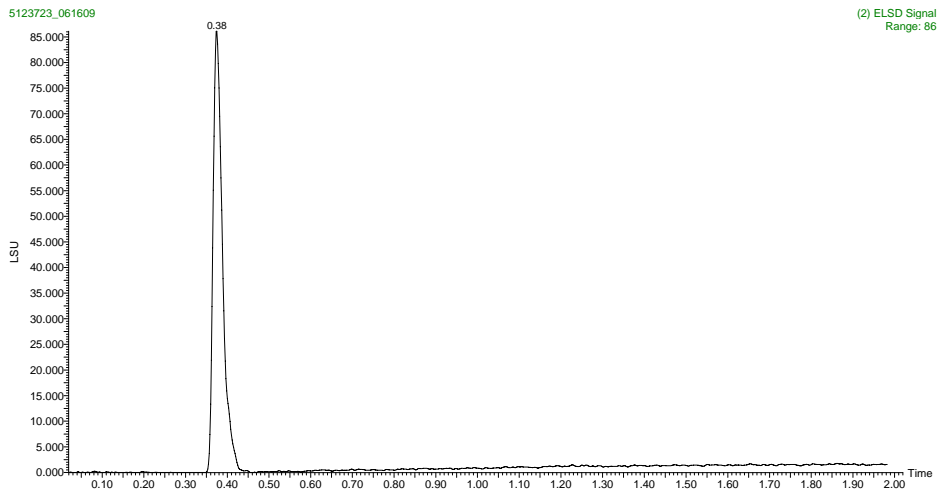
6 (SJ000126684) Parent Ion – Expected Mass +1: 242.1



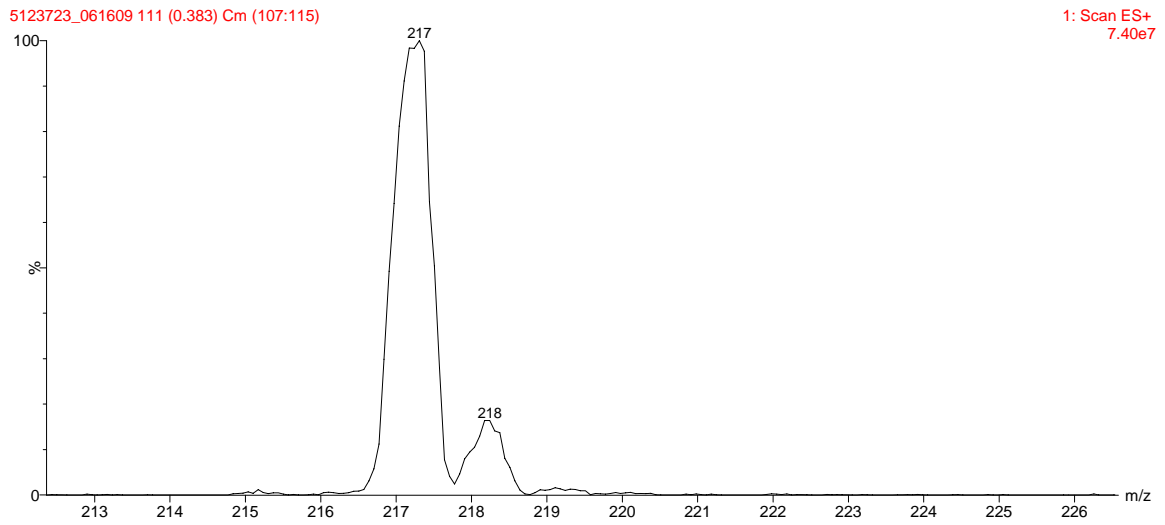
7 (SJ000360927) – UV-TIC – Purity = 92 % - product mass at 0.37 min



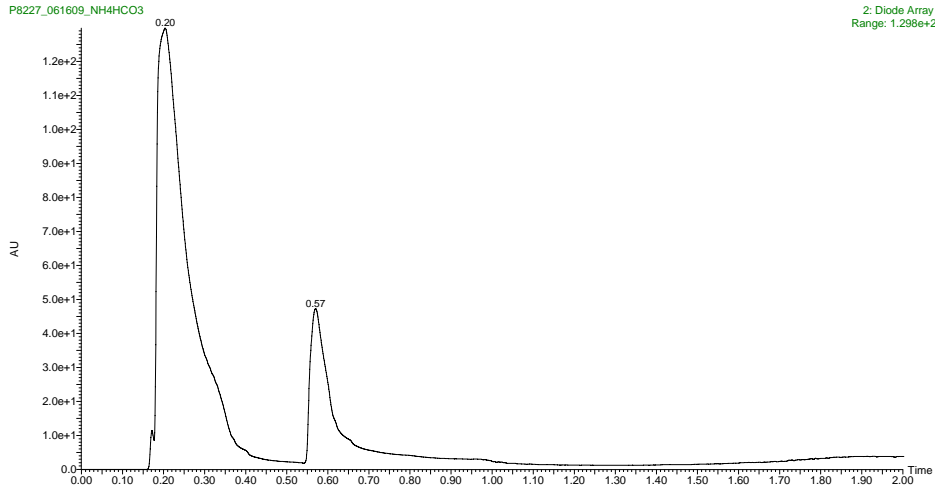
7 (SJ000360927) – ELSD Signal – Purity = >95% - product mass at 0.38 min



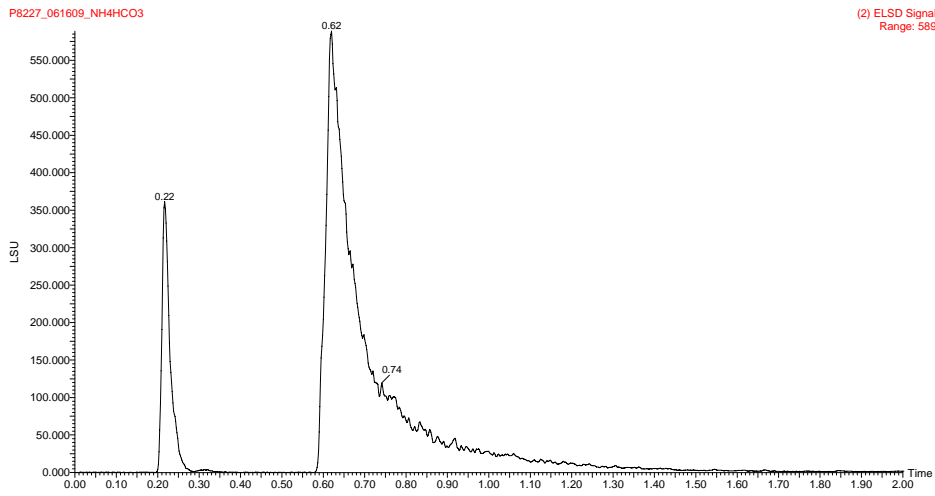
7 (SJ000360927) Parent Ion – Expected Mass +1: 217.1



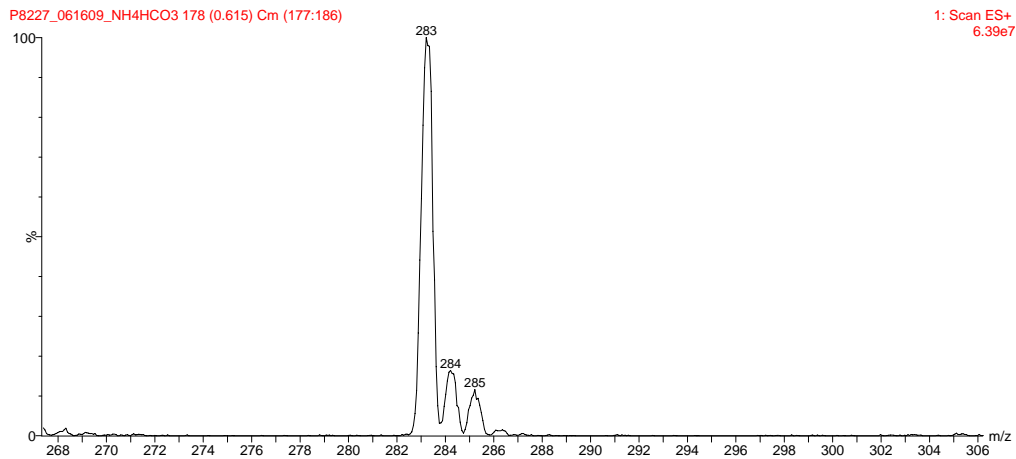
8 (SJ000288115) UV-TIC – Purity = >95% - Product Mass at 0.57 min



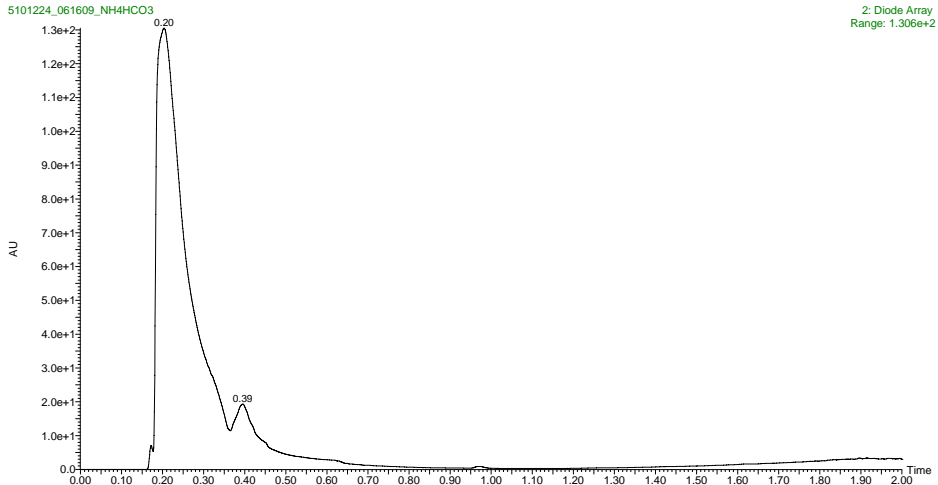
8 (SJ000288115) ELSD Signal – Purity = >95%



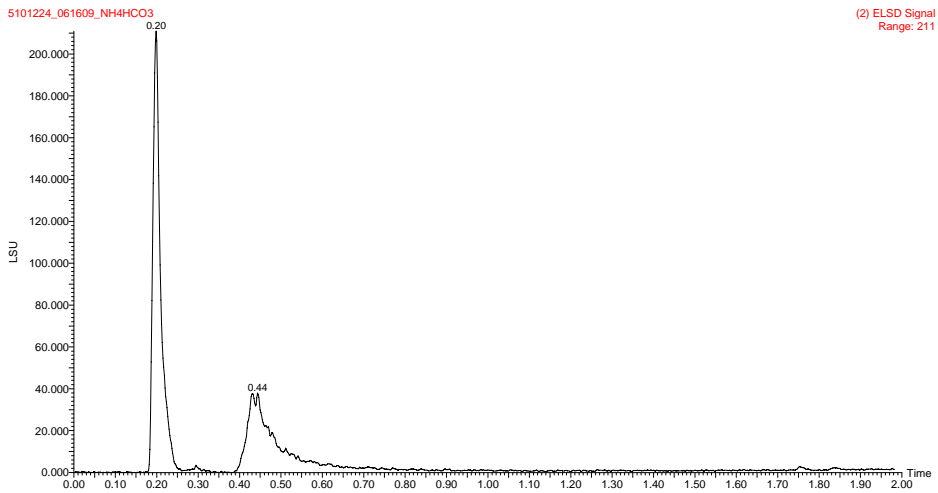
8 (SJ000288115) Parent Ion – Expected Mass +1: 283.1



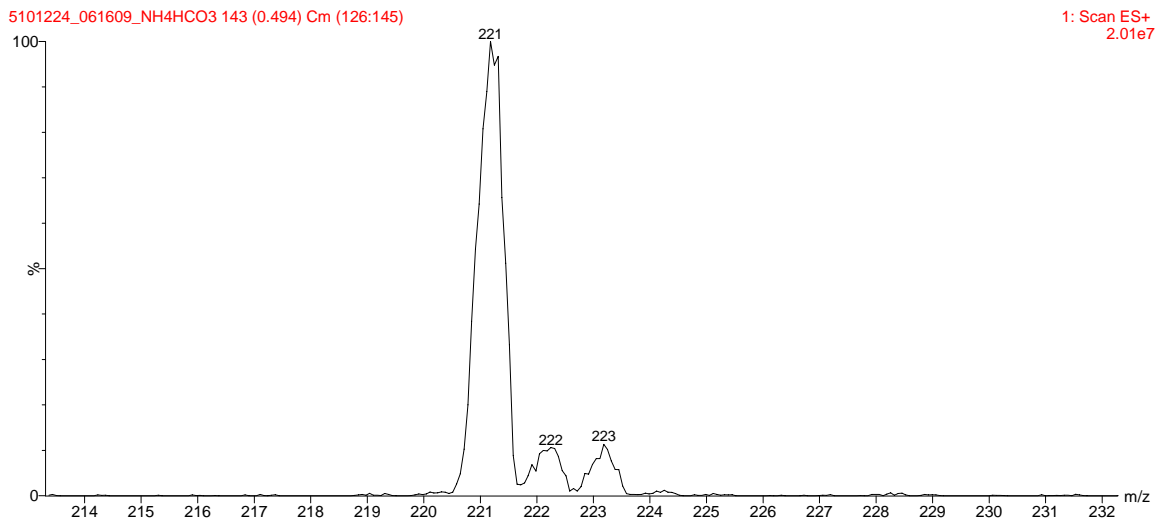
9 (SJ000359132) UV-TIC – Purity = >95%, product mass at 0.39 min



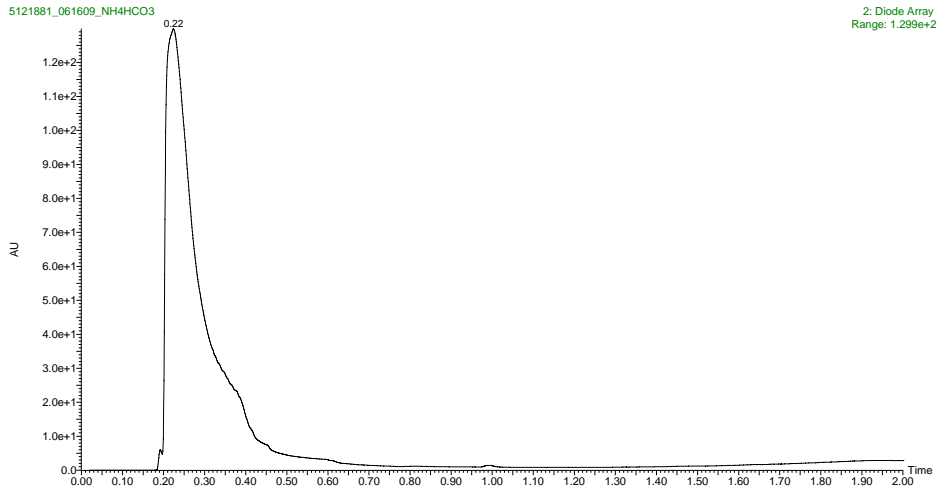
9 (SJ000359132) ELSD Signal – Purity = >95%, product mass at 0.44 min



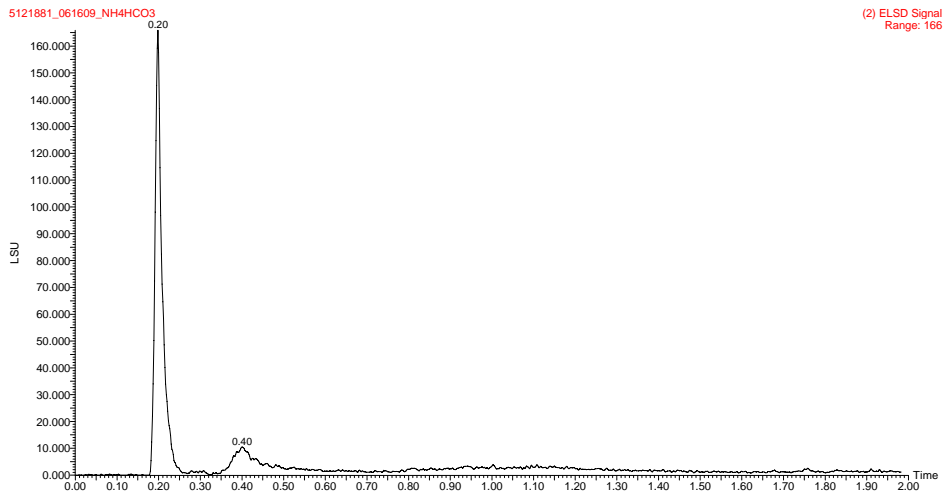
9 (SJ000359132) Parent Ion – Expected Mass +1: 221.1



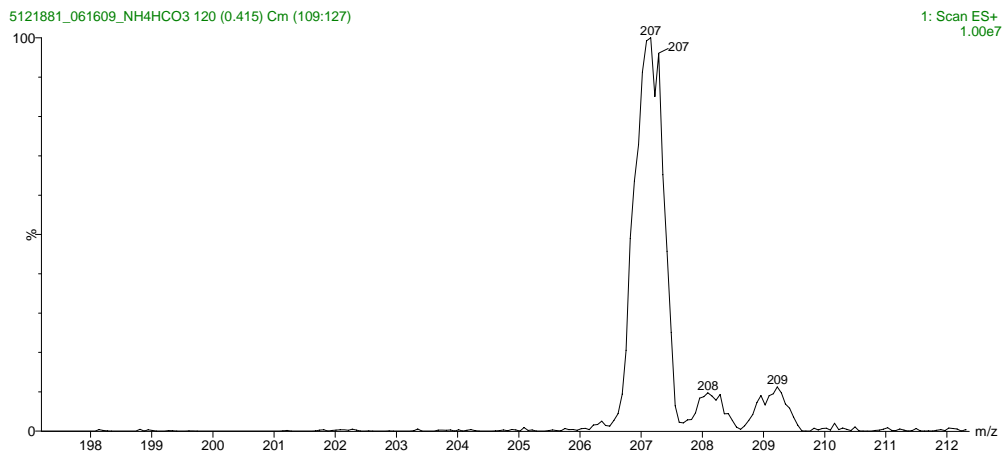
10 (SJ000359141) UV-TIC – No Detectable UV Signal



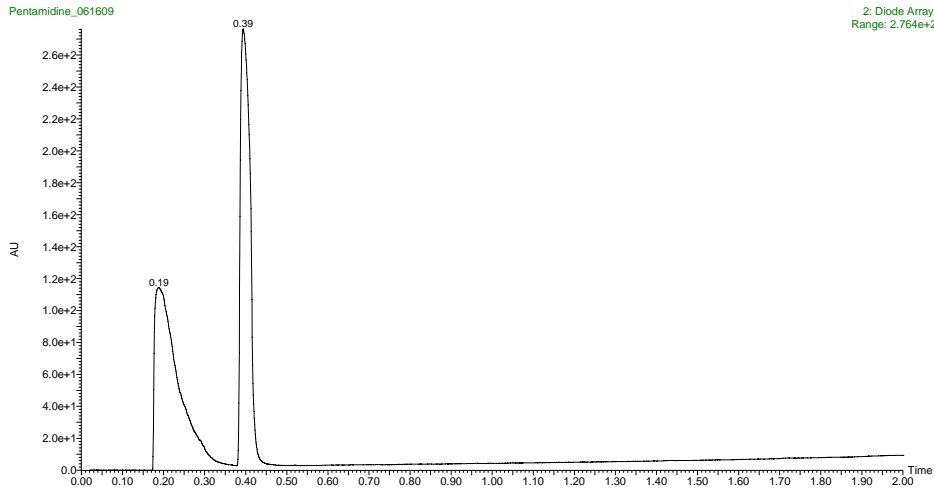
10 (SJ000359141) ELSD Signal – Purity = >95% - Product mass at 0.4 min



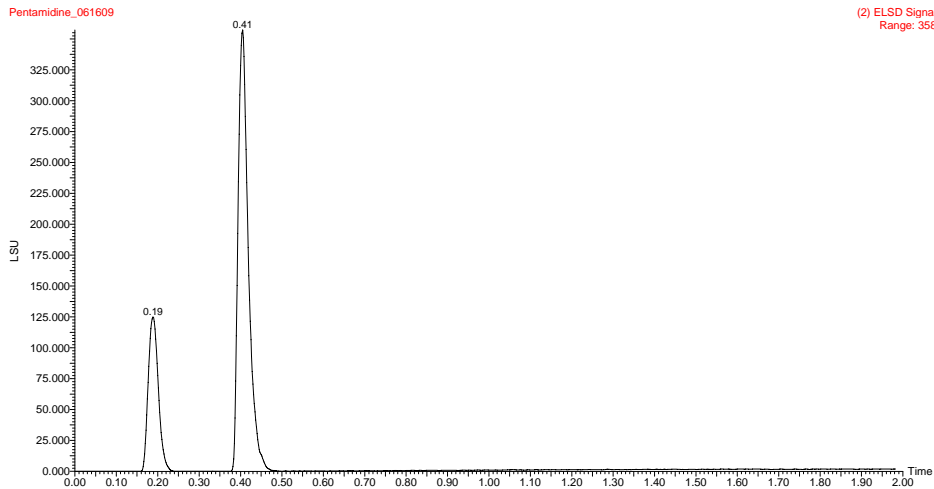
10 (SJ000359141) Parent Ion – Expected Mass +1: 207.1



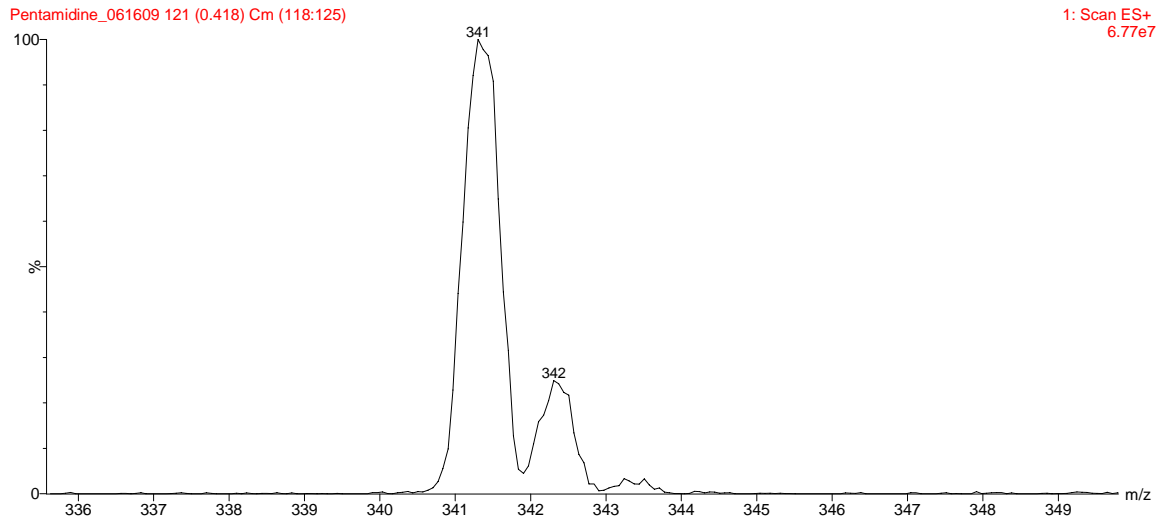
11 (SJ000285200) UV-TIC – Purity = >95% - product mass at 0.39 min



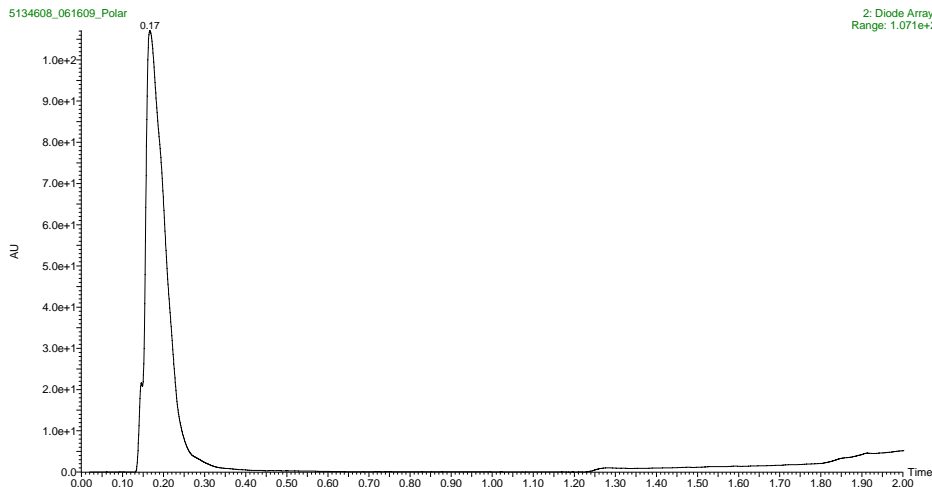
11 (SJ000285200) ELSD – Purity = 100 % - product mass at 0.41 min



11 (SJ000285200) Parent Ion – Expected Mass +1: 341.4



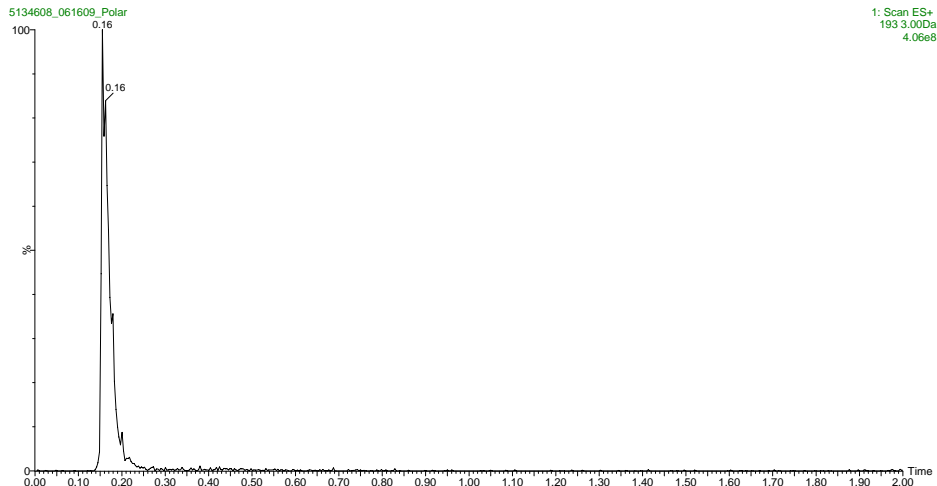
12 (SJ000359413) UV-TIC – Product in Solvent Peak – attempts at separation unsuccessful – no masses other than product and solvent were detected in solvent peak.



12 (SJ000359413) ELSD Signal – Product in Solvent Peak – attempts at separation unsuccessful



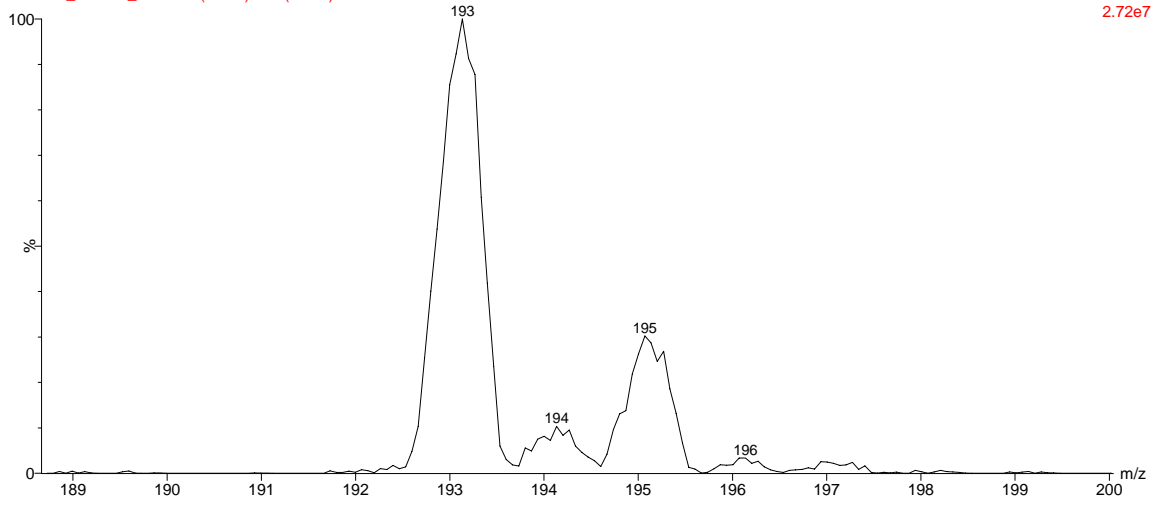
12 (SJ000359413) Product Parent Ion Chromatogram – Product is in solvent peak



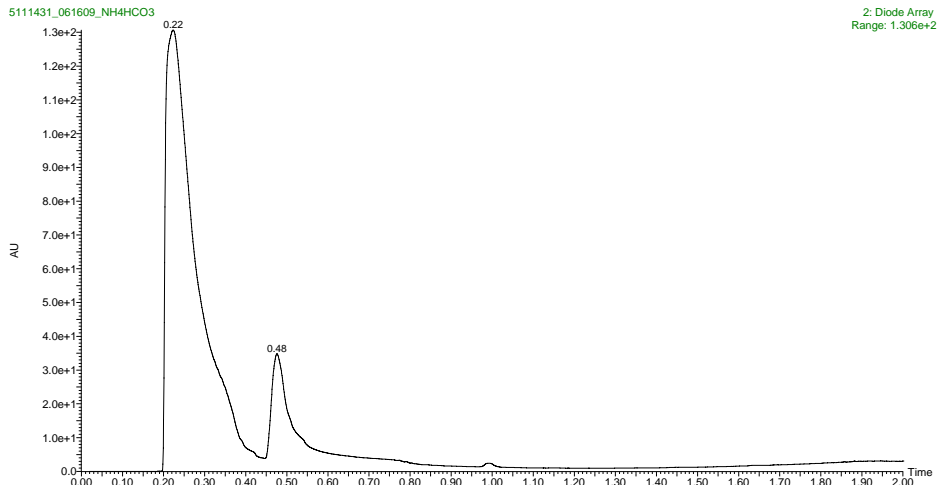
12 (SJ000359413) Parent Ion – Expected Mass +1: 192.1

5134608_061609_Polar 47 (0.162) Cm (44:52)

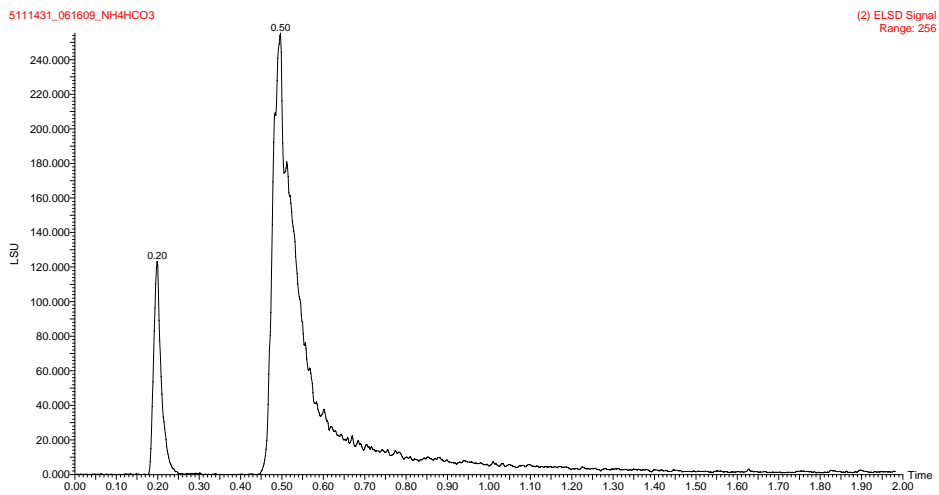
1: Scan ES+
2.72e7



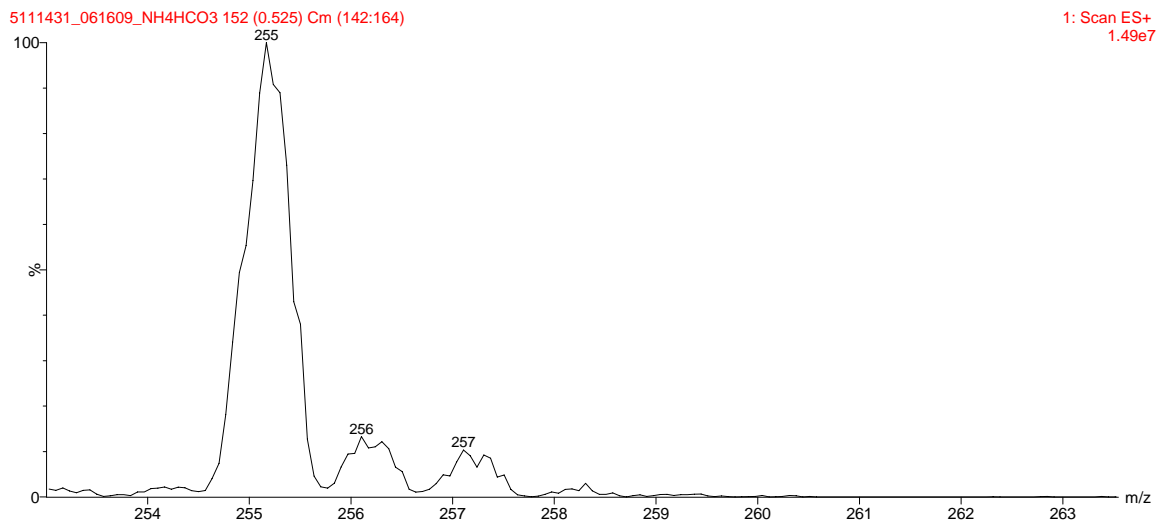
13 (SJ000359140) UV-TIC – Purity = >95% - product mass at 0.48 min



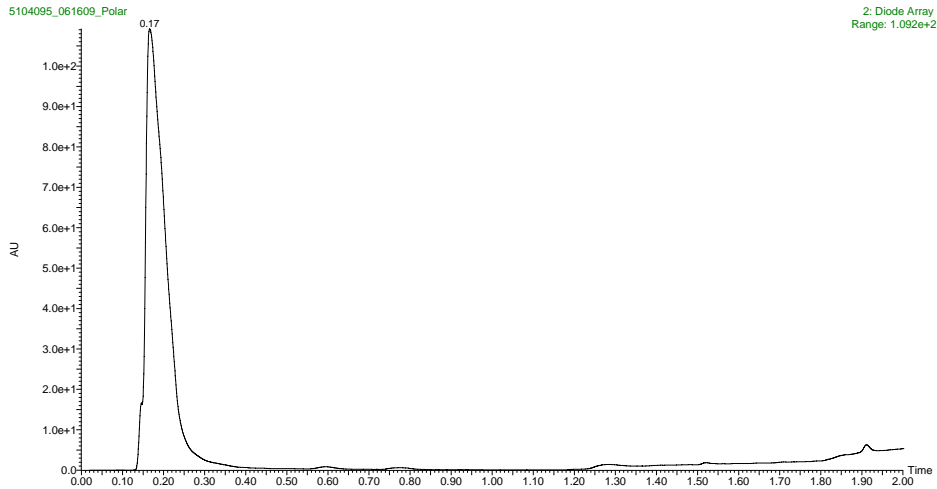
13 (SJ000359140) ELSD Signal – Purity = >95% - product mass at 0.50 min



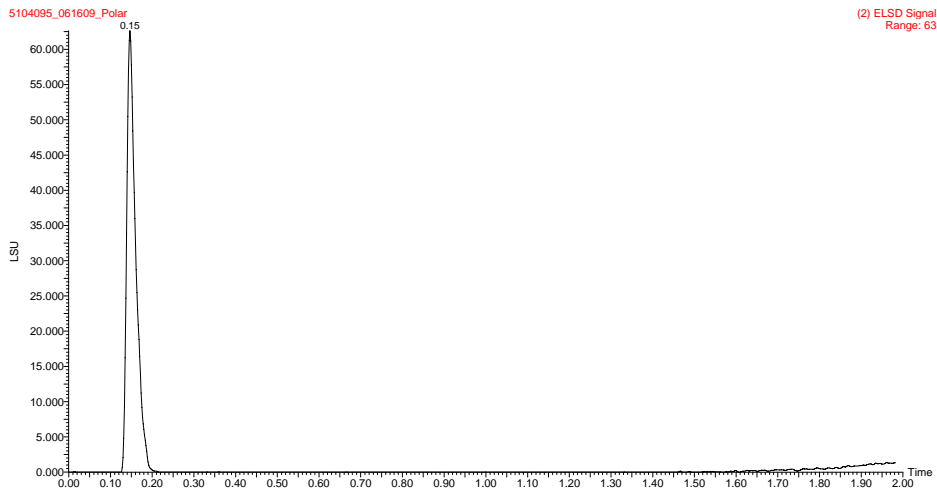
13 (SJ000359140) Parent Ion – Expected Mass +1: 255.1



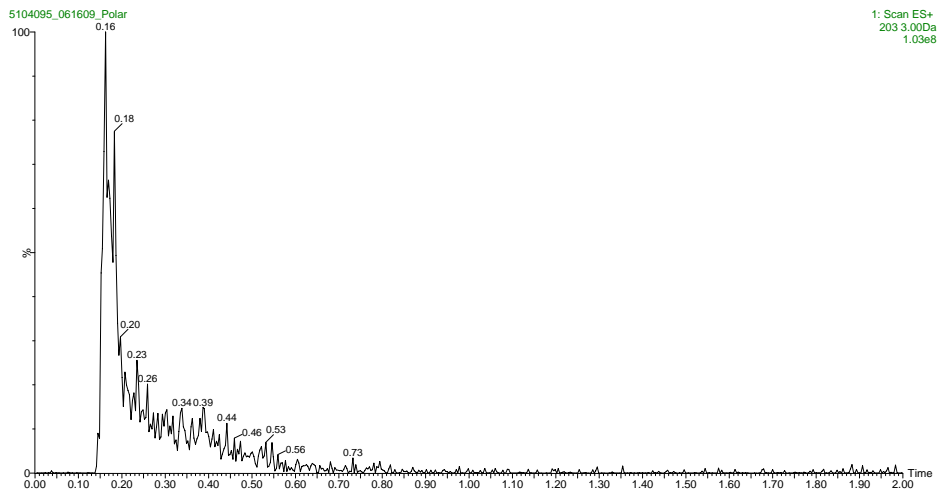
14 (SJ000359137) – UV-TIC – Product in Solvent Peak – attempts at separation unsuccessful – No other major components detected – Purity = >95%



14 (SJ000359137) – UV-TIC – Product in Solvent Peak – attempts at separation unsuccessful – No other major components detected – Purity = >95%



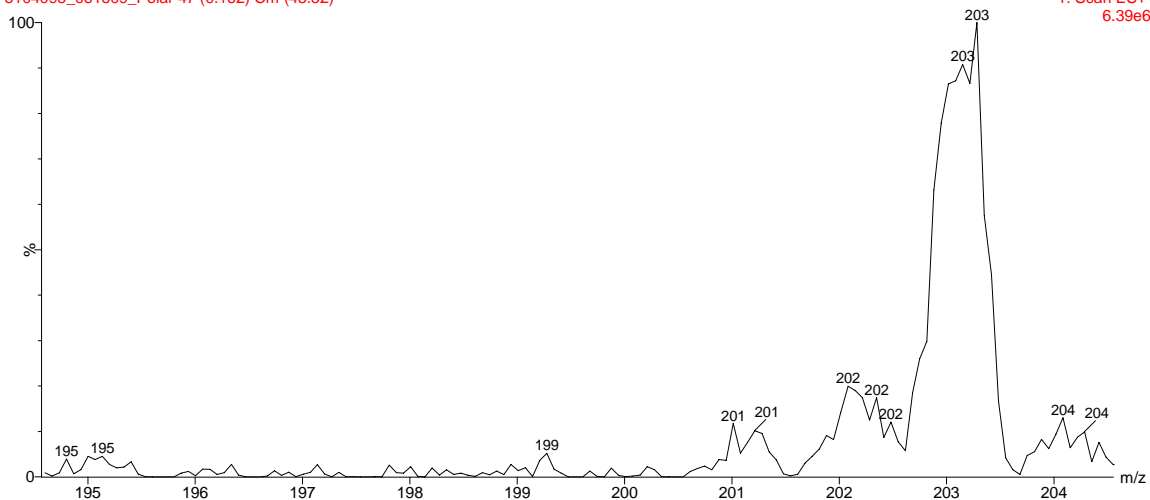
14 (SJ000359137) - Product Parent Ion Chromatogram – Product is in solvent peak



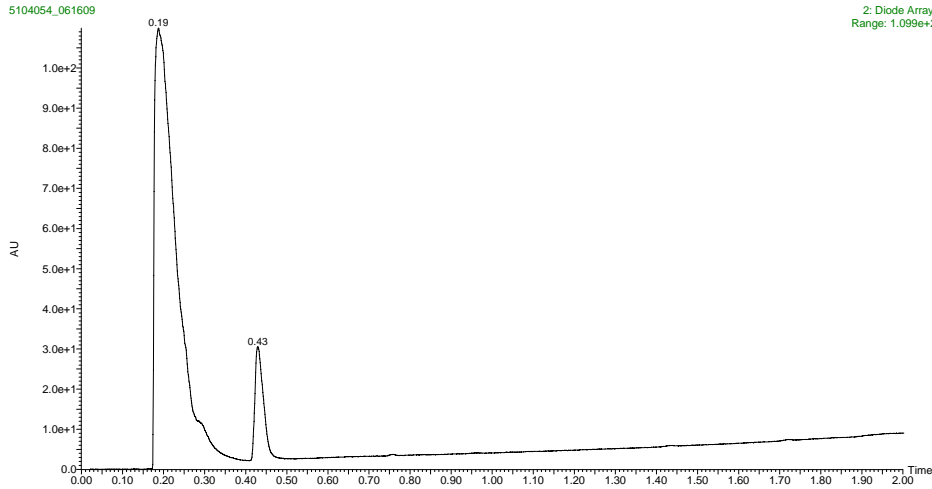
14 (SJ000359137) Parent Ion – Expected Mass +1: 203.0

5104095_061609_Polar 47 (0.162) Cm (45:52)

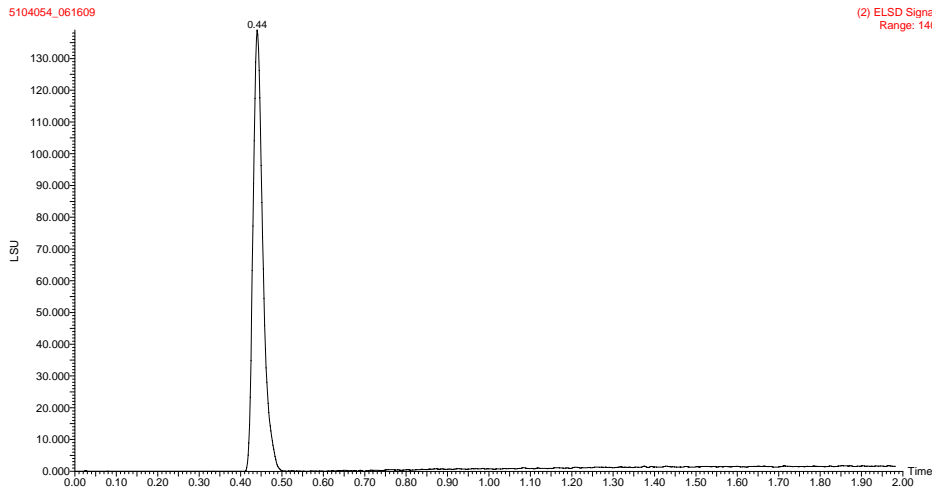
1: Scan ES+
6.39e6



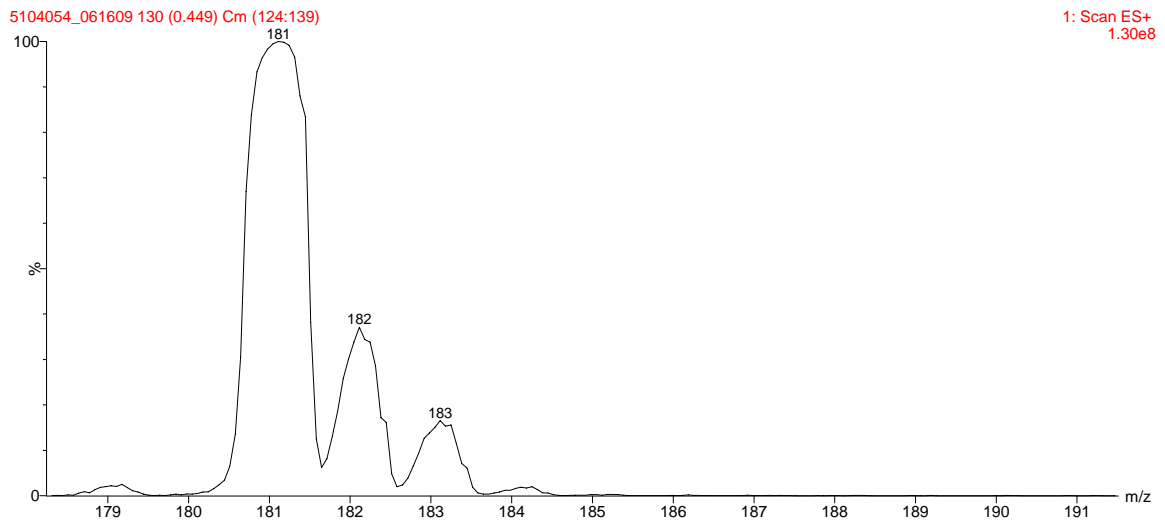
15 (SJ000359134) – UV-TIC – Purity = >95% - product mass at 0.43 min



15 (SJ000359134) – ELSD Signal – Purity = 100 % - product mass at 0.44 min



15 (SJ000359134) Parent Ion – Expected Mass +1: 181.1



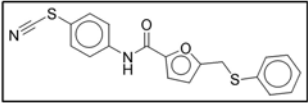
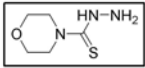
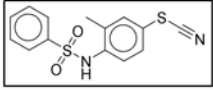
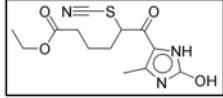
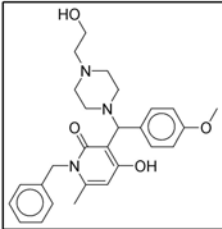
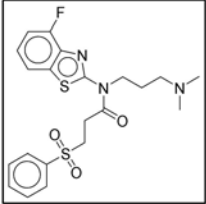
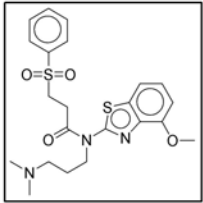
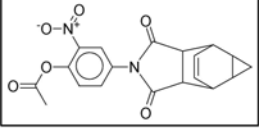
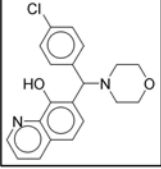
S4.11 Tables of All ODC High-throughput Screen Hits and Mode of inhibition

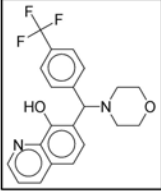
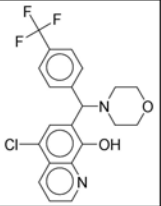
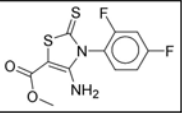
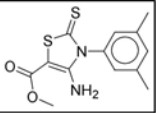
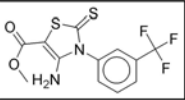
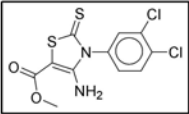
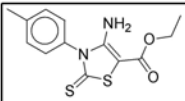
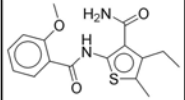
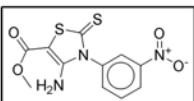
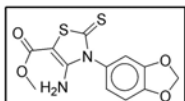
The following tables are a summary of all screening data from the ODC high-throughput screening effort. The compounds below are the re-ordered hit compounds plus small structure activity series which were not reported as validated hits in the main body of chapter 4. Most of these compounds displayed DTT dependent inhibition and required incubation with ODC in the absence of DTT in order to display inhibition. All compounds with reported EC₅₀ values versus TbODC displayed the doubling in rate when screened at 2x [ODC] which is characteristic of ODC dependant inhibition. Furthermore, none of the compounds displayed detectable inhibition of the linking enzymes in the 2-enzyme linked assay. Validated hits in the below table were not reported in the primary publication due to lack of pure compound, lack of preliminary SAR or irreversible inhibition. All compounds with reported EC₅₀ values versus whole cell *T. brucei* were evaluated for their ability to be rescued by the addition of 500 µM putrescine (sufficient to reverse growth inhibition by 1 mM DFMO) to the culture media. None displayed significant shifts in EC₅₀ values indicating that all had significant non-ODC related mechanisms of toxicity.

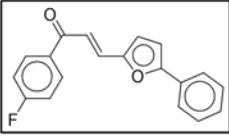
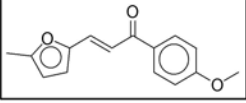
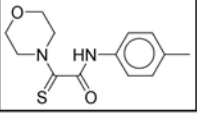
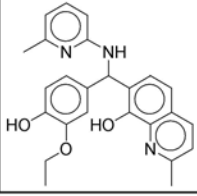
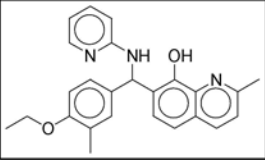
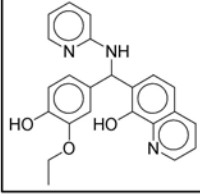
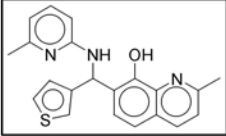
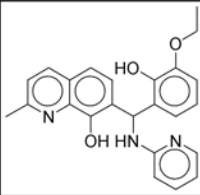
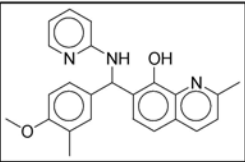
Field Definitions are below:

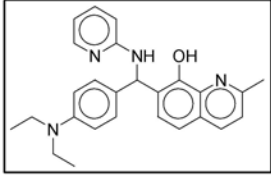
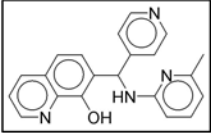
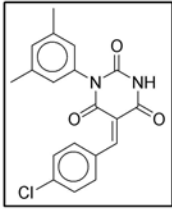
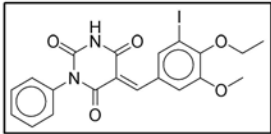
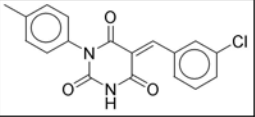
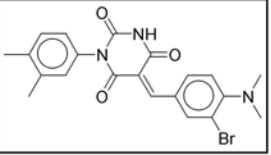
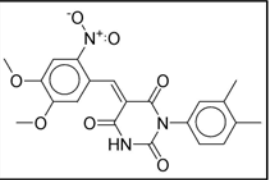
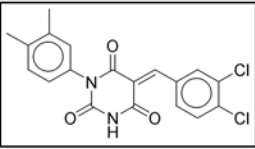
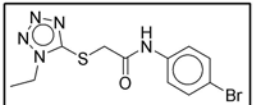
CompoundID:	Vendor Catalogue Number (SJ_Unique_ID field in St. Jude Chemical Biology Compound Registration Database)
TbODC EC ₅₀ (μM):	Enzyme-linked assay EC ₅₀ value as determined by fitting to a 4-parameter sigmoidal dose response curve. Value is a mean of 3 replicates. Compounds were pre-incubated with ODC and no DTT in this experiment. EC ₅₀ values were determined at 625 μM L-Orn and 60 μM PLP at room temperature.
<i>T. brucei</i> EC ₅₀ (μM):	EC ₅₀ values of compounds versus whole cell <i>T. brucei</i> as determined by the Cell-Titer-Glo Assay. Materials and methods for this experiment is on the following page.
Ornithine Mode of Inhibition:	Mode of inhibition with respect to varied L-ornithine concentrations. See materials and methods section of chapter 4 for full details. Compounds were pre-incubated with ODC and no DTT in this set of experiments.
PLP Mode of Inhibition:	Mode of inhibition with respect to varied pyridoxal-5'-phosphate concentrations. See materials and methods section of chapter 4 for full details. Compounds were pre-incubated with ODC and no DTT in this experiment.
Validated Hit:	Hits were designated as validated if full dose responses could be measured for both normal (compound+ODC+Linking enzymes followed by L-Orn+DTT+PLP) and reverse DTT (compound+ODC+DTT+PLP+Linking enzymes followed by L-Orn) linked enzyme assays.

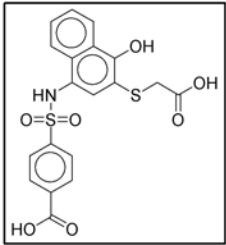
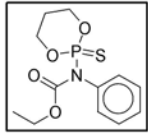
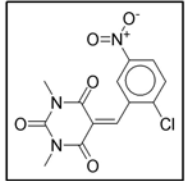
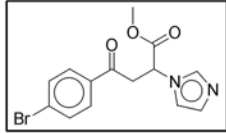
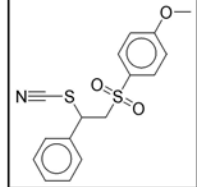
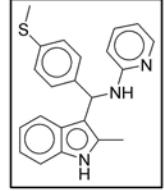
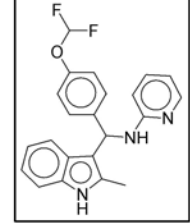
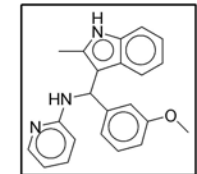
S4.11 Tables of All ODC High-throughput Screen Hits and Mode of inhibition

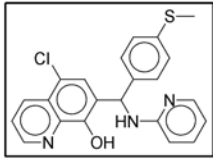
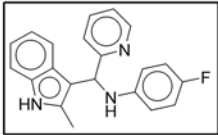
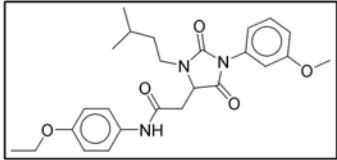
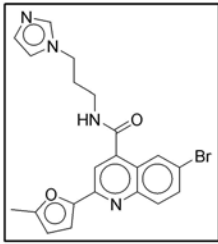
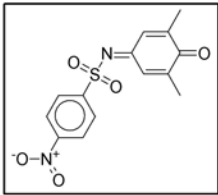
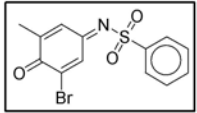
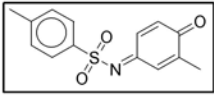
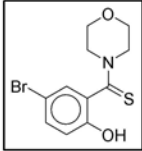
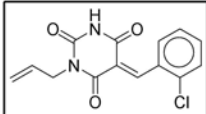
Structure	Compound ID	TbODC EC ₅₀ (μ M)	<i>T. brucei</i> EC ₅₀ (μ M)	Ornithine Mode of Inhibition	PLP Mode of Inhibition	Validated Hit?
	7992559	30.48	0.74	Un-Competitive	Non-Competitive	TRUE
	F1098-0070	9.81	0.14	Non-Competitive	Non-Competitive	TRUE
	7800304	30.62	4.09	Un-Competitive	Non-Competitive	TRUE
	C393-0024	13.10	0.01	Non-Competitive	Non-Competitive	TRUE
	F2074-0019	1.75	8.42	Non-Competitive	Non-Competitive	TRUE
	E677-1397	2.35	2.18	Non-Competitive	Non-Competitive	FALSE
	E677-1143	3.71	5.32	Non-Competitive	Non-Competitive	FALSE
	7144577	8.91	0.08	Non-Competitive	Non-Competitive	FALSE
	F1031-0071	3.30	3.19	Non-Competitive	Non-Competitive	FALSE

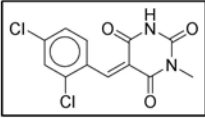
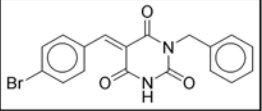
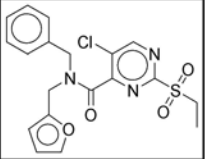
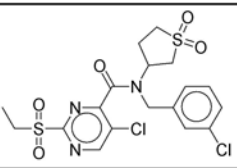
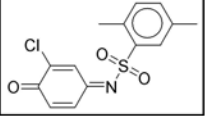
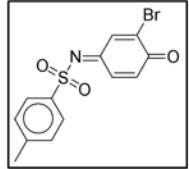
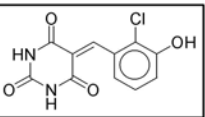
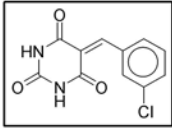
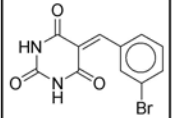
Structure	Compound ID	TbODC EC ₅₀ (μ M)	<i>T. brucei</i> EC ₅₀ (μ M)	Ornithine Mode of Inhibition	PLP Mode of Inhibition	Validated Hit?
	F0815-0045	ND	2.26	Inactive	Inactive	FALSE
	F1310-0007	ND	0.42	Inactive	Inactive	FALSE
	K286-4390	0.44	6.14	Non-Competitive	Non-Competitive	FALSE
	K286-4341	4.32	25.85	Non-Competitive	Non-Competitive	FALSE
	K286-4371	1.46	10.03	Non-Competitive	Non-Competitive	FALSE
	K286-4369	2.31	4.86	Non-Competitive	Non-Competitive	FALSE
	K286-4395	1.61	16.49	Non-Competitive	Non-Competitive	FALSE
	3366-3045	3.27	13.16	Non-Competitive	Un-Competitive	FALSE
	K286-4382	0.73	12.29	Non-Competitive	Non-Competitive	FALSE
	K286-4379	2.24	4.51	Non-Competitive	Non-Competitive	FALSE

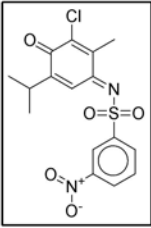
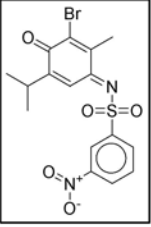
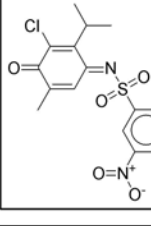
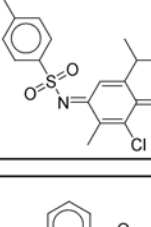
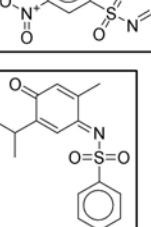
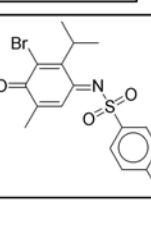

Structure	Compound ID	TbODC EC ₅₀ (μ M)	<i>T. brucei</i> EC ₅₀ (μ M)	Ornithine Mode of Inhibitor	PLP Mode of Inhibition	Validated Hit?
	5545617	Inactive	34.00	Inactive	Inactive	FALSE
	5223890	16.49	8.60	Non-Competitive	Non-Competitive	FALSE
	3448-2065	0.29	4.37	Non-Competitive	Un-Competitive	FALSE
	7485255	1.50	1.15	Non-Competitive	Non-Competitive	FALSE
	6375520	Inactive	8.21	Inactive	Inactive	FALSE
	6381814	1.04	0.86	Non-Competitive	Non-Competitive	FALSE
	6376401	2.93	6.35	Non-Competitive	Non-Competitive	FALSE
	6373722	6.48	9.86	Non-Competitive	Non-Competitive	FALSE
	7012006	2.18	5.47	Non-Competitive	Non-Competitive	FALSE

Structure	Compound ID	TbODC EC ₅₀ (μ M)	<i>T. brucei</i> EC ₅₀ (μ M)	Ornithine Mode of Inhibition	PLP Mode of Inhibition	Validated Hit?
	6633405	1.06	0.19	Non-Competitive	Non-Competitive	FALSE
	6372407	Inactive	5.03	Inactive	Inactive	FALSE
	2368-0065	4.85	Inactive	Non-Competitive	Non-Competitive	FALSE
	5964204	14.13	23.14	Non-Competitive	Non-Competitive	FALSE
	5965587	13.61	8.91	Non-Competitive	Non-Competitive	FALSE
	6324093	14.19	1.05	Non-Competitive	Non-Competitive	FALSE
	6320643	8.59	0.00	Non-Competitive	Non-Competitive	FALSE
	6327734	24.21	0.13	Non-Competitive	Non-Competitive	FALSE
	3448-9166	1.40	5.06	Non-Competitive	Non-Competitive	FALSE

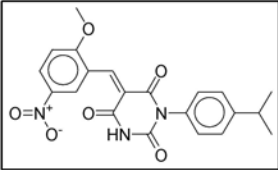
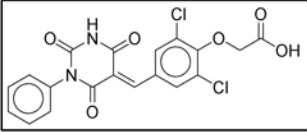
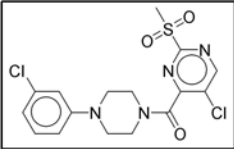
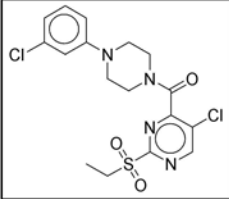
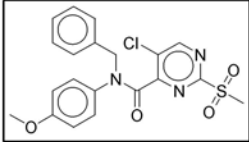
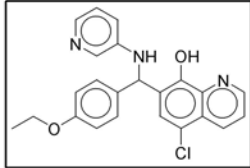
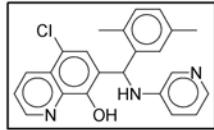
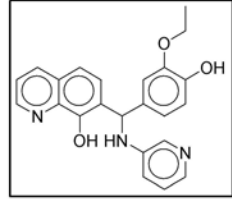
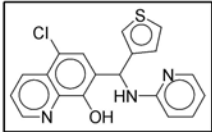
Structure	Compound ID	TbODC EC ₅₀ (μ M)	<i>T. brucei</i> EC ₅₀ (μ M)	Ornithine Mode of Inhibition	PLP Mode of Inhibition	Validated Hit?
	7202-3086	4.32	4.49	Non-Competitive	Non-Competitive	FALSE
	0094-0016	5.36	2.51	Non-Competitive	Competitive	FALSE
	2237-1807	1.61	10.22	Non-Competitive	Non-Competitive	FALSE
	7741221	2.77	1.42	Non-Competitive	Non-Competitive	FALSE
	5218493	34.91	7.38	Non-Competitive	Non-Competitive	FALSE
	F1387-0033	0.89	0.62	Non-Competitive	Non-Competitive	FALSE
	F1387-0032	3.55	5.07	Non-Competitive	Non-Competitive	FALSE
	F1387-0028	0.94	0.68	Non-Competitive	Non-Competitive	FALSE

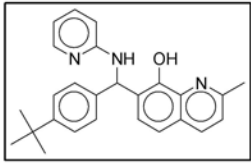
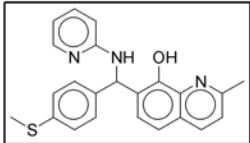
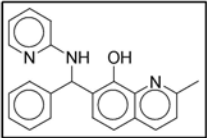
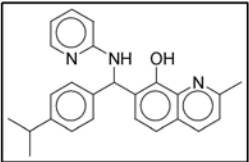
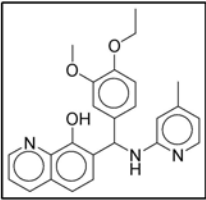
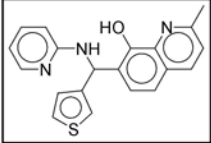
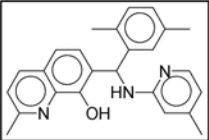
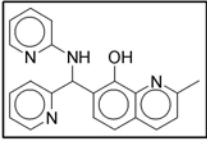
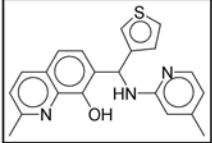
Structure	Compound ID	TbODC EC ₅₀ (μ M)	<i>T. brucei</i> EC ₅₀ (μ M)	Ornithine Mode of Inhibition	PLP Mode of Inhibition	Validated Hit?
	7925755	Inactive	1.17	Inactive	Inactive	FALSE
	F0815-0095	1.73	5.64	Non-Competitive	Non-Competitive	FALSE
	E750-0136	7.94	9.46	Non-Competitive	Non-Competitive	FALSE
	7923517	9.28	17.13	Non-Competitive	Non-Competitive	FALSE
	2548-0747	1.86	10.14	Non-Competitive	Non-Competitive	FALSE
	6629745	9.72	0.10	Non-Competitive	Non-Competitive	FALSE
	6629868	6.13	10.60	Non-Competitive	Non-Competitive	FALSE
	3405-0210	10.00	Inactive	Non-Competitive	Non-Competitive	FALSE
	5305098	4.16	6.13	Non-Competitive	Non-Competitive	FALSE

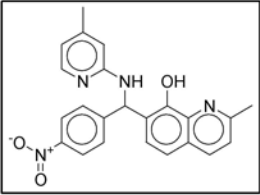
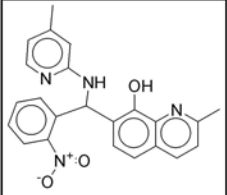
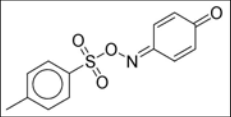
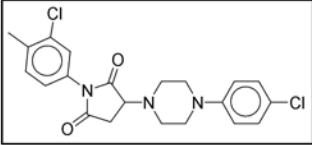
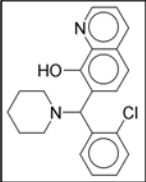
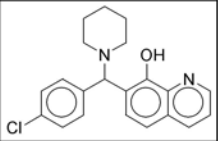
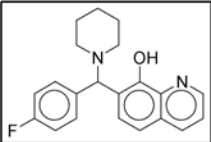
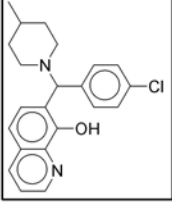
Structure	Compound ID	TbODC EC ₅₀ (μ M)	<i>T. brucei</i> EC ₅₀ (μ M)	Ornithine Mode of Inhibition	PLP Mode of Inhibition	Validated Hit?
	5240915	6.42	17.22	Non-Competitive	Non-Competitive	FALSE
	5240794	17.14	Inactive	Num_NonComp_2	undef	FALSE
	D053-0388	7.74	1.34	Non-Competitive	Non-Competitive	FALSE
	D053-0375	10.69	1.52	Non-Competitive	Non-Competitive	FALSE
	F0808-1812	0.59	7.61	Non-Competitive	Non-Competitive	FALSE
	5158531	12.19	2.83	Non-Competitive	Non-Competitive	FALSE
	7483938	7.66	0.02	Non-Competitive	Non-Competitive	FALSE
	6077688	8.95	17.01	Non-Competitive	Non-Competitive	FALSE
	5316000	5.90	7.94	Non-Competitive	Non-Competitive	FALSE

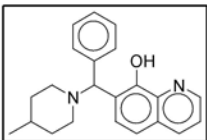
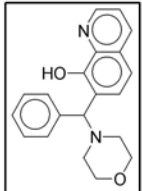
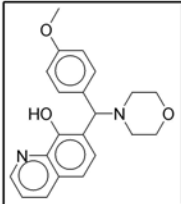
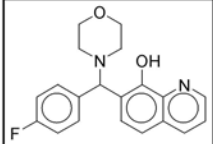
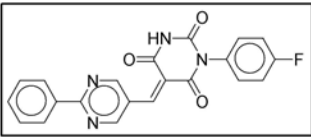
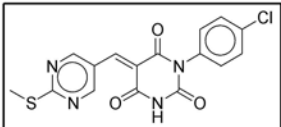
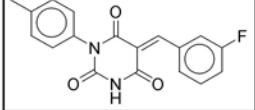
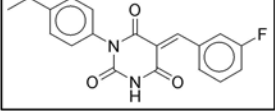
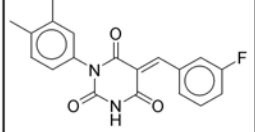
Structure	Compound ID	TbODC EC ₅₀ (μ M)	<i>T. brucei</i> EC ₅₀ (μ M)	Ornithine Mode of Inhibition	PLP Mode of Inhibition	Validated Hit?
	6653473	4.30	7.88	Non-Competitive	Non-Competitive	FALSE
	6653675	4.30	5.16	Non-Competitive	Non-Competitive	FALSE
	6680314	1.81	0.34	Non-Competitive	Non-Competitive	FALSE
	6389350	3.84	8.03	Non-Competitive	Non-Competitive	FALSE
	6656502	2.52	4.38	Non-Competitive	Non-Competitive	FALSE
	6627645	2.24	Non-Competitive	Non-Competitive	Non-Competitive	FALSE
	6657582	1.83	0.31	Non-Competitive	Non-Competitive	FALSE

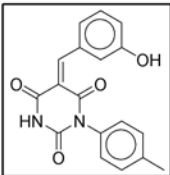
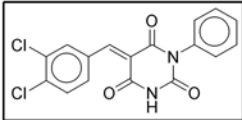
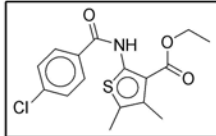
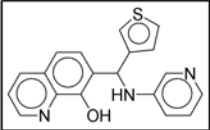
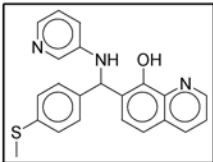
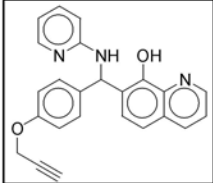
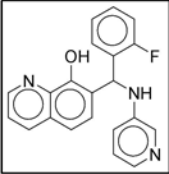
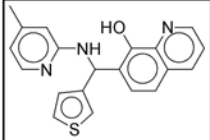
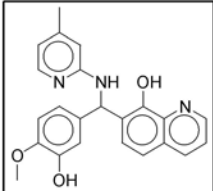
Structure	Compound ID	TbODC EC ₅₀ (μ M)	<i>T. brucei</i> EC ₅₀ (μ M)	Ornithine Mode of Inhibition	PLP Mode of Inhibition	Validated Hit?
	6627762	2.21	2.85	Non-Competitive	Non-Competitive	FALSE
	6658016	2.82	0.45	Non-Competitive	Non-Competitive	FALSE
	6625728	6.82	2.08	Non-Competitive	Non-Competitive	FALSE
	6631480	5.70	6.19	Non-Competitive	Non-Competitive	FALSE
	6631369	7.41	7.37	Non-Competitive	Non-Competitive	FALSE
	6626128	10.50	3.50	Non-Competitive	Non-Competitive	FALSE
	F0808-1801	1.56	28.18	Non-Competitive	Competitive	FALSE
	F0808-1800	3.07	22.42	Non-Competitive	Competitive	FALSE
	5960222	13.10	13.42	Non-Competitive	Non-Competitive	FALSE
	5960045	12.13	8.18	Non-Competitive	Non-Competitive	FALSE

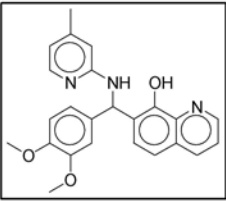
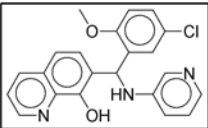
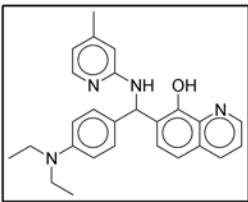
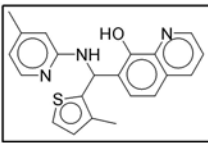
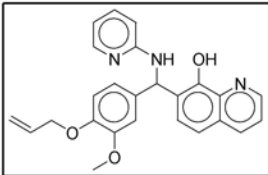
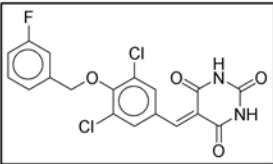
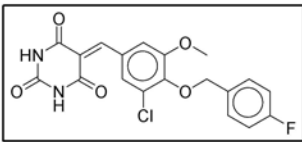
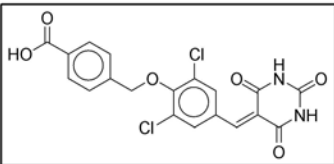
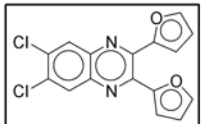
Structure	Compound ID	TbODC EC ₅₀ (μ M)	<i>T. brucei</i> EC ₅₀ (μ M)	Ornithine Mode of Inhibition	PLP Mode of Inhibition	Validated Hit?
	5963070	28.30	0.02	Non-Competitive	Non-Competitive	FALSE
	5968220	26.36	0.04	Non-Competitive	Non-Competitive	FALSE
	D053-0032	10.29	3.63	Non-Competitive	Non-Competitive	FALSE
	D053-0117	14.95	2.17	Non-Competitive	Non-Competitive	FALSE
	D053-0306	4.30	2.00	Non-Competitive	Non-Competitive	FALSE
	7969312	6.26	2.77	Non-Competitive	Non-Competitive	FALSE
	7967759	Inactive	3.28	Inactive	Inactive	FALSE
	7970161	0.95	0.64	Non-Competitive	Non-Competitive	FALSE
	7924532	Inactive	3.81	Inactive	Inactive	FALSE

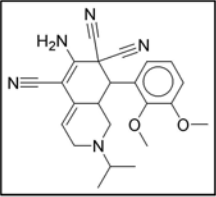
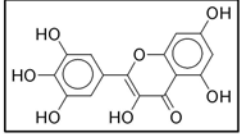
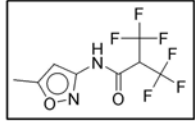
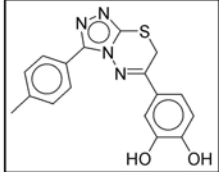
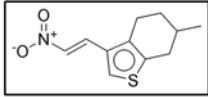
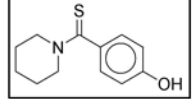
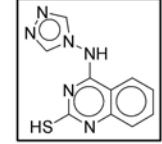
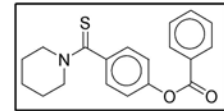
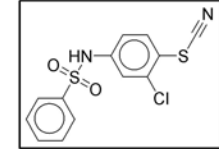
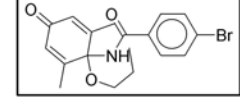
Structure	Compound ID	TbODC EC ₅₀ (μ M)	<i>T. brucei</i> EC ₅₀ (μ M)	Ornithine Mode of Inhibitor	PLP Mode of Inhibition	Validated Hit?
	6371621	Inactive	3.45	Inactive	Inactive	FALSE
	6378891	Inactive	7.30	Inactive	Inactive	FALSE
	6633774	Inactive	9.46	Inactive	Inactive	FALSE
	7016468	Inactive	3.99	Inactive	Inactive	FALSE
	5994-0447	1.00	1.12	Non-Competitive	Non-Competitive	FALSE
	6635495	5.19	7.85	Non-Competitive	Non-Competitive	FALSE
	7630880	Inactive	5.32	Inactive	Inactive	FALSE
	6378816	Inactive	12.29	Inactive	Inactive	FALSE
	7634527	2.98	4.48	Non-Competitive	Non-Competitive	FALSE

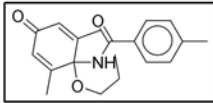
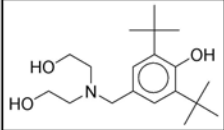
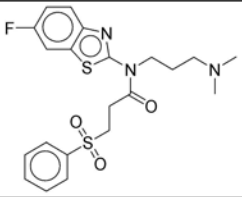
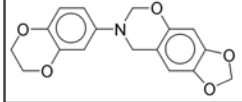
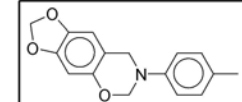
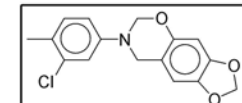
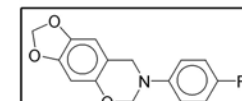
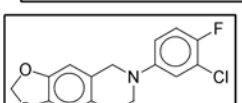
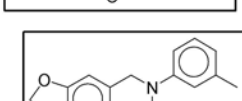
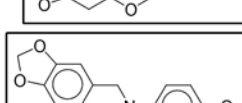
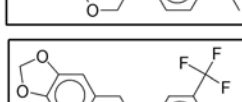
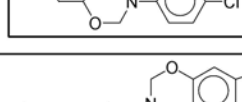
Structure	Compound ID	TbODC EC ₅₀ (μ M)	<i>T. brucei</i> EC ₅₀ (μ M)	Ornithine Mode of Inhibitor	PLP Mode of Inhibition	Validated Hit?
	7630693	Inactive	2.99	Inactive	Inactive	FALSE
	7630436	Inactive	5.35	Inactive	Inactive	FALSE
	5467940	15.27	0.24	Non-Competitive	Non-Competitive	FALSE
	5934605	41.43	14.67	Non-Competitive	Non-Competitive	FALSE
	F1031-0135	12.96	2.95	Non-Competitive	Non-Competitive	FALSE
	F0842-0019	18.10	3.08	Non-Competitive	Non-Competitive	FALSE
	F1031-0171	17.22	2.93	Non-Competitive	Non-Competitive	FALSE
	F1031-0043	Inactive	2.21	Inactive	Inactive	FALSE

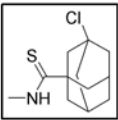
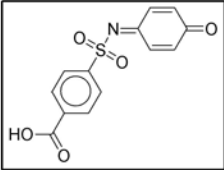
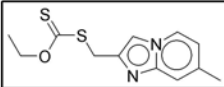
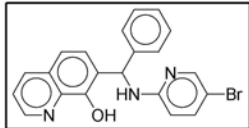
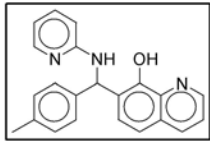
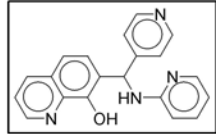
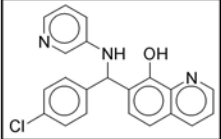
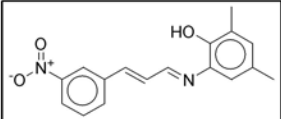
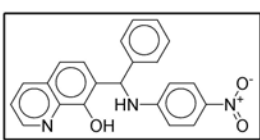
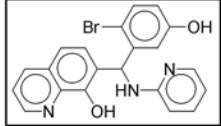
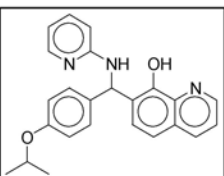
Structure	Compound ID	TbODC EC ₅₀ (μ M)	<i>T. brucei</i> EC ₅₀ (μ M)	Ornithine Mode of Inhibition	PLP Mode of Inhibition	Validated Hit?
	F1031-0061	21.12	4.15	Non-Competitive	Non-Competitive	FALSE
	F0870-0083	2.33	4.01	Non-Competitive	Non-Competitive	FALSE
	F1310-0022	1.05	5.89	Non-Competitive	Non-Competitive	FALSE
	F0842-0027	2.54	4.60	Non-Competitive	Non-Competitive	FALSE
	6586297	15.85	Inactive	Non-Competitive	Non-Competitive	FALSE
	6589006	6.85	50.00	Non-Competitive	Non-Competitive	FALSE
	5976843	11.27	0.06	Non-Competitive	Non-Competitive	FALSE
	7261142	17.22	0.03	Non-Competitive	Non-Competitive	FALSE
	6323011	13.10	0.02	Non-Competitive	Non-Competitive	FALSE

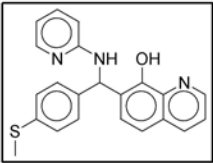
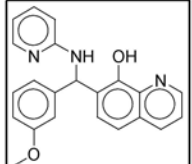
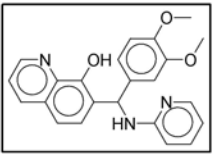
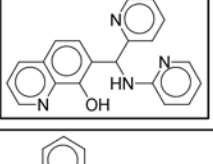
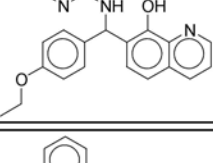
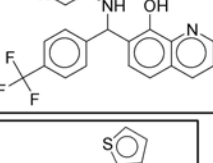
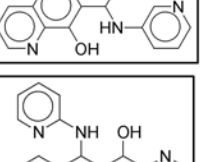
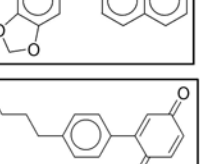
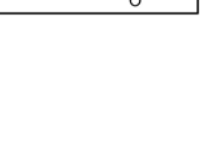
Structure	Compound ID	TbODC EC ₅₀ (μ M)	<i>T. brucei</i> EC ₅₀ (μ M)	Ornithine Mode of Inhibition	PLP Mode of Inhibition	Validated Hit?
	2368-0377	2.59	0.00	Non-Competitive	Non-Competitive	FALSE
	5966880	10.30	2.31	Non-Competitive	Non-Competitive	FALSE
	3297-0914	4.67	17.86	Non-Competitive	Non-Competitive	FALSE
	7968826	1.58	1.42	Non-Competitive	Non-Competitive	FALSE
	7968687	2.95	3.55	Non-Competitive	Non-Competitive	FALSE
	7925578	6.31	3.26	Non-Competitive	Non-Competitive	FALSE
	7968218	6.85	3.26	Non-Competitive	Non-Competitive	FALSE
	6374848	3.59	1.96	Non-Competitive	Non-Competitive	FALSE
	7011428	3.10	2.33	Non-Competitive	Non-Competitive	FALSE

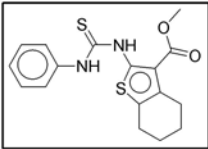
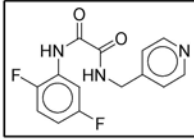
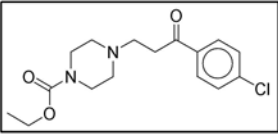
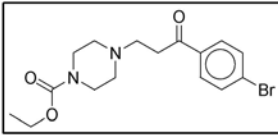
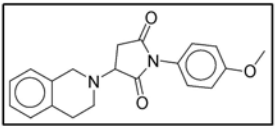
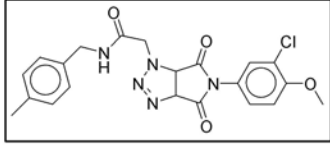
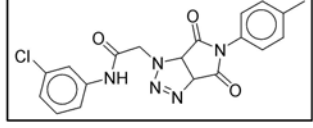
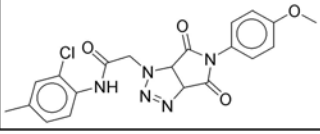
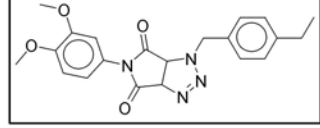
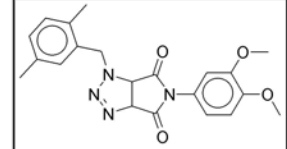
Structure	Compound ID	TbODC EC ₅₀ (μM)	<i>T. brucei</i> EC ₅₀ (μM)	Ornithine Mode of Inhibition	PLP Mode of Inhibition	Validated Hit?
	6372208	4.43	1.80	Non-Competitive	Non-Competitive	FALSE
	7967682	6.36	2.67	Non-Competitive	Non-Competitive	FALSE
	6372780	2.03	0.23	Non-Competitive	Non-Competitive	FALSE
	6375950	1.87	0.30	Non-Competitive	Non-Competitive	FALSE
	7926588	4.00	3.55	Non-Competitive	Non-Competitive	FALSE
	5977995	20.42	1.67	Non-Competitive	Non-Competitive	FALSE
	6290791	14.76	0.85	Non-Competitive	Non-Competitive	FALSE
	5970242	7.69	0.02	Non-Competitive	Non-Competitive	FALSE
	K079-0037	13.73	22.74	Non-Competitive	Non-Competitive	FALSE

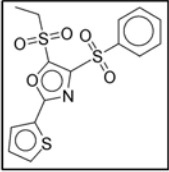
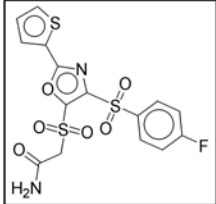
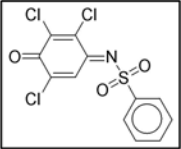
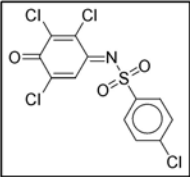
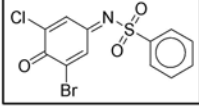
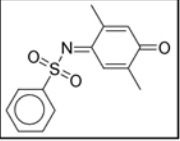
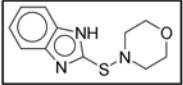
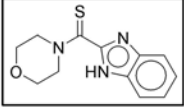
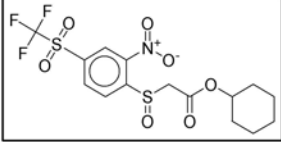
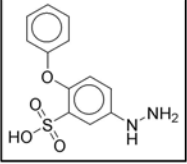
Structure	Compound ID	TbODC EC ₅₀ (μM)	<i>T. brucei</i> EC ₅₀ (μM)	Ornithine Mode of Inhibition	PLP Mode of Inhibition	Validated Hit?
	3132-0665	27.66	23.50	Non-Competitive	Non-Competitive	FALSE
	M 6760	Inactive	3.98	Inactive	Inactive	FALSE
	4770-1860	9.36	0.28	Non-Competitive	Non-Competitive	FALSE
	K243-0077	22.67	7.97	Non-Competitive	Non-Competitive	FALSE
	E540-1032	Inactive	0.62	Inactive	Inactive	FALSE
	3405-0201	16.82	13.65	Non-Competitive	Competitive	FALSE
	K297-0325	Inactive	0.28	Inactive	Inactive	FALSE
	3405-0009	14.70	3.56	Non-Competitive	Competitive	FALSE
	7833672	15.27	1.01	Non-Competitive	Non-Competitive	FALSE
	F1055-0007	10.04	13.96	Non-Competitive	Non-Competitive	FALSE

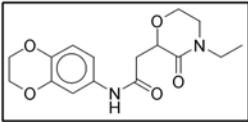
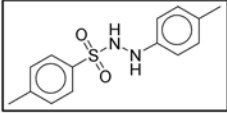
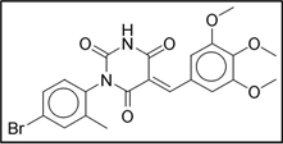
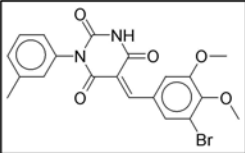
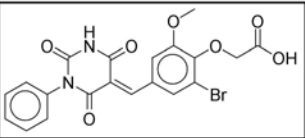
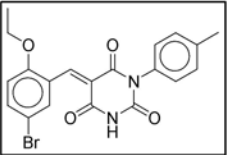
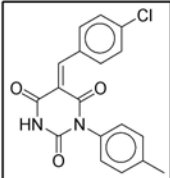
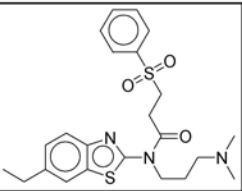
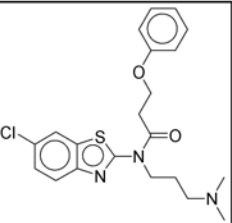
Structure	Compound ID	TbODC EC ₅₀ (μ M)	<i>T. brucei</i> EC ₅₀ (μ M)	Ornithine Mode of Inhibition	PLP Mode of Inhibition	Validated Hit?
	F1055-0005	Inactive	0.00	Inactive	Inactive	FALSE
	5243661	4.83	6.57	Non-Competitive	Non-Competitive	FALSE
	E677-0508	3.73	4.63	Non-Competitive	Non-Competitive	FALSE
	7982563	3.45	25.79	Non-Competitive	Non-Competitive	FALSE
	C276-0038	4.00	24.70	Non-Competitive	Non-Competitive	FALSE
	7906760	4.34	11.70	Non-Competitive	Non-Competitive	FALSE
	C276-0041	3.42	31.62	Non-Competitive	Non-Competitive	FALSE
	7918942	6.72	5.03	Non-Competitive	Non-Competitive	FALSE
	7906754	5.44	2.11	Non-Competitive	Non-Competitive	FALSE
	C276-0043	1.79	13.35	Non-Competitive	Non-Competitive	FALSE
	7906759	36.11	0.58	Non-Competitive	Non-Competitive	FALSE
	7918941	8.26	1.95	Non-Competitive	Non-Competitive	FALSE

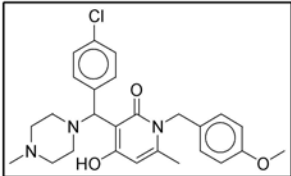
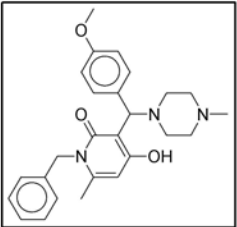
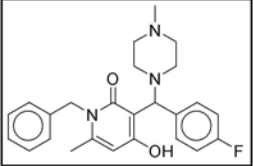
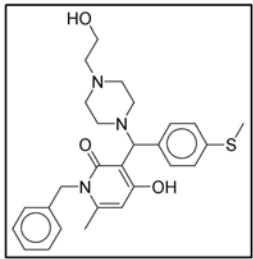
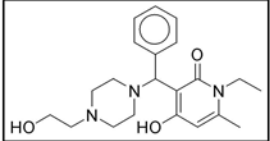
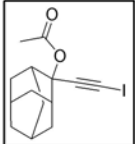
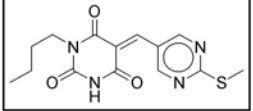
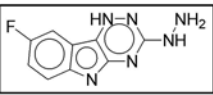
Structure	Compound ID	TbODC EC ₅₀ (μM)	<i>T. brucei</i> EC ₅₀ (μM)	Ornithine Mode of Inhibitor	PLP Mode of Inhibition	Validated Hit?
	0418-0093	Inactive	Inactive	Inactive	Inactive	FALSE
	7202-3000	1.32	23.91	Non-Competitive	Non-Competitive	FALSE
	F1387-0062	Inactive	50.00	Inactive	Inactive	FALSE
	5133157	Inactive	1.96	Inactive	Inactive	FALSE
	6372490	12.43	2.90	Non-Competitive	Non-Competitive	FALSE
	6376502	Inactive	7.75	Inactive	Inactive	FALSE
	7969927	6.82	5.16	Non-Competitive	Non-Competitive	FALSE
	0958-0297	19.95	4.65	Non-Competitive	Non-Competitive	FALSE
	5140792	Inactive	1.13	Inactive	Inactive	FALSE
	6371667	Inactive	2.02	Inactive	Inactive	FALSE
	6372717	22.39	3.67	Non-Competitive	Non-Competitive	FALSE

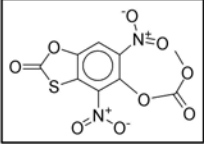
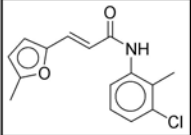
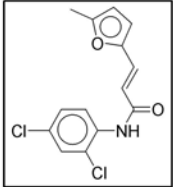
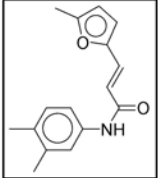
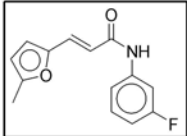
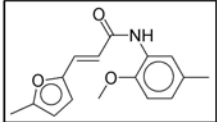
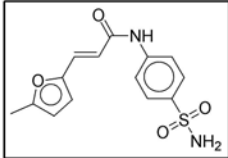
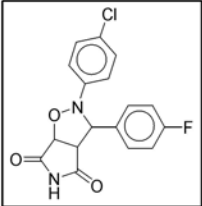
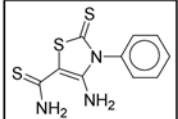
Structure	Compound ID	TbODC EC ₅₀ (μM)	<i>T. brucei</i> EC ₅₀ (μM)	Ornithine Mode of Inhibition	PLP Mode of Inhibition	Validated Hit?
	6377128	Inactive	2.60	Inactive	Inactive	FALSE
	6374081	Inactive	6.33	Inactive	Inactive	FALSE
	6376791	4.30	0.32	Non-Competitive	Non-Competitive	FALSE
	6371681	Inactive	6.18	Inactive	Inactive	FALSE
	6382061	6.57	3.16	Non-Competitive	Non-Competitive	FALSE
	7967495	Inactive	2.83	Inactive	Inactive	FALSE
	7970045	1.04	0.35	Non-Competitive	Non-Competitive	FALSE
	6371856	4.79	3.47	Non-Competitive	Non-Competitive	FALSE
	5924-0106	2.72	12.64	Non-Competitive	Non-Competitive	FALSE

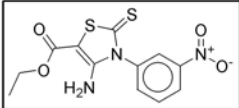
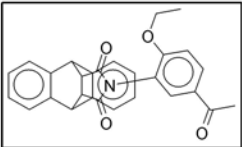
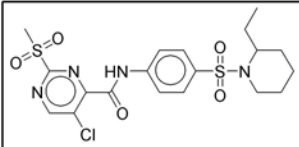
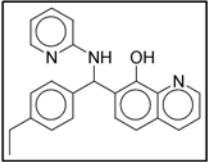
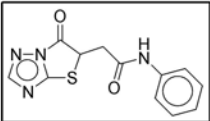
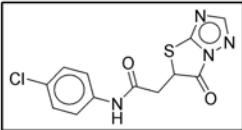
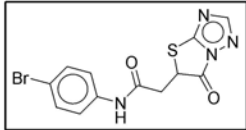
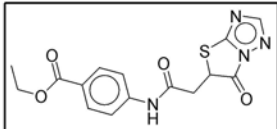
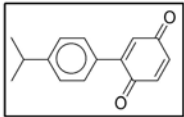
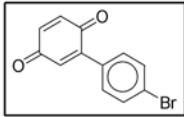
Structure	Compound ID	TbODC EC ₅₀ (μM)	<i>T. brucei</i> EC ₅₀ (μM)	Ornithine Mode of Inhibition	PLP Mode of Inhibition	Validated Hit?
	3261-1071	2.25	50.00	Non-Competitive	Non-Competitive	FALSE
	F2795-0512	Inactive	0.06	Inactive	Inactive	FALSE
	6350-0006	10.13	7.97	Non-Competitive	Non-Competitive	FALSE
	6350-0013	10.41	7.08	Non-Competitive	Non-Competitive	FALSE
	7174955	6.88	11.19	Non-Competitive	Non-Competitive	FALSE
	F3165-1168	32.91	0.04	Non-Competitive	Non-Competitive	FALSE
	C338-0072	15.92	0.21	Non-Competitive	Non-Competitive	FALSE
	C433-0076	3.05	0.02	Non-Competitive	Competitive	FALSE
	C433-0620	5.03	0.00	Non-Competitive	Competitive	FALSE
	C433-0614	5.48	0.06	Non-Competitive	Competitive	FALSE

Structure	Compound ID	TbODC EC ₅₀ (μM)	<i>T. brucei</i> EC ₅₀ (μM)	Ornithine Mode of Inhibition	PLP Mode of Inhibition	Validated Hit?
	D093-0045	2.44	0.96	Non-Competitive	Non-Competitive	FALSE
	D093-0073	8.18	7.10	Non-Competitive	Competitive	FALSE
	5158512	11.88	3.37	Non-Competitive	Non-Competitive	FALSE
	5158511	7.31	7.57	Non-Competitive	Non-Competitive	FALSE
	5228252	8.43	1.63	Non-Competitive	Non-Competitive	FALSE
	5149913	6.63	25.12	Non-Competitive	Non-Competitive	FALSE
	1069-0090	1.63	6.37	Non-Competitive	Non-Competitive	FALSE
	1332-0031	13.00	0.01	Num_NonComp_3	Undef_Comp_3	FALSE
	7568836	14.29	0.55	Competitive	Non-Competitive	FALSE
	5118904	8.41	5.01	Non-Competitive	Non-Competitive	FALSE

Structure	Compound ID	TbODC EC ₅₀ (μM)	<i>T. brucei</i> EC ₅₀ (μM)	Ornithine Mode of Inhibition	PLP Mode of Inhibition	Validated Hit?
	7817424	19.40	0.21	Non-Competitive	Non-Competitive	FALSE
	5142887	35.48	10.75	Un-Competitive	Non-Competitive	FALSE
	6006195	22.46	0.12	Non-Competitive	Non-Competitive	FALSE
	6005002	14.70	0.42	Non-Competitive	Non-Competitive	FALSE
	5964389	18.67	5.62	Non-Competitive	Non-Competitive	FALSE
	5965278	11.68	3.58	Non-Competitive	Non-Competitive	FALSE
	2368-0409	4.30	Inactive	Non-Competitive	Non-Competitive	FALSE
	E677-0889	5.22	1.12	Non-Competitive	Non-Competitive	FALSE
	E677-0564	8.16	1.65	Non-Competitive	Non-Competitive	FALSE

Structure	Compound ID	TbODC EC ₅₀ (μ M)	<i>T. brucei</i> EC ₅₀ (μ M)	Ornithine Mode of Inhibition	PLP Mode of Inhibition	Validated Hit?
	F2074-0207	29.11	27.40	Non-Competitive	Non-Competitive	FALSE
	F2074-0016	2.25	5.05	Non-Competitive	Non-Competitive	FALSE
	F2074-0085	20.53	0.01	Non-Competitive	Non-Competitive	FALSE
	F2074-0107	3.85	8.08	Non-Competitive	Non-Competitive	FALSE
	F2074-0285	41.43	Inactive	Non-Competitive	Non-Competitive	FALSE
	7267501	Inactive	2.78	Inactive	Inactive	FALSE
	6604418	9.04	11.53	Non-Competitive	Non-Competitive	FALSE
	6927-0961	1.39	0.47	Competitive	Non-Competitive	FALSE

Structure	Compound ID	TbODC EC ₅₀ (μM)	<i>T. brucei</i> EC ₅₀ (μM)	Ornithine Mode of Inhibition	PLP Mode of Inhibition	Validated Hit?
	0665-0081	10.28	1.21	Non-Competitive	Un-Competitive	FALSE
	6128194	30.21	0.81	Non-Competitive	Non-Competitive	FALSE
	6147058	Inactive	7.86	Inactive	Inactive	FALSE
	7253329	13.38	3.52	Non-Competitive	Non-Competitive	FALSE
	7285485	24.32	1.63	Non-Competitive	Non-Competitive	FALSE
	7246974	29.90	0.13	Non-Competitive	Non-Competitive	FALSE
	6005-0063	28.54	0.32	Non-Competitive	Competitive	FALSE
	6767933	10.00	0.09	Non-Competitive	Non-Competitive	FALSE
	6000-1760	0.39	11.68	Non-Competitive	Un-Competitive	FALSE

Structure	Compound ID	TbODC EC ₅₀ (μ M)	<i>T. brucei</i> EC ₅₀ (μ M)	Ornithine Mode of Inhibition	PLP Mode of Inhibition	Validated Hit?
	K286-4381	1.28	8.21	Non-Competitive	Competitive	FALSE
	2360-0539	5.24	2.23	Non-Competitive	Non-Competitive	FALSE
	D053-0279	11.66	0.85	Non-Competitive	Non-Competitive	FALSE
	6377846	Inactive	2.75	Inactive	Inactive	FALSE
	7803985	0.45	10.45	Non-Competitive	Non-Competitive	FALSE
	7776670	0.47	22.98	Non-Competitive	Non-Competitive	FALSE
	7521108	0.69	3.89	Non-Competitive	Non-Competitive	FALSE
	7788014	31.64	12.59	Non-Competitive	Non-Competitive	FALSE
	5924-0105	0.74	13.96	Non-Competitive	Non-Competitive	FALSE
	4663-0305	0.77	22.02	Non-Competitive	Non-Competitive	FALSE

S4.12 Table of All ODC High-Throughput Assay Hits Cytotoxicity Data and Reverse Addition Results

The following table shows the full cytotoxicity results for each re-ordered hit compound from table S4.11. It also includes the results for reverse DTT addition experiments and the selectivity for hODC versus TbODC.

Field Definitions are below:

CompoundID:	Vendor Catalogue Number (notebook_page field in St. Jude Chemical Biology Compound Registration Database)
Reverse Addition Hit:	If the compound displayed a full dose response curve when incubated with ODC and DTT, the compound was designated as a reverse addition hit. This assay was the most stringent of all secondary assays used.
hODC selectivity:	Compounds were designated as selective if there was a greater than 10-fold difference in IC ₅₀ values for hODC and TbODC as determined using the normal DTT addition linked enzyme assay. IC ₅₀ values were determined under isokinetic conditions at 1.5x K _m L-Orn and 60 μM PLP.
Therapeutic Index Fields:	All therapeutic index fields are defined as the ratio of the EC ₅₀ value of the compound versus the test cell line to the EC ₅₀ value of the compound versus <i>T. brucei</i> . If no activity was detected versus the test cell-line the therapeutic index was set to 1000x. Compounds were tested to a maximum concentration of 100 μM.

Compound ID	Reverse Addition Hit	hODC Selectivity	BJ Therapeutic Index	HepG2 Therapeutic Index	HEK293 Therapeutic Index	Raji Therapeutic Index
7992559	TRUE	Non-Selective	67.85	60.62	18.47	10.39
F1098-0070	TRUE	Non-Selective	353.97	71.11	187.99	79.78
7800304	TRUE	Non-Selective	4.56	13.76	6.15	3.99
C393-0024	TRUE	Non-Selective	7943.28	8891.40	5623.41	8891.40
F2074-0019	TRUE	Non-Selective	0.00	5.94	1.68	5.94
E677-1397	TRUE	TbODC Selective	6.28	3.94	9.20	2.79
E677-1143	TRUE	Non-Selective	4.23	1.19	3.25	0.57
7144577	FALSE	Non-Selective	658.76	1.32	1000.00	740.90
F1031-0071	FALSE	Non-Selective	13.99	1.99	2.09	0.52
F0815-0045	FALSE	Inactive	15.70	1.41	3.23	0.48
F1310-0007	FALSE	Inactive	118.88	11.48	11.58	6.73
K286-4390	FALSE	TbODC Selective	8.15	1000.00	1000.00	1000.00
K286-4341	FALSE	TbODC Selective	1.93	1000.00	1000.00	1000.00
K286-4371	FALSE	TbODC Selective	4.98	1000.00	4.45	1000.00
K286-4369	FALSE	TbODC Selective	1000.00	1000.00	1000.00	1000.00
K286-4395	FALSE	TbODC Selective	1000.00	1000.00	1000.00	1000.00
3366-3045	FALSE	TbODC Selective	1000.00	1000.00	1000.00	1000.00
K286-4382	FALSE	TbODC Selective	1.29	1000.00	1000.00	1000.00
K286-4379	FALSE	TbODC Selective	1000.00	1000.00	11.08	1000.00
5545617	FALSE	Inactive	1.11	1.65	1.26	0.69
5223890	FALSE	TbODC Selective	5.22	5.81	3.24	1.58
3448-2065	FALSE	TbODC Selective	11.43	1000.00	1000.00	1000.00
7485255	FALSE	Non-Selective	11.82	61.46	35.48	11.87
6375520	FALSE	Inactive	4.88	1000.00	3.21	6.14
6381814	FALSE	Non-Selective	14.70	25.12	17.50	9.10
6376401	FALSE	TbODC Selective	5.23	1000.00	7.87	6.27
6373722	FALSE	TbODC Selective	5.07	1000.00	5.07	5.08
7012006	FALSE	TbODC Selective	7.72	1000.00	3.94	9.16

Compound ID	Reverse Addition Hit	hODC Selectivity	BJ Therapeutic Index	HepG2 Therapeutic Index	HEK293 Therapeutic Index	Raji Therapeutic Index
6633405	FALSE	TbODC Selective	40.93	1000.00	97.08	78.12
6372407	FALSE	Inactive	3.25	0.93	0.45	0.81
2368-0065	FALSE	TbODC Selective	Inactive	Inactive	Inactive	Inactive
5964204	FALSE	Non-Selective	0.08	1000.00	1.72	1.15
5965587	FALSE	Non-Selective	1000.00	0.00	1000.00	2.16
6324093	FALSE	Non-Selective	47.60	0.04	69.19	60.06
6320643	FALSE	TbODC Selective	68117.92	52609.35	47284.70	26779.65
6327734	FALSE	Non-Selective	370.44	0.26	0.42	370.44
3448-9166	FALSE	TbODC Selective	1000.00	1000.00	1000.00	1000.00
7202-3086	FALSE	TbODC Selective	7.05	2.11	3.69	2.61
0094-0016	FALSE	TbODC Selective	25.12	1000.00	19.91	1000.00
2237-1807	FALSE	TbODC Selective	1000.00	2.92	0.87	0.10
7741221	FALSE	TbODC Selective	3.47	7.61	3.10	1.00
5218493	FALSE	Non-Selective	1000.00	1000.00	0.24	0.20
F1387-0033	FALSE	TbODC Selective	6.17	6.17	4.16	2.19
F1387-0032	FALSE	TbODC Selective	5.28	4.96	4.44	1.40
F1387-0028	FALSE	TbODC Selective	11.82	11.82	11.80	4.03
7925755	FALSE	Inactive	35.47	39.80	14.74	37.18
F0815-0095	FALSE	TbODC Selective	1.80	1.58	1.58	0.71
E750-0136	FALSE	TbODC Selective	0.07	5.30	10.58	4.21
7923517	FALSE	TbODC Selective	1000.00	2.92	3.68	1.36
2548-0747	FALSE	TbODC Selective	1000.00	4.93	8.79	4.94
6629745	FALSE	Non-Selective	502.13	1000.00	399.81	357.90
6629868	FALSE	TbODC Selective	2.87	1000.00	4.73	1.94
3405-0210	FALSE	TbODC Selective	Inactive	Inactive	Inactive	Inactive
5305098	FALSE	Non-Selective	8.15	1000.00	4.93	4.63
5240915	FALSE	Non-Selective	2.90	1000.00	1.38	1.79

Compound ID	Reverse Addition Hit	hODC Selectivity	BJ Therapeutic Index	HepG2 Therapeutic Index	HEK293 Therapeutic Index	Raji Therapeutic Index
5240794	FALSE	Non-Selective	Inactive	Inactive	Inactive	Inactive
D053-0388	FALSE	TbODC Selective	5.52	3.10	3.21	2.75
D053-0375	FALSE	Non-Selective	20.93	6.62	6.59	2.84
F0808-1812	FALSE	TbODC Selective	6.57	4.16	2.69	1.31
5158531	FALSE	TbODC Selective	18.39	1000.00	14.05	14.15
7483938	FALSE	Non-Selective	1000.00	1000.00	3925.08	3498.24
6077688	FALSE	Non-Selective	1000.00	0.00	1000.00	0.02
5316000	FALSE	Non-Selective	1000.00	1000.00	3.57	3.17
6653473	FALSE	TbODC Selective	0.62	1.40	0.54	0.19
6653675	FALSE	Non-Selective	0.94	3.92	0.83	0.36
6680314	FALSE	Non-Selective	8.91	49.84	5.49	3.94
6389350	FALSE	Non-Selective	0.48	2.52	0.45	0.16
6656502	FALSE	Non-Selective	1.89	7.84	1.92	1.87
6627645	FALSE	Non-Selective	2.41	8.80	2.46	1.29
6657582	FALSE	Non-Selective	10.48	36.56	8.08	6.18
6627762	FALSE	Non-Selective	0.84	7.23	0.82	0.43
6658016	FALSE	Non-Selective	16.16	121.59	15.22	8.86
6625728	FALSE	Non-Selective	10.14	24.00	9.64	5.41
6631480	FALSE	TbODC Selective	1.20	4.55	1.29	0.65
6631369	FALSE	TbODC Selective	1.46	0.00	0.78	0.93
6626128	FALSE	TbODC Selective	11.52	0.00	10.75	8.38
F0808-1801	FALSE	TbODC Selective	0.00	1.77	0.89	1.77
F0808-1800	FALSE	TbODC Selective	1000.00	2.23	2.23	2.23
5960222	FALSE	Non-Selective	4.01	1000.00	3.15	1.97
5960045	FALSE	Non-Selective	5.23	1000.00	3.89	4.02
5963070	FALSE	Non-Selective	1241.04	1000.00	1134.42	771.22

Compound ID	Reverse Addition Hit	hODC Selectivity	BJ Therapeutic Index	HepG2 Therapeutic Index	HEK293 Therapeutic Index	Raji Therapeutic Index
5968220	FALSE	Non-Selective	1000.00	1000.00	1000.00	1229.26
D053-0032	FALSE	Non-Selective	2.12	1.95	1.71	1.96
D053-0117	FALSE	Non-Selective	3.54	2.69	2.32	0.79
D053-0306	FALSE	TbODC Selective	2.92	2.71	4.02	0.86
7969312	FALSE	Non-Selective	4.57	15.09	6.05	4.30
7967759	FALSE	Inactive	4.85	11.80	4.24	3.89
7970161	FALSE	Non-Selective	12.83	78.49	19.33	12.74
7924532	FALSE	Inactive	7.39	9.43	7.49	10.15
6371621	FALSE	Inactive	2.25	2.58	1.44	14.49
6378891	FALSE	Inactive	3.89	1000.00	1.94	6.85
6633774	FALSE	Inactive	1000.00	1000.00	2.17	5.29
7016468	FALSE	Inactive	9.42	1000.00	1.01	11.26
5994-0447	FALSE	Non-Selective	20.04	2.28	2.09	1.04
6635495	FALSE	TbODC Selective	7.36	1000.00	6.37	6.37
7630880	FALSE	Inactive	9.40	1000.00	2.67	8.40
6378816	FALSE	Inactive	0.52	1000.00	0.65	0.74
7634527	FALSE	Non-Selective	11.16	1000.00	11.16	11.16
7630693	FALSE	Inactive	4.14	1.68	2.78	2.98
7630436	FALSE	Inactive	3.75	2.09	0.84	2.25
5467940	FALSE	Non-Selective	5.04	23.69	5.26	2.76
5934605	FALSE	TbODC Selective	3.41	1000.00	3.04	4.30
F1031-0135	FALSE	TbODC Selective	9.19	0.50	0.89	0.28
F0842-0019	FALSE	TbODC Selective	11.35	0.65	0.75	0.36
F1031-0171	FALSE	Non-Selective	14.69	0.77	0.74	0.40
F1031-0043	FALSE	Inactive	9.39	1.18	1.50	0.51
F1031-0061	FALSE	Non-Selective	3.40	0.61	0.63	0.29
F0870-0083	FALSE	TbODC Selective	14.23	1.26	1.32	0.44
F1310-0022	FALSE	TbODC Selective	3.96	0.68	0.55	0.30
F0842-0027	FALSE	TbODC Selective	9.88	1.10	1.04	0.27
6586297	FALSE	Non-Selective	Inactive	Inactive	Inactive	Inactive
6589006	FALSE	Non-Selective	1000.00	0.00	1000.00	1000.00
5976843	FALSE	Non-Selective	1000.00	1000.00	1.21	40.02

Compound ID	Reverse Addition Hit	hODC Selectivity	BJ Therapeutic Index	HepG2 Therapeutic Index	HEK293 Therapeutic Index	Raji Therapeutic Index
7261142	FALSE	Non-Selective	1000.00	8.64	1000.00	216.94
6323011	FALSE	Non-Selective	1000.00	3.59	8.03	1000.00
2368-0377	FALSE	Non-Selective	1000.00	22334.18	707.95	1000.00
5966880	FALSE	Non-Selective	24.36	0.02	1000.00	8.83
3297-0914	FALSE	TbODC Selective	1000.00	0.01	0.63	1000.00
7968826	FALSE	Non-Selective	10.65	22.31	12.60	16.76
7968687	FALSE	Non-Selective	3.87	4.53	5.22	7.29
7925578	FALSE	Non-Selective	10.58	3.00	5.26	8.75
7968218	FALSE	Non-Selective	12.71	2.09	3.08	1.68
6374848	FALSE	Non-Selective	14.44	10.59	9.90	15.62
7011428	FALSE	Non-Selective	14.81	7.32	7.42	12.10
6372208	FALSE	Non-Selective	19.85	7.11	4.60	12.64
7967682	FALSE	Non-Selective	5.41	6.00	6.10	12.48
6372780	FALSE	TbODC Selective	15.94	36.86	15.19	41.02
6375950	FALSE	TbODC Selective	22.46	85.12	12.02	55.36
7926588	FALSE	TbODC Selective	11.22	4.01	3.21	8.95
5977995	FALSE	Non-Selective	29.88	1000.00	35.05	37.70
6290791	FALSE	Non-Selective	104.66	0.08	58.72	104.66
5970242	FALSE	Non-Selective	1000.00	1000.00	11.06	1908.26
K079-0037	FALSE	Non-Selective	2.20	1000.00	2.20	1.56
3132-0665	FALSE	Non-Selective	0.00	2.13	0.04	1.90
M 6760	FALSE	Inactive	1000.00	8.91	14.12	14.12
4770-1860	FALSE	TbODC Selective	1000.00	177.41	0.03	158.49
K243-0077	FALSE	TbODC Selective	0.17	1.17	1.81	0.04
E540-1032	FALSE	Inactive	14.97	27.54	80.36	12.82
3405-0201	FALSE	TbODC Selective	0.00	1000.00	3.66	3.64
K297-0325	FALSE	Inactive	1000.00	1000.00	22.87	1000.00
3405-0009	FALSE	TbODC Selective	1000.00	1000.00	14.03	1000.00
7833672	FALSE	Non-Selective	49.52	49.52	49.52	14.56

Compound ID	Reverse Addition Hit	hODC Selectivity	BJ Therapeutic Index	HepG2 Therapeutic Index	HEK293 Therapeutic Index	Raji Therapeutic Index
F1055-0007	FALSE	Non-Selective	1000.00	3.58	3.81	2.75
F1055-0005	FALSE	Inactive	1000.00	211.61	3.98	56100.92
5243661	FALSE	Non-Selective	7.61	5.25	7.63	2.51
E677-0508	FALSE	TbODC Selective	2.96	1.26	2.76	1.08
7982563	FALSE	Non-Selective	1.94	1.23	1.73	0.69
C276-0038	FALSE	TbODC Selective	2.02	1.44	0.01	0.98
7906760	FALSE	Non-Selective	4.27	1.31	2.70	0.89
C276-0041	FALSE	Non-Selective	0.00	1.06	1.58	0.86
7918942	FALSE	Non-Selective	9.93	2.78	9.93	4.47
7906754	FALSE	TbODC Selective	13.51	13.39	26.77	15.02
C276-0043	FALSE	TbODC Selective	3.75	2.11	2.02	0.81
7906759	FALSE	Non-Selective	85.54	9.67	130.21	152.48
7918941	FALSE	Non-Selective	13.86	35.88	19.32	11.82
0418-0093	FALSE	Inactive	Inactive	Inactive	Inactive	Inactive
7202-3000	FALSE	TbODC Selective	1000.00	2.09	2.09	2.09
F1387-0062	FALSE	Inactive	1.00	1.23	1.05	1.53
5133157	FALSE	Inactive	2.35	2.02	1.15	7.64
6372490	FALSE	Non-Selective	13.77	17.22	2.34	7.81
6376502	FALSE	Inactive	0.75	0.52	0.44	0.60
7969927	FALSE	TbODC Selective	2.89	7.15	2.39	5.19
0958-0297	FALSE	TbODC Selective	10.75	4.84	7.31	1.31
5140792	FALSE	Inactive	17.23	2.41	1.00	2.00
6371667	FALSE	Inactive	15.40	3.13	2.41	9.62
6372717	FALSE	Non-Selective	4.08	1.86	3.01	10.15
6377128	FALSE	Inactive	11.74	3.60	1.79	12.89
6374081	FALSE	Inactive	4.60	2.35	1.63	4.94
6376791	FALSE	Non-Selective	113.82	18.20	23.15	14.77
6371681	FALSE	Inactive	1.29	1.05	0.85	1.00
6382061	FALSE	Non-Selective	12.59	3.98	3.56	11.73
7967495	FALSE	Inactive	9.00	5.60	3.12	6.66
7970045	FALSE	TbODC Selective	25.23	66.97	31.10	41.11
6371856	FALSE	TbODC Selective	12.86	3.05	2.49	6.82

Compound ID	Reverse Addition Hit	hODC Selectivity	BJ Therapeutic Index	HepG2 Therapeutic Index	HEK293 Therapeutic Index	Raji Therapeutic Index
5924-0106	FALSE	TbODC Selective	1.36	1.59	1.30	0.83
3261-1071	FALSE	TbODC Selective	0.63	0.75	0.42	1.00
F2795-0512	FALSE	Inactive	1000.00	1000.00	1000.00	879.51
6350-0006	FALSE	Non-Selective	6.27	3.05	5.60	0.30
6350-0013	FALSE	Non-Selective	7.06	2.35	7.08	0.37
7174955	FALSE	Non-Selective	5.40	10.03	7.96	3.88
F3165-1168	FALSE	TbODC Selective	0.23	1000.00	1000.00	1000.00
C338-0072	FALSE	TbODC Selective	1000.00	1000.00	0.17	243.28
C433-0076	FALSE	TbODC Selective	1.69	1000.00	707.95	761.23
C433-0620	FALSE	TbODC Selective	501.19	31.62	12.59	17740.67
C433-0614	FALSE	TbODC Selective	1000.00	889.14	6.31	889.14
D093-0045	FALSE	TbODC Selective	19.63	2.37	2.89	1.66
D093-0073	FALSE	TbODC Selective	7.04	2.71	5.92	3.04
5158512	FALSE	TbODC Selective	5.81	15.79	8.02	5.30
5158511	FALSE	TbODC Selective	2.18	4.71	3.82	1.90
5228252	FALSE	TbODC Selective	30.60	30.60	12.79	18.64
5149913	FALSE	Non-Selective	0.73	1.99	0.51	0.59
1069-0090	FALSE	TbODC Selective	1000.00	1000.00	1000.00	0.00
1332-0031	FALSE	TbODC Selective	56.23	1000.00	7924.47	7924.47
7568836	FALSE	Non-Selective	5.97	8.20	12.56	1.65
5118904	FALSE	TbODC Selective	9.98	1000.00	7.08	1000.00
7817424	FALSE	TbODC Selective	118.58	242.81	185.24	123.54
5142887	FALSE	TbODC Selective	4.65	1000.00	4.66	5.87
6006195	FALSE	Non-Selective	37.60	1000.00	421.35	531.71
6005002	FALSE	Non-Selective	117.78	1000.00	93.78	49.31
5964389	FALSE	Non-Selective	1000.00	1000.00	1000.00	3.22
5965278	FALSE	Non-Selective	6.43	5.78	3.00	4.80
2368-0409	FALSE	TbODC Selective	Inactive	Inactive	Inactive	Inactive

Compound ID	Reverse Addition Hit	hODC Selectivity	BJ Therapeutic Index	HepG2 Therapeutic Index	HEK293 Therapeutic Index	Raji Therapeutic Index
E677-0889	FALSE	TbODC Selective	8.12	2.63	9.00	1.42
E677-0564	FALSE	Non-Selective	7.08	6.09	8.29	7.63
F2074-0207	FALSE	TbODC Selective	1000.00	1.82	0.06	1.82
F2074-0016	FALSE	Non-Selective	1000.00	2.22	0.00	9.90
F2074-0085	FALSE	Non-Selective	1.78	1000.00	8891.40	8891.40
F2074-0107	FALSE	Non-Selective	0.00	6.19	6.19	0.62
F2074-0285	FALSE	TbODC Selective	Inactive	Inactive	Inactive	Inactive
7267501	FALSE	Inactive	10.98	11.60	8.56	2.22
6604418	FALSE	TbODC Selective	8.05	0.00	4.34	5.38
6927-0961	FALSE	Non-Selective	1000.00	12.97	105.70	7.23
0665-0081	FALSE	TbODC Selective	1000.00	1000.00	1000.00	1000.00
6128194	FALSE	Non-Selective	25.42	17.49	38.67	13.50
6147058	FALSE	Inactive	6.37	2.02	6.37	8.21
7253329	FALSE	Non-Selective	3.33	10.80	6.46	1.76
7285485	FALSE	Non-Selective	5.49	20.69	8.20	3.35
7246974	FALSE	TbODC Selective	1000.00	19.74	1000.00	89.12
6005-0063	FALSE	TbODC Selective	281.84	158.11	1000.00	158.11
6767933	FALSE	Non-Selective	562.90	1000.00	562.90	502.88
6000-1760	FALSE	TbODC Selective	1000.00	1000.00	1000.00	1000.00
K286-4381	FALSE	TbODC Selective	4.32	1000.00	1000.00	0.05
2360-0539	FALSE	TbODC Selective	1000.00	22.40	11.25	44.80
D053-0279	FALSE	TbODC Selective	9.61	6.37	8.01	2.74
6377846	FALSE	Inactive	6.01	2.23	2.69	7.96
7803985	FALSE	TbODC Selective	2.32	6.65	2.90	1.43
7776670	FALSE	TbODC Selective	0.94	2.18	0.97	0.35
7521108	FALSE	TbODC Selective	6.77	18.18	8.30	2.07
7788014	FALSE	TbODC Selective	2.47	6.31	2.51	2.01
5924-0105	FALSE	TbODC Selective	2.00	1.38	1.08	0.80
4663-0305	FALSE	TbODC Selective	1.10	1.06	0.69	0.69

S4.13 Table of ODC High-Throughput Assay Hit Purity and Concentration Data

The following table shows the purity and concentration data for each re-ordered hit compound from table **S4.11**. It also includes the EC₅₀ value for the reverse DTT addition experiment, the redox activities and the source of the compound (primary hit or non-primary hit).

Field Definitions are below:

CompoundID:	Vendor Catalogue Number (notebook_page field in St. Jude Chemical Biology Compound Registration Database)
Reverse Addition EC ₅₀ (μM):	The IC ₅₀ value for the compound under incubated with ODC and DTT, the compound was designated as a reverse addition hit. This assay was the most stringent of all secondary assays used.
ELSD/UV Purity:	This reflects the % purity as determined by UPLC analysis using both UV and ELSD detectors. See chapter 4 materials and methods section for a full description.
Pure:	Compounds above 75% pure by ELSD/UV were flagged as pure. See chapter 4 materials and methods section for a full description.
Redox Assay Activity:	The activity group from the redox-assay (see chapter 4 materials and methods for a full description of this assay). High activity is greater than 75% active, mid is between 40 and 75% active, low is between ~15 and 40% active and inactive reflects compounds which were statistically indistinguishable from the negative control population. Activities were normalized to positive and negative controls.
Primary Screen Hit:	If the compound was identified as a hit in the primary screen this field will be "TRUE". If it was part of a later SAR directed reorder compound set, it will be "FALSE".

Compound ID	Reverse	ELSD/UV	Pure	CLND	Redox Assay	Primary
	Addition EC ₅₀	Percent		Concentration		
	(μ M)	Purity		(mM)	Activity	Screen Hit
7992559	27.00	95.00	TRUE	10.00	INACT	TRUE
F1098-0070	6.31	95.00	TRUE	4.63	INACT	TRUE
7800304	7.94	100.00	TRUE	10.00	INACT	TRUE
C393-0024	38.15	95.00	TRUE	9.07	INACT	TRUE
F2074-0019	4.01	78.00	TRUE	2.57	INACT	TRUE
E677-1397	29.33	73.00	FALSE	7.20	INACT	TRUE
E677-1143	34.20	71.00	FALSE	8.77	INACT	TRUE
7144577	Inactive	80.00	TRUE	10.00	INACT	TRUE
F1031-0071	Inactive	95.00	TRUE	11.00	INACT	FALSE
F0815-0045	Inactive	95.00	TRUE	9.20	MID	FALSE
F1310-0007	Inactive	95.00	TRUE	10.90	MID	FALSE
K286-4390	Inactive	95.00	TRUE	7.93	INACT	TRUE
K286-4341	Inactive	95.00	TRUE	10.23	INACT	TRUE
K286-4371	Inactive	95.00	TRUE	9.30	HIGH	TRUE
K286-4369	Inactive	95.00	TRUE	8.45	INACT	TRUE
K286-4395	Inactive	95.00	TRUE	10.25	INACT	TRUE
3366-3045	Inactive	95.00	TRUE	8.93	INACT	TRUE
K286-4382	Inactive	95.00	TRUE	8.52	INACT	TRUE
K286-4379	Inactive	95.00	TRUE	8.50	HIGH	TRUE
5545617	Inactive	50.00	FALSE	10.00	INACT	TRUE
5223890	Inactive	100.00	TRUE	10.00	INACT	TRUE
3448-2065	Inactive	95.00	TRUE	6.35	INACT	FALSE
7485255	Inactive	95.00	TRUE	8.43	INACT	TRUE
6375520	Inactive	95.00	TRUE	11.30	INACT	FALSE
6381814	Inactive	ND	FALSE	ND	INACT	TRUE
6376401	Inactive	95.00	TRUE	12.20	INACT	FALSE
6373722	Inactive	95.00	TRUE	10.62	INACT	FALSE
7012006	Inactive	95.00	TRUE	11.20	INACT	FALSE
6633405	Inactive	20.00	FALSE	1.00	INACT	FALSE
6372407	Inactive	95.00	TRUE	13.95	HIGH	FALSE
2368-0065	Inactive	88.00	TRUE	5.70	INACT	TRUE
5964204	Inactive	40.00	FALSE	10.00	INACT	TRUE
5965587	Inactive	33.00	FALSE	10.00	INACT	TRUE
6324093	Inactive	47.00	FALSE	10.00	INACT	TRUE
6320643	Inactive	90.00	TRUE	8.32	INACT	TRUE
6327734	Inactive	40.00	FALSE	10.00	INACT	TRUE
3448-9166	Inactive	95.00	TRUE	5.67	INACT	FALSE
7202-3086	Inactive	90.00	TRUE	6.70	MID	TRUE
0094-0016	Inactive	95.00	TRUE	10.00	INACT	FALSE
2237-1807	Inactive	79.00	TRUE	5.33	INACT	TRUE
7741221	Inactive	68.00	FALSE	10.00	INACT	TRUE
5218493	Inactive	90.00	TRUE	10.00	INACT	TRUE
F1387-0033	Inactive	78.00	TRUE	2.13	MID	TRUE
F1387-0032	Inactive	ND	FALSE	ND	MID	TRUE
F1387-0028	Inactive	85.00	TRUE	2.97	HIGH	TRUE
7925755	Inactive	95.00	TRUE	10.57	INACT	FALSE
F0815-0095	Inactive	76.00	TRUE	5.30	MID	TRUE
E750-0136	Inactive	94.00	TRUE	10.60	INACT	TRUE

Compound ID	Reverse Addition EC ₅₀ (μM)	CLND/UV Percent Purity	Pure	CLND Concentration (mM)	Redox Assay Activity	Primary Screen Hit
7923517	Inactive	93.00	TRUE	7.95	INACT	TRUE
2548-0747	Inactive	69.00	FALSE	10.00	MID	TRUE
6629745	Inactive	15.00	FALSE	10.00	INACT	TRUE
6629868	Inactive	50.00	FALSE	10.00	INACT	TRUE
3405-0210	Inactive	95.00	TRUE	10.00	INACT	FALSE
5305098	Inactive	95.00	TRUE	5.73	INACT	TRUE
5240915	Inactive	100.00	TRUE	10.00	INACT	TRUE
5240794	Inactive	40.00	FALSE	10.00	INACT	TRUE
D053-0388	Inactive	95.00	TRUE	6.20	INACT	TRUE
D053-0375	Inactive	95.00	TRUE	9.67	INACT	TRUE
F0808-1812	Inactive	78.00	TRUE	4.40	MID	TRUE
5158531	Inactive	25.00	FALSE	10.00	INACT	TRUE
7483938	Inactive	100.00	TRUE	10.00	INACT	TRUE
6077688	Inactive	25.00	FALSE	10.00	INACT	TRUE
5316000	Inactive	70.00	FALSE	10.00	INACT	TRUE
6653473	Inactive	40.00	FALSE	10.00	INACT	TRUE
6653675	Inactive	50.00	FALSE	10.00	INACT	TRUE
6680314	Inactive	50.00	FALSE	10.00	INACT	TRUE
6389350	Inactive	50.00	FALSE	10.00	INACT	TRUE
6656502	Inactive	40.00	FALSE	10.00	INACT	TRUE
6627645	Inactive	75.00	FALSE	10.00	INACT	TRUE
6657582	Inactive	15.00	FALSE	10.00	INACT	TRUE
6627762	Inactive	15.00	FALSE	5.35	INACT	TRUE
6658016	Inactive	10.00	FALSE	10.00	INACT	TRUE
6625728	Inactive	25.00	FALSE	10.00	INACT	TRUE
6631480	Inactive	85.00	TRUE	10.00	INACT	TRUE
6631369	Inactive	50.00	FALSE	10.00	INACT	TRUE
6626128	Inactive	28.00	FALSE	10.00	INACT	TRUE
F0808-1801	Inactive	48.00	FALSE	10.00	INACT	TRUE
F0808-1800	Inactive	34.00	FALSE	10.00	MID	TRUE
5960222	Inactive	68.00	FALSE	10.00	INACT	TRUE
5960045	Inactive	72.00	FALSE	10.00	INACT	TRUE
5963070	Inactive	60.00	FALSE	10.00	INACT	TRUE
5968220	Inactive	40.00	FALSE	10.00	INACT	TRUE
D053-0032	Inactive	95.00	TRUE	9.73	INACT	TRUE
D053-0117	Inactive	95.00	TRUE	9.88	INACT	TRUE
D053-0306	Inactive	95.00	TRUE	10.17	INACT	TRUE
7969312	Inactive	87.00	TRUE	9.15	INACT	TRUE
7967759	Inactive	95.00	TRUE	11.18	INACT	FALSE
7970161	Inactive	ND	FALSE	ND	INACT	FALSE
7924532	Inactive	95.00	TRUE	13.40	INACT	FALSE
6371621	Inactive	95.00	TRUE	13.33	INACT	FALSE
6378891	Inactive	95.00	TRUE	12.72	INACT	FALSE
6633774	Inactive	95.00	TRUE	10.57	INACT	FALSE
7016468	Inactive	95.00	TRUE	9.27	INACT	FALSE
5994-0447	Inactive	95.00	TRUE	4.83	MID	TRUE
6635495	Inactive	95.00	TRUE	10.47	INACT	FALSE
7630880	Inactive	95.00	TRUE	10.40	INACT	FALSE

Compound ID	Reverse Addition EC ₅₀ (μM)	CLND/UV Percent Purity	Pure	CLND Concentration (mM)	Redox Assay Activity	Primary Screen Hit
6378816	Inactive	95.00	TRUE	11.86	INACT	FALSE
7634527	Inactive	95.00	TRUE	10.20	INACT	TRUE
7630693	Inactive	95.00	TRUE	9.91	INACT	FALSE
7630436	Inactive	95.00	TRUE	8.90	INACT	FALSE
5467940	Inactive	95.00	TRUE	7.80	INACT	TRUE
5934605	Inactive	100.00	TRUE	10.57	INACT	TRUE
F1031-0135	Inactive	95.00	TRUE	8.95	MID	FALSE
F0842-0019	Inactive	95.00	TRUE	9.85	HIGH	FALSE
F1031-0171	Inactive	95.00	TRUE	11.65	MID	FALSE
F1031-0043	Inactive	95.00	TRUE	11.50	MID	FALSE
F1031-0061	Inactive	95.00	TRUE	12.30	MID	FALSE
F0870-0083	Inactive	95.00	TRUE	12.00	INACT	FALSE
F1310-0022	Inactive	80.00	TRUE	10.90	INACT	TRUE
F0842-0027	Inactive	95.00	TRUE	11.85	INACT	FALSE
6586297	Inactive	50.00	FALSE	10.00	INACT	TRUE
6589006	Inactive	33.00	FALSE	2.76	INACT	TRUE
5976843	Inactive	46.00	FALSE	10.00	INACT	TRUE
7261142	Inactive	33.00	FALSE	10.00	INACT	TRUE
6323011	Inactive	45.00	FALSE	10.00	INACT	TRUE
2368-0377	Inactive	86.00	TRUE	4.85	INACT	TRUE
5966880	Inactive	50.00	FALSE	10.00	INACT	TRUE
3297-0914	Inactive	95.00	TRUE	10.00	INACT	FALSE
7968826	Inactive	93.00	TRUE	7.77	HIGH	TRUE
7968687	Inactive	90.00	TRUE	8.78	INACT	TRUE
7925578	Inactive	95.00	TRUE	9.63	INACT	TRUE
7968218	Inactive	95.00	TRUE	10.45	MID	TRUE
6374848	Inactive	95.00	TRUE	11.62	INACT	FALSE
7011428	Inactive	95.00	TRUE	9.97	INACT	TRUE
6372208	Inactive	95.00	TRUE	11.43	INACT	FALSE
7967682	Inactive	95.00	TRUE	11.32	INACT	TRUE
6372780	Inactive	40.00	FALSE	3.93	INACT	FALSE
6375950	Inactive	75.00	FALSE	8.43	INACT	FALSE
7926588	Inactive	95.00	TRUE	8.90	INACT	FALSE
5977995	Inactive	50.00	FALSE	10.00	INACT	TRUE
6290791	Inactive	50.00	FALSE	10.00	INACT	TRUE
5970242	Inactive	55.00	FALSE	3.35	INACT	TRUE
K079-0037	Inactive	ND	FALSE	ND	MID	FALSE
3132-0665	Inactive	95.00	TRUE	9.94	INACT	TRUE
M 6760	Inactive	95.00	TRUE	10.00	INACT	FALSE
4770-1860	Inactive	95.00	TRUE	8.55	INACT	TRUE
K243-0077	Inactive	95.00	TRUE	10.00	INACT	FALSE
E540-1032	Inactive	95.00	TRUE	3.60	INACT	TRUE
3405-0201	Inactive	95.00	TRUE	10.00	INACT	FALSE
K297-0325	Inactive	95.00	TRUE	10.00	INACT	
3405-0009	Inactive	95.00	TRUE	10.60	INACT	FALSE
7833672	Inactive	95.00	TRUE	9.95	INACT	TRUE
F1055-0007	Inactive	95.00	TRUE	9.70	INACT	TRUE

Compound ID	Reverse Addition EC ₅₀ (μM)	CLND/UV Percent Purity	Pure	CLND Concentration (mM)	Redox Assay Activity	Primary Screen Hit
F1055-0005	Inactive	95.00	TRUE	1.10	INACT	TRUE
5243661	Inactive	85.00	TRUE	8.10	INACT	TRUE
E677-0508	Inactive	95.00	TRUE	7.00	INACT	TRUE
7982563	Inactive	95.00	TRUE	7.90	INACT	FALSE
C276-0038	Inactive	95.00	TRUE	7.70	INACT	TRUE
7906760	Inactive	79.00	TRUE	5.40	INACT	FALSE
C276-0041	Inactive	95.00	TRUE	7.50	INACT	TRUE
7918942	Inactive	90.00	TRUE	10.00	INACT	FALSE
7906754	Inactive	95.00	TRUE	10.00	INACT	FALSE
C276-0043	Inactive	95.00	TRUE	5.90	INACT	TRUE
7906759	Inactive	60.00	FALSE	10.00	INACT	FALSE
7918941	Inactive	3.00	FALSE	6.00	INACT	FALSE
0418-0093	Inactive	95.00	TRUE	10.00	INACT	FALSE
7202-3000	Inactive	55.00	FALSE	10.00	MID	TRUE
F1387-0062	Inactive	95.00	TRUE	15.10	MID	TRUE
5133157	Inactive	95.00	TRUE	10.92	INACT	FALSE
6372490	Inactive	90.00	TRUE	9.38	INACT	FALSE
6376502	Inactive	95.00	TRUE	9.99	INACT	FALSE
7969927	Inactive	95.00	TRUE	12.10	HIGH	TRUE
0958-0297	Inactive	95.00	TRUE	10.00	INACT	FALSE
5140792	Inactive	95.00	TRUE	11.10	INACT	FALSE
6371667	Inactive	92.00	TRUE	11.67	INACT	FALSE
6372717	Inactive	95.00	TRUE	12.07	INACT	FALSE
6377128	Inactive	95.00	TRUE	11.12	INACT	FALSE
6374081	Inactive	95.00	TRUE	15.95	INACT	FALSE
6376791	Inactive	100.00	TRUE	8.07	INACT	TRUE
6371681	Inactive	95.00	TRUE	10.41	INACT	FALSE
6382061	Inactive	95.00	TRUE	10.55	INACT	FALSE
7967495	Inactive	95.00	TRUE	10.47	INACT	FALSE
7970045	Inactive	75.00	FALSE	5.30	INACT	TRUE
6371856	Inactive	95.00	TRUE	12.40	INACT	FALSE
5924-0106	Inactive	90.00	TRUE	10.00	INACT	TRUE
3261-1071	Inactive	90.00	TRUE	7.25	INACT	FALSE
F2795-0512	Inactive	95.00	TRUE	13.73	INACT	TRUE
6350-0006	Inactive	95.00	TRUE	8.00	INACT	TRUE
6350-0013	Inactive	95.00	TRUE	7.45	INACT	TRUE
7174955	Inactive	95.00	TRUE	15.23	INACT	TRUE
F3165-1168	Inactive	95.00	TRUE	6.14	INACT	TRUE
C338-0072	Inactive	95.00	TRUE	3.30	INACT	TRUE
C433-0076	Inactive	82.00	TRUE	4.96	INACT	TRUE
C433-0620	Inactive	95.00	TRUE	4.08	INACT	TRUE
C433-0614	Inactive	95.00	TRUE	4.48	INACT	TRUE
D093-0045	Inactive	95.00	TRUE	6.70	INACT	TRUE
D093-0073	Inactive	95.00	TRUE	9.40	INACT	TRUE
5158512	Inactive	70.00	FALSE	10.00	MID	TRUE
5158511	Inactive	25.00	FALSE	10.00	INACT	TRUE
5228252	Inactive	15.00	FALSE	10.00	MID	TRUE
5149913	Inactive	33.00	FALSE	10.00	INACT	TRUE


Compound ID	Reverse Addition EC ₅₀ (μM)	CLND/UV Percent Purity	Pure	CLND Concentration (mM)	Redox Assay Activity	Primary Screen Hit
1069-0090	Inactive	50.00	FALSE	4.55	INACT	FALSE
1332-0031	Inactive	95.00	TRUE	10.00	INACT	FALSE
7568836	Inactive	90.00	TRUE	1.85	INACT	TRUE
5118904	Inactive	70.00	FALSE	10.00	INACT	TRUE
7817424	Inactive	60.00	FALSE	10.00	INACT	TRUE
5142887	Inactive	15.00	FALSE	10.00	INACT	TRUE
6006195	Inactive	25.00	FALSE	10.00	INACT	TRUE
6005002	Inactive	32.00	FALSE	10.00	INACT	TRUE
5964389	Inactive	50.00	FALSE	10.00	INACT	TRUE
5965278	Inactive	90.00	TRUE	4.68	INACT	TRUE
2368-0409	Inactive	89.00	TRUE	6.95	INACT	TRUE
E677-0889	Inactive	86.00	TRUE	4.90	INACT	TRUE
E677-0564	Inactive	95.00	TRUE	6.37	INACT	TRUE
F2074-0207	Inactive	47.00	FALSE	10.00	INACT	TRUE
F2074-0016	Inactive	82.00	TRUE	3.07	INACT	TRUE
F2074-0085	Inactive	61.00	FALSE	10.00	INACT	TRUE
F2074-0107	Inactive	76.00	TRUE	2.73	INACT	TRUE
F2074-0285	Inactive	40.00	FALSE	10.00	MID	TRUE
7267501	Inactive	ND	FALSE	ND	INACT	TRUE
6604418	Inactive	75.00	FALSE	10.00	INACT	TRUE
6927-0961	Inactive	95.00	TRUE	5.23	INACT	TRUE
0665-0081	Inactive	ND	FALSE	ND	MID	FALSE
6128194	Inactive	95.00	TRUE	5.05	INACT	TRUE
6147058	Inactive	95.00	TRUE	9.30	INACT	TRUE
7253329	Inactive	95.00	TRUE	5.45	INACT	TRUE
7285485	Inactive	100.00	TRUE	10.95	INACT	TRUE
7246974	Inactive	100.00	TRUE	4.25	INACT	TRUE
6005-0063	Inactive	95.00	TRUE	8.05	INACT	TRUE
6767933	Inactive	100.00	TRUE	9.23	INACT	TRUE
6000-1760	Inactive	95.00	TRUE	8.22	INACT	FALSE
K286-4381	Inactive	95.00	TRUE	9.57	HIGH	FALSE
2360-0539	Inactive	90.00	TRUE	13.00	INACT	TRUE
D053-0279	Inactive	95.00	TRUE	8.03	INACT	TRUE
6377846	Inactive	95.00	TRUE	11.70	INACT	FALSE
7803985	Inactive	30.00	FALSE	10.00	INACT	TRUE
7776670	Inactive	25.00	FALSE	10.00	INACT	TRUE
7521108	Inactive	26.00	FALSE	10.00	INACT	TRUE
7788014	Inactive	30.00	FALSE	10.00	INACT	TRUE
5924-0105	Inactive	94.00	TRUE	10.00	INACT	TRUE
4663-0305	Inactive	90.00	TRUE	10.00	INACT	TRUE

Publishing Agreement

It is the policy of the University to encourage the distribution of all theses, dissertations, and manuscripts. Copies of all UCSF theses, dissertations, and manuscripts will be routed to the library via the Graduate Division. The library will make all theses, dissertations, and manuscripts accessible to the public and will preserve these to the best of their abilities, in perpetuity.

Please sign the following statement:

I hereby grant permission to the Graduate Division of the University of California, San Francisco to release copies of my thesis, dissertation, or manuscript to the Campus Library to provide access and preservation, in whole or in part, in perpetuity.



Author Signature

12-15-2009
Date